

**Influence of Non-thermal Plasma-based Biological  
Decontamination Processes on the Surface Properties  
of Plasma-exposed Polymers**

Inauguraldissertation

zur

Erlangung des akademischen Grades

doctor rerum naturalium (Dr. rer. nat.)

an der Mathematisch-Naturwissenschaftlichen Fakultät

der

Ernst-Moritz-Arndt-Universität Greifswald

vorgelegt von: Katja Fricke

geboren am 30.10.1982

in Rostock

Greifswald, 20. September 2012



Dekan: Prof. Dr. Klaus Fesser

1. Gutachter: Prof. Dr. Thomas von Woedtke

2. Gutachter: Prof. Dr. Michael Wertheimer

Tag der Promotion: 18.12.2012





# CONTENTS

<b>I</b>	<b><u>OUTLINE OF THE THESIS</u></b>	<b>7</b>
<b>II</b>	<b><u>LIST OF PUBLICATIONS</u></b>	<b>9</b>
<b>III</b>	<b><u>ZUSAMMENFASSUNG/SUMMARY</u></b>	<b>11</b>
<b>1</b>	<b><u>NON-THERMAL PLASMA</u></b>	<b>19</b>
1.1	Introduction	19
1.2	Low-pressure plasma	22
1.3	Atmospheric pressure plasma	23
1.3.1	Dielectric barrier discharge (DBD) (applied in publication 5.6)	23
1.3.2	Atmospheric pressure plasma jet (applied in publication 5.1 - 5.5)	25
<b>2</b>	<b><u>NON-THERMAL PLASMA IN BIOLOGY AND MEDICINE</u></b>	<b>26</b>
2.1	Plasma-based bio-decontamination and sterilization	26
2.1.1	Mechanism of bio-decontamination	27
2.1.2	Impact of plasma agents on micro-organisms	29
2.1.3	Removal/etching of micro-organisms and biofilms	31
2.1.4	Bio-decontamination of polymers	34
2.2	Interaction between plasma/gaseous phase and polymer	36
2.2.1	Surface etching	37
2.2.2	Cross-linking	38
2.2.3	Surface modification/functionalization	39
2.3	Plasma-assisted surface modification of biomaterials for improved cell proliferation	42
<b>3</b>	<b><u>OUTLOOK: ATMOSPHERIC PRESSURE PLASMA FOR BIO-DECONTAMINATION OF LIVING SURFACES</u></b>	<b>44</b>
<b>4</b>	<b><u>REFERENCES</u></b>	<b>47</b>
<b>5</b>	<b><u>ORIGINAL PUBLICATIONS</u></b>	<b>53</b>
5.1	“On the Use of Atmospheric Pressure Plasma for the Bio-Decontamination of Polymers and Its Impact on Their Chemical and Morphological Surface Properties”	55
5.2	“Atmospheric Pressure Plasma: A high-performance tool for the efficient removal of biofilms”	73
5.3	“High Rate etching of Polymers by Means of an Atmospheric Pressure Plasma Jet”	83
5.4	“Investigation of Surface Etching of Poly(ether ether ketone) by Atmospheric Pressure Plasmas”	93

5.5	“Comparison of nonthermal Plasma Processes on the Surface Properties of Polystyrene and their Impact on Cell Growth”	107
5.6	“New nonthermal atmospheric pressure plasma sources for decontamination of human extremities”	119

<b><u>IV</u></b>	<b><u>EIDESSTATTLICHE ERKLÄRUNG/AFFIRMATION</u></b>	<b><u>129</u></b>
------------------	---	-------------------

<b><u>V</u></b>	<b><u>CURRICULUM VITAE</u></b>	<b><u>131</u></b>
-----------------	--------------------------------	-------------------

<b><u>VI</u></b>	<b><u>LIST OF ALL PUBLICATIONS</u></b>	<b><u>133</u></b>
------------------	--	-------------------

<b><u>VII</u></b>	<b><u>ACKNOWLEDGEMENT</u></b>	<b><u>139</u></b>
-------------------	-------------------------------	-------------------

# I Outline of the Thesis

This thesis focuses on the application of non-thermal physical plasmas in the biomedical research area related to inactivation of micro-organisms which is also referred to as plasma-based bio-decontamination. The investigations are mainly restricted to the inactivation of biological systems on abiotic polymeric surfaces by using an atmospheric pressure plasma jet operated with argon gas or argon gas with different admixtures of molecular oxygen. Additionally to the capability of the applied plasma jet in killing microbes the efficacy of this plasma jet for the removal of complex biological systems, in particular biofilms is shown. To model cell constituents of bacteria different synthetic polymers were chosen to gain insight into the decomposition process responsible for biofilm degradation. By investigating the impact of atmospheric pressure plasma on physico-chemical surface properties of various synthetic aliphatic and aromatic polymers the interaction mechanisms between plasma and plasma-exposed material are discussed. These studies are accompanied by applying different optical plasma diagnostic techniques to obtain information on the plasma gas phase which contribute to the elucidation of the reaction mechanisms occurring during plasma exposure. Moreover, it is presented to which extent the plasma treatment influences the surface properties of polymers during the plasma-based bio-decontamination process and further, the beneficial functionalization of plasma-treated polymeric surfaces for biomedical application is discussed.

The thesis is organized as follows:

The first chapter will give a brief introduction into physical plasmas and introduce the different types of non-thermal plasmas and finally, presents the atmospheric pressure plasma jet applied in this work.

The application of non-thermal plasmas in biomedical research fields are introduced in chapter two. The basic theory of plasma-based bio-decontamination will be discussed including the inactivation of micro-organisms as well as the elimination of microbes and biomolecules. This chapter is accompanied by the depiction of fundamental processes of plasma polymer interactions and outlined the resulting changes in the physico-chemical properties of the plasma-exposed polymer surface.

Chapter three comprises the potential application of plasma-based functionalization processes for biomedical purposes. The main interest is focusing on the use of polymers for biomaterials and which functional requirements have to be fulfilled for this specific application.

In chapter four a short outlook in the state-of-the-art application of atmospheric pressure plasma for bio-decontamination of living surfaces like human tissue is given.

The last chapter comprises the original publications on which the thesis is based on.



## II List of Publications

This thesis is based on the following peer-reviewed publications:

- **On the Use of Atmospheric Pressure Plasma for the Bio-Decontamination of Polymers and Its Impact on Their Chemical and Morphological Surface Properties**

K. Fricke, H. Tresp, R. Bussiahn, K. Schröder, Th. von Woedtke, K.-D. Weltmann  
*Plasma Chem. Plasma Process.*, vol. 32, pp. 801-816, 2012

Own contribution: K.F. designed and performed the experiments with the help of H.T. and R.B. K.F. wrote the manuscript. It was edited by all co-authors.

- **Atmospheric Pressure Plasma: A high-performance tool for the efficient removal of biofilms**

K. Fricke, I. Koban, H. Tresp, L. Jablonowski, K. Schröder, A. Kramer, K.-D. Weltmann, Th. von Woedtke, Th. Kocher  
*PLOS ONE*, vol. 7, no. 8, pp. 1-8, 2012

Own contribution: K.F. and K.S. designed the experiments. K.F. performed the experiments with the help of I.K. and H.T. The manuscript was written by K.F. which was edited by all co-authors.

- **High rate etching of polymers by means of an atmospheric pressure plasma jet**

K. Fricke, H. Steffen, K. Schröder, Th. von Woedtke, K.-D. Weltmann  
*Plasma Process. Polym.*, vol. 8, no. 1, pp. 51-58, 2011

Own contribution: K.F. designed and performed the experiments and wrote the manuscript which was edited by all co-authors.

- **Investigation of Surface Etching of Poly(ether ether ketone) by an Atmospheric Pressure Plasma Jet**

K. Fricke, S. Reuter, D. Schröder, V. Schulz-von der Gathen, K.-D. Weltmann, Th. von Woedtke  
*IEEE Trans. Plasma Sci.*, 2012, DOI: 10.1109/TPS.2012.2212463

Own contribution: K.F. designed and performed the experiments with the help of S.R. and D.S. The manuscript was written by K.F., S.R., D.S., and V. SvG.

- **Comparison of nonthermal Plasma Processes on the Surface Properties of Polystyrene and their Impact on Cell Growth**

K. Fricke, K. Duske, A. Quade, B. Nebe, K. Schröder, K.-D. Weltmann, Th. von Woedtke  
*IEEE Trans. Plasma Sci.*, 2012. DOI: 10.1109/TPS.2012.2204904

Own contribution: K.F. designed and performed the experiments with the help of K.D. and A.Q. K.F. wrote the manuscript which was edited by all co-authors.

➤ **New nonthermal atmospheric pressure plasma sources for decontamination of human extremities**

K.-D. Weltmann, K. Fricke, M. Stieber, R. Brandenburg, Th. von Woedtke, U. Schnabel

*IEEE Trans. Plasma Sci.*, 2012, DOI: 10.1109/tps.2012.2204279

Own contribution: K.F. was involved in performing the experiments and contributed to write the manuscript.

Confirmed: Greifswald, den 20.09.2012

---

Prof. Dr. Thomas von Woedtke

### III Zusammenfassung/Summary

In der Medizintechnik gehört die biologische Dekontamination bzw. Sterilisation zu den wesentlichen Verfahrensschritten sowohl bei der Herstellung als auch bei der Aufbereitung von Medizinprodukten. Da immer mehr polymerbasierte medizintechnische Produkte verwendet werden, stoßen verfügbare Verfahren an ihre Grenzen. Konventionelle Sterilisations- und Desinfektionsverfahren auf der Basis hoher Temperaturen, toxischer Gase oder ionisierender Strahlung können sich nachteilig auf Polymere auswirken und damit die Funktionalität der behandelten Produkte gefährden. Aus diesem Grund sind alternative, materialschonende und effiziente Dekontaminationsverfahren erforderlich. Ein möglicher Weg ist der Einsatz von nichtthermischen physikalischen Plasmen. Durch den Verzicht auf Vakuumtechnik und die daraus resultierenden Vorteile für die praktische Einsatzfähigkeit ist die Atmosphärendruck-Plasmatechnik von besonderem Interesse. Die vielseitigen Wirkmechanismen von Plasmen ermöglichen eine effiziente Abtötung bzw. Inaktivierung von Mikroorganismen, die nach aktuellem Kenntnisstand auf dem Zusammenwirken von plasmagenerierten reaktiven Sauerstoff- und Stickstoffspezies (ROS, RNS) sowie der vom Plasma emittierten (V)UV-Strahlung basiert. Sogenannte kalte Plasmen eignen sich aufgrund moderater Gastemperaturen (ungefähr bei Raumtemperatur) vor allem für die Behandlung von hitzeempfindlichen Materialien, wie z.B. Polymeren, ohne deren Volumeneigenschaften zu beeinträchtigen.

Inhalt der vorliegenden Arbeit ist die Untersuchung von Plasmaverfahren zur mikrobiologischen Dekontamination von Polymeren bei Atmosphärendruck. Dabei sollen vor allem Erkenntnisse zum Einfluss variierteter Plasma-Prozessparameter auf die inaktivierende Wirkung auf Mikroorganismen einerseits und die Beeinflussung der Materialeigenschaften andererseits gewonnen werden. Als Gegenstand der Untersuchungen dient ein hochfrequenzangeregter Atmosphärendruck-Plasmajet (aus der Reihe „kINPen“) mit Argon (Ar) und Argon-Sauerstoff-Gemischen (Ar/O<sub>2</sub>) als Arbeitsgas.

Drei wesentliche Aspekte wurden analysiert:

1. Die Wirkung des Plasmas auf die Vitalität von Mikroorganismen in Abhängigkeit von Arbeitsgas, Behandlungszeit und Probenabstand (Abstand zwischen der Jetdüse und dem Substrat).
2. Der plasmabasierte Abtrag von mikrobiellen Biofilmen.
3. Die Auswirkungen der Plasmabehandlung auf die Oberflächeneigenschaften ausgewählter Polymere.

Für die Studien zur Wirksamkeit von Ar- und Ar/O<sub>2</sub>-Plasma auf die Inaktivierung von Mikroorganismen wurden *Bacillus-atrophaeus*-Sporen verwendet, da diese wegen ihrer widerstandsfähigen Zellschichten besonders resistent gegenüber herkömmlichen Sterilisationsverfahren sind und daher auch als Bioindikatoren zur Sterilisationskontrolle verwendet werden. Polymerstreifen (Polyethylen und Polystyrol) wurden mit einer Sporensuspension punktuell kontaminiert, getrocknet und anschließend mit Plasma behandelt. Es konnte gezeigt werden, dass für eine effiziente Reduktion der Kontamination das Prozessgas einen entscheidenden Einfluss hat. So wurde durch die Zumischung von moleku-

larem Sauerstoff die sporeninaktivierende Wirkung des Plasmas im Vergleich zu reinem Ar als Arbeitsgas deutlich erhöht. Auf Grund der Sauerstoffzumischung von 1 Vol.-% wurde eine Reduktion der Anzahl koloniebildender Einheiten um 4 Log<sub>10</sub>-Stufen nach 300 s Plasmabehandlung erreicht. Zusätzlich hat sich gezeigt, dass ebenso der Probenabstand einen erheblichen Einfluss auf die Inaktivierung von Sporen hat, so dass mit zunehmendem Abstand die mikrobizide Wirkung des Plasmas reduziert ist.

Da die mikrobielle Wirkung den im Plasma generierten ROS/RNS sowie der (V)UV-Strahlung zugeschrieben werden, wurde zur Identifizierung angeregter Plasmaspezies die optische Emissionsspektroskopie (OES) verwendet, mit deren Hilfe eine Korrelation zwischen der mikrobiziden Effizienz in Abhängigkeit von Prozessgas und Arbeitsabstand gezeigt wurde. In der vorliegenden Arbeit erklärt sich die antimikrobielle Wirkung von sauerstoffhaltigen Plasmen durch die Bildung von ROS. Während das Emissionsspektrum von reinem Ar-Plasma hauptsächlich durch Emissionslinien von Hydroxylradikalen (bei  $\lambda = 308$  nm), von dem zweiten positiven System von Stickstoff (bei  $\lambda = 337$  nm) und von Argon (im Bereich zwischen  $\lambda = 700$ -900 nm) dominiert wurde, konnte im Spektrum vom Ar/O<sub>2</sub>-Plasma eine hohe Intensität von Emissionslinien von atomarem Sauerstoff (bei  $\lambda = 777$  nm und  $\lambda = 844$  nm) nachgewiesen werden. Die mit zunehmendem Probenabstand nachlassende letale Wirkung des Plasmas wird unter anderem auf das Abreagieren von kurzlebigen reaktiven Spezies in der Umgebungsluft zurückgeführt. Mit zunehmendem Abstand erreichen daher immer weniger reaktive Teilchen die Oberfläche. Dies wurde in den OES-Spektren beider Arbeitsgase in einer Intensitätsabnahme der Emissionslinien der angeregten Plasmaspezies sichtbar.

Plasma bewirkt nicht nur eine Inaktivierung von Mikroorganismen sondern kann auch zum Abtrag von biologischem Material führen. In einem Modellversuch wurden 7 Tage alte Biofilme von *Candida albicans* mit Ar- bzw. Ar/O<sub>2</sub>-Plasma behandelt. Der Nachweis der Biofilmentfernung wurde mit Hilfe eines Lichtmikroskops dokumentiert. Übereinstimmend mit den Inaktivierungsversuchen zeigte sich auch bei dem Abtrag des Biofilms eine bessere Wirkung des Ar/O<sub>2</sub>-Plasmas im Vergleich zu reinem Ar-Plasma. Die vollständige Entfernung des Biofilms wurde nach 300 s Ar/O<sub>2</sub>-Plasmabehandlung (mit einer Zumischung von 1 Vol.-% O<sub>2</sub>) erreicht. Dies führte zur Schlussfolgerung, dass Sporeninaktivierung und Biofilmaustrag auf weitgehend identische Wirkparameter zurückzuführen sind.

Zum Verständnis der Wirkmechanismen des plasmabasierten Biofilmaustrags wurden synthetische aliphatische und aromatische Polymere als Modelloberflächen untersucht, da analog zu Polymeren Mikroorganismen bzw. Biofilme hauptsächlich aus aliphatischen und aromatischen Kohlenwasserstoffverbindungen sowie diversen Anteilen von Sauerstoff- und Stickstoffgruppen bestehen. Zum Einsatz kamen Polyethylen, Polymethylmethacrylat, Polystyrol, Polypropylen, Polycarbonat, und Polyetheretherketon. Es wurde die abtragen- (ätzende) Wirkung des Plasmas auf Polymeroberflächen untersucht, wobei die Bestimmung der Ätzrate sowie die Aufklärung des Ätzmechanismus im Mittelpunkt standen. Die Ätzrate wurde quantitativ durch Bestimmung des Masseverlustes und durch Messung von Ätzprofilen mittels der Profilometrie ermittelt. Dabei wurden für die untersuchten Polymere Ätzraten von 50 bis 300 nm/s nach Ar/O<sub>2</sub>-Plasmabehandlung (1 Vol.-% O<sub>2</sub>) berechnet. Die gemessenen Ätzprofile zeigten, dass Ar-Plasma ohne direkte Sauerstoffzu-



mischung zwar einen Materialabtrag bewirkt, dieser allerdings hauptsächlich außerhalb der eigentlichen Plasmazone stattfindet, d.h. in dem Bereich, in dem eine intensive Zumischung von Umgebungsluft erfolgt. Der atmosphärische Sauerstoff kann durch das Verwirbeln mit dem Plasma angeregt und dissoziiert werden, was zum Ätzen der Polymeroberfläche führt. Bei direkter Zumischung von molekularem Sauerstoff zum Ar-Plasma wurde die Ätzrate um ein Vielfaches erhöht, darüber hinaus erfolgte das Ätzen unmittelbar in der Plasmazone. Für Absolutmessungen der Sauerstoffdichte in reaktiven Plasmaentladungen wurde in dieser Arbeit die Zwei-Photonen angeregte laserinduzierte Fluoreszenzspektroskopie (TALIF) verwendet. Damit war es möglich einen direkten Zusammenhang zwischen der Sauerstoffzumischung und der Intensität des Materialabtrages herzustellen. So konnte gezeigt werden, dass mit zunehmender Sauerstoffzumischung (von 0 bis 1.5 Vol.-%) die atomare Sauerstoffdichte steigt, jedoch mit zunehmendem Abstand sinkt. Weiterhin wurde gezeigt, dass sich die abgetragene Masse proportional zu der Sauerstoffdichte verhält, d.h. es konnte eindeutig nachgewiesen werden, dass im Plasma erzeugte Sauerstoffspezies für den Ätzprozess verantwortlich sind.

Somit konnte in der vorliegenden Arbeit unter Verwendung von repräsentativen Polymeren, die sowohl strukturelle Analogien zu Bestandteilen von Mikroorganismen und Biofilmen aufweisen als auch als Materialien in Medizinprodukten zur Anwendung kommen nachgewiesen werden, dass erwünschte antimikrobielle und biofilmaustragende Plasmaeffekte und eventuell unerwünschte Ätzwirkungen auf die plasmabehandelten Materialien auf weitgehend identischen Wirkkomponenten und -mechanismen beruhen. Diese Erkenntnisse sind folglich bei der Steuerung plasmabasierter Sterilisations- und Dekontaminationsverfahren von Polymermaterialien zu berücksichtigen.

Auch bei der Vermeidung von materialabtragenden Plasmaparametern ist während der Plasmaexposition das zu dekontaminierende Substrat unweigerlich dem Beschuss energiereicher und reaktiver Plasmaspezies ausgesetzt, die mit der Substratoberfläche wechselwirken können. Aus diesem Grund wurde der Einfluss der Plasmabehandlung auf charakteristische Oberflächeneigenschaften der Polymere untersucht. Insbesondere wurden die Veränderungen in der Wasserbenetzbarkeit, der chemischen Oberflächenzusammensetzung und der Topografie, sowie deren Veränderungen in Zusammenhang mit variablen Prozessparametern analysiert. Detaillierte Erkenntnisse zur polymerspezifischen Wirkung des Plasmas wurden durch die oberflächenanalytischen Untersuchungen zur chemischen Zusammensetzung mittels Röntgenphotoelektronenspektroskopie (XPS) gewonnen. Durch die XPS-Analysen von unbehandelten und behandelten Polymeren konnte ein erhöhtes Sauerstoff/Kohlenstoff-Verhältnis und die Bildung sauerstoffhaltiger funktioneller Gruppen auf der Oberfläche wie beispielsweise C-O (Hydroxyl, Ether), O-C=O (Säuren, Ester) und C=O (Aldehyde, Ketone) nach der Plasmabehandlung nachgewiesen werden. Die Wasserkontaktwinkelmessungen bestätigten, dass diese polaren Gruppen eine Hydrophilisierung der Oberfläche bewirken. Bereits nach einer Sekunde Plasmabehandlung wurde die Benetzbarkeit von hydrophoben Polymeroberflächen verbessert. Analog zu den Untersuchungen zur Inaktivierung von Mikroorganismen konnte gezeigt werden, dass die Gaszusammensetzung und der Abstand des Plasmas zur Substratoberfläche die Plasma-Oberflächen-Wechselwirkungen beeinflussen. Beispielsweise wurde durch die

Zumischung von Sauerstoff zum Ar-Plasma nochmals eine Verringerung des Wasserkontaktwinkels im Vergleich zur Wirkung reinen Ar-Plasmas bei einigen Polymeren erreicht. Die Variation des Substratabstandes ergab, dass die beobachteten Effekte mit zunehmendem Abstand abnehmen. Die erhobenen Daten zeigten insgesamt, dass auch diese Oberflächenfunktionalisierungen im erheblichen Maße auf die Wirkung von im Plasma generierten ROS zurückzuführen sind. Bei längeren Behandlungszeiten ( $> 60$  s) wurde darüber hinaus eine Änderung in der Topografie mittels Rasterkraftmikroskopie (AFM) festgestellt und eine Zunahme der Rauheit in Abhängigkeit von der Plasmabehandlung gemessen, was darauf hindeutet, dass es einen Übergang zwischen plasmabasierter Oberflächenfunktionalisierung und beginnenden Ätzeffekten gibt.

Im Gegensatz zu meist eher unerwünschtem makroskopischem Materialabtrag im Ergebnis der Sterilisation bzw. Dekontamination von Polymermaterialien durch Atmosphärendruckplasma kann die Erzeugung plasmachemischer Oberflächenfunktionalisierungen zur Steuerung der Adhäsion von Zellen oder Biomolekülen auf Biomaterialien genutzt werden. Untersuchungen zum Zellwachstum von humanen Osteoblasten (MG-63) auf den plasmamodifizierten Oberflächen zeigten keinen negativen Einfluss auf die Bioverträglichkeit. Weiterhin war im Vergleich zu der unbehandelten Oberfläche eine verbesserte Zellausbreitung nach der Plasmabehandlung zu sehen.

Letztendlich bewirkt die entsprechende Wahl der Plasma-Prozessparameter sowohl eine Inaktivierung bzw. einen Abtrag von Mikroorganismen als auch eine gezielte Veränderung der Oberflächeneigenschaften des Materials, die für die anschließende biomedizinische Verwendung des Materials durchaus vorteilhaft sein kann.

## Summary

The biological decontamination and sterilization is a crucial processing step in producing and reprocessing of medical devices. Since polymer-based materials are increasingly used for the production of medical devices, the application of conventional sterilization processes are restricted to a certain extent. Conventional sterilization techniques on the basis of high temperatures, toxic gases, or ionizing radiation can be detrimental to the functionality and performance of polymeric materials. For this reason, alternative, gentle, and efficient decontamination processes are required. One possible approach is the use of non-thermal physical plasmas. Especially atmospheric pressure plasma is receiving great interest due to the absence of vacuum systems which is highly attractive for the practical applicability. Its mechanisms of action enable the efficient killing and inactivation of micro-organisms which are attributed to the interaction of plasma-generated reactive oxygen and nitrogen species (ROS, RNS) as well as plasma-emitted (V)UV radiation. Owing to the moderate gas temperatures (near or at room temperature) so-called “cold plasmas” are well-suitable for the treatment of heat-sensitive materials, such as polymers, without affecting their bulk properties.

The present work focuses on the investigation of atmospheric pressure plasma processes for the biological decontamination of polymers. The objective is to help elucidate on the one hand the impact of varied plasma process parameters on the inactivation of micro-organisms and on the other hand the influence of plasma on the surface properties of the substrate. The investigations were performed by means of a high-frequency driven plasma jet (from the product line “kINPen”) operated with argon (Ar) and argon-oxygen (Ar/O<sub>2</sub>) mixtures.

Three main aspects were analyzed:

1. The effect of plasma on the viability of micro-organisms dependent on working gas, treatment time, and the sample distance (distance between the jet nozzle and the substrate).
2. The plasma-based removal of microbial biofilms.
3. The effects of the plasma treatment on the surface properties of selected polymers.

For the studies on the efficiency of Ar-plasma and Ar/O<sub>2</sub>-plasma on the inactivation of micro-organisms, *Bacillus atrophaeus* spores were used which are highly resistant against conventional sterilization methods due to their protective layer composed of coat proteins. Furthermore, spores are commonly used as bioindicator in the validation of sterilization processes. Polymer strips (polyethylene and polystyrene) were punctually contaminated with a spore suspension, dried, and subsequently exposed to plasma. It was shown that the choice of the process gas determines the efficient reduction of the contamination. Hence, the admixture of molecular oxygen led to a remarkable increase of the lethal effect as compared to Ar-plasma only. The admixture of 1 vol% oxygen resulted in 4 log<sub>10</sub>-reduction of the colony forming units after 300 s plasma treatment. Furthermore, it was

shown that with increasing jet-nozzle-to-substrate distance the lethal effect of plasma was reduced.

Since the bactericidal effect of plasma is attributed to plasma-generated ROS and/or RNS as well as (V)UV radiation, optical emission spectroscopy (OES) was applied to identify plasma-excited species. Based on these measurements it was possible to show a correlation between the lethal effect of plasma and the applied process parameters by varying the process gas and the jet-nozzle-to-substrate distance. The antimicrobial effect of oxygen-containing plasmas is mainly explained by the formation of ROS. The emission spectrum of pure Ar-plasma was mainly dominated by emission lines of hydroxyl radicals (at  $\lambda = 308$  nm), the second positive system of nitrogen (at  $\lambda = 337$  nm) and emission lines of argon (in the range of  $\lambda = 700$ -900 nm), while in the OES spectrum of Ar/O<sub>2</sub>-plasma high intensities of emission lines of atomic oxygen were detected (at  $\lambda = 777$  nm and  $\lambda = 844$  nm). The decrease of the bactericidal effect with increasing jet-nozzle-to-substrate distance is assigned to the depletion of short-lived reactive species in ambient air. Therefore, with increasing distance to the gas discharge less reactive species are left in reaching the substrate surface which was confirmed by the decrease in the intensity of the emission lines of excited plasma species in the OES spectra of the two working gases.

Plasma causes not only an inactivation of micro-organisms but initiates the removal of biological material, too. In a proof of principle 7 day old biofilms of *Candida albicans* were treated with Ar-plasma and Ar/O<sub>2</sub>-plasma. The detection of the biofilm removal was documented by using a light microscope. In agreement with the aforementioned results of the inactivation experiments, Ar/O<sub>2</sub>-plasma was most effective in biofilm removal in comparison to pure Ar-plasma. Hence, a complete removal of biofilms was achieved after 300 s Ar/O<sub>2</sub>-plasma treatment with an oxygen admixture of 1 vol%. Consequently, it has been concluded that both, inactivation of micro-organisms and removal of micro-organisms is generally based on the same mechanisms.

To gain insight into the mechanisms of the plasma-based biofilm removal, synthetic aliphatic and aromatic polymers were used as model surfaces for biological cell compounds. Analogous to synthetic polymers, micro-organisms are mainly composed of aliphatic and aromatic hydrocarbon compounds, as well as various amounts of oxygen and nitrogen groups. The investigations were focused on the following synthetic polymers: polyethylene, poly(methyl methacrylate), polystyrene, polypropylene, polycarbonate, and poly(ether ether ketone). The etching effect of plasma on these polymers was studied whereas the determination of the etching rate, as well as the elucidation of the etching mechanism was in the focus of interest. The etching rate was estimated quantitatively by the determination of the mass loss and by measuring the etched surface profile by stylus profilometry after plasma treatment. For the investigated polymers etching rates of 50 nm/s up to 300 nm/s were calculated after Ar/O<sub>2</sub>-plasma treatment (1 vol% O<sub>2</sub>). The measured surface profiles showed that Ar-plasma initiates material erosion but, this occurred mainly adjacent to the active plasma zone, where an admixture of ambient air takes place. The oxygen-containing ambient air can be excited and dissociated by the plasma, resulting in the etching of the polymer surface. In contrast, the direct admixture of molecular oxygen to the Ar gas flow led to an increased etching effect and further, it was observed that the etching

process occurred directly on-axis of the jet, thus in the plasma zone. Measurements of the atomic oxygen density in the gas discharge plasma were realized by using two-photon laser-induced fluorescence spectroscopy (TALIF) which revealed a correlation between the amount of added oxygen and the efficiency of the etching process. It was shown that with increased admixture of oxygen, from 0 to 1.5 vol%, the density of atomic oxygen was increased. Furthermore, a proportional relationship between the etched mass and the oxygen density was found. Hence, it could be clearly demonstrated that oxygen species generated in the plasma are responsible for the etching process.

Consequently, by using polymers, which present chemical and structural analogies to cell compounds of micro-organisms or biofilms and which are used for the production of medical devices, it was demonstrated that the desired antimicrobial effect and biofilm removal as well as usually undesired material erosion are based on substantially identical reactive plasma components and mechanisms. These findings are therefore to be considered in the control of plasma-based sterilization and decontamination methods of polymeric materials.

Substantial erosion of the plasma-exposed substrate can be avoided by the choice of the plasma process parameters, but during the plasma exposure the substrate to be decontaminated is still subjected to the bombardment of reactive plasma species which can interact with the substrate's surface in different ways. For this reason, a further aspect of this work was to investigate the influence of the plasma treatment on characteristic surface properties of the polymers. In particular, changes in the wettability, in the chemical composition, and in the topography of the surface dependent on varied process parameters were studied. Detailed insights into plasma-based alteration of surface properties were obtained by surface analytical studies on the chemical composition using X-ray photoelectron spectroscopy (XPS). XPS analyses of untreated and plasma-treated polymers revealed a higher oxygen/carbon ratio and the formation of oxygen-containing functional groups on the surface, including C-O (hydroxyl, ether), O-C=O (acids, esters), and C=O (aldehyde, ketone), after plasma treatment. Water contact angle measurements confirmed that these polar groups cause a hydrophilicity of the surface. Even after a second plasma treatment, the wettability of hydrophobic polymer surfaces was improved. In agreement with the studies concerning the inactivation of micro-organisms, it was shown that the gas composition and the distance of the plasma to the substrate affect the plasma-surface interactions. For example, by adding molecular oxygen a further reduction in water contact angle was achieved for several polymers compared to the effect of Ar-plasma only. Furthermore, the variation of the jet-nozzle-to-substrate distance showed that the observed surface effects decline with increasing distance. Besides surface functionalization processes, changes in the topography with prolonged plasma treatment time (> 60 s) were observed, too. By applying atomic force microscopy (AFM) an increase in surface roughness as a function of plasma treatment was shown which indicates that a well-defined boundary between surface functionalization and surface etching exists.

In contrast to undesired macroscopic material erosion which might be initiated by plasma-based sterilization and decontamination processes, the generation of plasma-chemical surface modifications can be used to control the adhesion of cells or bio-

molecules on biomaterials. Cell growth of human osteoblasts (MG-63) was examined on plasma-modified surfaces which revealed no negative influence on the biocompatibility. Moreover, plasma-treated surfaces led to an improved cell proliferation in comparison to untreated surfaces.

Summarizing, a careful choice of plasma process parameters results in both, the inactivation/removal of micro-organisms and the tailoring of the surface properties which can be beneficial for subsequent biomedical application of the material.



# 1 Non-thermal Plasma

Non-thermal plasmas have reached considerable importance in various plasma processing applications due to its ability to provide enhanced gas phase chemistry with high concentrations of chemically active species without the need for elevated gas temperatures [1]. Accordingly, cold gas discharge plasmas are highly attractive in fields where moderate temperatures are required such as in material processing and biomedical applications [2]. Plasma technology has been used for industrial application since the 1970s [3]. Especially low-pressure plasma processes have been applied in the microelectronic and semiconductor market. In recent years a lot of efforts have been made in the development of plasma sources, new types of excitation and further, the interest in plasmas operating at atmospheric pressure plasma was continuously growing [4]. The progress in newly designed plasma sources and novel plasma-specific applications opened up new research areas and further, obtained more interests in industrial fields and in the field of life sciences related to biomedical applications [5].

## 1.1 Introduction

Physical plasma is (partially) ionized gas which is also referred to as the fourth state of matter, the most prevalent state of matter (99% of the apparent universe is in the plasma state). It is composed of photons, electrons, positive and negative ions, atoms, free radicals and excited or non-excited molecules [4]. Plasma is a quasi-neutral particle system (in macroscopic dimension) exhibiting a collective behavior due to long-range Coulomb interactions [6]. Plasmas are generated at low, atmospheric, and high pressure. The presence of free electric charges (electrons and ions) is responsible for the electrical conductivity of plasma and the strong response to electromagnetic fields. From the historical viewpoint, Sir William Crookes identified plasma as “radiant matter” in 1879. But the term “plasma” for ionized gas was first used by Irving Langmuir in 1928 related to blood plasma which carries red and white corpuscles like an electrified fluid carries electrons and ions [7]:

*“...the ionized gas contains ions and electrons in about equal numbers so that the resultant space charge is very small. We shall use the name **plasma** to describe this region containing balanced charges of ions and electrons.”*

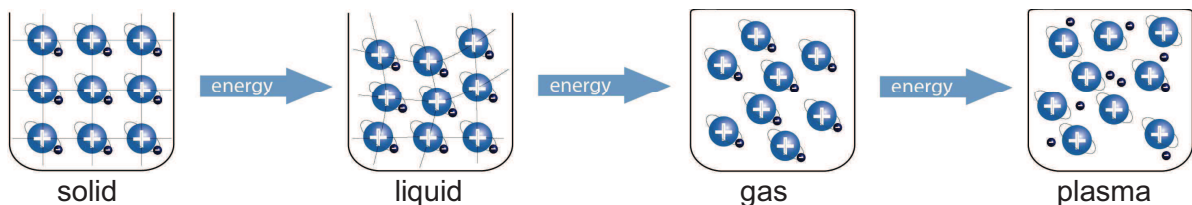


**Figure 1.1: Matter can exist in several states.** The most common states are known as solid, liquid, gas, and plasma. The supply of energy affects the motion of molecules. As the energy of the moving molecules overcomes the molecular attraction forces, the matter will change its state from solid to liquid to gas. When the energy supply proceeds intense collision processes among the constituents occur. The atoms themselves begin to break down: electrons are stripped from their orbit causing the atom to become a positively charged ion. The resulting mixture of neutral atoms, free electrons, and charged ions is called plasma.

The fourth state of matter results from progressively provided energy to matter for the transition from the solid to the liquid up to the gas state as schematically shown in Fig. 1.1. By supplying further energy, gas is converted into plasma when the energy is sufficient to ionize atoms of the gas [3, 8]. In laboratories plasma is generated by coupling energy to a gaseous medium through thermal energy or by applying voltage or by injecting electromagnetic radiation [9]. In terms of electron density and temperature ( $T_e$ : electron temperature,  $T_{ion}$ : ion temperature,  $T_{gas}$ : gas temperature) plasmas are generally divided into two main groups: high-temperature plasmas and low-temperature plasmas. Low-temperature plasmas are further subdivided into thermal plasma and non-thermal plasma. The typical classification of different kinds of plasmas and an overview of the main characteristics are presented in Tab. 1.1.

**Table 1.1: Plasma classification according to [4] and [9].**

Plasma	Characteristics	Example
<b>High temperature plasma</b> (equilibrium plasma)	$T_e \approx T_{ion} \approx T_{gas} = 10^6 - 10^8 \text{ K}$ electron density: $\geq 10^{20} \text{ m}^{-3}$	fusion plasma
<b>Low-temperature plasma</b>		
Thermal plasma (local equilibrium plasma)	$T_e \approx T_{ion} \approx T_{gas} \leq 2 \cdot 10^4 \text{ K}$ electron density: $10^{21} - 10^{26} \text{ m}^{-3}$	Arc plasma, plasma torches
Non-thermal plasma (non-equilibrium plasma)	$T_e \gg T_{ion}$ $T_e \leq 10^5 \text{ K}$ ( $\approx 10 \text{ eV}$ ) $T_{ion} \approx T_{gas} \approx 300 - 10^3 \text{ K}$ electron density: $< 10^{19} \text{ m}^{-3}$	glow discharge, corona, barrier discharge

Species produced in high-temperature plasmas are in thermal equilibrium, hence electrons and heavy ions have high temperatures. In case of low-temperature plasmas, thermal plasmas are characterized by the same electron and gas temperature which is based on elastic collisions between electrons and heavy particles (ions, molecules, and atoms). The energy of electrons is consumed by the heavy particles which results in heating of them. Thermal plasmas are characterized by an almost local thermodynamic equilibrium between electrons and heavy particles. For non-thermal plasmas the electron temperature is remarkable higher compared to the ion and neutral gas temperature. This temperature difference depends on the collision rate between electrons among themselves and with heavy particles. Due to the small kinetic transfer in elastic collisions between electrons and heavy particles the electrons energy remains high [10]. Consequently, non-thermal plasmas do not present a local thermodynamic equilibrium. Since the neutral gas temperature remains near or at room temperature, non-thermal plasmas are often referred to as “cold plasmas” [11]. Regarding the different neutral gas temperatures, thermal plasmas are used for application where heat is required, for instance for welding, cutting, or spraying. In contrast, non-thermal plasmas are applied for processes where high temperatures need to be avoided, such as for surface processing of heat-sensitive materials [12].

In the gas discharge very complex physical and chemical processes occur simultaneously which are described by means of various elementary processes [13]. The reactivity of plasma is reached by ionization of particles. Hence, for the generation of plasma the



ionization of neutral atoms and/or molecules of the medium is the key process [13]. Ionization occurs by collisions of energetic particles, by ionizing radiation, or by the impact of electric fields on electrons. The degree of ionization is defined as the density of the charged particles in the plasma. High-temperature plasma is completely ionized plasma; the ionization degree is close to unity. Plasma is called partially ionized when the ionization degree is low. Hence, the total density of charged particles is lower than the total density of neutral species which is the case in non-thermal plasma (degree of ionization:  $10^{-6}$ - $10^{-4}$ ) [14]. In non-thermal plasmas the energy required for chemical reactions is mainly transferred by the electrons. They transfer the energy provided by the external electric field to the gaseous medium. Due to their low mass electrons are easily accelerated and absorb the largest amount of the applied energy. This energy is transferred through collisions to the molecules of the gas initiating their ionization and dissociation. Collisions between electrons and heavy particles can be either elastic or inelastic. In terms of elastic collisions the internal energies of colliding particles do not change. Hence, this type of collision does not result in excitation of heavy particles. Inelastic collisions are characterized by energy transfer from the kinetic energy of electrons to internal energy of heavy particles leaving the heavy particle in an excited or ionized state. Hence, the electrons excite the gas molecules to higher energy levels by losing their own energy. Due to the short lifetime of the excited species photons are emitted on their transition to the ground state (the excitation – relaxation process is responsible for the glow).

The basic feature of generating non-thermal plasmas is that the electrical energy is mainly used for the production of energetic electrons without heating the gaseous medium. To generate and sustain non-thermal plasmas the input of electrical power is necessary for dissociation and excitation of atoms and molecules with subsequent production of radicals and metastable molecular states. This is achieved by various electric power sources operating at alternating current (AC) or direct current (DC), low frequency ( $\sim 50$  kHz) or high frequency including radio frequency (RF) and microwave ( $\sim 2.45$  GHz). Furthermore, according to the possibility to ignite plasma in a broad spectrum of gas pressure, reaching from low-pressure to atmospheric pressure ( $0.1 \dots 10^6$  Pa), different types of gas discharges can be obtained. All these different methods of applying the gas discharge power enable a wide variety of types of plasmas. Depending on the mechanism used for the generation of non-thermal plasma it can be distinguished between the following discharges: glow discharge, capacitively coupled plasma, inductively coupled plasma generated at low-pressure as well as corona discharge, dielectric barrier discharge, plasma jet operating at atmospheric pressure [15].

Since non-thermal plasmas provide a high reaction chemistry at low gas temperatures they are of particular importance for technological and biomedical application. Plasma-emitted species are sources of energy which induce chemical reactions in the plasma itself as well as at the interface on surfaces. The appropriate choice of operating conditions (process gas, energy input, and reactor geometry) leads to specific technological and biomedical process applications [16]. Hereinafter gas discharge modes well-suited for biomedical application including material processing and bio-decontamination are shown. Furthermore, the approaches to generate plasmas presented below were chosen because

of their extensive use for bio-decontamination and industrial processes. Since the subjects of this thesis are non-thermal plasmas operating at atmospheric pressure, the section about low-pressure plasma is only briefly discussed.

## 1.2 Low-pressure plasma

Gas discharges generated at reduced pressure are referred to as low-pressure plasmas. A number of researches related to surface modification are focused on low-pressure gas discharges which led to the development of a number of low-pressure gas discharges over the past. Low-pressure plasmas are of great interest in fundamental research as well as in microelectronic industry and material processing (e.g. for surface etching and surface coating) [17]. This type of plasma is associated with a low density of atoms in the gas phase and hence, with low collision rates among the plasma-generated species due to the long mean free paths between electrons and heavy particles which inhibit electrons to transfer their energy to the gas. For the generation of low-pressure plasma vacuum systems are required which in fact implies long pump down times but enables the production of large-scaled uniform plasma processes with a well-controlled and stable plasma chemistry [4]. Hence, various plasma-assisted processing techniques are intensively used to design substrate surfaces by grafting chemical functionalities. These techniques cover the range from plasma functionalization/modification over thin-film deposition in plasma polymerization up to chemical micro-patterning [18].

The characteristics of this type of gas discharge plasma are controlled by utilizing the proper reactor architecture and operating parameters including discharge frequency, delivered power, choice of the working gas or gas mixture and its flow rate, and the gas pressure [19]. For surface treatment different setups are used: (I) for the capacitively coupled RF discharge two electrodes are mounted into a vacuum chamber where the process gas is introduced with a typical pressure of some Pascal. (II) Another setup uses a MW excitation where no electrodes are necessary and a higher degree of ionization can be achieved compared to the RF excitation. (III) Also a combination of these two setups can be applied which is called “mixed” (or dual-) frequency plasma [20].

Besides surface modification processes low-pressure plasmas are successfully applied for bio-decontamination of surfaces (e.g. medical devices, pharmaceutical packing and filling), too [21, 22]. Further, in 1990s two sterilizing processes were commercialized using low-pressure plasma technology, namely Sterrad® and Plazlyte® Sterilization System [23]. Nevertheless, both systems are not plasma-based but rather plasma-assisted because gas mixtures that contain components with germicidal properties (e.g.  $\text{H}_2\text{O}_2$ , aldehyde) are used before gas discharge ignition. Plasma-based decontamination processes use non-toxic gas mixtures (for instance Ar,  $\text{H}_2$ ,  $\text{O}_2$ ,  $\text{N}_2$ , air etc.) which produce reactive species and (V)UV radiation at relatively low temperatures [24]. Hence, in many studies and reviews different potential mechanisms of its action have been shown which led to the commercialization of plasma sterilization reactors operating only with non-toxic gases [25].

As already stated, low-pressure plasmas are fundamental processes in plasma technology but suffer some drawbacks too. Because of the need of vacuum systems low-

pressure plasmas are highly expensive, time-consuming, and require high maintenance. Furthermore, the size of the objects to be plasma-treated is limited by the size of the vacuum chamber. Therefore, plasma sources operating at atmospheric pressure are in focus of interest due to the economical and operational advantages. Furthermore, for objects that cannot be easily evacuated, e.g. substrates with huge amount of adsorbed material and moisture, low-pressure plasmas are not practicable and additionally, it is more and more desirable that plasma can be ignited and sustain in open air suited for the treatment of living material (e.g. tissue) or liquids [26].

### 1.3 Atmospheric pressure plasma

In comparison to low-pressure plasma, atmospheric pressure plasma operates in the open air, hence at atmospheric pressure. For this reason, this type of plasma is very attractive for various industrial applications because of its potential of fast and efficient in-line processing fabrication without the need of expensive vacuum equipment. Hence, technological atmospheric-pressure plasmas including arc plasma, atmospheric-pressure glow discharge (APGD), corona, and dielectric barrier discharge are used in a wide variety for industrial processes such as surface modification of polymers [27]. However, since working in ambient air often includes the influence of species of the surrounding air on the gas discharge, the plasma phase chemistry is not as well-controlled as compared to low-pressure plasma.

To generate non-thermal atmospheric pressure plasmas different principles for the energy input from diverse sources have been developed (e.g. corona discharge, dielectric barrier discharge, atmospheric pressure plasma jet, and the plasma needle). In the following section two setups for the generation of non-thermal atmospheric pressure plasma applied in this work for decontamination of micro-organisms are presented. Both gas discharge modes are suitable plasma sources for the generation of cold plasma at atmospheric pressure. These types of gas discharges provide room temperature conditions, the possibility for different geometrical shapes of experimental arrangements and for scaling-up to large dimensions.

#### 1.3.1 Dielectric barrier discharge (DBD) (applied in publication 5.6)

The characteristic of the dielectric barrier discharge is that at least one of the electrodes is covered by a thin layer of dielectric or highly resistive material (made of glass, quartz, ceramic, polymers or other materials of low dielectric loss and high breakdown strength) [28]. This gas discharge is typically generated between two electrodes commonly driven by a HF electric current (in the kHz range). DBDs mostly generate micro-discharges (filamentary mode) which appear randomly between the electrodes. Under special conditions there exists a diffuse (glow-like) mode, too, which is also called atmospheric pressure glow discharge (APGD). The dielectric layer is responsible for proper function of this type of gas discharge [14]. Due to charge accumulation on the dielectric surface an electrical potential is created which opposes the applied voltage and, hence, limits the discharge current and impede the glow to arc transition [29]. Additionally, it facilitates the distribution of the micro-discharges over the complete electrode. The DBD is also referred to as the

silent discharge due to the absence of sparks, which are characterized by local overheating, generation of local shock waves and noise [30]. DBDs are intensively applied for industrial processes such as in ozone generation, in CO<sub>2</sub> lasers, as source for VUV/UV radiation, and for surface treatment to improve wettability and adhesion [31]. Furthermore, for recent years dielectric barrier discharges are investigated for biomedical application e.g. treatment of skin diseases [32]. Depending on the applied process gas and voltage the distance of the electrodes varies between micrometers and centimeters [33]. The DBD operates in a wide range of configurations e.g. volume discharge, surface discharge, and coplanar or planar discharge schematically shown in Fig. 1.2.

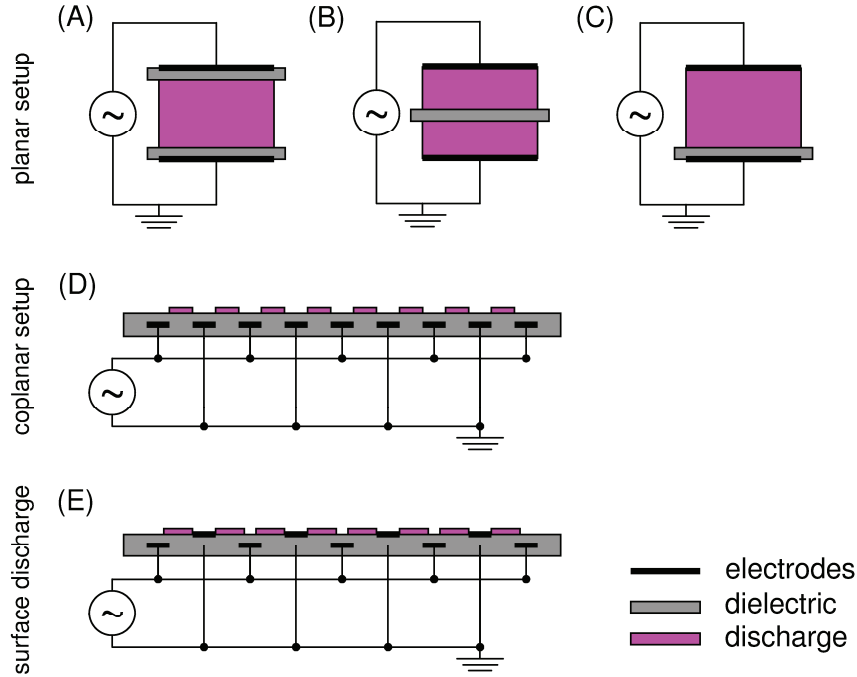


**Figure 1.2: Setups for DBD.** Planar configuration: (A) dielectric layer on both electrodes, (B) dielectric in the discharge, and (C) dielectric layer on one electrode. (D) Coplanar arrangement where the electrodes are embedded in the dielectric. (E) Surface discharge with only one electrode embedded in the dielectric (according to [33]).

There are two basic configurations of DBDs: firstly, the volume DBD where the object to be treated serves as the second electrode [32, 34] and secondly, the surface DBD which is characterized by two electrodes in direct contact with the dielectric where the plasma is generated around the electrodes. If both electrodes are embedded in the dielectric a coplanar configuration is present. In this setup the plasma is produced at the dielectric, too. In the set-up of the surface DBD and the coplanar dielectric barrier discharge the object to be treated is not part of the electrode arrangement. All these mentioned gas discharges can be applied for surface treatment of non-living and living material. Owing to the effortless discharge ignition nearly every combination of gases can be applied and further, due to the low gas flow (down to 100 standard cubic centimeters (sccm) and less) these plasma sources are highly attractive [33]. Also the versatile electrode configurations which enable an excellent adaptability (even over several meters a homogeneous discharge can be generated) is very advantageous.

### 1.3.2 Atmospheric pressure plasma jet (applied in publication 5.1 - 5.5)

Cold atmospheric pressure plasma jets generate stable gas discharges for surface modification of heat-sensitive materials, inactivation of micro-organisms, and recently, for direct application on living surfaces. Atmospheric pressure plasma jets can be operated with different gases including noble gases (e.g. helium, argon) with gas flow rates up to some standard liters per minute (slm) and small admixtures of reactive gases (e.g. nitrogen or oxygen). The plasma characteristics depend on the jet configuration and electrical excitation and therefore, differ considerably [1, 35]. The wide spectrum covers dc jets, kilohertz frequency pulsed and sinusoidal jets, radio frequency and microwave excited jets [35]. In general, atmospheric pressure plasma jets consist of two electrodes in different arrangements [33]. Figure 1.3 shows a schematic of the atmospheric pressure plasma jet applied for the studies in publication 5.1-5.5. This jet has been developed by the Leibniz Institute for Plasma Science and Technology (INP Greifswald e.V.) and is called kINPen®.

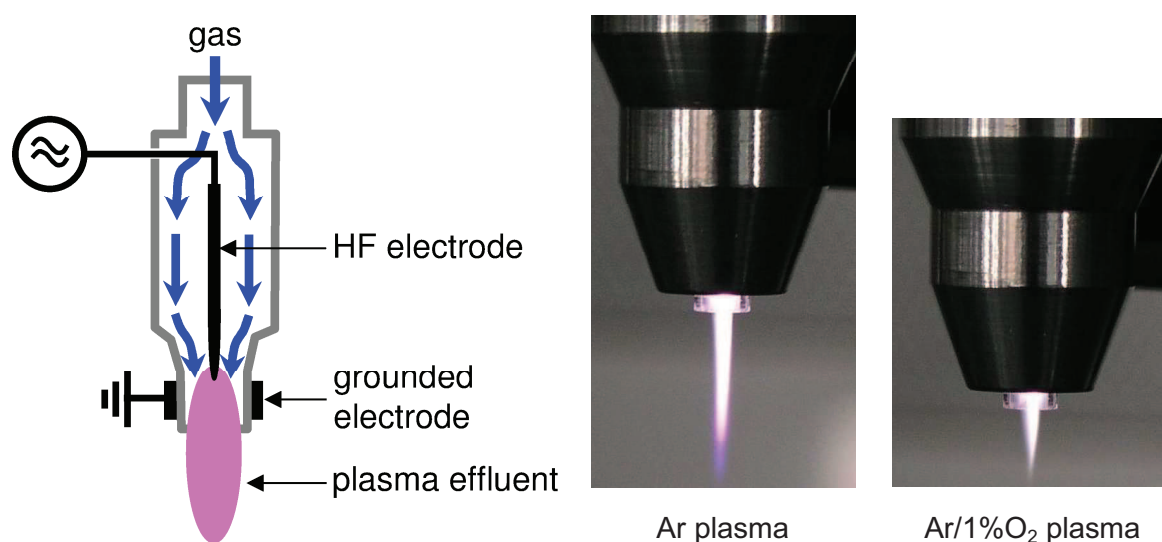


**Figure 1.3: Atmospheric Pressure Plasma Jet.** Left: Schematic setup of the plasma jet (according to [32]). Photograph of Ar plasma jet (effluent length of 12 mm) and Ar/1%O<sub>2</sub> plasma jet (effluent length of 6 mm).

The inner rod electrode is coupled to high frequency power (1.1-1.8 MHz). The operating gas flows between the outer grounded and the inner electrode. The gas discharge is ignited from the top of the central pin-type electrode (1 mm diameter) where electrons are produced by applying HF power. The electrons interact with gas molecules via inelastic collisions. On this way generated high velocity plasma effluent expands to the surrounding air outside the jet nozzle. Depending on the process gas the jet effluent reaches a length of up to 12 mm (Fig. 1.3). During the gas discharge ions and electrons undergo recombination processes, but the flowing effluent still contains metastable species and radicals which interact with the non-living or living material. The neutral gas temperature is about 330 K (measured at the tip of the plasma effluent) which is determined by the high gas flow and the low power consumption. By means of special electrical input signals (burst mode: alternating plasma on and plasma off periods) a further decrease in gas temperature can be achieved down to room temperature [36]. Due to the small plasma dimensions the treatment area of plasma jets is restricted in the range of a few millimeters for localized applications. But this is also the main advantage of plasma jets in combination with



the treatment of narrow gaps or cavities difficult to access. Hence, atmospheric pressure plasma jets exhibit an excellent ability to penetrate into small structures which is beneficial for the precise treatment of micro-structures such as capillaries or, for biomedical application, e.g. root canals [37]. If large-area treatment is required different arrangements can be applied which consist of several plasma jets which can also be adapted to special geometries [32].

## 2 Non-thermal Plasma in Biology and Medicine

Non-thermal plasmas have reached many breakthroughs in the field of biology and medicine by combining a broad interdisciplinary research on physics, biology, chemistry, medicine, and engineering. Although at the beginning of the application of non-thermal plasmas for biomedical purposes low-pressure plasmas were in the focused of interests, new possibilities arose from the development of plasma devices which operate stable at atmospheric pressure close to ambient temperature. The development of dielectric barrier discharges and non-thermal plasma jets opened up new application possibilities of physical plasmas. A recent emerging activity is the application of plasma in health care which leads to the formation of a new field titled “Plasma Medicine” [38]:

*“Recent demonstrations of plasma technology in the treatment of living cells, tissues, and organs are creating a new field at the intersection of plasma science and technology with biology and medicine – Plasma Medicine.”*

Non-thermal plasmas are efficient in providing highly reactive species to initiate complex biochemical processes leading to physical and chemical modifications of non-living surfaces and biological matter [2]. By adjusting the process parameters (e.g. process gas, source of input energy, frequency) the amount and type of plasma-generated components can be controlled. This enables a variety of combinations of reactive chemical species to create a desired effect. Especially the effect of plasma on biological systems is of importance. Recently, three different research areas related to biomedical and clinical purposes have been developed which are summarized in the field Plasma medicine: plasma-based bio-decontamination/sterilization, plasma-assisted modification of biomaterials, and the direct plasma interaction with living systems for therapeutic approaches (e.g. plasma treatment of wounds) [39]. The development of non-thermal atmospheric pressure plasmas in 1990s set initial focus on the research field of bio-decontamination procedures [40]. Therefore, cold atmospheric pressure plasma sources and their antimicrobial activity on various microorganisms have been intensively studied which is also the main topic in this thesis.

### 2.1 Plasma-based bio-decontamination and sterilization

The major drawbacks of conventional sterilization techniques using dry heat (oven), moist heat (autoclave), or chemicals like gaseous ethylene oxide or hydrogen peroxide are the high processing temperature, the long-time treatment, the use of toxic chemicals which can remain on the surface after the process and thus, constitute an unacceptable risk. Furthermore, high temperatures can damage the material which affect adversely their

quality and shorten their lifetime. Another sterilization process is the application of gamma or electron-beam irradiation which may implicate changes in the bulk of the material being treated and further, requires high security equipment [41]. The mentioned limitations of the traditional sterilization techniques and the case that several materials and equipments such as polymer-based goods are incompatible towards conventional sterilization techniques have encouraged the development of alternative methods like plasma treatment. Atmospheric pressure plasmas are able to inactivate many different types of micro-organisms such as bacteria and fungi. Hence, their capability for clinical application has attracted much attention. According to the moderate gas temperature of non-thermal plasmas (near or at room temperature) this technology enables the treatment of temperature-sensitive non-living materials like polymers. Additionally, recent plasma bio-decontamination research is devoted to living systems like biological tissue to reduce microbial load and to enhance the healing process [42]. Furthermore, non-thermal plasmas facilitate not only bio-decontamination of diverse materials but also the removal of dead cells and organic compounds [43-45].

### 2.1.1 Mechanism of bio-decontamination

The idea of using non-thermal plasma for sterilization arose by Menashi *et al.* in 1968 who patented a corona-based plasma sterilization system [46]. Thenceforth, a lot of experiments have been carried out to prove the antimicrobial effect with different plasma sources and extensive literature and reviews can be found devoted to this topic [33, 47, 48]. It has been shown, that the germicidal effect of plasma is very specific. For the determination of the efficacy of decontamination processes the technology is tested against model organisms such as bacterial spores. Spores of *Bacillus spp.* are very resistant to many treatments including harsh chemicals, UV radiation, wet and dry heat. Therefore, these spores have been used as biological indicator for biological decontamination and/or sterilization processes [49]. The high level of bacterial spore resistance is owing to the spore's structure and chemical composition. For instance the thick proteinaceous coat and the inner membrane serve as protective barrier characterized by very low permeability to hydrophilic molecules which provides protection against toxic chemicals [50].

In general, to evaluate the lethal effect of plasma on micro-organisms the most widely used method is the determination of survival curves. Survival curves are usually depicted as semi-logarithmic plots of the number of viable micro-organisms as a function of the treatment time. Those provided after plasma treatment often display curves with different shapes (multi-slope survival curves) indicating a time-dependent killing but with different time constants within the inactivation process. A schematic illustration of a two-slope survival curve is shown in Fig. 2.1.

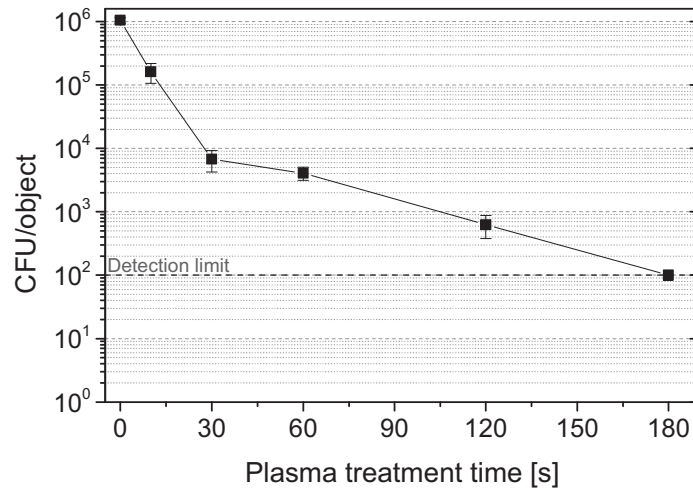


**Figure 2.1: Inactivation kinetic:** Example of a two-slope survival curve of *Bacillus atrophaeus* spores immobilized on polyethylene strips exposed to Ar/O<sub>2</sub> atmospheric pressure plasma.

The inactivation curve is composed of two successive lines with different slopes. The first phase is characterized by a fast inactivation, followed by a much slower inactivation. The multi-slope inactivation curves can be explained as follows: the first phase of inactivation is initiated by plasma-emitted species reacting with the outer membrane of isolated micro-organisms or of the first layers of stacked micro-organisms resulting in damaging [51]. In the next phase the inactivation is slower according to the shielded micro-organisms which results in a decreased inactivation efficacy [52]. Furthermore, impinging plasma-generated species (e.g. atomic oxygen, hydroxyl radicals) lead to erosion of micro-organisms. The micro-organisms in the upper layers are eroded and the species reach the biological material of those below. This observed biphasic inactivation curve illustrates, that the inactivation of micro-organisms by plasma processes is different from those obtained after conventional sterilization processes which usually exhibits an exponential function of time.

In the literature different terms are used to describe the inactivation/killing of micro-organisms. It can be distinguished between biological decontamination (bio-decontamination) and sterilization. *Bio-decontamination* means the general inactivation or removal of biological compounds (micro-organisms, fungi, viruses, and pyrogens) [53]. The term *sterilization* was defined by the pharmacopoeias as the complete absence of viable micro-organisms including viruses whereas a sterility assurance level (SAL) of  $10^{-6}$  is accepted for pharmacopoeial sterilization procedures. [54]. In other words, the SAL value indicates a probability of not more than one viable micro-organism in one million sterilized items of the final product. Hence, sterility requirements are based on the conventional SAL concept. Because the inactivation curves obtained after plasma treatment are different, alternative concepts such as “tiered sterility assurance levels” have been suggested [55]. Furthermore, concerning microbiological safety a differentiation in pharmaceutical sterilization (SAL =  $10^{-6}$ ), high-level sterilization (SAL =  $10^{-4}$ ), low-level sterilization (SAL =  $10^{-3}$ ) - all designated for heat-resistant materials -, and the proof of antimicrobial efficacy on the highest experimentally accessible level for heat-sensitive devices has been proposed [53].



Several scientists have shown that the shape of inactivation curves depends on the type of micro-organisms, the applied gas compositions, and the location of the samples during the plasma treatment (direct treatment: samples are in direct contact with the plasma, remote treatment: samples are located away from the discharge volume or in a second chamber) which reveal the complexity of both, plasma-based processes and biology. The observed differences in inactivation mechanisms of micro-organisms can be attributed for instance to the fact that bacteria differ in their cell wall. Gram-positive bacteria (*Staphylococcus aureus*) are characterized by a thicker cell wall than that of Gram-negative bacteria (*Escherichia coli*). These differences in cell-wall structure influence the lethal effect of plasma. Therefore, non-thermal plasma is more effective against Gram-negative than Gram-positive bacteria [56].

### 2.1.2 Impact of plasma agents on micro-organisms

For the bio-decontamination or sterilization of surfaces several plasma species, such as (V)UV photons, charged particles, neutral (radicals), heat, and electromagnetic fields are considered to interact with bacterial cells. Figure 2.2 summarizes the microbicidal plasma species and shows their impact on micro-organisms.

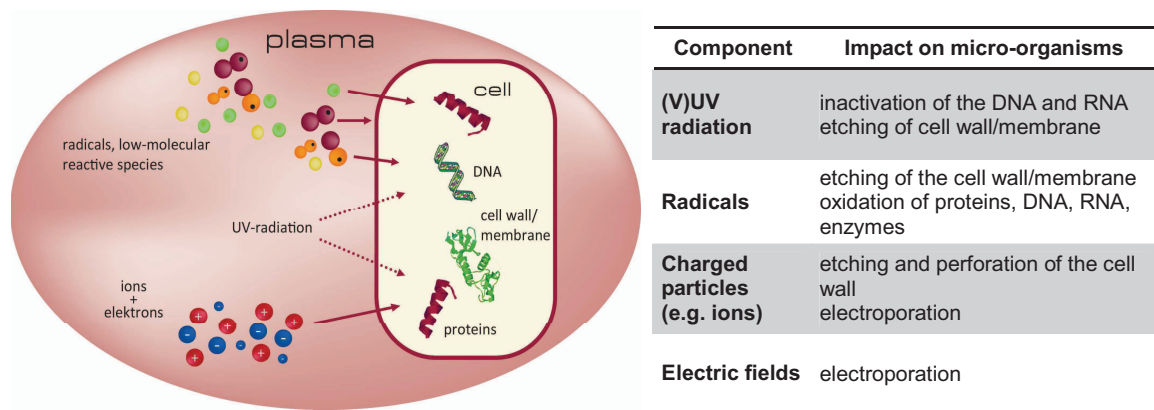


**Figure 2.2: Schematic illustration of plasma-emitted biologically active components:** Interaction between plasma components and cell.

- VUV and UV radiation

Plasma emits UV radiation with different wavelengths ( $\lambda = 200\text{--}400\text{ nm}$ ). UVC in the range of 200–290 nm is known for its lethal effect on micro-organisms and is the most damaging type of UV radiation. Especially in low-pressure plasmas the content of UV photons can be considerable high. The absorption of UV photons through cellular macro molecules results in impairment of the DNA, proteins, and lipids which is based on changes in the cellular redox state (oxidative stress) [57]. The direct UV radiation leads to the modification of the DNA and to agglomeration of protein- and peptide-chains. The main effect of UV photons is the dimerization of thymine bases in bacterial DNA strands. This disturbs the helical structure which inhibits the replication and transcription of bacteria cells [23]. Furthermore, the energetic photons initiate the generation of intracellular reactive species causing oxidative degradation of lipids and DNA. Also photo-induced etching has to be considered resulting in bacteria killing [58].

Depending on the process gas it is further possible that photons in the vacuum ultraviolet spectral range (VUV,  $\lambda = 110\text{-}200\text{ nm}$ ) are emanated from the plasma. Due to the high energy of VUV photons the photodesorption and erosion effect can eventually be enhanced which in turns results in a strong antimicrobial activity [59].

- Reactive species (radicals)

Depending on the process gas various chemically reactive species are generated including  $\text{NO}^\bullet$ ,  $\text{NO}_2^\bullet$ ,  $\text{O}^\bullet$ ,  $\text{O}_2^-$ ,  $\text{O}_3$ ,  $\text{O}_2^{\bullet-}$ ,  $\text{ONOO}^-$ , and  $\text{HO}^\bullet$  which make a significant contribution to the inactivation of micro-organisms [60]. Reactive oxygen species (ROS) and reactive nitrogen species (RNS) have a strong oxidizing effect on cell structures. This oxidizing effect damages organic molecules such as lipids and amino acids. Produced ozone is known to interfere with the respiration system of cells. Furthermore, ozone can react with organic double bonds initiating the generation of ROS. Also the presence of moisture contributes to the germicidal effect of plasma, due to the generation of hydroxyl radicals ( $\text{HO}^\bullet$ ) which was reported by several authors [61]. The cell membrane is a lipid double layer comprised of saturated and unsaturated fatty acids providing the characteristic gel-like structure [62]. Based on the semi-permeability, one of the most important characteristics of the membrane is its function as diffusion barrier.  $\text{HO}^\bullet$  attacks unsaturated fatty acids to initiate lipid peroxidation which influences the barrier function of the membrane [63] in such a way that the infiltration of plasma-generated ROS and RNS can be increased. In the case of RNS,  $\text{NO}^\bullet$  and  $\text{NO}_2^\bullet$  influence the metabolic pathway causing inactivation of micro-organisms, too.

- Charged particles

Charged particles are considered to initiate rupture of the outer membrane of bacterial cells. The charge accumulation on the outer surface induces electrostatic forces which overcome the tensile strength of the membrane leading to rupture. For instance Laroussi *et al.* observed morphological changes of *E. coli* after plasma exposure and postulated that the smaller the radius of the micro-organism the stronger the electrostatic force [23].

- Electric fields

Pulses of electric fields are able to control membrane transport processes and function of cells. Local electric fields can initiate electroporation which can enhance the invasion of plasma-generated ROS or RNS in the cell. Consequently, the impact of high electric fields leads to irreversible damage of the membrane [64].

- Heat

Since non-thermal plasmas can be operated at relatively low temperatures ( $\leq 50^\circ\text{C}$ ) no substantial thermal effects on bacterial cells are expected. Hence, heat is not the major contributor to the inactivation process especially if bacterial spores, e.g. endospores of *Bacillus atrophaeus*, are used as test organisms which are known to be very resistant against heat.

---

**Publication 5.1: On the Use of Atmospheric Pressure Plasma for the Bio-Decontamination of Polymers and Its Impact on Their Chemical and Morphological Surface Properties – Part I**

---

The first part of this publication demonstrates the plasma-based bio-decontamination efficiency of the atmospheric pressure plasma jet operated with argon and different admixtures of molecular oxygen. Plasma inactivation kinetics of *Bacillus atrophaeus* spores revealed a maximum reduction of viable number of micro-organisms after 180 s argon oxygen (with an admixture of 1 vol% oxygen) plasma exposure. The dependence of the lethal effect on the applied process gas was studied by varying the admixture of molecular oxygen. Furthermore, the influence of the distance between the jet-nozzle and the substrate on inactivation effect was examined. In summary, it is shown that reactive oxygen species emanated from the gas discharge play a determinative role in non-thermal plasma bio-decontamination.

---

**2.1.3 Removal/etching of micro-organisms and biofilms**

Another aspect of bio-decontamination of objects and in current focus of interest is the degradation of biomolecules (e.g. protein, lipids) and removal of pathogens from surfaces by using gas discharges. Surgical instruments and medical devices are contaminated by residual micro-organisms and infectious biomolecules after cleaning process [65]. Biological remnants (dead bacteria) or pyrogenic substances (constituent parts of bacterial cell walls causing fever) are capable to entertain inflammatory processes in the adjacent tissues. Hence, for clinical practice the elimination of harmful organic substances and biomolecules from surfaces that are in direct contact with the patient is of importance. This includes most of all surfaces of reused medical equipment like endoscopes, surgical instruments, or dental tools. Since present sterilization processes are insufficient in completely removing resistant and infectious biomolecules, e.g. prions, from surfaces, non-thermal plasmas represent an alternative method by providing a rich gas-phase chemistry capable for the erosion of micro-organisms and biomolecules under atmospheric pressure as well as low-pressure conditions [22, 66].

A further issue which should be considered is that most studies elucidating the lethal effect of plasma are based on using free living bacteria (planktonic cells). But the predominant appearance of microbes attached to inert or living surfaces, in natural as well as in clinical environments, is their growth in microbial communities, known as biofilms [67]. Moreover, micro-organisms aggregated in biofilms are the source of most persistent infections [67]. Biofilms are composed of many bacteria cells embedded in a self-made matrix comprising different extracellular produced substances including proteins, nucleic acid, and polysaccharides, resulting in the formation of a multilayer structure of several micrometers. These extracellular polymeric substances provide to a certain degree resistance toward high doses of antibiotics and increase the tolerance toward host immune defense [68]. Consequently, it is more difficult to kill cells in the form of biofilms than in the form of individual cells and longer plasma treatment times are often required for an efficient inactivation of biofilms [69, 70]. Biofilms can be found on artificial surfaces in oral cavities

(denture or implants) and further, are a serious problem in the pathogenesis of chronic wound infections [44, 71]. Hence, microbes are involved in a number of implant-related biofilm infections (e.g. nosocomial infections caused by a variety of bacteria and fungi) and non-device-related chronic infections.

By tailoring the chemistry of the plasma gas phase, through appropriate tuning of the process parameters, the inactivation as well as the etching effectiveness of the gas discharge on microbes and biomolecules can be optimized. In this way, it is possible to inactivate bacterial cells by the diffusion of plasma-emitted species into the biofilm and to erode and to remove organic compounds at the same time. Additionally, when the architecture of the biofilm is damaged it is conceivable that the plasma-generated species infiltrate deeper into the biofilm which facilitates the detachment of biofilm fragments or loosely packed bacterial clusters [72].

---

#### **Publication 5.2: Atmospheric Pressure Plasma: A high-performance tool for the efficient removal of biofilms**

So far, little is reported on the application of atmospheric pressure plasma for etching of complex biological systems (e.g. biofilms). In this publication the removal of a 7-day old *Candida albicans* biofilm by means of the atmospheric pressure plasma jet is demonstrated quantitatively by microscopically analysis. The biofilm-forming *Candida albicans* was chosen since Candidiasis, caused by *Candida* species, is the most common fungal infection in humans.

The optimal plasma conditions for the most effective biofilm removal were investigated by comparing different process gases and treatment times. In particular, the influence of Ar plasma and Ar + 1 vol% O<sub>2</sub> admixture on the etching efficacy was studied. It is shown that an almost complete elimination of biofilm was achieved by adding molecular oxygen to the argon gas discharge. Furthermore, the estimation of the biofilm thickness before and after plasma exposure enabled the calculation of etching rates which was found to be in the range of 33 - 67 nm/s. Since the plasma device used in this study can be further developed for clinical use, plasma jets might be an effective tool in medicine for bacterial inactivation and the removal of organic compounds.

---

Summarizing, gas discharges can be successively applied to remove biomolecules from surfaces. However, the interaction mechanisms between plasma and biomolecules are not yet fully understood but are mandatory to elucidate for proper functioning of the plasma procedure. In general, micro-organisms are composed of several natural polymers including proteins, lipids, and hydrocarbon-like compounds [73]. Hence, for understanding the fundamental reaction processes of plasma-based etching of micro-organisms and biomolecules representative synthetic polymers can be used as model constituents for microbial cells. Polymers are macromolecules composed of repeating units which are linked by covalent bonds [74]. They are subdivided into aliphatic and aromatic polymers. Aliphatic polymers are characterized by linear or branched chain molecules which are saturated (called alkanes) or unsaturated (called alkenes or alkynes) whereas aromatic

polymers are composed of ring-shaped structures like phenyl rings. Micro-organisms are composed of aliphatic and aromatic structures, too. Moreover, the surface chemical composition of micro-organisms, deduced from XPS data, reveals that micro-organisms mainly consist of carbon, oxygen, and nitrogen. In detail, for different strains (Gram-positive, Gram-negative, and yeast strains) and species the ratio of oxygen to carbon varies between 0.2 and 0.6 whereas the nitrogen to carbon ratio are found to be between 0.03 and 0.2 [73]. Additionally, deduced from the elemental composition and peak fitting procedures information on the functional groups can be obtained which are indicative of the structural cell surface features [75]. Hence, the analysis of functional groups enables a rough attribution to the three major classes of cell compounds (proteins and peptides, sugars and polysaccharides, and lipids) where each is characterized by limited number of chemical functions [75]. As provided by XPS, the elemental composition of synthetic polymers is in some way comparable to cell components of micro-organisms which was already discussed by Pelletier *et al.* as referenced in [76]. Therefore, using synthetic polymers as reference material for cell compounds enables the investigation of the impact of chemically active plasma species on polymeric substances dependent on their elemental composition and chemical structure. Furthermore, it allows a detailed study on the etching mechanism including the determination of etching rates.

---

**Publication 5.3: High Rate etching of Polymers by Means of an Atmospheric Pressure Plasma Jet**

In this study, the etching efficacy of the atmospheric pressure plasma jet on different polymers (polyethylene, polypropylene, poly(methyl methacrylate), polystyrene, polycarbonate, poly(ether ether ketone), and cellulose) is investigated. Polymeric materials were exposed to pure argon and argon/oxygen plasma. The influence of oxygen admixture (up to 1 vol%) and jet-nozzle to substrate distance on etching rates was studied. Two strategies were applied for the determination of the etching rates: 1. calculation of the mass difference by weighing and 2. by measuring the surface etching profile after plasma treatment. The experiments showed that reactive oxygen species play an important role in the polymer removal which results in etching rates of 50 nm/s up to 300 nm/s depending on the polymeric material.

---

Despite intensive investigations about the surface properties, detailed knowledge of the plasma chemistry is required too, in order to understand the reactions occurring between plasma and plasma-exposed surfaces. Based on these information and in combination with various surface analysis techniques more information on plasma-initiated surface reactions can be obtained. Moreover, the extent of plasma-initiated surface processes depends strongly on the species of the applied plasma source. For this purpose different non-invasive plasma diagnostic tools can be applied for the characterization of the gas phase. Among the different diagnostic techniques, optical plasma diagnostic methods have the advantage that the gas discharge remains undisturbed [77]. Hence, optical emission spectroscopy (OES) and two-photon absorption laser-induced fluorescence (TALIF) spectroscopy are widely used to determine the plasma properties. OES gives



direct access only to excited particles in the visible and the (V)UV spectral range. This technique offers high spatial and temporal resolution. In the measured optical emission spectra the intensity of excited species is depicted as function of the wavelength. Deduced from these spectra information on the type of the excited particles in the plasma can be obtained and further, the rotation and vibration temperatures can be calculated [78]. Quantitative determination of individual particle densities and fluxes can be received by using TALIF spectroscopy [79].

As previously stated, the germicidal effect of atmospheric pressure plasmas has been proven for several process gases where a fast inactivation was mainly achieved by using or admixing reactive process gases like oxygen, nitrogen, or air [33]. In the experiments mentioned above (publication 5.1-5.3) several indications were found that plasma-generated oxygen species are key-role species having a dominant influence in both, the inactivation of micro-organisms and in the plasma-polymer interactions. Hence, TALIF measurements can be applied to obtain information on the atomic ground state density of oxygen and to get an insight into plasma chemistry [80].

---

#### ***Publication 5.4: Investigation of Surface Etching of Poly(ether ether ketone) by Atmospheric Pressure Plasmas***

An atmospheric pressure argon plasma jet with varying admixtures of molecular oxygen was used to study the etching mechanism of poly(ether ether ketone) (PEEK). Spatial atomic oxygen density profiles of the gas discharge are investigated by TALIF spectroscopy and compared to the etching surface profiles of PEEK. Furthermore, a correlation between plasma-based etching processes on PEEK with the generation of chemically reactive plasma species is proposed. In detail, the dependence of the atomic oxygen density on different gas mixtures and axial distances as well as its correlation to the etching efficiency was examined. The results exhibited an increased density of atomic oxygen with increasing admixture of molecular oxygen with an oxygen density up to  $1.75 \times 10^{15} \text{ cm}^{-3}$  and a lower oxygen density with increased distance to the jet effluent. Analogous to these results an increased etching behavior with increasing admixture of oxygen was observed. Hence, a linear behavior between etching and oxygen density was proven. Furthermore, a comparison of the shape of the depth profile and the radial profile of the oxygen density showed that the radial depth profiles nearly followed the radial evolution of the oxygen density. Deduced from these results it can be concluded that the etching process is proportional to the processes involved in the generation of reactive oxygen species.

---

#### **2.1.4 Bio-decontamination of polymers**

For the fabrication of medical/therapy devices, disposables, and packaging material polymers are used or at least are part of the final product. The intensive application of polymers for biomedical purposes is based on the number of advantageous properties, such as processability, recyclability, mechanical properties, and low cost. Hence, a wide variety of polymers are applied as artificial biomaterials including polyethylene (PE), poly-

styrene (PS), poly(methyl methacrylate) (PMMA), polyvinyl alcohol (PVA), polycarbonate (PC), poly(ether ether ketone) (PEEK). A number of polymers and its biomedical applications are listed in Tab. 2.1.

**Table 2.1 Biomedical applications of polymers (according to [81]).**

<b>Polymer</b>	<b>Biomedical application</b>
Polyethylene	Tubes, catheters
Polypropylene	Part of medical devices, blood transfusion bags
Poly(methyl methacrylate)	Dentures, contact lenses, bone cement
Polycarbonate	Blood pumps, syringes, arterial tubules, hard-tissue replacement, surgical instruments
Polystyrene	Disposal, cell culture material
Poly(tetrafluoroethylene)	Vascular and auditory prostheses, tubes, catheters
Polyurethane	Dental materials, blood-contacting devices, artificial heart
Poly(ether ether ketone)	Orthopedic and spinal implants
Polyester	Vascular grafts, resorbable system

Owing to their sensitive properties (for instance sensitive to heat) gentle non-thermal bio-decontamination procedures are required. But, plasma-emitted species are carrying a large amount of energy which can be transferred to the plasma-exposed surface. Hence, polymeric materials or medical devices composed of polymers that are bio-decontaminated by plasma-based processes are exposed to the same reactive species and the same plasma-initiated processes. Consequently, abiotic surfaces exposed to plasma can also undergo changes in the surface properties. Especially plasma in contact with polymers can result in physico-chemical and topological modifications at the surface like the generation of reactive sites or changes in cross-linking. For the modified polymer surface altered properties, such as wettability, adhesion, and biocompatibility have to be considered, too.

---

***Publication 5.1: On the Use of Atmospheric Pressure Plasma for the Bio-Decontamination of Polymers and Its Impact on Their Chemical and Morphological Surface Properties – Part II***

---

The second part of this publication exhibits the influence of gas discharges on the surface properties of polyethylene and polystyrene. The changes in the physico-chemical surface properties (wettability and elemental composition) and the surface topology for different process gases were examined. For the given plasma conditions, both polymers showed an improved wettability. The chemical composition, analyzed by XPS, showed an incorporation of oxygen and the formation of oxygen-containing functional groups. The surface topography was studied by means of atomic force microscopy which revealed for instance the formation of a spike-like texture after plasma treatment. Hence, depending on the process gas different surface properties have been observed.

---

Finally, the results, presented in publication 5.1-5.4, have confirmed that the inactivation of micro-organisms as well as their plasma-initiated removal is mostly based on reactive

oxygen species while using atmospheric pressure argon or argon-oxygen plasma. Additionally, synthetic polymers used for modeling bacterial cell components for the investigation of the degradation process of biological matter by plasma, have shown, that atmospheric pressure plasma is capable to affect the surface properties of plasma-exposed polymers intensively. Hence, in terms of the safety of the surface properties of the material to be decontaminated, finding the balance between the inactivation of microorganisms and the modification of surface properties is a difficult task. Certainly, a combination of the lethal effect and the alteration of surface properties by applying plasma are not necessarily detrimental. For instance, many conventional synthetic polymers and natural polymers (e.g. cellulose) have to be equipped with surface properties for specific biomedical application, since the presence or absence of functional groups at the polymer surface determine its response to the environment.

Therefore, an overview of potential plasma-polymer-interactions is given in the following chapter which has to be considered when atmospheric pressure plasmas are applied for the bio-decontamination of polymeric surfaces.

## 2.2 Interaction between plasma/gaseous phase and polymer

Polymers exposed to plasma are subjected to a continuous bombardment by plasma-generated species. Moreover, in non-polymerizing gas discharges many processes occur simultaneously with complex synergetic manner leading to different surface interactions, schematically shown in Fig. 2.3 (according to [82]).

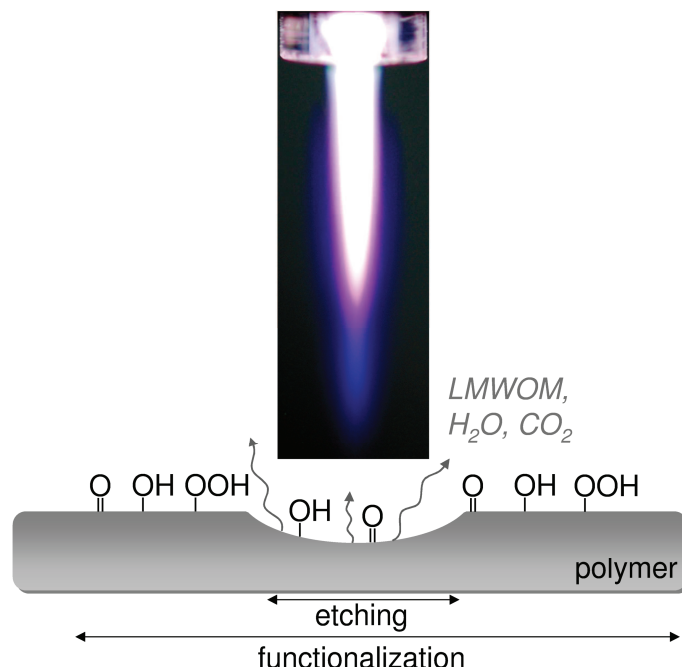


**Figure 2.3:** Schematic representation of changes in surface properties of plasma-exposed polymers: Plasma-induced functionalization and etching processes by means of the atmospheric pressure plasma jet. (LMWOM: low-molecular weight oxidized material)



It can be distinguished between:

- *Polymer etching*: Removal of material in chemical and/or physical ways from the surface or etching of the polymer surface with the release of volatile species and the formation of low-molecular weight oxidized material (LMWOM).
- *Cross-linking*: Cross-linking processes are mainly based on impinging (V)UV radiation and occur in the subsurface layer of the material.
- *Surface functionalization*: Impinging energetic particles break the covalent bonds at the surface which result in the formation of surface radicals. The latter react with plasma species to form functional groups at the surface. Typically gases used for surface functionalization are Ar, He, O<sub>2</sub>, N<sub>2</sub>, Air, and NH<sub>3</sub>.

In the following section the effect of plasma species on polymeric materials in terms of the different mentioned plasma-surface interactions are briefly outlined.

### 2.2.1 Surface etching

Polymers are very susceptible to degradation processes initiated by reactive plasma species during plasma treatment which results in the generation of volatile polymer fragments and the formation of non-volatile oligomers called low-molecular weight oxidized material (LMWOM) [83]. Commonly, intensive surface etching is not desirable for biomedical application because the degradation products can lead to the formation of a weak boundary layer on the treated surface which can have a detrimental effect on applications where good adhesion is required [84]. The extent of the generated LMWOM depends on the type of polymer and process conditions. Prolonged plasma treatment initiates stronger etching processes which result in the release of gaseous degradation products including CO<sub>2</sub>, CO, and H<sub>2</sub>O and further, initiates changes in the morphology/topology of the surface through plasma-based roughening. The extent of etching mainly depends on the chemical reactivity of the plasma gas and the type of polymer. For example, using oxygen plasma results in higher etching rates compared to argon plasma. With regard to the properties of the polymer etching processes appear differently according to the varying sensitivity of polymers [85]. For instance, amorphous structures are preferably etched whereas highly ordered (crystalline) regions are more resistant. Furthermore, etching processes are inhibited by the aromaticity of the polymers or by the tendency of polymers to undergo cross-linking processes during plasma exposure (e.g. PE) [27]. Cross-linkages produce structures of high densities which diminish etching reactions on the plasma-treated polymer, too. The presence of oxygen in the polymer backbone increases the etching effect [86]. However, plasma-induced surface etching influences the morphology and topology of the polymeric material which is shown in Fig. 2.4 for polymers of different chemical structure.

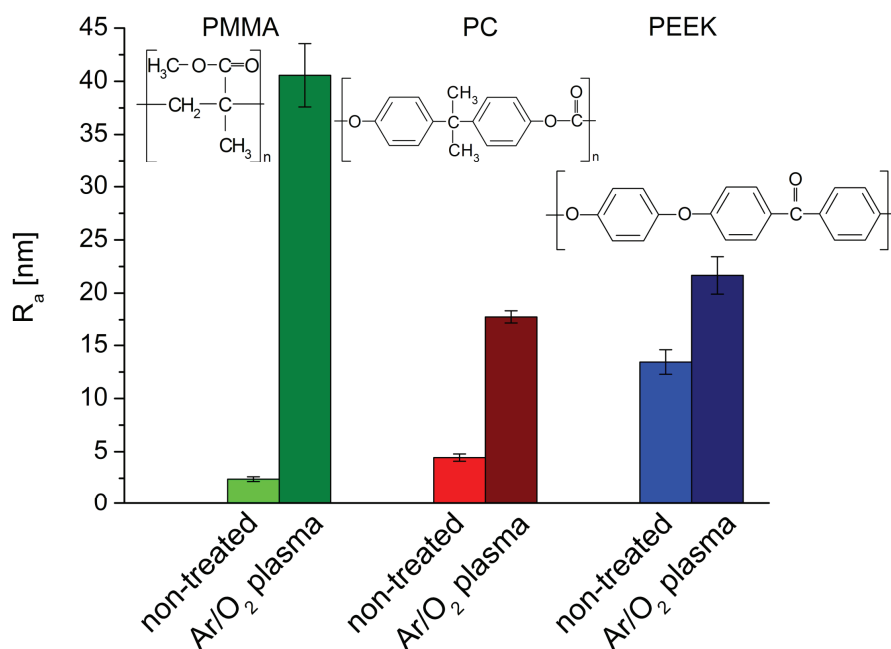


**Figure 2.4: Plasma-induced surfaces roughness:** Arithmetic roughness ( $R_a$ ) of non-treated polymers and of polymers exposed to argon-oxygen atmospheric pressure plasma (treatment time: 60 s) ( $10 \times 10 \mu\text{m}$ , mean  $\pm$  SD,  $n = 5$  each).

Consequently, plasma-etching results in an increased surface roughness in relation to the non-treated polymer. Furthermore, according to the different etching rates of the polymer (PMMA > PC > PEEK) the extent of plasma in changing the topology varies remarkably.

### 2.2.2 Cross-linking

Noble gas plasma species and VUV/UV photons can initiate surface cross-linking on a polymer which is characterized by the formation of links (covalent bonds) between the molecular chains [87, 88]. C-C and C-H  $\sigma$ -bonds in organic polymers absorb UV radiation between  $\lambda = 60\text{-}160 \text{ nm}$  (vacuum UV radiation) which can result in ionization and dissociation of chain molecules. Additionally, due to the electron transition in the  $\pi$ -electron system, e.g. in phenyl rings, UV absorption occurs between  $\lambda = 150\text{-}285 \text{ nm}$  in aromatic polymers. At  $\lambda < 200 \text{ nm}$  ( $> 6.2 \text{ eV}$ ) chain scissions in the polymer are most likely to occur which result in the formation of radical sites as well as in the formation of C=C double bonds [89]. Furthermore, VUV radiation results in cross-linking of the polymer, too. (V)UV photons are mainly emitted in low-pressure plasma by using noble gases, hydrogen, or oxygen. Since (V)UV radiation is highly energetic, the impact of these photons can be up to micrometers in depth of the surface layer depending on the wavelength and the absorption properties of the polymer [90]. A cross-linked surface yields a stable ordered structure with high density which acts like a barrier to the diffusion of molecules between the surface and the bulk and hence, limiting the random movement of the polymer chain [88]. For the stability of the surface properties a higher degree of cross linking can be beneficial.

However, in atmospheric pressure plasmas UV photons are only dominant under specific operation conditions. Nevertheless, the results obtained in this work revealed that UV

photons emitted by argon or argon-oxygen plasmas played a minor role in plasma-surface-interactions.

### 2.2.3 Surface modification/functionalization

Polymers, especially polyolefins, are chemically inert due to the absence of polar and reactive functional groups. Plasma-based surface modification of polymers is related to generate new functional groups on the surface (surface functionalization) which supply new surface properties. Plasma treatment mostly affects the wettability of the polymeric surface. Hence, changes in the water contact angle can be observed which is shown in Fig. 2.5.

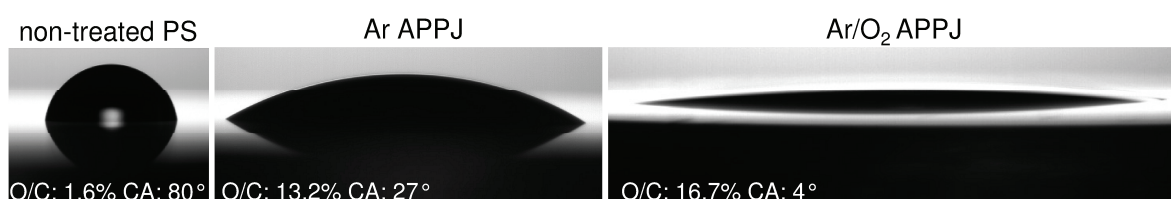


**Figure 2.5: Changes in the wetting properties after plasma exposure:** Wettability of non-treated PS and PS exposed to Ar and Ar/O<sub>2</sub> atmospheric pressure plasma (treatment time: 60 s). Also shown are the O/C ratios and the measured water contact angle (CA) before and after plasma exposure.

The wettability of the surface is determined by measuring the contact angle (CA) which is defined as the angle between the solid surface plane and the tangent of the liquid-vapor interface of a drop [91]. A comparison between the wettability of non-treated and plasma-treated polymer surfaces reveals an enhanced wetting behavior after plasma exposure (see Fig. 2.5). Furthermore, the corresponding data on the changes in the elemental composition, here expressed as the ratio of the oxygen content to the carbon content (O/C), exhibit that the wettability is enhanced with increased O/C ratio and thus, with increased oxygen-containing functionalities. Altered wetting properties result most of all from the modification of the chemical composition of the surface. This plasma-based surface functionalization is based on the continuous flow of energetic particles which initiates covalent bond breaking of the polymer surface. Some typical bonds for organic molecules and their dissociation energy are presented in Tab. 2.2.

**Table 2.2** Dissociation energies of different covalent bonds in organic molecules [27].

Type of bond	Dissociation energy [eV]
C-C/C-H	3.6 – 4.3
C=C in benzene	6.1
C=O	7.8
C-O	3.7
C-N	3.2
C=N	9.3

The high-energy tail of the electron energy distribution of plasma-emitted species and UV photons is in the range of several electron volts which is sufficient to react with the surface macromolecules or diffuse into the polymer surface, transferring their energy to

the polymer, leading to dissociation of chemical bonds in polymers [92]. Consequently, the impact of these species result in the formation of active reaction sites (i.e. surface radicals) used for surface grafting by incorporation of functional groups. This surface modification proceeds via H-abstraction or ablation of side-chains and attachment of atoms provided by the gas discharge to the surface radicals which is commonly accompanied by C-C bond scissions, too. Along with chain scissions of the polymer loosely bonded polymer fragments are created on the surface. Carbon radicals formed during plasma exposure recombine by forming cross-linkages, while neighboring carbon radicals produce C=C double bonds. Depending on the used gas a variety of plasma-formed functional groups are introduced on the polymer surface. For instance, applying oxygen plasma results in the formation of oxygen-containing groups such as hydroxyls, ketones, or carboxylic groups which can be determined by surface analytical techniques like X-ray photoelectron spectroscopy (XPS). XPS provides information about the quantitative and qualitative changes in the chemistry of the subsurface of materials exposed to plasma [90]. During XPS measurements X-rays impinge on the surface resulting in the emission of photoelectrons from the sample surface whose kinetic energy is measured. This energy is specific for each element which enables the identification of the elements (except hydrogen) present in the outer 10 nm of the surface. Additional to the chemical composition, XPS provides information on the chemical bonds of the surface. Therefore, high-energy resolution spectra of characteristics peaks of elements like, C 1s, N 1s, or O 1s are analyzed. From the binding energy of the peaks, used for the peakfit of the element spectrum, the chemical bonding can be identified by means of reference data from the literature [93]. Figure 2.6 exemplarily shows the highly-resolved measured C 1s peak including its peakfit of non-treated PS and PS exposed to atmospheric pressure Ar/O<sub>2</sub> plasma.

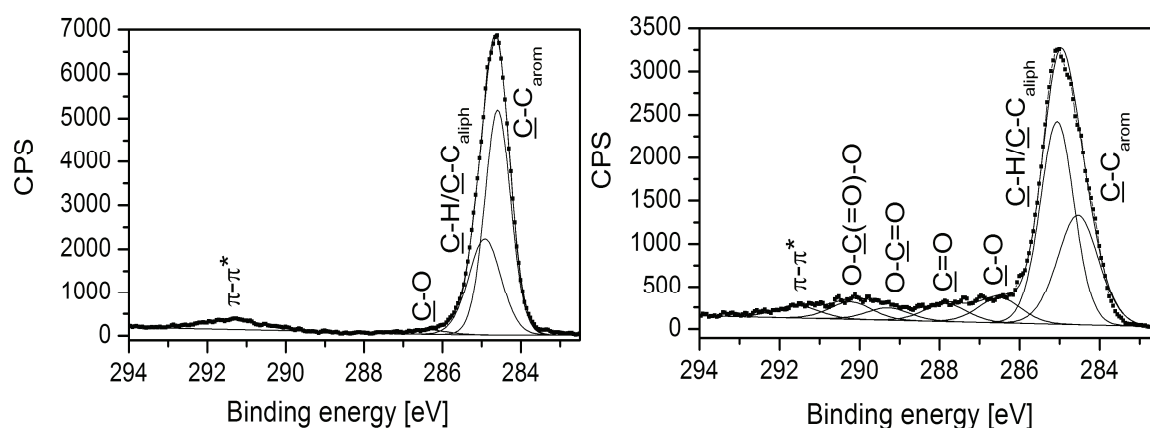


**Figure 2.6: Comparison of the chemical bindings of PS before and after plasma treatment:** Highly resolved C 1s peak of the XPS spectrum of (left) non-treated PS and (right) PS exposed to Ar/O<sub>2</sub> atmospheric pressure plasma (treatment time: 60 s).

As evident plasma treatment results in a broadening of the C 1s peak. The fitting procedures of the C 1s peak of non-treated PS and plasma-exposed PS revealed the formation of new groups assigned to different oxygen-containing functionalities after plasma treatment.

Surface functionalization occurs not only during the plasma treatment, any radicals that remain on the surface after plasma exposure can react with ambient air which results in

further incorporation of oxygen. Regarding the stability of the functionalized surface it has to be considered that the functionalization undergoes aging processes which result in a gradual decline of the prior incorporated functionalities through diffusion of those from the outermost layer to the bulk or by oxidation processes in ambient air. This thermodynamically driven mobility of functional groups is also called “hydrophobic recovery” which leads in some cases to the lost of beneficial functionalization after a few weeks [84].

However, a further limiting factor in the degree of surface functionalization and hence, the amount of incorporated functional groups is the plasma-induced degradation of the polymer. This can be observed by analyzing the influence of the plasma treatment time on the functionalization degree expressed as O/C ratio which is shown in Fig. 2.7.

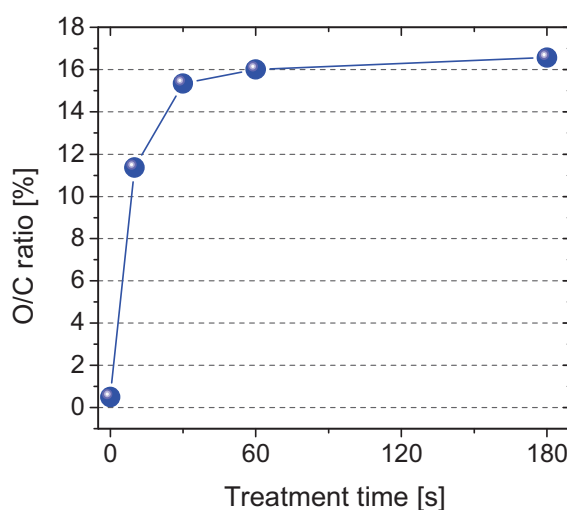


**Figure 2.7: Influence of the treatment time:** Development of the O/C ratio of PS exposed to Ar/O<sub>2</sub> atmospheric pressure plasma depending on the treatment time.

Figure 2.7 shows the exponential increase of the O/C ratio of polystyrene exposed to atmospheric pressure plasma. It is well known that with prolonged treatment time a plateau-like region in oxygen (or nitrogen if nitrogen-containing operating gases such as NH<sub>3</sub> are used) introduction is reached (constant modified surface layer). This steady state of functionalization is attributed to the transition of the modification into the etching process. Hence, in steady state both processes occur simultaneously. This can be explained as follows: Initial plasma-based oxidation occur on the topmost molecular layer of the surface. Afterwards the subjacent layers are oxidized successively with lower functionalization degree (Fig. 2.7: 30-60 s) whereas the topmost layer has reached the maximum O/C ratio [27]. Hence, further oxidation is accompanied by the release of CO<sub>2</sub>, H<sub>2</sub>O, and CO as well as the formation of LMWOM. Moreover, the prior functionalized surface can be destroyed by etching processes [94].

All these introduced changes in surface properties can be beneficial for further biomedical application. Moreover, different plasma-based surface treatment strategies have been developed to graft materials with desired and specific surface properties to overcome the poor adhesion properties of polymeric materials. In terms of plasma-based surface modification for biomedical applications, the intended aim is the grafting of surface either by incorporation of oxygen- or nitrogen-containing functionalities or by the deposition of func-



tional thin organic films to improve for instance the wettability, adhesion, and biocompatibility. Especially surface properties of materials that are used in medical devices or in contact with biological systems, i.e. biomaterials, are subject of the mentioned plasma processes.

### 2.3 Plasma-assisted surface modification of biomaterials for improved cell proliferation

Biomaterials are primarily used for medical applications which include materials that are used for devices designed to replace a part of a function of the human body (e.g. bone implants and dental implants), but they are also used to grow cells in culture or as disposables for biomedical diagnostics in the clinical laboratory [95]. The biocompatibility of these surfaces is of particular importance for cell attachment and proliferation which can be controlled by the material's surface properties whereas the surface chemistry and structure are considered to be the most determined factors [96]. Hence, polymers intended for biomedical application, must provide specific surface properties for proper functioning of medical devices and for the acceptance of implants. Therefore, in recent years plasma-assisted surface modification techniques received increasing interest and became an important topic for surface grafting of biomaterials [97]. Especially two plasma-based processes are most frequently applied: either surface functionalization or plasma polymerization (deposition of nanometer-thick films).

In terms of functionalization the plasma-treated surface is grafted with functional groups by using different gases or gas mixtures operating at low-pressure or at atmospheric pressure. Depending on the applied process gas the plasma-functionalized materials exhibit oxygen functional groups and/or nitrogen functional groups which result in enhanced cell attachment and cell growth [98]. Figure 2.8 exemplarily shows cell culture results of osteoblastic cells (MG-63) grown on non-treated polycarbonate and on ammonia plasma-treated polycarbonate.

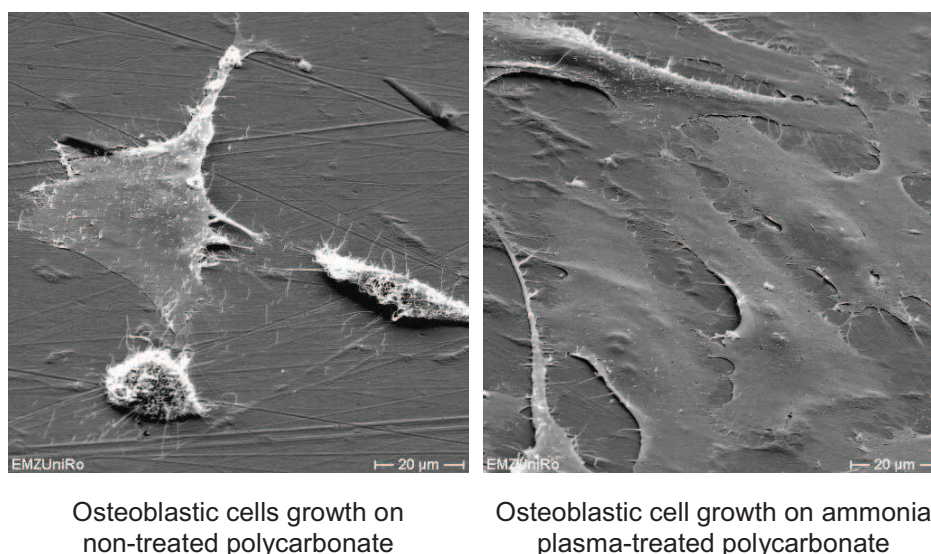


**Figure 2.8: Influence of surface properties on cell spreading behavior:** Osteoblastic cells (MG-63) cultivated for 24 h on polycarbonate (left) and plasma-treated polycarbonate (right). Surface treatment conditions: low-pressure microwave plasma (20 Pa, 2.45 GHz), 120 s treatment time.

Due to the hydrophobic and non-polar character of polycarbonate, cells are not well attached and well-spread on this surface. In contrast, plasma-treated polycarbonate results in alteration of the surface properties which improves cell attachment and cell growth.

Plasma polymerization is a well-suited method to prepare defined polymeric-like thin films predominantly on metals and ceramics, but also on polymeric materials. During the plasma enhanced chemical vapor deposition (PECVD) the organic monomer (precursor) undergoes dissociation and excitation with subsequent deposition and polymerization of the excited species on the substrate surface. In contrast to surface functionalization plasma polymerization allows the deposition of high densities of certain surface functionalities realized by the choice of precursor and by tuning processing conditions. Many investigations exist concerning plasma polymer films for biomedical application which are mainly obtained by applying low-pressure plasma [99]. But recently, promising atmospheric pressure plasma-assisted techniques have been reported [100]. However, for the thin-film deposition, intended for improved biocompatibility, different precursors are applied such as acrylic acid to increase the amount of carboxylate groups or a number of nitrogen-containing substances including allylamine or ethylenediamine providing high density of amino groups.

---

***Publication 5.5: Comparison of non-thermal Plasma Processes on the Surface Properties of Polystyrene and their Impact on Cell Growth***

---

Initial adhesion and spreading of cells are crucial factors for successful performance of synthetic biomaterial used for cell culture disposables or human medical devices (e.g. implants). Surface properties which allow the control of attachment of cells are decisive for the acceptance of the provided material. Hence, different surface preparation techniques are used to equip surfaces with functional groups to improve initial surface interactions. In this study polystyrene (PS) surfaces were modified by using different non-thermal plasma processes. In particular, low-pressure plasma and atmospheric pressure plasma were applied to modify surfaces or to deposit thin films on surfaces. Furthermore, the behavior of human osteoblastic cells with respect to cell viability and cell growth on differently plasma treated polystyrene surfaces are investigated. A comparison is made between plasma-grafted polystyrene and commercially available polystyrene – such as tissue culture PS (TCPS) and Primaria<sup>TM</sup>. The cell studies were accompanied by surface analysis comprising atomic force microscopy (AFM), determination of surface energies, and X-ray photoelectron spectroscopy (XPS) measurements. This work demonstrates that the functionalization of PS substrates by applying low-pressure and atmospheric pressure plasma processes are equally effective in improvement of cell attachment and proliferation. Furthermore, it is shown that the enhanced metabolic activity and spreading behavior of osteoblastic cells correlate with an increase in surface wettability and the introduction of polar oxygen- and/or nitrogen-containing functional groups after plasma treatment.

---

### 3 Outlook: Atmospheric Pressure Plasma for Bio-Decontamination of Living Surfaces

As previously shown it is quite feasible to use the atmospheric pressure plasma jet for an efficient inactivation of micro-organisms without causing substantial damage to the material's surface properties. Moreover, recent advances in the development of cold atmospheric pressure plasma sources (less than 40°C at the point of application) and their proven high antiseptic efficacy provide the possibility to extend plasma treatment to human or animal skin. In particular, the development of plasma sources operating at low power allowed the utilization of plasmas without causing thermal damage revealing a low risk connected with skin treatment which is of importance for a clinical setting [101]. Furthermore, the improvement of techniques for the production of stable plasmas at atmospheric pressure is essential for *in vivo* applications.

The bactericidal effect of non-thermal plasma can be used for instance for tissue where the use of chemicals for bio-decontamination possess a risk in damaging or for skin diseases where antibiotic resistant bacteria are encountered. Therefore, a prospective field of application will be therapies of infectious skin diseases like athlete's foot, yeast infections, or acne, where the skin is injured but the protective skin barrier is more or less intact [39]. Preliminary investigations concerning the biological decontamination of skin have been successfully applied with an atmospheric pressure plasma jet which is similar to that applied in this work [102]. Furthermore, neither damage to the skin barrier nor skin dryness has been determined after plasma treatment [103].

A further application might be its use for chronic wound disinfection as an addition or even alternative to antiseptic or antibiotic therapy. Hence, cold atmospheric plasma treatment of living tissue has become a popular topic in modern plasma physics and in medical sciences.

However, essential for the success of the application of non-thermal plasma on living surfaces in the future is a deeper fundamental understanding of the physics, chemistry, and biology of plasma-living tissue interaction. Moreover, to demonstrate a successful reduction in bacterial load on skin diseases, the implementation of clinical trials is mandatory. Additionally, the effect of plasma on the complete wound-healing process needs further investigations.

---

#### ***Publication 5.6: New non-thermal atmospheric pressure plasma sources for decontamination of human extremities***

The aim of this publication is to present two newly developed plasma sources, based on the principle of surface dielectric barrier discharges, and to show their potential application for the treatment of infectious skin diseases. Furthermore, an electrode arrangement directly applicable on human extremities is shown. The presented plasma sources are characterized by a good adaption on complex structured objects. The plasma parameters and composition and thus antimicrobial effects can be controlled by operation parameters and gas.



Both plasma sources operate in a moderate temperature range applicable for therapeutic utilization. The *in vitro* testing on micro-organisms exhibits promising results. Plasma inactivation kinetics of *E. coli*, *S. aureus*, and *C. albicans*, which were chosen as possible colonizer of skin and wounds, revealed lethal effects already after 60 s plasma exposure.

---

---



## 4 References

- [1] M. Laroussi, and T. Akan, "Arc-free atmospheric pressure cold plasma jets: A review," *Plasma Process. Polym.*, vol. 4, no. 9, pp. 777-788, 2007.
- [2] G. Y. Park, S. J. Park, M. Y. Choi, I. G. Koo, J. H. Byun, J. W. Hong, J. Y. Sim, G. J. Collins, and J. K. Lee, "Atmospheric-pressure plasma sources for biomedical applications," *Plasma Sources Sci. Technol.*, vol. 21, pp. 1-21, 2012.
- [3] R. d'Agostino, P. Favia, Y. Kawai, H. Ikegami, N. Sato, and F. Arefi-Khonsari, "Advanced Plasma Technology," Weinheim: Wiley-VCH Verlag GmbH & Co. KGaA, 2008
- [4] R. Hippler, H. Kersten, M. Schmidt, and K. H. Schoenbach, "Low Temperature Plasmas: Fundamentals, Technologies, and Techniques," Weinheim: Wiley VCH 2008
- [5] S. Samukawa, M. Hori, S. Rauf, K. Tachibana, P. Bruggeman, G. Kroesen, J. C. Whitehead, A. B. Murphy, A. F. Gutsol, S. Starikovskaia, U. Kortshagen, J. P. Boeuf, T. J. Sommerer, M. J. Kushner, U. Czarnetzki, and N. Mason, "The 2012 Plasma Roadmap," *J. Phys. D-Appl. Phys.*, vol. 45, no. 25, pp. 1-37, 2012.
- [6] M. Perucca, "Introduction to Plasma and Plasma Technology," *Plasma Technology for Hyperfunctional Surfaces*, H. Rauscher, M. Perucca and G. Buyle, eds., Weinheim: Wiley-VCH Verlag GmbH & co., 2010.
- [7] I. Langmuir, "Oscillations in ionized gases," *Proceedings of the National Academy of Sciences of the United States of America*, vol. 14, pp. 627-637, 1928.
- [8] H. Conrads, and M. Schmidt, "Plasma generation and plasma sources," *Plasma Sources Sci. Technol.*, vol. 9, no. 4, pp. 441-454, 2000.
- [9] C. Tendero, C. Tixier, P. Tristant, J. Desmaison, and P. Leprince, "Atmospheric pressure plasmas: A review," *Spectroc. Acta Pt. B-Atom. Spectr.*, vol. 61, no. 1, pp. 2-30, 2006.
- [10] J. Meichsner, "Low Temperature Plasmas," *Plasma Physics*, A. Dinklage, T. Klinger, G. Marx *et al.*, eds., Berlin Heidelberg: Springer, 2005.
- [11] K. H. Becker, U. Kogelschatz, K. H. Schoenbach, and R. J. Barker, "Non-equilibrium air plasmas at atmospheric pressure," London: IOP Publishing, 2005
- [12] A. Bogaerts, E. Neyts, R. Gijbels, and J. van der Mullen, "Gas discharge plasmas and their applications," *Spectroc. Acta Pt. B-Atom. Spectr.*, vol. 57, no. 4, pp. 609-658, 2002.
- [13] A. Fridman, *Plasma Chemistry*, New York: Cambridge University Press, 2008.
- [14] B. Eliasson, and U. Kogelschatz, "Nonequilibrium Volume Plasma Chemical Processing," *IEEE Trans. Plasma Sci.*, vol. 19, no. 6, pp. 1063-1077, 1991.
- [15] V. Nehra, A. Kumar, and H. K. Dwivedi, "Atmospheric Non-Thermal Plasma Sources," *Int. J. Eng.*, vol. 2, no. 1, pp. 53-68, 2008.
- [16] R. d'Agostino, P. Favia, C. Oehr, and M. R. Wertheimer, "Low-temperature plasma processing of materials: Past, present, and future," *Plasma Process. Polym.*, vol. 2, no. 1, pp. 7-15, 2005.
- [17] D. B. Graves, "Plasma Processing," *IEEE Trans. Plasma Sci.*, vol. 22, no. 1, pp. 31-42, 1994.
- [18] F. Hempel, H. Steffen, H. Busse, B. Finke, J. B. Nebe, A. Quade, H. Rebl, C. Bergemann, K.-D. Weltmann, and K. Schröder, "On the Application of Gas Discharge Plasmas for the Immobilization of Bioactive Molecules for Biomedical and Bioengineering Applications," *Biomedical Engineering - Frontiers and Challenges*, R. Fazel-Rezaei, ed., pp. 297-318: InTech, 2011.
- [19] L. Martinu, M. R. Wertheimer, and J. E. Klemberg-Sapieha, "Recent advances in plasma deposition of functional coatings on polymers," *Plasma Deposition and Treatment of Polymers*, W. W. Lee, R. D'Agostino and M. R. Wertheimer, eds.: Materials Research Society, 1999.
- [20] E. M. Liston, L. Martinu, and M. R. Wertheimer, "Plasma surface modification of polymers for improved adhesion: a critical review," *J. Adhes. Sci. Technol.*, vol. 7, no. 10, pp. 1091-1127, 1993.
- [21] F. Rossi, O. Kylian, H. Rauscher, M. Hasiwa, and D. Gilliland, "Low pressure plasma discharges for the sterilization and decontamination of surfaces," *New J. Phys.*, vol. 11, pp. 1-33, 2009.
- [22] A. von Keudell, P. Awakowicz, J. Benedikt, V. Raballand, A. Yanguas-Gil, J. Opretzka, C. Flotgen, R. Reuter, L. Byelykh, H. Halfmann, K. Stapelmann, B. Denis, J. Wunderlich, P. Muranyi, F. Rossi, O. Kylian, N. Hasiwa, A. Ruiz, H. Rauscher, L. Sirghi, E. Comoy, C. Dehen, L. Challier, and J. P. Deslys, "Inactivation of Bacteria and Biomolecules by Low-Pressure Plasma Discharges," *Plasma Process. Polym.*, vol. 7, no. 3-4, pp. 327-352, 2010.

- [23] M. Laroussi, "Low temperature plasma-based sterilization: Overview and state-of-the-art," *Plasma Process. Polym.*, vol. 2, no. 5, pp. 391-400, 2005.
- [24] F. Rossi, O. Kylian, and M. Hasiwa, "Decontamination of surfaces by low pressure plasma discharges," *Plasma Process. Polym.*, vol. 3, no. 6-7, pp. 431-442, 2006.
- [25] B. Denis, S. Steves, E. Semmler, N. Bibinov, W. Novak, and P. Awakowicz, "Plasma Sterilization of Pharmaceutical Products: From Basics to Production," *Plasma Process. Polym.*, vol. 9, no. 6, pp. 619-629, 2012.
- [26] R. Itatani, "Remark on Production of Atmospheric Pressure Non-thermal Plasmas for Modern Applications," *Advanced Plasma Technology*, R. d'Agostino, P. Favia, Y. Kawai *et al.*, eds., Weinheim: Wiley-VCH Verlag GmbH 2008.
- [27] J. Friedrich, *The Plasma Chemistry of Polymer Surfaces - Advanced Techniques for Surface Design*, Weinheim: Wiley-VCH Verlag GmbH, 2012.
- [28] U. Kogelschatz, "Dielectric-barrier discharges: Their history, discharge physics, and industrial applications," *Plasma Chem. Plasma Process.*, vol. 23, no. 1, pp. 1-46, 2003.
- [29] F. Iza, G. J. Kim, S. M. Lee, J. K. Lee, J. L. Walsh, Y. T. Zhang, and M. G. Kong, "Microplasmas: Sources, particle kinetics, and biomedical applications," *Plasma Process. Polym.*, vol. 5, no. 4, pp. 322-344, 2008.
- [30] A. Fridman, A. Chirokov, and A. Gutsol, "Non-thermal atmospheric pressure discharges," *J. Phys. D-Appl. Phys.*, vol. 38, no. 2, pp. R1-R24, 2005.
- [31] H. E. Wagner, R. Brandenburg, K. V. Kozlov, A. Sonnenfeld, P. Michel, and J. F. Behnke, "The barrier discharge: basic properties and applications to surface treatment," *Vacuum*, vol. 71, no. 3, pp. 417-436, 2003.
- [32] K. D. Weltmann, E. Kindel, T. von Woedtke, M. Hähnel, M. Stieber, and R. Brandenburg, "Atmospheric-pressure plasma sources: Prospective tools for plasma medicine," *Pure Appl. Chem.*, vol. 82, no. 6, pp. 1223-1237, 2010.
- [33] J. Ehlbeck, U. Schnabel, M. Polak, J. Winter, T. von Woedtke, R. Brandenburg, T. von dem Hagen, and K. D. Weltmann, "Low temperature atmospheric pressure plasma sources for microbial decontamination," *J. Phys. D-Appl. Phys.*, vol. 44, no. 1, pp. 1-18, 2011.
- [34] G. Fridman, G. Friedman, A. Gutsol, A. B. Shekhter, V. N. Vasilets, and A. Fridman, "Applied plasma medicine," *Plasma Process. Polym.*, vol. 5, no. 6, pp. 503-533, 2008.
- [35] J. L. Walsh, F. Iza, N. B. Janson, V. J. Law, and M. G. Kong, "Three distinct modes in a cold atmospheric pressure plasma jet," *J. Phys. D-Appl. Phys.*, vol. 43, no. 7, pp. 1-14, 2010.
- [36] K. D. Weltmann, E. Kindel, R. Brandenburg, C. Meyer, R. Bussiahn, C. Wilke, and T. von Woedtke, "Atmospheric Pressure Plasma Jet for Medical Therapy: Plasma Parameters and Risk Estimation," *Contrib. Plasma Phys.*, vol. 49, no. 9, pp. 631-640, 2009.
- [37] X. P. Lu, Y. G. Cao, P. Yang, Q. Xiong, Z. L. Xiong, Y. B. Xian, and Y. Pan, "An RC Plasma Device for Sterilization of Root Canal of Teeth," *IEEE Trans. Plasma Sci.*, vol. 37, no. 5, pp. 668-673, 2009.
- [38] M. Laroussi, and A. Fridman, "Plasma Medicine," *Plasma Process. Polym.*, vol. 5, no. 6, pp. 501-501, 2008.
- [39] K. D. Weltmann, and T. von Woedtke, "Campus PlasmaMed-From Basic Research to Clinical Proof," *IEEE Trans. Plasma Sci.*, vol. 39, no. 4, pp. 1015-1025, 2011.
- [40] M. Laroussi, "Sterilization of contaminated matter with an atmospheric pressure plasma," *IEEE Trans. Plasma Sci.*, vol. 24, no. 3, pp. 1188-1191, 1996.
- [41] M. Moreau, N. Orange, and M. G. J. Feuilleux, "Non-thermal plasma technologies: New tools for bio-decontamination," *Biotechnol. Adv.*, vol. 26, no. 6, pp. 610-617, , 2008.
- [42] E. Martines, M. Zuin, R. Cavazzana, E. Gazza, G. Serianni, S. Spagnolo, M. Spolaore, A. Leonardi, V. Deligianni, P. Brun, M. Aragona, and I. Castagliuolo, "A novel plasma source for sterilization of living tissues," *New J. Phys.*, vol. 11, pp. 1-8, 2009.
- [43] A. G. Whittaker, E. M. Graham, R. L. Baxter, A. C. Jones, P. R. Richardson, G. Meek, G. A. Campbell, A. Aitken, and H. C. Baxter, "Plasma cleaning of dental instruments," *J. Hosp. Infect.*, vol. 56, no. 1, pp. 37-41, 2004.
- [44] S. Rupf, A. N. Idlibi, F. Al Marrawi, M. Hannig, A. Schubert, L. von Mueller, W. Spitzer, H. Holtmann, A. Lehmann, A. Rueppell, and A. Schindler, "Removing Biofilms from Microstructured Titanium Ex Vivo: A Novel Approach Using Atmospheric Plasma Technology," *Plos One*, vol. 6, no. 10, pp. 9, 2011.

- 
- [45] I. Koban, R. Matthes, N. O. Hübner, A. Welk, P. Meisel, B. Holtfreter, R. Sietmann, E. Kindel, K.-D. Weltmann, A. Kramer, and T. Kocher, "Treatment of *Candida albicans* biofilms with low-temperature plasma induced by dielectric barrier discharge and atmospheric pressure plasma jet," *New J. Phys.*, vol. 12, pp. 1-16, 2010.
  - [46] W. P. Menashi: *Treatment of surfaces* U.S. Patent 3,3863,163, 1968.
  - [47] M. Laroussi, "Nonthermal decontamination of biological media by atmospheric-pressure plasmas: Review, analysis, and prospects," *IEEE Trans. Plasma Sci.*, vol. 30, no. 4, pp. 1409-1415, 2002.
  - [48] M. Moisan, J. Barbeau, S. Moreau, J. Pelletier, M. Tabrizian, and L. H. Yahia, "Low-temperature sterilization using gas plasmas: a review of the experiments and an analysis of the inactivation mechanisms," *Int. J. Pharm.*, vol. 226, no. 1-2, pp. 1-21, 2001.
  - [49] A. D. Russell, "Bacterial-spores and chemical sporicidal agents," *Clin. Microbiol. Rev.*, vol. 3, no. 2, pp. 99-119, 1990.
  - [50] P. Setlow, "Spores of *Bacillus subtilis*: their resistance to and killing by radiation, heat and chemicals," *J. Appl. Microbiol.*, vol. 101, no. 3, pp. 514-525, 2006.
  - [51] K. Kelly-Wintenberg, T. C. Montie, C. Brickman, J. R. Roth, A. K. Carr, K. Sorge, L. C. Wadsworth, and P. P. Y. Tsai, "Room temperature sterilization of surfaces and fabrics with a One Atmosphere Uniform Glow Discharge Plasma," *J. Ind. Microbiol. Biotechnol.*, vol. 20, no. 1, pp. 69-74, 1998.
  - [52] M. Moisan, J. Barbeau, M. C. Crevier, J. Pelletier, N. Philip, and B. Saoudi, "Plasma sterilization. Methods mechanisms," *Pure Appl. Chem.*, vol. 74, no. 3, pp. 349-358, 2002.
  - [53] T. von Woedtke, A. Kramer, and K. D. Weltmann, "Plasma sterilization: What are the conditions to meet this claim?," *Plasma Process. Polym.*, vol. 5, no. 6, pp. 534-539, 2008.
  - [54] A. Kramer, and O. Assadian, "Wallhäußers Praxis der Sterilisation, Desinfektion, Antiseptik und Konservierung," Stuttgart, New York: Georg Thieme Verlag, 2008.
  - [55] T. von Woedtke, and A. Kramer, "The limits of sterility assurance," *GMS Krankenhaushygiene interdisziplinär*, vol. 3, no. 3, pp. 1-10, 2008.
  - [56] S. A. Ermolaeva, A. F. Varfolomeev, M. Y. Chernukha, D. S. Yurov, M. M. Vasiliev, A. A. Kaminskaya, M. M. Moisenovich, J. M. Romanova, A. N. Murashev, Selezneva, II, T. Shimizu, E. V. Sysolyatina, I. A. Shaginyan, O. F. Petrov, E. I. Mayevsky, V. E. Fortov, G. E. Morfill, B. S. Naroditsky, and A. L. Gintsburg, "Bactericidal effects of non-thermal argon plasma in vitro, in biofilms and in the animal model of infected wounds," *J. Med. Microbiol.*, vol. 60, no. 1, pp. 75-83, 2011.
  - [57] M. G. Kong, G. Kroesen, G. Morfill, T. Nosenko, T. Shimizu, J. van Dijk, and J. L. Zimmermann, "Plasma medicine: an introductory review," *New Journal of Physics*, vol. 11, pp. 35, 2009.
  - [58] A. Majumdar, R. K. Singh, G. J. Palm, and R. Hippler, "Dielectric barrier discharge plasma treatment on *E. coli*: Influence of CH<sub>4</sub>/N<sub>2</sub>, O<sub>2</sub>, N<sub>2</sub>/O<sub>2</sub>, N<sub>2</sub>, and Ar gases," *J. Appl. Phys.*, vol. 106, no. 8, pp. 5, 2009.
  - [59] R. Brandenburg, H. Lange, T. von Woedtke, M. Stieber, E. Kindel, J. Ehlbeck, and K.-D. Weltmann, "Antimicrobial Effects of UV and VUV Radiation of Nonthermal Plasma Jets," *IEEE Trans. Plasma Sci.*, vol. 37, no. 6, pp. 877-883, 2009.
  - [60] L. F. Gaunt, C. B. Beggs, and G. E. Georgiou, "Bactericidal action of the reactive species produced by gas-discharge nonthermal plasma at atmospheric pressure: A review," *IEEE Trans. Plasma Sci.*, vol. 34, no. 4, pp. 1257-1269, 2006.
  - [61] M. Hähnel, T. von Woedtke, and K. D. Weltmann, "Influence of the Air Humidity on the Reduction of *Bacillus* Spores in a Defined Environment at Atmospheric Pressure Using a Dielectric Barrier Surface Discharge," *Plasma Process. Polym.*, vol. 7, no. 3-4, pp. 244-249, 2010.
  - [62] M. Laroussi, and F. Leipold, "Evaluation of the roles of reactive species, heat, and UV radiation in the inactivation of bacterial cells by air plasmas at atmospheric pressure," *Int. J. Mass Spectrom.*, vol. 233, no. 1-3, pp. 81-86, 2004.
  - [63] J. M. C. Gutteridge, "Lipid Peroxidation and Antioxidants as Biomarkers of Tissue Damage," *Clin. Chem.*, vol. 41, no. 12B, pp. 1819-1828, 1995.
  - [64] K. H. Schoenbach, S. Katsuki, R. H. Stark, E. S. Buescher, and S. J. Beebe, "Bioelectrics - New applications for pulsed power technology," *IEEE Trans. Plasma Sci.*, vol. 30, no. 1, pp. 293-300, 2002.
  - [65] H. C. Baxter, G. A. Campbell, A. G. Whittaker, A. C. Jones, A. Aitken, A. H. Simpson, M. Casey, L. Bountiff, L. Gibbard, and R. L. Baxter, "Elimination of transmissible spongiform encephalopathy infectivity and decontamination of surgical instruments by using radio-frequency gas-plasma treatment," *J. Gen. Virol.*, vol. 86, pp. 2393-2399, 2005.

- [66] B. J. Park, D. H. Lee, J. C. Park, I. S. Lee, K. Y. Lee, S. O. Hyun, M. S. Chun, and K. H. Chung, "Sterilization using a microwave-induced argon plasma system at atmospheric pressure," *Physics of Plasmas*, vol. 10, no. 11, pp. 4539-4544, 2003.
- [67] J. W. Costerton, P. S. Stewart, and E. P. Greenberg, "Bacterial biofilms: A common cause of persistent infections," *Science*, vol. 284, no. 5418, pp. 1318-1322, 1999.
- [68] T. Bjarnsholt, N. Hoiby, G. Donelli, C. Imbert, and A. Forsberg, "Understanding biofilms - are we there yet?," *FEMS Immunol. Med. Microbiol.*, vol. 65, no. 2, pp. 125-126, 2012.
- [69] K. Becker, A. Koutsospyros, S. M. Yin, C. Christodoulatos, N. Abramzon, J. C. Joaquin, and G. Brelles-Marino, "Environmental and biological applications of microplasmas," *Plasma Phys. Control. Fusion*, vol. 47, pp. B513-B523, 2005.
- [70] Y. Akishev, M. Grushin, V. Karalnik, N. Trushkin, V. Kholodenko, V. Chugunov, E. Kobzev, N. Zhirkova, I. Irkhina, and G. Kireev, "Atmospheric-pressure, nonthermal plasma sterilization of microorganisms in liquids and on surfaces," *Pure Appl. Chem.*, vol. 80, no. 9, pp. 1953-1969, 2008.
- [71] S. Ermolaeva, O. Petrov, N. Zigangirova, M. Vasiliev, E. Sysolyatina, S. Antipov, M. Alyapyshev, N. Kolkova, A. Mukhachev, B. Naroditsky, T. Shimizu, A. Grigoriev, G. Morfill, V. E. Fortov, and A. Gintsburg, "Low Temperature Atmospheric Argon Plasma: Diagnostic and Medical Applications," *Plasma for Bio-Decontamination, Medicine and Food Security*, Z. Machala, K. Hensel and Y. Akishev, eds.: Springer, 2012.
- [72] C. Traba, and J. F. Liang, "Susceptibility of *Staphylococcus aureus* biofilms to reactive discharge gases," *Biofouling*, vol. 27, no. 7, pp. 763-772, 2011.
- [73] H. C. van der Mei, J. de Vries, and H. J. Busscher, "X-ray photoelectron spectroscopy for the study of microbial cell surfaces," *Surf. Sci. Rep.*, vol. 39, no. 1, pp. 3-24, 2000.
- [74] H.-G. Elias, *Makromoleküle*, Weinheim: Wiley-VCH, 2003.
- [75] P. G. Rouxhet, and M. J. Genet, "XPS analysis of bio-organic systems," *Surface and Interface Analysis*, vol. 43, no. 12, pp. 1453-1470, 2011.
- [76] S. Lerouge, M. R. Wertheimer, R. Marchand, M. Tabrizian, and L. Yahia, "Effect of gas composition on spore mortality and etching during low-pressure plasma sterilization," *J. Biomed. Mater. Res.*, vol. 51, no. 1, pp. 128-135, 2000.
- [77] U. Fantz, "Basics of plasma spectroscopy," *Plasma Sources Sci. Technol.*, vol. 15, no. 4, pp. S137-S147, 2006.
- [78] C. O. Laux, T. G. Spence, C. H. Kruger, and R. N. Zare, "Optical diagnostics of atmospheric pressure air plasmas," *Plasma Sources Sci. Technol.*, vol. 12, no. 2, pp. 125-138, 2003.
- [79] M. Geigl, S. Peters, O. Gabriel, B. Krames, and J. Meichsner, "Analysis and kinetics of transient species in electrode near plasma and plasma boundary sheath of RF plasmas in molecular gases," *Contrib. Plasma Phys.*, vol. 45, no. 5-6, pp. 369-377, 2005.
- [80] K. Niemi, V. Schulz-von der Gathen, and H. F. Döbele, "Absolute atomic oxygen density measurements by two-photon absorption laser-induced fluorescence spectroscopy in an RF-excited atmospheric pressure plasma jet," *Plasma Sources Sci. Technol.*, vol. 14, no. 2, pp. 375-386, 2005.
- [81] N. Gomathi, A. Sureshkumar, and S. Neogi, "RF plasma-treated polymers for biomedical applications," *Current Science*, vol. 94, no. 11, pp. 1478-1486, 2008.
- [82] K. S. Siow, L. Britcher, S. Kumar, and H. J. Griesser, "Plasma methods for the generation of chemically reactive surfaces for biomolecule immobilization and cell colonization - A review," *Plasma Process. Polym.*, vol. 3, no. 6-7, pp. 392-418, 2006.
- [83] M. Strobel, C. Dunatov, J. M. Strobel, C. S. Lyons, S. J. Perron, and M. C. Morgen, "Low-molecular-weight materials on corona-treated polypropylene," *J. Adhes. Sci. Technol.*, vol. 3, no. 5, pp. 321-335, 1989.
- [84] S. Guimond, and M. R. Wertheimer, "Surface degradation and hydrophobic recovery of polyolefins treated by air corona and nitrogen atmospheric pressure glow discharge," *J. Appl. Polym. Sci.*, vol. 94, no. 3, pp. 1291-1303, 2004.
- [85] G. N. Taylor, and T. M. Wolf, "Oxygen plasma removal of thin polymer films," *Polym. Eng. Sci.*, vol. 20, no. 16, pp. 1087-1092, 1980.
- [86] C. M. Weikart, and H. K. Yasuda, "Modification, degradation, and stability of polymeric surfaces treated with reactive plasmas," *J. Polym. Sci. Pol. Chem.*, vol. 38, no. 17, pp. 3028-3042, 2000.



- 
- [87] M. R. Wertheimer, A. C. Fozza, and A. Holländer, "Industrial processing of polymers by low-pressure plasmas: the role of VUV radiation," *Nucl. Instrum. Methods Phys. Res. Sect. B-Beam Interact. Mater. Atoms*, vol. 151, no. 1-4, pp. 65-75, 1999.
  - [88] C. Borcia, G. Borcia, and N. Dumitrascu, "Atmospheric-Pressure Dielectric Barrier Discharge for Surface Processing of Polymer Films and Fibers," *IEEE Trans. Plasma Sci.*, vol. 37, no. 6, pp. 941-945, 2009.
  - [89] F. E. Truica-Marasescu, and M. R. Wertheimer, "Vacuum ultraviolet photolysis of hydrocarbon polymers," *Macromol. Chem. Phys.*, vol. 206, no. 7, pp. 744-757, 2005.
  - [90] A. Holländer, R. Wilken, and J. Behnisch, "Subsurface chemistry in the plasma treatment of polymers," *Surf. Coat. Technol.*, pp. 788-791, 1999.
  - [91] M. Strobel, and C. S. Lyons, "An Essay on Contact Angle Measurements," *Plasma Process. Polym.*, vol. 8, no. 1, pp. 8-13, 2011.
  - [92] J. F. Friedrich, R. Mix, R. D. Schulze, A. Meyer-Plath, R. Joshi, and S. Wettmarshausen, "New plasma techniques for polymer surface modification with monotype functional groups," *Plasma Process. Polym.*, vol. 5, no. 5, pp. 407-423, 2008.
  - [93] G. Beamson, and D. Briggs, *High resolution XPS of organic polymers. The Scienta ESCA 300 data base*, Chichester: John Wiley & Sons, 1992.
  - [94] C. Bergemann, A. Quade, F. Kunz, S. Ofe, E. D. Klinkenberg, M. Laue, K. Schröder, V. Weissmann, H. Hansmann, K.-D. Weltmann, and B. Nebe, "Ammonia Plasma Functionalized Polycarbonate Surfaces Improve Cell Migration Inside an Artificial 3D Cell Culture Module," *Plasma Process. Polym.*, vol. 9, no. 3, pp. 261-272, 2012.
  - [95] B. D. Ratner, A. S. Hoffmann, F. J. Schoen, and J. E. Lemons (B. D. Ratner, A. S. Hoffmann, F. J. Schoen, and J. E. Lemons), "Biomaterials Science: An Introduction to Materials in Medicine," Academic Press, 2004
  - [96] K. Anselme, A. Ponche, and M. Bigerelle, "Relative influence of surface topography and surface chemistry on cell response to bone implant materials. Part 2: biological aspects," *Proc. Inst. Mech. Eng. Part H-J. Eng. Med.*, vol. 224, no. H12, pp. 1487-1507, 2010.
  - [97] T. Jacobs, R. Morent, N. De Geyter, P. Dubruel, and C. Leys, "Plasma Surface Modification of Biomedical Polymers: Influence on Cell-Material Interaction," *Plasma Chem. Plasma Process.*, pp. 1-35, 2012.
  - [98] B. Nebe, B. Finke, F. Luethen, C. Bergemann, K. Schröder, J. Rychly, K. Liefeth, and A. Ohl, "Improved initial osteoblast functions on amino-functionalized titanium surfaces," *Biomol. Eng.*, vol. 24, no. 5, pp. 447-454, 2007.
  - [99] B. Finke, F. Hempel, H. Testrich, A. Artemenko, H. Rebl, O. Kylian, J. Meichsner, H. Biederman, B. Nebe, K.-D. Weltmann, and K. Schröder, "Plasma processes for cell-adhesive titanium surfaces based on nitrogen-containing coatings," *Surf. Coat. Technol.*, vol. 205, pp. S520-S524, 2011.
  - [100] F. Truica-Marasescu, P. L. Girard-Lauriault, A. Lippitz, W. E. S. Unger, and M. R. Wertheimer, "Nitrogen-rich plasma polymers: Comparison of films deposited in atmospheric- and low-pressure plasmas," *Thin Solid Films*, vol. 516, no. 21, pp. 7406-7417, 2008.
  - [101] E. Stoffels, I. E. Kieft, R. E. J. Sladek, L. J. M. van den Bedem, E. P. van der Laan, and M. Steinbuch, "Plasma needle for in vivo medical treatment: recent developments and perspectives," *Plasma Sources Sci. Technol.*, vol. 15, no. 4, pp. S169-S180, 2006.
  - [102] G. Daeschlein, S. Scholz, R. Ahmed, T. von Woedtke, H. Haase, M. Niggemeier, E. Kindel, R. Brandenburg, K.-D. Weltmann, and M. Juenger, "Skin decontamination by low-temperature atmospheric pressure plasma jet and dielectric barrier discharge plasma," *J. Hosp. Infect.*, vol. 81, no. 3, pp. 177-183, 2012.
  - [103] G. Daeschlein, S. Scholz, R. Ahmed, A. Majumdar, T. von Woedtke, H. Haase, M. Niggemeier, E. Kindel, R. Brandenburg, K. D. Weltmann, and M. Junger, "Cold plasma is well-tolerated and does not disturb skin barrier or reduce skin moisture," *J. Dtsch. Dermatol. Ges.*, vol. 10, no. 7, pp. 509-515, 2012.





## 5 Original Publications



**5.1 “On the Use of Atmospheric Pressure Plasma for the Bio-Decontamination of Polymers and Its Impact on Their Chemical and Morphological Surface Properties”**

Katja Fricke, Helena Tresp, René Bussiahn, Karsten Schröder, Thomas von Woedtke, and Klaus-Dieter Weltmann

*Plasma Chemistry and Plasma Processing*, vol. 32, no. 4, pp. 801-816, **2012**



## On the Use of Atmospheric Pressure Plasma for the Bio-Decontamination of Polymers and Its Impact on Their Chemical and Morphological Surface Properties

K. Fricke · H. Tresp · R. Bussiahn · K. Schröder · Th. von Woedtke · K.-D. Weltmann

Received: 21 April 2011 / Accepted: 12 April 2012 / Published online: 11 May 2012  
© Springer Science+Business Media, LLC 2012

**Abstract** Low temperature atmospheric pressure plasma processes can be applied to inactivate micro-organisms on products and devices made from synthetic and natural polymers. This study shows that even a short-time exposure to Ar or Ar/O<sub>2</sub> plasma of an atmospheric pressure plasma jet leads to an inactivation of *Bacillus atrophaeus* spores with a maximum reduction of 4 orders of magnitude. However, changes in the surface properties of the plasma exposed material have to be considered, too. Therefore, polyethylene and polystyrene are used as exemplary substrate materials to investigate the effect of plasma treatment in more detail. The influence of process parameters, such as type of operating gas or jet-nozzle to substrate distance, is examined. The results show that short-time plasma treatment with Ar and Ar/O<sub>2</sub> affects the surface wettability due to the introduction of polar groups as proofed by X-ray photoelectron spectroscopy. Furthermore, atomic force microscopy images reveal changes in the surface topography. Thus, nano-structures of different heights are observed on the polymeric surface depending on the treatment time and type of process gas.

**Keywords** Atmospheric pressure plasma jet · Polymers · Decontamination · Modification · XPS · AFM

### Introduction

Heat sensitive materials like polymers used for biomedical applications (e.g. medical implants) often undergo various pre-treatments to obtain desired physico-chemical surface characteristics to ensure reliable functionality in the biological environment [1–3]. For further processing, an activation of the substrate surface is required as well as a sterile handling. In this case, gas-discharge plasma-based processes are the method of choice, combining the change of chemical and physical properties of only the outermost layer of

---

K. Fricke (✉) · H. Tresp · R. Bussiahn · K. Schröder · Th. von Woedtke · K.-D. Weltmann  
INP Greifswald e.V., Leibniz Institute for Plasma Science and Technology, Felix-Hausdorff-Str. 2,  
17489 Greifswald, Germany  
e-mail: k.fricke@inp-greifswald.de

the polymer surface without affecting the bulk properties and the ability to bio-decontaminate the surface at the same time. Furthermore, plasmas have a great potential to modify and/or bio-decontaminate small and complex-shaped products regarding the inherent advantages of gas phase processes [4]. A physical plasma is created from a gas that is dissociated and ionized. It is a quasineutral particle system composed of positively and negatively charged ions, radicals, electrons, and neutral particles (atoms, molecules) [5]. Owing to the moderate neutral gas temperatures (at or near ambient temperature), non-thermal plasmas are more suitable for the sterilization or modification of thermolabile polymeric surfaces. In particular, atmospheric plasma processes are of growing interest, since they do not require expensive vacuum systems which reduces the process cost significantly. Therefore, the number of newly developed plasma sources designed for surface functionalization and biological decontamination has grown considerably within the last years [6–9]. Non-thermal plasmas provide several types of active species including charged particles, radicals, excited metastables, electric fields, and (V)UV radiation, which are considered to be effective sterilizing agents [10, 11]. However, these plasma-generated species are not only capable to inactivate micro-organisms, they may also initiate reactions with polymer surfaces [12]. Hence, it is necessary to investigate the plasma induced surface modification during antimicrobial treatment in detail, as surfaces modified in this manner exhibit changes in wettability, elemental composition, and texture (roughness) leading to alteration of the functionalities [13, 14]. It is thus possible to obtain required surface bio-decontamination and at the same time improved surface properties to accomplish biocompatibility, which is especially for biomedical materials of importance. For instance, chemical functionalities such like hydroxyls, carboxyl groups, ketones, and aldehydes can be created on the surface during plasma exposure causing an increase of surface energy and subsequently an improved wettability, which in turn enables a better adhesion and proliferation of cells [15, 16]. Nevertheless, changes in the surface morphology and topology induced by the plasma treatment facilitate an appropriate biological response, too [17, 18].

Since gas plasma bio-decontamination/sterilization of heat sensitive materials is considered to be a prospective alternative to commercial available methods, the present work is focused on the inactivation of *Bacillus atrophaeus* spores using argon and argon oxygen plasma. Furthermore, the inactivation efficiency was compared dependent on the process gas, treatment time, and operating distance. In parallel with the antimicrobial studies, the changes in the physico-chemical surface properties of polyethylene (PE) and polystyrene (PS) were also examined. Therefore, water contact angle measurements, atomic force microscopy (AFM), and X-ray photoelectron spectroscopy (XPS) were applied. Additional optical emission spectroscopy (OES) studies were performed to obtain more information on the species present in the plasma.

## Experimental Set Up

### Miniaturized Atmospheric Pressure Plasma Jet

The principal set up of the high-frequency (HF) driven (1.7 MHz) miniaturized atmospheric pressure plasma jet (kINPen, INP Greifswald, Germany) is schematically shown in Fig. 1. The device consists of a grounded ring electrode and a centered rod electrode inside a quartz capillary (with an inner diameter of 1.6 mm and an outer diameter of 4 mm) which is coupled to the power source via a matching network. Throughout the experiments



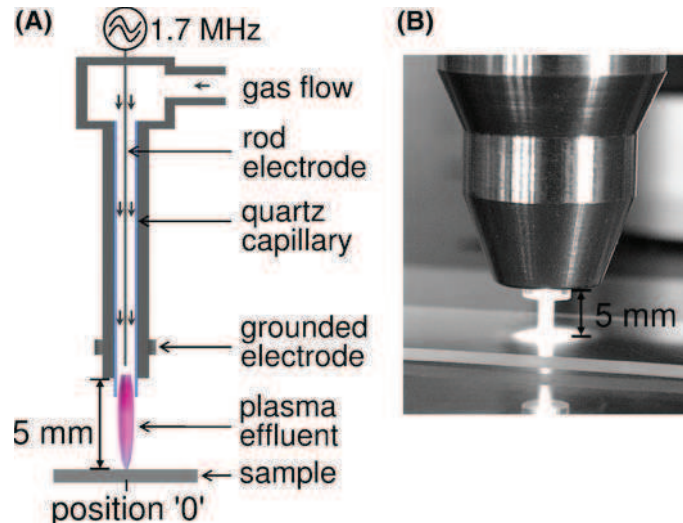


**Fig. 1** **a** Experimental set-up and scheme of the plasma jet (kINPen). **b** Photograph of the Ar plasma jet impinging on a PS substrate at a jet-nozzle to substrate distance of 5 mm

the overall electric power applied to the device was held constant at 65 W (as measured at the generator output). The plasma source was operated with argon at a flow rate of 5 standard liter per minute (slm) and small admixtures of molecular oxygen of up to 0.05 slm (1 %O<sub>2</sub>). Under these conditions, the length of the Ar plasma jet expanding into the surrounding air was observed to be 12 mm and with 1 % oxygen admixture 5–6 mm from the nozzle outlet. It has to be noted, that for this reason at a jet-nozzle to substrate distance (also called axial distance) of 5 mm the Ar plasma jet spreads on the polymeric substrate. Thus, the impinging jet affects a surface area in the range of 5–7 mm. Further details on this type of jet are described elsewhere [19, 20]. The plasma treatments were performed only at one position (localized treatment) of the polymer surfaces which is labeled as position '0'.

#### Polymeric Materials

The experiments were carried out with polyethylene (PE, 200  $\mu\text{m}$  thick, 0.94 g/cm<sup>3</sup>, Goodfellow, Germany) and polystyrene (PS, 125  $\mu\text{m}$  thick, 1.02 g/cm<sup>3</sup>, Greiner, Germany) as substrate materials. Polyethylene and polystyrene are hydrocarbon polymers with a simple chemical structure containing no chemical functional groups which facilitates clear information on the impact of plasma on the chemical surface composition. Furthermore, these polymers were selected because of their particular relevance in biomedical applications.

#### Microbiological Tests

For the microbiological tests endospores of *B. atrophaeus* spores were used due to their standardized usage for sterilization processes [22]. Endospores are inactive or dormant forms of bacteria. Compared to vegetative forms (actively growing) spores are most

resistant to chemical and environmental factors such as chemical agents, heat, radiation, and changes in pH.

Inactivation kinetics of micro-organisms by plasma have been realized using polyethylene and polystyrene strips ( $3 \times 0.9$  cm) contaminated punctually with 25  $\mu$ l of a suspension of *B. atrophaeus* spores (drop diameter: 3–4 mm) and dried under aseptic conditions. The plasma-treated strips as well as the non-treated strips (control) were transferred into tubes containing 10 ml sterile tryptic soy broth and agitated for 15 min on a Bühler shaker to remove vital and destroyed spores. Afterwards, the culture vessels were put into a water bath of 80 °C for 10 min to destroy vegetative germs. The spore concentration was quantified via dilution series by the surface-spread plate count method using agar plates (Caso, Merck) and is given as colony forming units per object (CFU/object). The plates were incubated for at least 20 h at 36 °C. For each experiment three samples were treated at a time under the same conditions for statistics.

### Surface Analysis

Contact angle measurements on the polymer surfaces were performed under ambient air at room temperature by the sessile drop method using a Digidrop contact angle analyzer (GBX Instrumentation Scientifique, France) and a drop of distilled water with a defined volume (0.5  $\mu$ l). The contact angle was measured through the zone of the locally plasma-treated polymer (line scan) with a step width of 3 mm. The contact angle of the resting drop was determined utilizing the software Windrop. The chemical composition of the surfaces was measured ex-situ with X-ray photoelectron spectroscopy (XPS) (Axis Ultra, Kratos, Manchester, UK) utilizing monochromatic aluminum  $K_{\alpha}$  irradiation at 1,486.6 eV. Charge neutralization was implemented by low energy electrons, injected in the magnetic field of the lens from a filament located directly atop the sample. The spot size was ca. 250  $\mu$ m in diameter. Wide scans and element spectra were recorded at a pass energy of 80 eV for the estimation of the chemical element composition and at a pass energy of 10 eV for the highly resolved measurements of the C 1s peak, respectively. Data acquisition and processing were carried out using the software CasaXPS, version 2.14.dev29 (Casa Software Ltd., Teignmouth, UK). A line scan through the centre of the plasma-treated zone of the polymeric substrates was recorded with a step size of 0.5 mm. All values are given in XPS atomic percent. Curve-fitting of the highly resolved C 1s region was performed to characterize the chemical structure of the polymeric surface using Gaussian–Lorentzian distribution and a linear baseline. The full width at half maximum of the C 1s components was 1.2 eV for high energy resolution measurements. Atomic force microscopy (AFM) provides the determination of the surface topography before and after plasma treatment. The AFM analysis was performed with a scanning probe microscope diCP-II (Veeco Instruments, Santa Barbara, USA) in the non contact mode, especially tapping mode. An area of  $10 \times 10$   $\mu$ m was scanned using a pyramidal silicon tip doped with n-type phosphorus with a resonance frequency of 273–389 kHz and a force constant of 20–80 N/m (Veeco, RTESPA-CP). Five areas were recorded for each sample and analyzed by means of the software SPMLab Ver. 6.0.2 (Veeco).

### Optical Emission Spectroscopy

For the optical emission spectroscopy (OES) a dual channel fiber optical spectrometer (Avantes AvaSpec 2048-2-USB2) was used. The first channel operated in the range of UV/VIS (200–450 nm) with a grating (600 lines/mm, Blaze 250 nm) and a 25  $\mu$ m slit. The

resolution of this channel was 0.6 nm. Channel two operated in the range of 450–950 nm (25  $\mu\text{m}$  slit, 600 lines/mm, Blaze 500 nm) with a resolution of 0.7 nm. The channels were linked to a y-cable, which had a 0.6 mm core and was coupled with a second fiber (diameter 1 mm). The spectra were normalized to the exposure time and relatively calibrated. The OES spectra were recorded side-on, i.e. the fiber was located lateral to the jet plasma, from the jet-nozzle up to the end of the plasma jet and analyzed using the software Spectrum Analyzer [21].

## Results and Discussion

### Antimicrobial Treatment

Bio-decontamination (inactivation or removal of micro-organisms on surfaces) or sterilization (complete absence of all viable micro-organisms) of surfaces has become one of the most important topics in gas-discharge based surface treatment [22, 23]. Especially for sensitive surfaces and goods which cannot be treated with conventional sterilization methods, such like heat sterilization, alternative and non-invasive approaches have to be evaluated. Gas-discharges are well-suited for treating sensitive substrate surfaces, e.g. of thermolabile substrates like polymers. Therefore, different plasma sources were developed with the purpose of bio-decontamination and additionally, the process of plasma-induced inactivation of bacteria cells is well discussed [4, 22]. Hence, only a brief outline is given here about the bio-decontamination potential of the applied plasma jet by using *B. atrophaeus* spores as test organism.

Plasma inactivation kinetics of *B. atrophaeus* spores for different operating gases and axial distances are depicted in Fig. 2. In particular, in Fig. 2a the spore viability (counts of colony forming units (CFU)) after plasma exposure applying different gas mixtures as a function of treatment time is plotted. As process gases pure argon and argon with admixtures of 0.2 and 1 % oxygen were used. The dashed line in this figure represents the detection limit of 100 CFU/object caused by the used method. If no spores were found on the samples the value of the detection limit was used. As shown in Fig. 2a the number of CFU was reduced with increasing treatment time. In terms of the process gas an enhanced plasma inactivation efficacy of *B. atrophaeus* spores was observed when oxygen was added. Particularly, for treatment times above 30 s considerable differences concerning the microbicidal efficiency of Ar and Ar/O<sub>2</sub> plasma were observed. Thus, by using oxygen admixtures an increase of the lethal effect by one log reduction was observed. Furthermore, dependent on the amount of added oxygen an improved lethal effect was achieved with the highest feasible oxygen admixture of 1 %. Hence, a maximum reduction of four orders of magnitude of the initial concentration was obtained after a treatment time of 180 s using Ar/O<sub>2</sub> (1 % O<sub>2</sub>) plasma (see Fig. 2a). The mechanism of the microbicidal action of plasma results from different plasma-generated species. In detail, the lethal effect of argon plasma is mainly based on (V)UV radiation validated by optical emission spectroscopy, which for example exhibits lines in the UV-B, UV-A, and VUV region [19, 20, 24]. Lange and von Woedtke investigated the influence of (V)UV radiation of the atmospheric pressure plasma jet on the inactivation of *B. atrophaeus* spores and found that this radiation is crucial for the lethal effect when pure argon is used [22]. However, when oxygen is admixed to the argon plasma reactive species like O and O<sub>3</sub> are generated, which are known for their antimicrobial effect and consequently increase the bacteria inactivation significantly [25, 26]. Figure 3 exemplarily shows optical emission spectra of Ar plasma and Ar/O<sub>2</sub>

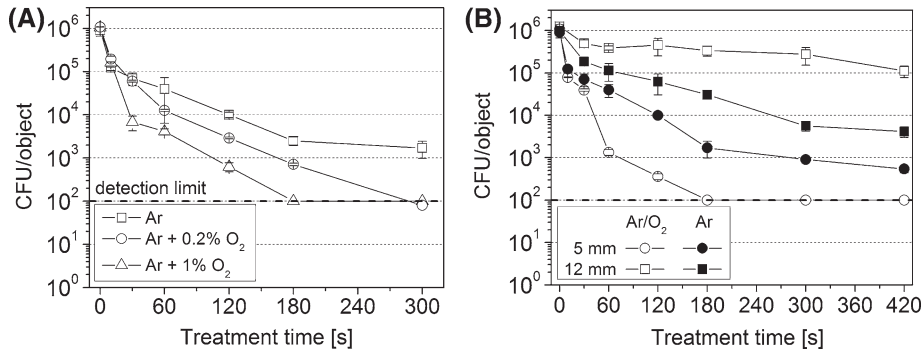


**Fig. 2** Inactivation curves of *B. atrophaeus* spores (number of viable micro-organisms in CFU/object): **a** after Ar (open square), Ar + 0.2 % O<sub>2</sub> (open circle), and Ar + 1 % O<sub>2</sub> (open triangle) plasma treatment on punctually contaminated PS strips. The jet-nozzle to substrate distance was 5 mm. **b** exposed to Ar (filled symbols) and Ar + 1 % O<sub>2</sub> (open symbols) plasma at jet-nozzle to substrate distances of 5 mm (circles) and 12 mm (squares) on punctually contaminated PE strips. The dashed horizontal line indicates the detection limit. (mean  $\pm$  SD,  $n = 3$  each)

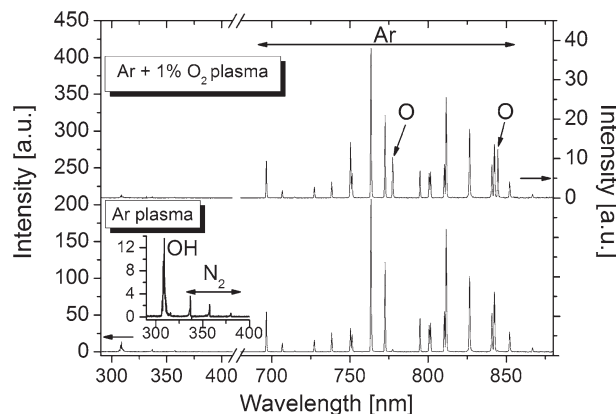


**Fig. 3** Typical optical emission spectra of Ar (lower graph) and Ar/O<sub>2</sub> (1 % O<sub>2</sub>) (upper graph) plasma recorded side-on close to the jet-nozzle (axial position of 3 mm). The inset in the lower graph shows the magnification for wavelengths between 290 and 400 nm in the Ar gas discharge

(1 % O<sub>2</sub>) plasma recorded at a distance of 3 mm from the nozzle outlet. The emission spectrum of the argon discharge in the visible range was dominated by atomic lines of argon whereas in the region between 300 and 400 nm emission of OH at 308 nm and of the second positive system of molecular nitrogen N<sub>2</sub> at 337 nm were observed. The OES spectrum of argon-oxygen plasma showed high intensity lines of atomic oxygen at 777 nm and at 844.6 nm which are caused by the dissociative excitation and the direct excitation processes. The intensities of OH and N<sub>2</sub> lines were comparatively weak. Consequently, the admixture of oxygen results in quenching of N<sub>2</sub> and OH lines [27]. The spectrum of Ar plasma showed also a slight emission of oxygen but the emission intensity of atomic O ( $I_O$ ) at 844.6 nm compared to the emission intensity of Ar ( $I_{Ar}$ ) at 750.4 nm for the two different process gases showed distinctive differences. The  $I_O/I_{Ar}$  ratio of the Ar discharge was 0.07 whereas an  $I_O/I_{Ar}$  ratio of 0.87 was determined for the Ar/O<sub>2</sub> discharge. Thus, the

emission of excited atomic oxygen was ten fold higher when 1 % oxygen was added. According to this result and due to the fact that the excitation and generation of  $N_2$  and OH is suppressed when oxygen is added it can be assumed, that the enhanced lethal effect of Ar/O<sub>2</sub> plasma might derive from the presence of plasma-generated reactive oxygen species. Dobrynin et al. [28] also studied the influence of the gas composition on the inactivation of bacteria and pointed out that oxygen is required for fast and effective bio-decontamination. However, not only the process gas has an influence on the inactivation efficacy but also the operating distance which is displayed in Fig. 2b for Ar and Ar/O<sub>2</sub> (1 % O<sub>2</sub>) plasma. For this purpose polymeric samples were positioned at a distance of 5 mm up to 12 mm from the jet-nozzle. Figure 2b shows that the inactivation efficiency was decreased when the jet-nozzle to substrate distance was increased, most of all when oxygen was admixed. This experimental observation can be attributed to the longer pathway of reactive species, the short lifetimes of oxygen atoms (in the range of ms [29]), and the reaction with ambient air, so that the number of reactive species reaching the surface and potentially inactivating the micro-organisms is reduced. Additionally, it can be assumed that the area of the polymer strip covered by the plasma is distinctly lessens with increasing operating distance, especially when oxygen is added due to the reduced length of the jet's effluent. Therefore, at a jet-nozzle to substrate distance of 12 mm a reduction by one order of magnitude was observed after 420 s of Ar/O<sub>2</sub> plasma exposure while at a jet-nozzle to substrate distance of 5 mm only 30 s were needed to obtain the same result. Based on these observations further OES measurements were performed to investigate the axial distribution of excited species generated by Ar (Fig. 4a) and Ar/O<sub>2</sub> plasma (Fig. 4b, note that the axial distance is reduced to 7 mm because of the shortened plasma jet when oxygen is admixed). The results obtained from the optical emission spectroscopy revealed that the intensity of the excited species of Ar, OH, and O was highest close to the nozzle outlet and decreased towards the end of the plasma jet. This observation correlates very well with the decreased lethal effect of plasma at higher axial distances. In contrast, the intensity of the second positive system of  $N_2$  increased with the distance to the jet-nozzle showing a maximum at a distance of 9 mm in the Ar discharge (Fig. 4a) which was also observed by Bornholdt et al. [30]. This result indicates the interaction of the ambient air with the jet effluent leading to the excitation of nitrogen. Bornholdt et al. assumed that

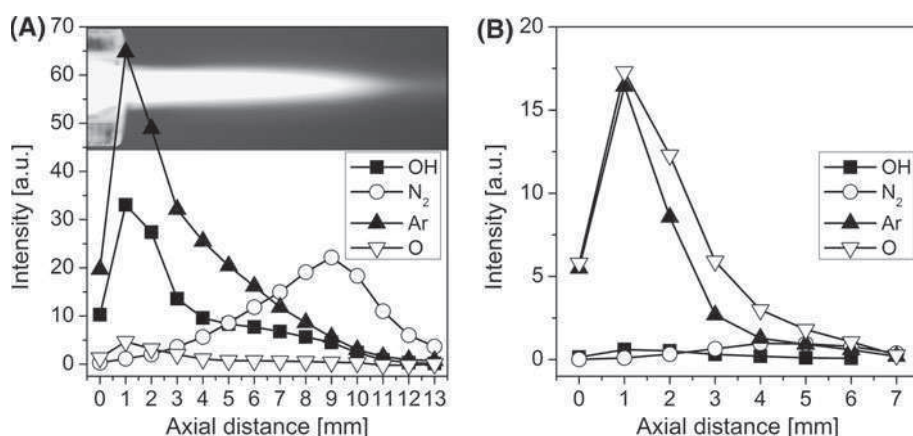


**Fig. 4** Intensity of excited species (Ar: 750.4 nm, O: 844.6 nm; OH: 308 nm N<sub>2</sub>: 337 nm) in **a** Ar plasma and **b** Ar/O<sub>2</sub> (1 % O<sub>2</sub>) plasma depending on the axial distance

especially excited (metastable) argon atoms and UV radiation are involved in the generation of  $N_2$ .

It should be noted that the influence of heat produced by the plasma jet on the inactivation of *B. atrophaeus* spores can be excluded here. Spores of *B. atrophaeus* are coated with a complex multilayer (spore coat) composed of several proteins which increase the resistance to the antimicrobial effect of chemical and physical components [31]. Furthermore, Brandenburg et al. showed that a hot air stream with temperatures between 80 and 90 °C did not reduce the initial spore concentration due to the high temperature resistance of *B. atrophaeus* spores [32]. Additionally, the atmospheric pressure plasma jet offers the possibility to operate in the burst mode (constant period of HF voltage supply—plasma on—is followed by a break period—plasma off) which can reduce the temperature load of the target without losing the antimicrobial efficacy. For detailed information the interested reader is referred to Weltmann et al. [19].

Summarizing, the admixture of oxygen and a short distance between the jet-nozzle and the substrate are needed with this plasma jet for a sufficient bio-decontamination. Similar results were published by Lim et al. [26]. He achieved the best inactivation adding oxygen to the argon plasma jet operating at short exposure distances with a reduction factor of 6 after 30 s Ar/O<sub>2</sub> plasma. Whereas Brandenburg et al. [32] obtained a reduction of 4 orders of magnitude after 420 s using pure argon plasma at atmospheric pressure.

#### Surface Modification

Besides the antimicrobial effects the plasma-induced physico-chemical properties of the polymeric surfaces were studied as well. In particular the influence of the plasma treatment on the polymer modification and etching was of interest here. The physico-chemical properties are of importance since they determine adhesion, repulsion, and wettability of the newly generated interface.

The radial profile of the wettability after plasma treatment, in detail the evolution of the water contact angle on polyethylene and polystyrene along a line crossing the substrate centre with a step size of 3 mm, is shown in Fig. 5. Note, that '0' represents the position of

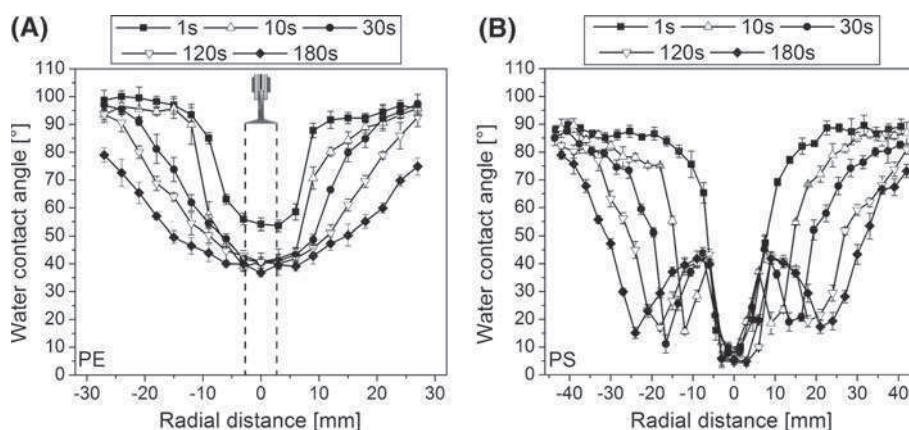


**Fig. 5** Radial profile of the water contact angle on **a** PE and on **b** PS after Ar plasma treatment depending on treatment time (mean  $\pm$  SD,  $n = 3$  each). The jet-nozzle to substrate distance was 5 mm. Also shown in Fig. 5a is a schematic plot of the dimension of the active plasma zone under the given treatment conditions



the localized jet treatment. These measurements were performed to obtain initial information on the altered surface properties immediately after plasma treatment. Since the water contact angle measurements were restricted to the sessile drop method the data presented here indicate changes in the wettability of the polymer only. Furthermore, the variation of the contact angle across the substrate exhibited the extensive impact of the plasma on the surface properties. Anyway, it was possible to receive general information on the influence of the plasma treatment on the surface wettability. E.g., the initial contact angle of  $100^\circ$  was reduced to a minimum contact angle of  $40^\circ$  after 30 s plasma treatment for PE (Fig. 5a) and from  $90^\circ$  to  $5^\circ$  after 1 s plasma treatment for PS (Fig. 5b), respectively. Furthermore a time-dependent broadening of the profile was observed due to a radial flowing afterglow of the plasma jet [33, 34]. Thus, a surface modification beyond the impinging jet was caused after a few seconds, already. Additionally, the contact angle measurements showed that the maximum contact angle reduction was achieved within a few seconds of plasma exposure and that it reached a constant value shortly after. The radial distribution of the contact angle showed different profiles for PE and PS. For PE a single minimum at the centre of the substrate (at position '0') was observed with a broadened profile with increasing treatment time (Fig. 5a). PS showed a similar tendency for short treatment times only. After longer treatment time ( $>10$  s) another effect was observed. In addition to the center dip a ring-shaped minimum appeared, indicated as two side-minima in the radial profile of PS (Fig. 5b). The width of the centre dip was nearly constant for all treatment times whereas a broadening of the total modified area with treatment time was observed too. The influence of the jet-nozzle to substrate distance on the wettability of PE and PS showed minimal changes. The inset in Fig. 6 displays the evolution of the water contact angle of PE determined at different axial distances after 60 s Ar plasma treatment. Even at higher axial distances (above 15 mm) a hydrophilicity of the polymer surface was observed. In comparison to small distances, where the contact angles varied between  $33$  and  $44^\circ$ , the contact angles were here between  $48$  and  $52^\circ$ . Regarding the effect of the process gas on the surface wettability, different oxygen admixtures (up to 1 %) did not result in remarkable differences compared to pure Ar plasma [33]. For a more detailed understanding of the plasma-assisted surface functionalization the chemical

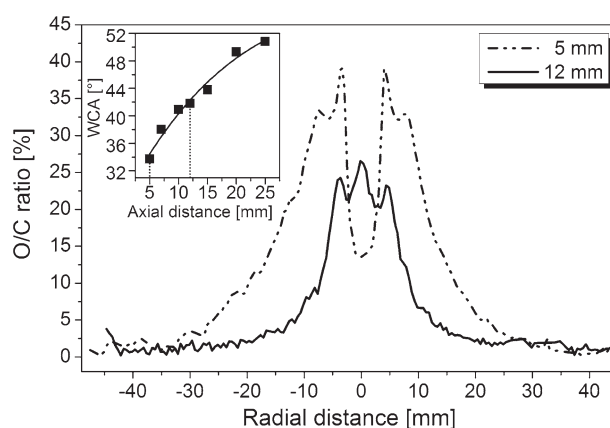


**Fig. 6** Radial profile of the O/C ratio of PE exposed to Ar plasma for 60 s at jet-nozzle to substrate distances of 5 (straight line with dash) and 12 mm (straight line). Inset: Dependence of the water contact angle (WCA) on the jet-nozzle to substrate distance (Treatment conditions: Ar plasma, 60 s)



composition of the polymer surface and the carbon binding state of PE and PS before and after plasma treatment was investigated by XPS. Table 1 contains the elemental composition of PE and PS dependent on the process gas and treatment time determined at position '0' of the polymeric surface. In general, non-treated PE and PS are only composed of hydrocarbons. Nevertheless, XPS analysis revealed residues of oxygen (O/C <0.5 %) on non-treated PE and PS associated with contaminations of the surrounding air. However, the results presented in Table 1 indicate a significant oxidation of plasma-treated surfaces which is shown by the remarkable increase in the oxygen-content after plasma exposure which is caused by reactions of plasma-generated active surface sites with oxygen-containing radicals from the plasma or by post-plasma processes with ambient air. Furthermore, with prolonged treatment time the O/C ratio of the PE and PS surface was increased. In terms of different process gases a further increase of the O/C ratio after Ar/O<sub>2</sub> (1 % O<sub>2</sub>) plasma was observed. Besides oxygen also nitrogen and silicon were detected. Nitrogen was observed on PE and PS after Ar plasma treatment only but not after Ar/O<sub>2</sub> exposure ascribe to the suppression of the N<sub>2</sub> production when oxygen is admixed. The silicon originated probably from the quartz capillary of the jet or from contamination of the polymer caused by the manufacturing process because silicon was not detected for every measurement after plasma treatment. Since the plasma-modified surfaces showed remarkable changes in the carbon and oxygen content, only the O/C ratio will be discussed in more detail. Radial profiles of the O/C ratio for PE and PS after 60 s Ar plasma exposure are exemplarily shown in Figs. 6 and 7. In particular, Fig. 6 shows the radial profile of the O/C ratio on plasma-treated PE dependent on the jet-nozzle to substrate distance. It was found that at an axial distance of 5 mm, the evolution of the O/C ratio on the PE surface can be observed across 50 mm, while the modified area at an axial distance of 12 mm was reduced to a width of 20 mm. Furthermore, the maximum O/C ratio decreased with axial distance which consequently resulted in a decreased hydrophilicity which is shown in the inset of Fig. 6. Besides the decreasing wettability with decreasing O/C ratio, further differences concerning the variation of the O/C ratio can be observed. Whereas at a jet-nozzle to substrate distance of 5 mm the incorporation of oxygen starts far away of the impinging jet, the oxygen content determined at a distance of 12 mm was highest in the centre of the plasma treatment. However, a comparison of the radial profile of the O/C ratio obtained for PE (Fig. 6, dashed line) and PS (Fig. 7, solid line) after 60 s Ar plasma treatment showed

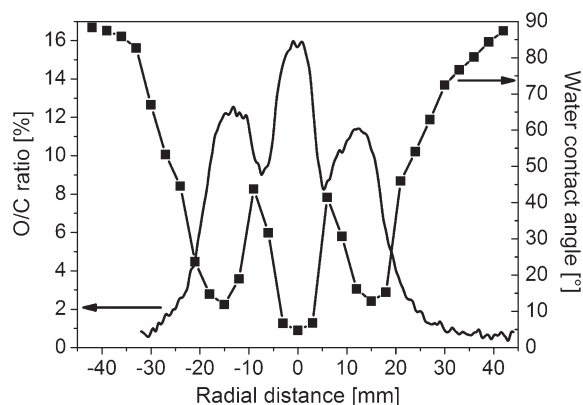
**Table 1** Surface chemical composition (in atom %) of PE and PS dependent on the treatment time and the gas mixture composition (5 slm Ar and 5 slm Ar + 0.05 slm O<sub>2</sub>)

	PE			PS		
	C	O	O/C	C	O	O/C
Non-treated	99.7	0.3	0.3	99.5	0.5	0.5 <sup>b</sup>
30 s Ar	84.9	15.1	17.8	88.9	10.1	11.4
30 s Ar/O <sub>2</sub>	85.1	14.9	17.5	85.6	13.3	15.5 <sup>b</sup>
60 s Ar	86.1	13.2	15.5 <sup>a</sup>	86.6	13.4	15.5
60 s Ar/O <sub>2</sub>	85.9	14.1	16.4	86.2	13.8	16.0
180 s Ar	86.0	13.4	15.6 <sup>b</sup>	84.5	14.0	16.6 <sup>a,b</sup>
180 s Ar/O <sub>2</sub>	84.1	15.8	18.8 <sup>b</sup>	83.5	15.7	18.8 <sup>b</sup>

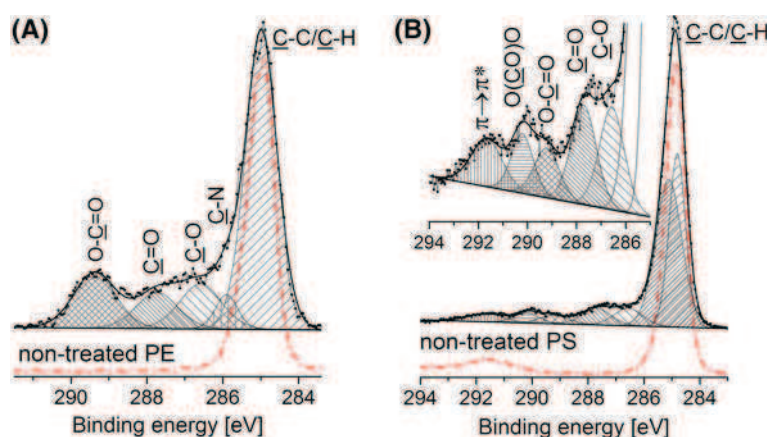
<sup>a</sup> Traces of N <0.9 %

<sup>b</sup> Traces of Si <0.8 %

**Fig. 7** Radial profile of the O/C ratio (*straight line*) and the water contact angle (*straight line with box*) of PS after 60 s Ar plasma treatment obtained at a jet-nozzle to substrate distance of 5 mm



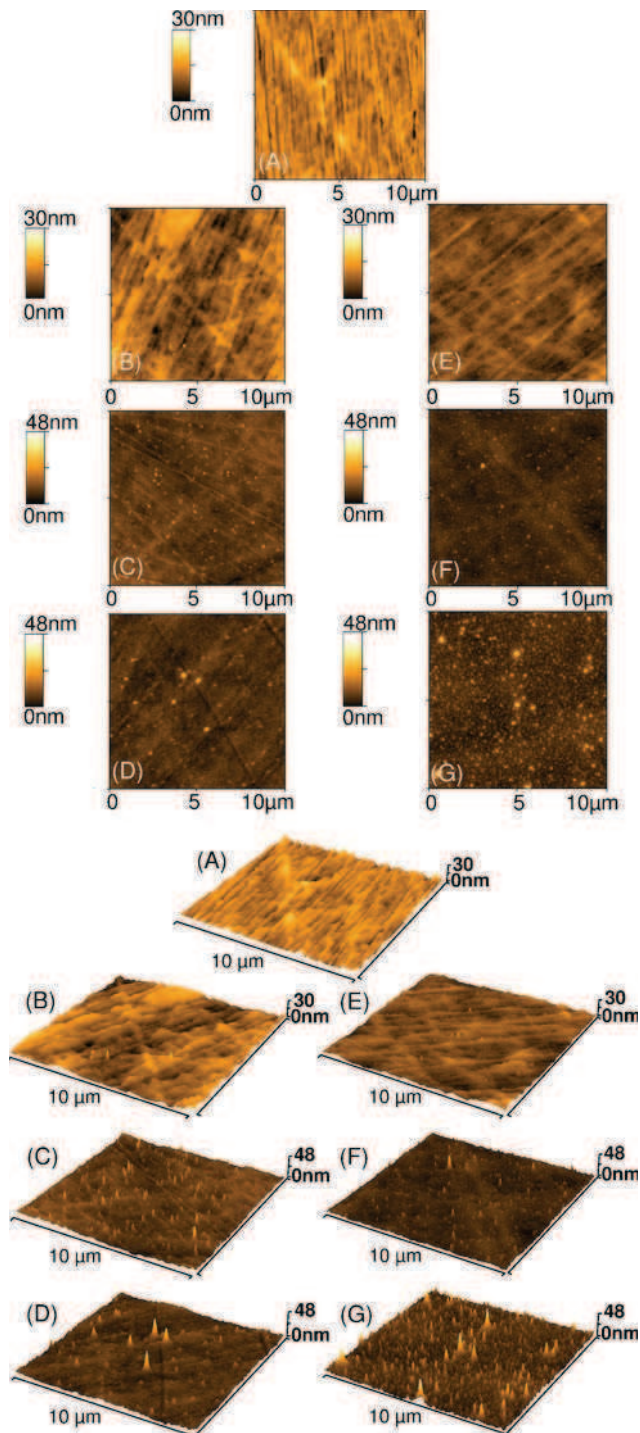
some distinct differences. While the O/C ratio on PS was at its maximum in the centre of the polymer (position '0') (Fig. 7), the highest O/C ratio on PE was besides the area where the jet directly impinged the surface (Fig. 6). Furthermore, Fig. 7 clearly indicates the correlation between the radial profile of the wettability and the radial distribution of the O/C ratio of PS. The lowest water contact angle was measured where the highest O/C ratio was determined. It is well known that the incorporation of oxygen on the polymeric surface results in the formation of functional groups. Therefore, the changes in carbon bindings were analyzed by fitting the high resolution C 1s peak. Figure 8 shows the highly resolved measured C 1s spectra of non-treated PE (Fig. 8a) and PS (Fig. 8b) compared to the treated ones. The C 1s spectrum of non-treated PE (dashed line) showed the expected C–H/C–C<sub>aliph</sub> binding at a binding energy (BE) of 285.0 eV whereas the C 1s spectrum of non-treated PS (dashed line) was mainly composed of C–C<sub>arom</sub> binding at BE of 284.6 eV (carbon atoms in the phenyl ring), C–H/C–C<sub>aliph</sub> at BE of 285.0 eV (aliphatic carbon), and the characteristic  $\pi \rightarrow \pi^*$  shake-up transition at BE of 291.7 eV arising from the electrons of the aromatic ring [35]. Curve-fitting of the highly resolved C 1s peak of PE after 60 s Ar



**Fig. 8** Highly resolved measured C 1s peak of: **a** non-treated PE (*straight line with dash*) and Ar plasma-treated PE. Also shown is the peak fit of plasma-exposed PE. **b** non-treated PS (*straight line with dash*) and Ar plasma-treated PS. The inset contains the magnification of the peak fit of plasma-treated PS. (Treatment conditions: 5 mm jet-nozzle to substrate distance, 60 s)

**Fig. 9**  $10 \times 10 \mu\text{m}$  AFM images (2-D and 3-D) of PS exposed to Ar (for **b**: 30 s; **c**: 60 s; **d**: 180 s) and Ar + 1 %  $\text{O}_2$  (for **e**: 30 s; **f**: 60 s; **g**: 180 s) plasma. The jet-nozzle to substrate distance was 5 mm. Image **a** represents non-treated PS. The AFM images were recorded at position '0' of the polymeric substrate

plasma treatment exhibited five components positioned at binding energies of 285.0, 286.0, 286.6, 287.9, and 289.3 eV assigned to  $-\text{C}-\text{C}/-\text{C}-\text{H}$ ,  $-\text{C}-\text{N}$ ,  $-\text{C}-\text{O}$  (hydroxyl, ether),  $-\text{C}=\text{O}$  (ketone, aldehyde), and  $-\text{O}-\text{C}=\text{O}$  (carboxylic groups, ester), respectively (Fig. 8a). For PS an additional peak at 290.3 eV can be observed after plasma treatment, which was attributed to  $-\text{O}-(\text{C}=\text{O})-\text{O}$  (carbonate) groups. The appearance of  $-\text{O}-(\text{CO})-\text{O}$  bindings represents highly oxidized carbon which is characterized by the maximum concentration of bonded oxygen. The formation of  $-\text{O}-(\text{CO})-\text{O}$  is based on the interaction of oxygen with the aromatic phenyl rings which results in ring breaking. Therefore, the C 1s high resolution spectrum of PS before and after plasma treatment showed a decrease in the intensity of the  $\pi \rightarrow \pi^*$  shake-up peak from 6.5 to 2.6 % as well as a decrease in the intensity of the  $\text{C}-\text{C}_{\text{arom}}$  binding from 62.4 to 49.5 % after plasma treatment. Besides the functionalization of hydrocarbons by oxidation reactions, the surface ablation process is a further effect of plasma treatment which becomes more and more dominant at longer plasma exposure [36]. It is most likely that etching processes are based on chemically reactive species produced by admixture of oxygen. Thus, a breaking of  $\text{C}-\text{C}/\text{C}-\text{H}$  bonds is initiated, causing the release of low molecular weight fragments,  $\text{CO}_2$ , and  $\text{H}_2\text{O}$  [37]. Certainly, the etch process influences the surface texture which in turn depends on the process gas [38, 39]. The change in the surface topography of PS with respect to the type of gas and treatment time (30, 60, and 180 s) is shown by selected representative  $10 \times 10 \mu\text{m}$  2-D and 3-D AFM images in Fig. 9. Figure 9a displays the surface topography of non-treated PS characterized by a lamellar structure due to manufacturing process. After 30 s exposure to Ar (Fig. 9b) and Ar/ $\text{O}_2$  (1 %  $\text{O}_2$ ) plasma (Fig. 9e), the topography of PS showed no significant changes, the lamellar structure is still visible, only a few surface grains appeared at the surface which was also observed by Teare et al. [40]. PS samples exposed to Ar and Ar/ $\text{O}_2$  plasma for 60 s exhibited initial changes in the surface topography characterized by the appearance of several nanostructures on their surfaces (Fig. 9c, f). Long-time plasma treatment with exposure times above 180 s led to an increase of the number of grains and the formation of spikes of considerable height. The difference between the surfaces treated with Ar and Ar/ $\text{O}_2$  plasma is noticeable: after Ar/ $\text{O}_2$  plasma treatment the surface was characterized by a multitude of spikes and grains, the lamellar structure of the non-treated PS was not recognizable anymore. Furthermore, the spikes on the Ar plasma treated PS surface were not as dense packed as on PS after 180 s Ar/ $\text{O}_2$  plasma exposure. These dramatic changes in the surface topography can be attributed to the admixture of oxygen leading to the generation of chemically reactive species etching the polymer surface. The results of the determined surface roughness  $R_{\text{rms}}$  and  $R_a$  varied between 2–3 nm for  $R_a$  and 2–4 nm for  $R_{\text{rms}}$ , respectively, independent on whether the PS surface is exposed to plasma or not. Hence, the  $R_{\text{rms}}$  and  $R_a$  values are not indicative of showing differences concerning the topography of non-treated and plasma-treated PS. Nevertheless, some insight can be gained from the information on the particle size extracted from the corresponding histogram of the AFM images depicted in Fig. 10. The histogram of an AFM image is a height distribution function and provides information on the probability that a spot has a defined height on the scanned area. Figure 10 shows, that the distribution of the particles sizes after plasma treatment was different compared to that of the non-treated PS. Whereas the particle size of the structure on the non-treated PS surface (Fig. 10a) varied between 20 and 40 nm a shift was observed to smaller size values after plasma treatment (Fig. 10b–d),



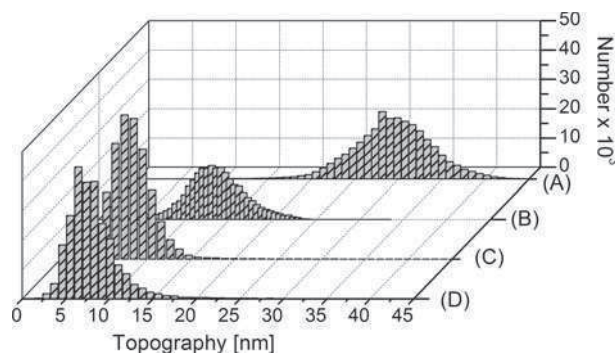


**Fig. 10** Histogram derived from the topographic AFM data of: **a** non-treated PS, **b** after 30 s Ar plasma, **c** after 180 s Ar plasma, and **d** after 180 s Ar/O<sub>2</sub> plasma, respectively

most of all after long-time plasma treatment (Fig. 10c, d). Briefly, 180 s Ar/O<sub>2</sub> plasma exposure led to the formation of a uniform surface with spike-like structures and grains showing particle sizes between 5 and 10 nm (Fig. 10d). A similar result was observed for plasma-treated PE. Figure 11 shows a characteristic selection of AFM images of non-treated PE (Fig. 11a) and of PE exposed to Ar plasma (Fig. 11b) and to Ar/O<sub>2</sub> (1 % O<sub>2</sub>) plasma (Fig. 11c) for 180 s. The non-treated PE surface was found to be considerably rougher (the  $R_{\text{rms}}$  value varied between 20 nm and 30 nm) compared to PS and its structure was more granular and hilly. However, a change in the topography of PE was observed after plasma treatment, too. The Ar plasma-treated PE surface was uniformly covered with spikes of similar height whereas Ar/O<sub>2</sub> plasma-treated PE exhibited a surface of densely packed spikes containing many huge spikes. The influence of the jet-nozzle to substrate distance on the morphological changes of the polymers was also investigated. For instance, PS exposed to Ar/O<sub>2</sub> plasma for 180 s at a jet-nozzle to substrate distance of 12 mm showed no morphological differences compared to the non-treated PS (data not shown). After 180 s Ar plasma exposure a few little grains were found on the PS surface. Deduced from these results it can be assumed that etching processes decline with increasing distances to the jet-nozzle which was already reported previously [33].

## Conclusions and Outlook

The presented study demonstrated the plasma-based bio-decontamination efficiency of an atmospheric pressure plasma jet operated with argon and different admixtures of molecular oxygen. Plasma inactivation kinetics of *B. atrophaeus* spores indicated that the optimum lethal effect depends on the type of feed gas and the jet-nozzle to substrate distance. Therefore, a maximum reduction of viable number of micro-organisms was achieved after 180 s argon-oxygen (with an admixture of 1% oxygen) plasma operating close to the jet-nozzle. Moreover, it was demonstrated that reactive oxygen species play a determinative role in non-thermal plasma bio-decontamination. Furthermore, this contribution showed to what extent the plasma dose, required for bio-decontamination, influenced the chemical and morphological surface properties of polymers. For the given plasma conditions, all polymers showed a decrease of the contact angle after a few seconds treatment time. Despite the localized plasma treatment in the centre of the substrate, a considerably larger



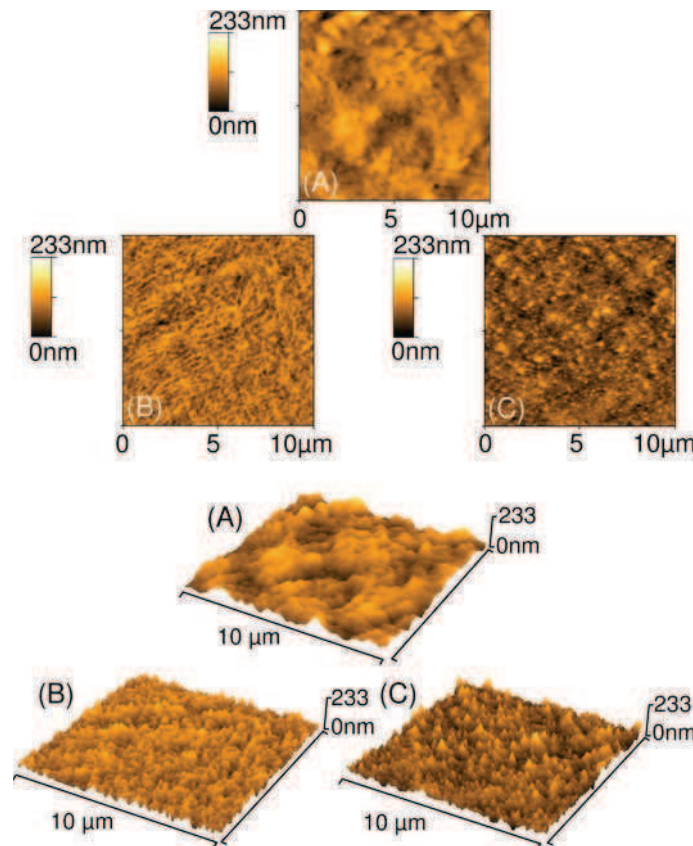


**Fig. 11**  $10 \times 10 \mu\text{m}$  AFM images (2-D and 3-D) of PE. **a** non-treated PE, **b** after 180 s Ar plasma treatment, **c** after 180 s Ar + 1 %  $\text{O}_2$  plasma treatment. The jet-nozzle to substrate distance was 5 mm. The AFM images were recorded at position '0' of the polymeric substrate

region was modified far away from the impinging jet. The elemental distribution of PE and PS recorded by X-ray photoelectron spectroscopy showed an incorporation of oxygen due to C–C/C–H bond breaking and the formation of oxygen-containing functional groups, especially C–O,  $\text{–C=O–}$ , and  $\text{O=C–O}$  groups. Apart from surface functionalization, also etching processes occurred during the plasma treatment. Etching processes resulted in the formation of a spike-like texture of PE and PS especially when oxygen was added to the argon plasma. Summarizing, short plasma treatment times led to inactivation of micro-organisms and to an effective change in surface properties, for instance of the surface wettability. The plasma assisted improved hydrophilicity and the creation of specific oxygen functionalities on the polymer surface revealed the possibility to enhance the field of applications. Thus, a careful choice of plasma parameters allows for a user-defined tailoring of the surface properties. Since the atmospheric pressure plasma jet can be operated at low temperatures, it offers a promising method of decontamination and modification of heat sensitive material. With regard to cell adhesion, biological response to polymeric materials depends strongly on surface chemistry and structure. Further studies will be performed to investigate the effect of plasma functionalization on cell behavior.

## References

1. Chu PK, Chen JY, Wang LP, Huang N (2002) *Mater Sci Eng R Rep* 36:143
2. van Kooten TG, Spijker HT, Busscher HJ (2004) *Biomaterials* 25:1735
3. Noeske M, Degenhardt J, Strudthoff S, Lommatzsch U (2004) *Int J Adhes Adhes* 24:171
4. Moisan M, Barbeau J, Crevier MC, Pelletier J, Philip N, Saoudi B (2002) *Pure Appl Chem* 74:349
5. Hippler R, Kersten H, Schmidt M, Schoenbach KH (2008) *Low temperature plasmas: fundamentals, technologies, and techniques*. Wiley VCH vol. 1, Weinheim
6. Laroussi M, Alexeff I, Kang WL (2000) *IEEE Trans Plasma Sci* 28:184
7. Rupf S, Lehmann A, Hannig M, Schafer B, Schubert A, Feldmann U, Schindler A (2010) *J Med Microbiol* 59:206
8. Stoffels E, Kieft IE, Sladek REJ, van den Bedem LJM, van der Laan EP, Steinbuch M (2006) *Plasma Sources Sci Technol* 15:169
9. Weltmann KD, Brandenburg R, von Woedtke T, Ehlbeck J, Foest R, Stieber M, Kindel E (2008) *J Phys D Appl Phys* 41:6
10. Laroussi M (2005) *Plasma Process Polym* 2:391
11. Moreau M, Orange N, Feuilleux MGJ (2008) *Biotechnol Adv* 26:610
12. Ionita ER, Ionita MD, Stancu EC, Teodorescu M, Dinescu G (2009) *Appl Surf Sci* 255:5448
13. Gomathi N, Mishra D, Maiti TK, Neogi S (2009) *J Adhes Sci Technol* 23:1861
14. Lommatzsch U, Pasedag D, Baalman A, Ellinghorst G, Wagner HE (2007) *Plasma Process Polym* 4:1041
15. Siow KS, Britcher L, Kumar S, Griesser HJ (2006) *Plasma Process Polym* 3:392
16. Pavithra D, Doble M (2008) *Biomed Mater* 3:13
17. Gessner C, Bartels V, Betker T, Matucha U, Penache C, Klages CP (2004) *Thin Solid Films* 459:118
18. Junkar I, Cvelbar U, Lehocky M (2011) *Mater Tehnol* 45:221
19. Weltmann KD, Kindel E, Brandenburg R, Meyer C, Bussiahn R, Wilke C, von Woedtke T (2009) *Contrib Plasma Phys* 49:631
20. Lange H, Foest R, Schaefer J, Weltmann KD (2009) *IEEE Trans Plasma Sci* 37:859
21. Navratil Z, Trunec D, Smid R, Lazar L (2006) *Czech J Phys* 56:B944
22. Ehlbeck J, Schnabel U, Polak M, Winter J, von Woedtke T, Brandenburg R, von dem Hagen T, Weltmann KD (2011) *J Phys D-Appl Phys* 44:18
23. Shintani H, Sakudo A, Burke P, McDonnell G (2010) *Exp Ther Med* 1:731
24. Foest R, Bindemann T, Brandenburg R, Kindel E, Lange H, Stieber M, Weltmann KD (2007) *Plasma Process Polym* 4:460
25. Laroussi M (2002) *IEEE Trans Plasma Sci* 30:1409
26. Lim JP, Uhm HS, Li SZ (2007) *Phys Plasmas* 14:6
27. Schulz-von der Gathen V, Schaper L, Knake N, Reuter S, Niemi K, Gans T, Winter J (2008) *J Phys D-Appl Phys* 41:6
28. Dobrynin D, Fridman G, Friedman A, Fridman A (2009) *New J Phys* 11:26
29. Xiong Z, Lu XP, Feng A, Pan Y, Ostrikov K (2010) *Phys Plasmas* 17:6
30. Bornholdt S, Wolter M, Kersten H (2010) *Eur Phys J D* 60:653
31. Setlow P (2006) *J Appl Microbiol* 101:514
32. Brandenburg R, Ehlbeck J, Stieber M, von Woedtke T, Zeymer J, Schluter O, Weltmann KD (2007) *Contrib Plasma Phys* 47:72
33. Fricke K, Quade A, Ohl A, Schröder K, von Woedtke Th (2009) In: von Keudell A, Winter J, Böke M, Schulz-von der Gathen V (eds) *Proceedings of the 19th international symposium on plasma chemistry (ISPC 19)*, Bochum (Germany) edited by, contr. P1.8.29 ([www.ispc-conference.org](http://www.ispc-conference.org))
34. Vogelsang A, Ohl A, Steffen H, Foest R, Schröder K, Weltmann KD (2010) *Plasma Process Polym* 7:16
35. Beamson G, Briggs D (1992) *The Scienta ESCA 300 data base*. John Wiley & Sons, Chichester
36. Fricke K, Steffen H, von Woedtke T, Schroeder K, Weltmann KD (2011) *Plasma Process Polym* 8:51
37. Egitto FD (1990) *Pure Appl Chem* 62:1699
38. Ataefard M, Moradian S, Mirabedini M, Ebrahimi M, Asiaban S (2008) *Plasma Chem Plasma Process* 28:377
39. Coen MC, Dietler G, Kasas S, Groning P (1996) *Appl Surf Sci* 103:27
40. Teare DOH, Ton-That C, Bradley RH (2000) *Surf Interface Anal* 29:276



## **5.2 “Atmospheric Pressure Plasma: A high-performance tool for the efficient removal of biofilms”**

Katja Fricke, Ina Koban, Helena Tresp, Lukasz Jablonowski, Karsten Schröder, Axel Kramer, Klaus-Dieter Weltmann, Thomas von Woedtke, and Thomas Kocher

*PLOS ONE*, vol. 7, no. 8, pp. 1-8, Aug, **2012**



# Atmospheric Pressure Plasma: A High-Performance Tool for the Efficient Removal of Biofilms

Katja Fricke<sup>1\*</sup>, Ina Koban<sup>2</sup>, Helena Tresp<sup>1,3</sup>, Lukasz Jablonowski<sup>2</sup>, Karsten Schröder<sup>1</sup>, Axel Kramer<sup>4</sup>, Klaus-Dieter Weltmann<sup>1</sup>, Thomas von Woedtke<sup>1</sup>, Thomas Kocher<sup>2</sup>

**1** Leibniz Institute for Plasma Science and Technology e.V. (INP Greifswald), Greifswald, Germany, **2** Unit of Periodontology, Dental School, University of Greifswald, Greifswald, Germany, **3** Centre for Innovation Competence Plasmatis, Greifswald, Germany, **4** Institute for Hygiene and Environmental Medicine, University of Greifswald, Greifswald, Germany

## Abstract

**Introduction:** The medical use of non-thermal physical plasmas is intensively investigated for sterilization and surface modification of biomedical materials. A further promising application is the removal or etching of organic substances, e.g., biofilms, from surfaces, because remnants of biofilms after conventional cleaning procedures are capable to entertain inflammatory processes in the adjacent tissues. In general, contamination of surfaces by micro-organisms is a major source of problems in health care. Especially biofilms are the most common type of microbial growth in the human body and therefore, the complete removal of pathogens is mandatory for the prevention of inflammatory infiltrate. Physical plasmas offer a huge potential to inactivate micro-organisms and to remove organic materials through plasma-generated highly reactive agents.

**Method:** In this study a *Candida albicans* biofilm, formed on polystyrene (PS) wafers, as a prototypic biofilm was used to verify the etching capability of the atmospheric pressure plasma jet operating with two different process gases (argon and argon/oxygen mixture). The capability of plasma-assisted biofilm removal was assessed by microscopic imaging.

**Results:** The *Candida albicans* biofilm, with a thickness of 10 to 20  $\mu\text{m}$ , was removed within 300 s plasma treatment when oxygen was added to the argon gas discharge, whereas argon plasma alone was practically not sufficient in biofilm removal. The impact of plasma etching on biofilms is localized due to the limited presence of reactive plasma species validated by optical emission spectroscopy.

**Citation:** Fricke K, Koban I, Tresp H, Jablonowski L, Schröder K, et al. (2012) Atmospheric Pressure Plasma: A High-Performance Tool for the Efficient Removal of Biofilms. PLoS ONE 7(8): e42539. doi:10.1371/journal.pone.0042539

**Editor:** Maria Gasset, Consejo Superior de Investigaciones Científicas, Spain

**Received:** February 22, 2012; **Accepted:** July 9, 2012; **Published:** August 6, 2012

**Copyright:** © 2012 Fricke et al. This is an open-access article distributed under the terms of the Creative Commons Attribution License, which permits unrestricted use, distribution, and reproduction in any medium, provided the original author and source are credited.

**Funding:** This work was supported by a grant from Bundesministerium für Bildung und Forschung (BMBF) - Federal Ministry of Education and Research, grant no. 13N9779 and 13N11188. The funders had no role in study design, data collection and analysis, decision to publish, or preparation of the manuscript.

**Competing Interests:** The authors have declared that no competing interests exist.

\* E-mail: k.fricke@inp-greifswald.de

## Introduction

Physical plasmas are fully or partially ionized gases which are generated by supplying energy to gaseous medium leading to dissociation of molecular bonds and ionization reactions. Hence, plasma consists of positively and negatively charged ions, electrons as well as neutral atoms and molecules (e.g. radicals) [1]. Furthermore, depending on the ionized gas, ultraviolet radiation can be emitted. Plasma can be categorized in high temperature or low temperature plasmas. The latter group of plasmas is subject of the present paper. In low temperature plasmas noble gases, such as argon and helium, and chemically active gases (e.g. oxygen and nitrogen) are commonly used. Moreover, low temperature plasmas are classified by the temperature of all species (electrons, ions, and neutral species) in thermal and non-thermal plasmas [1]. Owing to its low neutral gas temperature (near or around room temperature) non-thermal plasmas may offer new biomedical applications such as bio-decontamination or sterilization of heat sensitive materials (e.g. polymers) and modification of surfaces for subsequent medical applications [2]. Furthermore, due to the moderate gas temper-

ature of non-thermal plasmas and, above all, the possibility of their generation at atmospheric pressure conditions, the application of these plasmas on living tissues is possible [3]. The effect of non-thermal plasmas on the inactivation of micro-organisms has been extensively studied over the past decade [4] concluding that effective inactivation of micro-organisms is based on plasma-generated highly reactive agents including UV photons, oxygen species ( $\text{O}_2^-$ ,  $\text{O}_3$ ,  $\text{O}$ ), charged particles as well as electric fields [5,6,7,8]. Inactivation of microbial pathogens is important, but a further challenging task is the complete removal of killed micro-organisms and their organic remnants by physical plasmas. Plasma appears to be a promising technique to eliminate organic material from surfaces without having toxic residue effects [9] and without damaging the underlying surface.

Biofilms are a serious medical problem [10,11]. They consist of a complex system of micro-organisms embedded within a self-produced extracellular matrix [12]. The extracellular matrix stabilizes the biofilm architecture, embeds essential materials like nutrients from the surrounding environment, and provides a certain degree of resistance against environmental threats,

antimicrobial agents, and the host immune response [13]. Pathogenic biofilms are involved in 65% or more of nosocomial infections [14]. For instance, *C. albicans* is considered as the most prevalent fungal biofilm-forming pathogen which causes life-threatening infections by colonizing polymers used for medical devices, such as dental material, stents, prostheses, implants, and catheters [13]. Therefore, *C. albicans* biofilm was used as a prototypic biofilm in this study. To minimize the risk of infections, surfaces can be cleaned and disinfected with different methods including ultrasound, ionizing radiation, and antimicrobial agents [15]. In general, for the removal of biofilms the mechanical procedure is the method of choice, because antimicrobial agents cannot penetrate into and inactivate biofilms [11,16]. But among the conventional techniques, research efforts have led to the development of alternative methods for the elimination of micro-organisms by applying non-thermal plasmas. The possibility to remove biological contaminants using physical plasmas was first mentioned by Whittaker *et al.*, which investigated the application of low-pressure plasma for cleaning of endodontic files [17]. Since then, only few scientists have done investigations in the field of plasma-assisted etching of biological substances. Baxter *et al.* studied the removal of prions from surgical instruments exposed for one hour to Ar/O<sub>2</sub> low-pressure plasma [18]. Rossi *et al.* reported an etching rate of 20 nm/s for a protein layer of bovine albumin which was exposed to Ar/O<sub>2</sub> plasma at low-pressure [19]. However, these studies were focused on using vacuum plasma technologies to eliminate proteins. In recent years, a lot of effort has been put into the development of non-thermal plasma devices operating at atmospheric pressure. But so far, little is reported on the application of atmospheric pressure plasma for etching of organic substances. In particular, the capability of atmospheric pressure plasma for the elimination of complex biological systems (e.g. biofilms) is not extensively studied, yet. Ermolaeva *et al.* investigated the bactericidal effect of several minutes of Ar plasma on *Pseudomonas aeruginosa* biofilms [20]. Rupf *et al.* studied the removal of dental biofilms by means of an atmospheric pressure plasma jet operating with helium as well as a combination of plasma and water spray [21].

In preliminary studies the impact of plasma-generated species, provided by the atmospheric pressure plasma jet, on synthetic polymers was already investigated to obtain detailed information on the plasma-initiated etching mechanism (e.g. influence of the applied process gas and of the operating distance on the etching efficacy) [22]. Furthermore, synthetic polymers were chosen since the elemental compositions of these polymers are in some way similar to those of cell constituents of micro-organisms. Hence, the studied polymers can be considered as model constituents for cell compounds whose elemental composition mainly include C, H, O, N, and P. For instance, the cell wall of *C. albicans* is predominantly composed of 80–90% of carbohydrates, 6–25% of proteins, and 1–7% of lipids [23], whereas the biofilm matrix of *C. albicans* mainly contains polysaccharides [24]. Therefore, the present study is focused on the transition of the investigations obtained on abiotic surfaces to living micro-organisms organized in a biofilm to determine the efficacy of the atmospheric pressure plasma jet in etching of micro-organisms. Besides, based on its similar and, most important, its well defined chemical composition, synthetic polymers can be easily analyzed by surface techniques under defined conditions compared to complex microbial systems. Thus, the etching rates of these materials will be compared to etching rates estimated for the biofilm. Furthermore, the use of synthetic polymers allows a more detailed look into the mechanistic pathway of substance removal.

This contribution is focused on analyzing: 1. The etching efficacy of argon (Ar) and argon/oxygen (Ar/O<sub>2</sub>) atmospheric pressure plasma jet on 7-day old *C. albicans* biofilms. 2. Estimation of etching rates by the determination of the biofilm thickness. 3. The dimension of the plasma-influenced area, by using the synthetic polymer poly(ether ether ketone) (PEEK) as model for the biofilm, as it features similar etching rates. 4. The influence of plasma-generated species on the etching process by performing optical emission spectroscopy (OES).

## Results and Discussion

The investigations demonstrate the removal or etching of biofilms by means of an atmospheric pressure plasma jet and extend our previous data, in which the efficacy of the plasma jet in killing, but not in removal of micro-organisms, was shown [25,26]. Figure 1 shows representative images of *C. albicans* biofilms before and after 60 s (A) Ar/O<sub>2</sub> gas flow (control), (B) Ar plasma, and (C) Ar/O<sub>2</sub> plasma exposure. Initial removal - apparent as bright spots representing the PS subsurface - of *C. albicans* biofilm was observed after 60 s Ar plasma treatment (Fig. 1 (B)). Distinct biofilm removal, however, could be observed only with Ar/O<sub>2</sub> plasma (Fig. 1 (C)). Figure 2 depicts a comparison of non-treated biofilm and biofilm exposed to (D) Ar and (E) Ar/O<sub>2</sub> gas discharge plasma for 300 s. As can be seen in Fig. 2 D, longer Ar plasma exposure time did not result in substantial etching of the biofilm. In contrast, an almost complete removal of biofilm was obtained after Ar/O<sub>2</sub> plasma treatment (Fig. 2 (E)). Consequently, to obtain increased biofilm removal, long time exposure was required. All control samples exposed to non-ionized Ar and Ar/O<sub>2</sub> gases for 60 s and 300 s showed no biofilm etching. Hence, the process gas alone did not result in biofilm removal. To estimate the etching efficacy of the plasma jet, the biofilm-covered surface area of each sample was calculated before and after plasma exposure. The results of plasma-etched surface areas, i.e. the difference of the biofilm-covered area before and after exposure to gas discharge plasma, depending on treatment times and process gases, are displayed in Fig. 3. As previously noted, even longer treatment times with Ar plasma did not significantly increase the etched biofilm surface area. After 300 s Ar plasma exposure a maximum surface area of 5000 μm<sup>2</sup> of initial 35171 μm<sup>2</sup> (mean of the untreated biofilm-covered surface area) was etched. Compared to Ar plasma treatment, the admixture of oxygen increased the biofilm removal considerably, especially for treatment times above 60 s. Further shown in Fig. 3, is the percentage decrease of the biofilm (right y-axis). A reduction in biofilm-covered surface area of only 12% was attained with 300 s Ar plasma. In contrast, already after 180 s Ar/O<sub>2</sub> plasma exposure, approximately 95% of the biofilm was etched. Consequently, the admixture of oxygen is crucial to obtain a sufficient efficacy in biofilm removal.

To gain further insight into the mechanism of biofilm etching and to identify reactive plasma species that are involved in the surface effects induced by plasma exposure, the plasma was characterized by performing optical emission spectroscopy. The spectral characteristics in the ultraviolet/visible (UV/VIS) range of Ar and Ar/O<sub>2</sub> plasma are plotted in Fig. 4. The emission spectrum of the Ar gas discharge was mainly dominated by atomic lines of Ar between 670 and 850 nm in the visible range. Furthermore, emission lines of OH at 309 nm and of the second positive system of molecular nitrogen N<sub>2</sub> at 337 nm were identified in the UV range (240–400 nm). The OH radical was probably formed from water vapors present in the ambient air [27]. In contrast, the optical emission spectrum of Ar/O<sub>2</sub> plasma showed additional emission lines of high intensity of atomic oxygen at 777.4 nm and



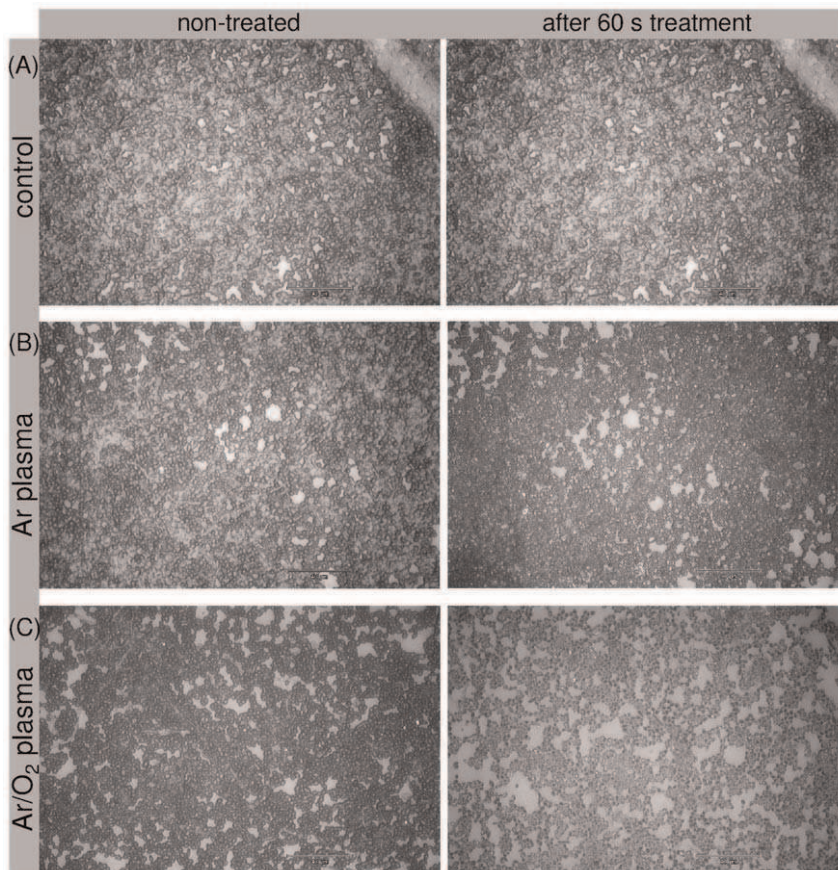


**Figure 1. Influence of different gas discharge plasmas on 7-day old *Candida albicans* biofilms grown on polystyrene wafer.** The samples were washed and dried by air flow before plasma treatment. The microscopic images were taken with a magnification of 200 at the same sample position before (left column) and after plasma treatment (right column) A: The control sample was only exposed to the Ar/O<sub>2</sub> gas flow for 60 s without plasma ignition. B: The biofilm sample was exposed to 5 slm Ar plasma. C: The biofilm sample was exposed to plasma composed of a gas mixture of 5 slm Ar and 0.05 slm O<sub>2</sub> (total admixture of 1% O<sub>2</sub>).  
doi:10.1371/journal.pone.0042539.g001

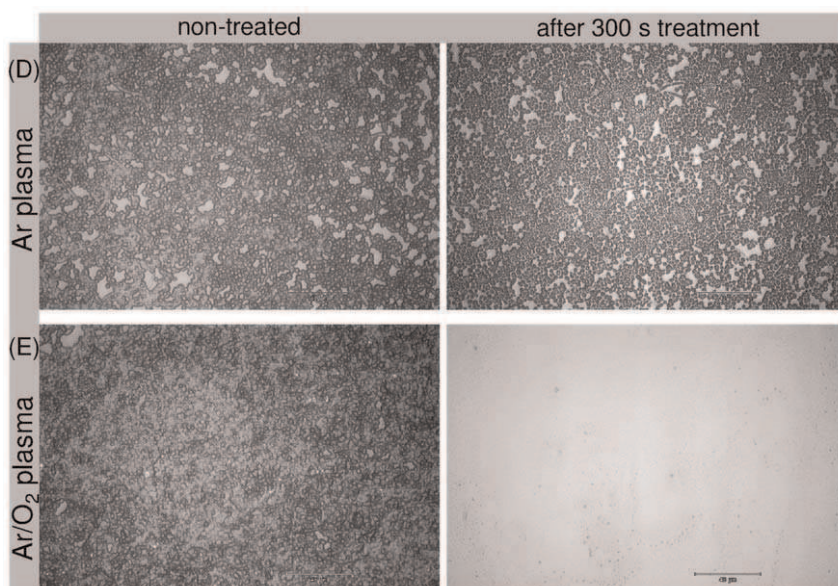


**Figure 2. Plasma-dependent removal of 7-day old *Candida albicans* biofilms grown on polystyrene wafer.** exposed to: (D) Ar gas discharge plasma (5 slm Ar) and (E) Ar/O<sub>2</sub> gas discharge plasma (5 slm Ar+0.05 slm O<sub>2</sub>) for 300 s.  
doi:10.1371/journal.pone.0042539.g002

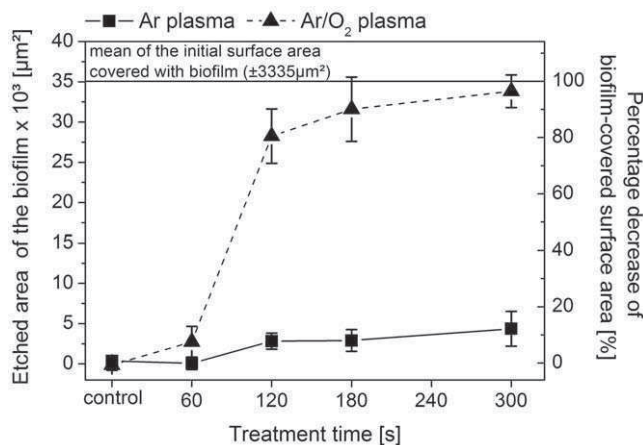


**Figure 3. Comparison between Ar plasma (—■—) and Ar/O<sub>2</sub> plasma (---▲---) on etched surface area of 7-day old *Candida albicans* biofilms depending on the plasma treatment time (n = 5; mean ± SD).** The biofilm-covered surface area was measured before and after plasma treatment. The control represents samples exposed to the gas flow without plasma ignition for 60 and 300 s. The initial surface area of the biofilm was  $35171 \pm 3335 \mu\text{m}^2$  (n = 60). The right y-axis represents the percentage decrease of the biofilm-covered surface area.

doi:10.1371/journal.pone.0042539.g003

844.6 nm in the visible region which were caused by dissociative excitation and direct excitation processes. Neither emission lines of OH nor of N<sub>2</sub> were observed in the UV range of Ar/O<sub>2</sub> plasma. Consequently, the admixture of oxygen resulted in collisional quenching of N<sub>2</sub> and OH lines [28] which suppressed the excitation and production mechanisms. Since the previous results indicated a reduced etching efficacy by using Ar plasma, it is most likely that UV radiation had a little effect on biofilm etching. Furthermore, the comparison of the ratio of the intensity of the emission lines of O (I<sub>O</sub>) at 844.6 nm and Ar (I<sub>Ar</sub>) at 750.4 nm of both gas discharges revealed an I<sub>O</sub>/I<sub>Ar</sub> ratio of 0.6 for Ar/O<sub>2</sub> plasma and an I<sub>O</sub>/I<sub>Ar</sub> ratio of 0.05 for Ar plasma. Hence, the portion of oxygen in the spectrum of Ar/O<sub>2</sub> plasma is remarkable higher. Deduced from these results it can be assumed that reactive oxygen species played a major role for biofilm removal and hence, that plasma-assisted etching was mainly a chemically driven process.

In preliminary studies synthetic polymers were investigated with respect to the capability of the applied plasma jet to etch hydrocarbon based aliphatic and aromatic polymers [22]. Especially, the impact of different process gases (argon and different argon/oxygen mixtures) and the influence of the chemical structure on etching rates were examined. Briefly, the etching rates of aliphatic polymers (polyethylene, polypropylene, and poly(methyl methacrylate)) varied between  $R = 180 \text{ nm/s}$  and  $R = 300 \text{ nm/s}$ , whereas the etching rates of aromatic polymers (polystyrene, polycarbonate, and poly(ether ether ketone)) were comparatively lower, ranging from  $R = 50 \text{ nm/s}$  for poly(ether ether ketone) up to  $R = 150 \text{ nm/s}$  for polycarbonate. Consequently, the etching rate depends not only on the process gas, but also on the chemical structure of the material to be etched.

The calculation of the etching rate requires the measurement of the thickness of the *C. albicans* biofilm, which equaled the distance between the lowest position (surface of the PS wafer) and the highest position (top of the biofilm). Since the best result in biofilm removal was achieved using Ar/O<sub>2</sub> gas discharge plasma with treatment times of 300 s, the etching rates were estimated only for

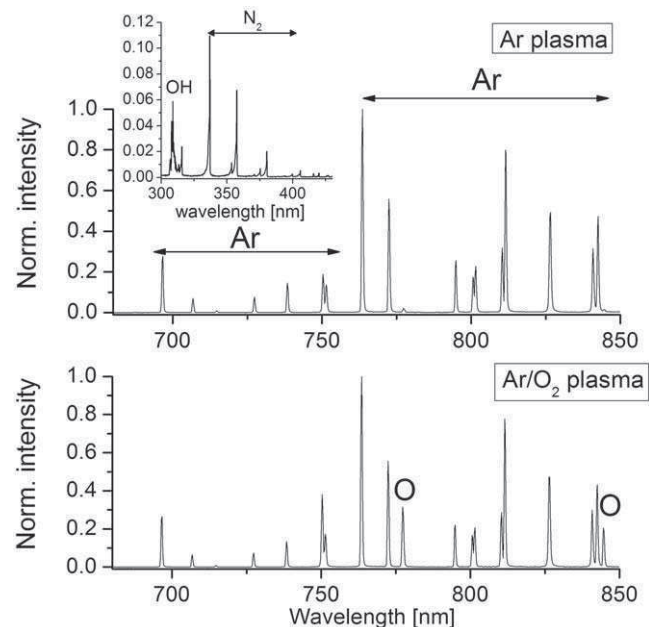


**Figure 4. Intensity of excited plasma-generated species in the Ar and Ar/O<sub>2</sub> gas discharge.** Overview optical emission spectra in the visible range (680–850 nm) of Ar plasma (5 slm Ar) and Ar/O<sub>2</sub> plasma (5slm Ar+0.05 slm O<sub>2</sub>) measured at a distance of 7 mm to the jet-nozzle by means of a dual channel fiber optical spectrometer (Avantes AvaSpec 2048-2-USB2). The spectra were relative calibrated, normalized to the exposure time, and analyzed using the software Spectrum Analyzer. In the upper spectrum excited species generated in the Ar gas discharge are shown, in particular atomic Ar in the range of 680–850 nm. The inset figure shows the emission spectrum of Ar plasma in the UV range (300–430 nm) which exhibits emission lines of OH at 309 nm and of the 2nd positive system of N<sub>2</sub> at 337–391 nm. The lower spectrum exhibits excited species generated in Ar/O<sub>2</sub> plasma which is dominated by emission lines of atomic Ar and additional emission lines of atomic O at 777.4 nm and 844.6 nm. Not shown is the emission spectrum in the UV range due to the absence of emission lines.

doi:10.1371/journal.pone.0042539.g004

this exposure time. Hence, before plasma treatment, the biofilm thickness was measured revealing a minimum biofilm thickness of approximately 10 μm and a maximum biofilm thickness of approximately 20 μm (these data are obtained from 5 biofilm-covered PS wafers; n = 3 on each sample). These variations in thicknesses were due to the inhomogeneous biofilm formation. Consequently, biofilm etching rates of  $R = 33 \text{ nm/s}$  (for the biofilm thickness of 10 μm) to  $R = 67 \text{ nm/s}$  (for the biofilm thickness of 20 μm) with Ar/O<sub>2</sub> plasma could be computed.

Since the investigations on biofilms revealed some drawbacks, such as the restricted thickness of biofilms to several micrometers, the variation of the thickness due to its inhomogeneous growth, and their sensitivity towards some surface analysis techniques, the polymer PEEK, as a substitute for biofilm, was used to overcome these limitations. Furthermore, the use of a model ensured consistent and reproducible conditions for a detailed analysis of the etching process. Additionally, PEEK was chosen since its etching rate is similar to the etching rates of the biofilm obtained in this study [22].

An important aspect of biofilm removal was the localized effect of the plasma treatment. Figure 5 exemplarily shows that the effective biofilm removal was restricted to a few millimeters after 180 s Ar/O<sub>2</sub> plasma exposure. The dark regions represent the densely packed *C. albicans* biofilm, whereas the bright areas display



the pristine PS surface. The diameter of the etched surface was in the range of 1.5 to 2 mm. Since the thickness of the biofilm varied, some regions were completely free of micro-organisms, whereas some areas were still covered with remnants. Additionally, Fig. 5 shows a sharp boundary between the plasma-affected area, where most of the biofilm was etched, and unaffected biofilm. Similar observation was reported by Koban *et al.* [29]. To get more details on the real extent of the plasma-etched surface, a surface profiling system was applied. Since the texture of the biofilm was too soft for this technique, the surface analysis was carried out on PEEK surfaces; otherwise the biofilm would be scraped off the surface by the diamond needle of the surface profiler. The surface profile of the plasma-treated substrate was measured through the zone of the localized plasma treatment on the polymer (line scan) (see Fig. 6 with inset). Figure 6 displays the surface profile of PEEK exposed to Ar/O<sub>2</sub> gas discharge for 60, 120, 180, and 300 s, respectively. Note that '0' represents the position of the localized plasma treatment. The surface profiles exhibit that the etching depth increased with prolonged plasma exposure. Furthermore, the most intensive etching process occurred directly on axis of the Ar/O<sub>2</sub> plasma jet (see also [22]). Hence, the removal of PEEK was mainly restricted to an area of 2 mm in diameter, which corresponds to the finding of the biofilm-etched area in Fig. 5. However, the observed distinct border between unaffected and etched-area after Ar/O<sub>2</sub> plasma (see Fig. 5) might be due to the localized presence of reactive plasma species. Hence, the distribution of selected optical emission lines of atomic Ar at 750.4 nm and atomic O at 844.6 nm was analyzed along the radial distance which is shown in Fig. 7. Further shown in Fig. 7 is the radial surface profile of PEEK after 180 s Ar/O<sub>2</sub> plasma exposure to illustrate the correlation between plasma species and surface etching. It can be seen that the etching profile of PEEK proceeds along with the intense optical emission of Ar and O. Hence, the highest intensities of emission lines were directly obtained in the region of the impinging plasma jet. Beyond the gas discharge, the emission intensity declined with increased radial distance. According to the radial measured OES spectra, the surface profile of PEEK showed an enhanced etching effect in the range of the highest emission intensities of Ar and O. Consequently, it can be assumed that the localized etching process is attributed to the presence of reactive species in the impinging plasma effluent, whose effectiveness in surface etching decreases with radial distance. Although OES is a suitable technique to verify excited species, it is not applicable to measure densities of species in the ground state. For this purpose laser-based plasma diagnostic (e.g. photon absorption laser induced fluorescence – TALIF) will be used in future studies to elucidate the influence of O and O<sub>3</sub> in plasma-assisted etching processes in more detail.

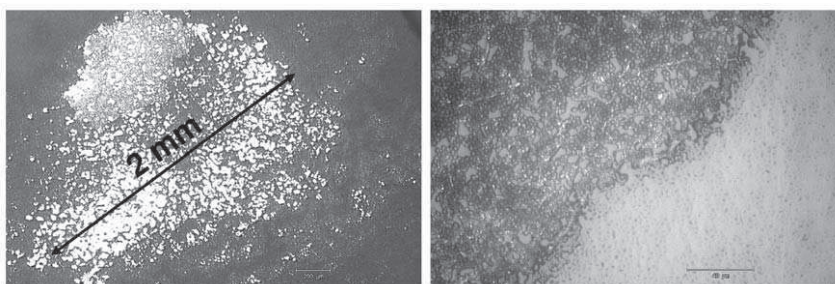


**Figure 5. Extent of the plasma-etched surface area after 180 s Ar/O<sub>2</sub> plasma exposure.** Images taken at 50-fold magnification on the left and at 200-fold magnification on the right. Left: The dark area represents the densely packed biofilm whereas the bright areas display the PS wafer surface. An etched area of 2 mm in diameter was measured. Right: Sharp boundary between the plasma-affected area and the still present biofilm. doi:10.1371/journal.pone.0042539.g005

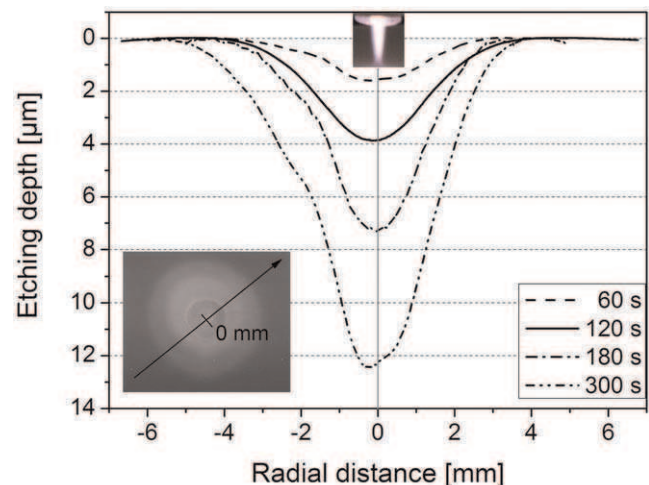


**Figure 6. Effectively plasma-etched surface of poly(ether ether ketone) (PEEK) dependent on the treatment time.** Radial surface profile of PEEK exposed to Ar/O<sub>2</sub> gas discharge plasma (5 slm Ar+0.05 slm O<sub>2</sub>) for 60, 120, 180, and 300 s at a jet-nozzle to substrate distance of 7 mm recorded by a stylus surface profiler. '0' represents the position of the localized plasma treatment. Inset figure: depiction of the surface profile measurement on PEEK. In the centre of the polymer (position 0 mm) the etched crater can be observed. doi:10.1371/journal.pone.0042539.g006

The mechanisms of plasma etching at atmospheric pressure are not yet fully understood, but it is most likely that the main mechanism is based on the chemical process of oxidation which might be described as follows: (i) impinging plasma-emitted reactive species like excited atoms/molecules and radicals result in bond-breaking of molecules, particularly hydrocarbon compounds; (ii) in following reactions two main processes occur simultaneously: modification and etching of plasma-created open bonds on the surface of micro-organisms, leading for instance to the formation of molecular fragments and volatile compounds emanating from the cells. Hence, plasma-exposed micro-organisms exhibit morphological changes, such as reduction in cell size [30,31,32] or the appearance of deep etch channels in the cell [33] up to complete cellular destruction [34]. Especially the presence of chemically reactive species, like atomic oxygen and ozone, easily react with these open bonds, which facilitates a faster etching of molecules [22,33].

Summarizing, the results of this study provide evidence that non-thermal atmospheric pressure plasmas are efficient in etching of 7-day old *Candida albicans* biofilms. Moreover, it was shown that



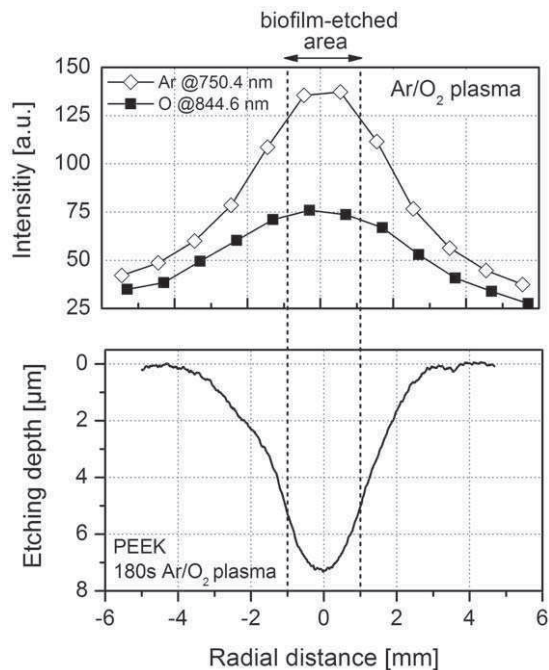


**Figure 7. Radial distribution of plasma-generated species in the Ar/O<sub>2</sub> gas discharge plasma and the direct relation to the radial etching profile of poly(ether ether ketone) (PEEK).** The upper graph shows the intensity of atomic Ar at 750.4 nm and atomic O at 844.6 nm depending on the radial distance recorded end-on at a distance of 7 mm to the jet-nozzle by means of a dual channel fiber optical spectrometer (Avantes AvaSpec 2048-2-USB2). The spectra were relative calibrated, normalized to the exposure time, and analyzed using the software Spectrum Analyzer. '0' represents the position of the atmospheric pressure plasma jet. In the lower figure the radial etching profile of PEEK after 180 s Ar/O<sub>2</sub> plasma exposure is displayed. The surface profile was recorded by means of a stylus surface profiler (Dektak 3ST, Veeco, USA). The dashed lines mark the extent of the biofilm-etched surface (see Fig. 5). doi:10.1371/journal.pone.0042539.g007

an almost complete elimination of biofilm was achieved by adding molecular oxygen to the argon gas discharge plasma. Hence, Ar/O<sub>2</sub> plasma efficiently removes biofilms with an etching rate of approximately 33 to 67 nm/s. This etching rate corresponds to rates on previously studied synthetic polymers. The high chemical activity of Ar/O<sub>2</sub> gas discharge is based on the presence of reactive atomic and molecular radicals interacting with organic materials resulting in etching. These findings may help to modulate plasma processes, which enhance the production of desired reactive species for improved process efficiency. Consequently, the atmospheric pressure plasma jet offers the possibility to eliminate micro-organisms.

## Materials and Methods

### Pre-treatment of the PS wafer

*Candida albicans* biofilms were cultured on polystyrene (PS) wafers (diameter of 10 mm) purchased from Becton Dickinson (Falcon™ Ref 351016). PS wafers were used because of their uniformly flat surfaces which enable a better microscopic imaging and simplify the measurement of the biofilm thickness. Previous cultivation experiments have shown that the formation of *Candida albicans* biofilm on pristine PS surfaces was not homogenous and partly washable by water. Therefore, the PS wafers were amino-functionalized in a low-pressure microwave (2.54 GHz) plasma

processing reactor (Plasma-Finish, Schwedt, Germany) using 40 sccm pure ammonia to support the adhesion of *Candida albicans* cells. The PS wafers were exposed for 30 s in the downstream region of the gas discharge plasma. Further information about the reactor as well as the functionalization procedure is described in [35]. The ammonia plasma-treated PS surfaces showed a non-washable dense packed *Candida* biofilm after cultivation.

### Biofilm formation

The strongly biofilm-forming strain *Candida albicans* ATCC 10231 (ATCC = American Type Culture Collection, Rockville, MD, USA) was used [36]. *C. albicans* was suspended into YPD Broth (Yeast Extract Peptone Dextrose, Sigma, Steinheim, Germany). The sterile test objects (PS wafers) were positioned in 24-well microtitre plates (Techno Plastic Products AG, Trasadingen, Switzerland). 1 ml micro-organism suspension (concentration of 10<sup>6</sup> cells/ml) was added, and incubated aerobically at 37°C. Every 24 h the medium was changed. After 7 days the medium was drawn off and the PS wafers were washed with 0.9% NaCl solution.

### Plasma source and plasma treatment

For the experiments a high-frequency (1.7 MHz, 2–6 kV<sub>pp</sub>) driven atmospheric pressure plasma jet (kINPen08, developed at the INP Greifswald) was applied (see Fig. 8). This plasma device consists of a pin-type electrode mounted in a quartz capillary (inner diameter of 1.6 mm and outer diameter of 4 mm) with an overall electric power of 65 W. The neutral gas temperature was below 80°C under the experimental conditions. A more detailed description of this type of plasma jet, version kINPen09, can be found in [25]. The influence of two different process gases on the removal of biofilms was investigated. In particular, argon (Ar) as feed gas with a gas flow of 5 standard liter per minute (slm) and a gas mixture of argon and oxygen (O<sub>2</sub>) with an admixture of 0.05 slm molecular O<sub>2</sub> (1% O<sub>2</sub>). Previous studies have shown that the highest etching rate is achieved at small distances between the nozzle-outlet and the substrate surface [22]. Hence, the samples were located at a constant distance of 7 mm from the jet-nozzle. At this working distance the tip of the Ar/O<sub>2</sub> plasma jet comes in contact with the substrate surface, whereas the Ar gas discharge plasma, with a total length of 12 mm, spreads on the treated surface. The biofilm samples were treated for 60, 120, 180, and 300 s. The control samples were exposed to the gas flow without plasma ignition. Before plasma treatment each sample was washed for several minutes using distilled water and dried by air flow to ensure that the substrate is covered with an adherent, non-washable biofilm.

### Light Microscope

The opaque biofilms were analyzed with a reflected light microscope (Zeiss Axiovert 200 M, Carl Zeiss Jena GmbH, Jena, Germany). Images were taken with a 50 and 200 fold magnification and the biofilm-covered surface area was quantified (200× magnification) with an image analysis program (analySIS® pro V. 3.0, Olympus soft imaging solutions, Münster, Germany). To obtain the biofilm-covered surface area before and after plasma treatment, the surface area of each biofilm, grown on PS, was manually traced and labeled by using analySIS®pro which subsequently calculated the marked surface area. The initial biofilm covered an averaged surface area of 35171±3335 μm<sup>2</sup> (n = 60, before treatment). To ensure that before and after plasma treatment the same position was microscopically analyzed every PS wafer was marked on the back side.

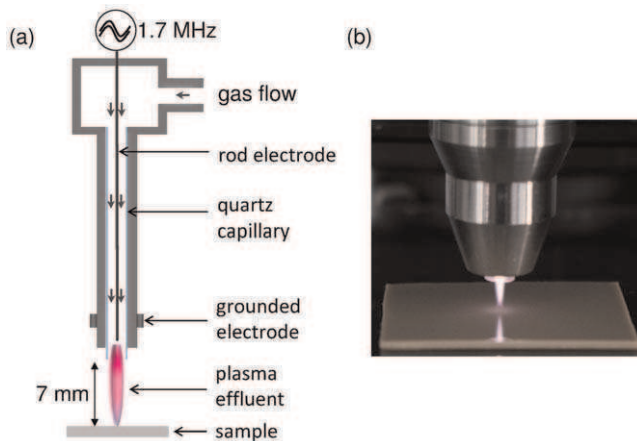


**Figure 8. The atmospheric pressure plasma jet (kINPen08, INP Greifswald, Germany).** (a) Schematic set-up of the plasma jet which consists of a pin-type electrode centered inside a quartz capillary with an inner diameter of 1.6 mm and an outer diameter of 4 mm. A high-frequency voltage (1.7 MHz, 2–6 kV<sub>pp</sub>) is coupled to the electrode. The overall electric power of the plasma device is 65 W. The plasma jet was positioned perpendicular to the sample surface with a distance of 7 mm between the nozzle outlet and the substrate surface. (b) Photograph of the plasma jet, driven with 5 slm Ar and 0.05 slm O<sub>2</sub>, impinging the PEEK surface.  
doi:10.1371/journal.pone.0042539.g008

In order to estimate an approximate etching rate  $R$  the thickness of the initial biofilm was calculated using a digital optical microscope system. Therefore, a stereoscopic image reproduction with spatial depth using the Zeiss microscope, a CCD-Camera as well as digital electronics for the processing of image data were applied. Data processing proceeds in the following way: an exposure series with constant focus position is taken. The relative movement between the sample plane and sample is carried out in a stepwise manner, where surface configuration of the sample is reconstructed from a set of optical section images to be calculated. Deduced from these images a 3-D image is generated from which the thickness of the biofilm was obtained.

### Statistical analysis

All data presented are means  $\pm$  standard deviation. For each process gas and treatment time the experiments were repeated five

times on five independent biofilm-covered PS wafers (total number of PS wafers:  $n = 60$ ), whereas for the determination of the biofilm thickness three different positions on the same sample was investigated of at least five selected samples.

### Optical emission spectroscopy (OES)

For the characterization of the plasma phase in the ultraviolet/visible (UV/VIS) spectral range, optical emission spectroscopy was applied, which is a commonly used diagnostic technique to identify excited species (e.g. atoms and molecules) present in the plasma. This method is easy to apply, very sensitive, and most important non-invasive [37]. A dual channel fiber optical spectrometer (Avantes AvaSpec 2048-2-USB2) was used. The channels were linked by an optical fiber to a cosine corrector. A quartz glass was in front of the cosine corrector. The emission lines of the plasma irradiation were measured in the range of 200 to 962 nm. OES spectra were relative calibrated, normalized to the exposure time, and analyzed using the software Spectrum Analyzer [38]. In order to analyze the radial distribution of the plasma species the fiber optics were mounted end-on by a movable holder.

### Polymer treatment and surface profilometry

The depth profile was recorded crossing the centre of the plasma-treated polymer with a stylus surface profiling system (Dektak 3ST, Veeco, USA) with a scan speed of 40  $\mu\text{m/s}$  and a force of the stylus tip on the surface of 10 mg. These investigations were focused on poly(ether ether ketone) (PEEK, purchased from Goodfellow, Germany) because of its very smooth and inflexible surface, being highly suitable for these investigations. According to the treatment of the biofilms, PEEK samples were exposed for 60, 180, 120, and 300 s to Ar/O<sub>2</sub> plasma (1% O<sub>2</sub>) at a jet-nozzle to substrate distance of 7 mm (see Fig. 8 b).

### Acknowledgments

The authors gratefully acknowledge Urte Kellner, Dagmar Jasinski, and Aniko Karpati (INP Greifswald e.V.) for excellent assistance.

### Author Contributions

Conceived and designed the experiments: KF IK KS TK. Performed the experiments: KF IK HT. Analyzed the data: KF IK HT LJ KS TK. Wrote the paper: KF IK LJ KS AK KDW TvW TK.

### References

- Hippler R, Kersten H, Schmidt M, Schoenbach KH, editors (2008) Low Temperature Plasmas: Fundamentals, Technologies, and Techniques. Weinheim: Wiley VCH
- Weltmann KD, von Woedtke T (2011) Campus PlasmaMed-From Basic Research to Clinical Proof. IEEE Trans Plasma Sci 39: 1015–1025.
- Lloyd G, Friedman G, Jafri S, Schultz G, Fridman A, et al. (2010) Gas Plasma: Medical Uses and Developments in Wound Care. Plasma Process Polym 7: 194–211.
- Ehlbeck J, Schnabel U, Polak M, Winter J, von Woedtke T, et al. (2011) Low temperature atmospheric pressure plasma sources for microbial decontamination. J Phys D-Appl Phys 44: 1–18.
- Dobrynin D, Fridman G, Friedman G, Fridman A (2009) Physical and biological mechanisms of direct plasma interaction with living tissue. New J Phys 11: 26.
- Moreau M, Orange N, Feuilloley MGJ (2008) Non-thermal plasma technologies: New tools for bio-decontamination. Biotechnol Adv 26: 610–617.
- Boudam MK, Moisan M, Saoudi B, Popovici C, Gherardi N, et al. (2006) Bacterial spore inactivation by atmospheric-pressure plasmas in the presence or absence of UV photons as obtained with the same gas mixture. J Phys D-Appl Phys 39: 3494–3507.
- Gaunt LF, Beggs CB, Georgiou GE (2006) Bactericidal action of the reactive species produced by gas-discharge nonthermal plasma at atmospheric pressure: A review. IEEE Trans Plasma Sci 34: 1257–1269.
- Sureshkumar A, Sankar R, Mandal M, Neogi S (2010) Effective bacterial inactivation using low temperature radio frequency plasma. Int J Pharm 396: 17–22.
- Kim J, Sudbery P (2011) Candida albicans, a Major Human Fungal Pathogen. Journal of Microbiology 49: 171–177.
- Hoiby N, Ciofu O, Johansen HK, Song ZJ, Moser C, et al. (2011) The clinical impact of bacterial biofilms. International Journal of Oral Science 3: 55–65.
- Davey ME, O'Toole GA (2000) Microbial biofilms: from ecology to molecular genetics. Microbiol Mol Biol Rev 64: 847–867.
- Harriott MM, Noverr MC (2009) Candida albicans and Staphylococcus aureus Form Polymicrobial Biofilms: Effects on Antimicrobial Resistance. Antimicrob Agents Chemother 53: 3914–3922.
- Mah TFC, O'Toole GA (2001) Mechanisms of biofilm resistance to antimicrobial agents. Trends Microbiol 9: 34–39.
- Otto C, Zahn S, Rost F, Zahn P, Jaros D, et al. (2011) Physical Methods for Cleaning and Disinfection of Surfaces. Food Eng Rev 3: 171–188.
- Ramage G, Vande Walle K, Wickes BL, Lopez-Ribot JL (2001) Characteristics of biofilm formation by Candida albicans. Rev Iberoam Micol 18: 163–170.
- Whittaker AG, Graham EM, Baxter RL, Jones AC, Richardson PR, et al. (2004) Plasma cleaning of dental instruments. J Hosp Infect 56: 37–41.
- Baxter HC, Campbell GA, Whittaker AG, Jones AC, Aitken A, et al. (2005) Elimination of transmissible spongiform encephalopathy infectivity and

- decontamination of surgical instruments by using radio-frequency gas-plasma treatment. *J Gen Virol* 86: 2393–2399.
19. Rossi F, Kylian O, Rauscher H, Hasiwa M, Gilliland D (2009) Low pressure plasma discharges for the sterilization and decontamination of surfaces. *New J Phys* 11: 33.
  20. Ermolaeva SA, Varfolomeev AF, Chernukha MY, Yurov DS, Vasiliev MM, et al. (2011) Bactericidal effects of non-thermal argon plasma in vitro, in biofilms and in the animal model of infected wounds. *J Med Microbiol* 60: 75–83.
  21. Rupf S, Idlibi AN, Al Marrawi F, Hannig M, Schubert A, et al. (2011) Removing Biofilms from Microstructured Titanium Ex Vivo: A Novel Approach Using Atmospheric Plasma Technology. *PLoS ONE* 6: 9.
  22. Fricke K, Steffen H, von Woedtke T, Schroeder K, Weltmann KD (2011) High Rate Etching of Polymers by Means of an Atmospheric Pressure Plasma Jet. *Plasma Process Polym* 8: 51–58.
  23. Chaffin WL, Lopez-Ribot JL, Casanova M, Gozalbo D, Martinez JP (1998) Cell wall and secreted proteins of *Candida albicans*: Identification, function, and expression. *Microbiol Mol Biol Rev* 62: 130–180.
  24. Al-Fattani MA, Douglas LJ (2006) Biofilm matrix of *Candida albicans* and *Candida tropicalis*: chemical composition and role in drug resistance. *J Med Microbiol* 55: 999–1008.
  25. Weltmann KD, Kindel E, Brandenburg R, Meyer C, Bussiahn R, et al. (2009) Atmospheric Pressure Plasma Jet for Medical Therapy: Plasma Parameters and Risk Estimation. *Contrib Plasma Phys* 49: 631–640.
  26. Koban I, Holtfreter B, Hübner NO, Matthes R, Sietmann R, et al. (2011) Antimicrobial efficacy of non-thermal plasma in comparison to chlorhexidine against dental biofilms on titanium discs in vitro - proof of principle experiment. *J Clin Periodontol* 38: 956–965.
  27. Machala Z, Janda M, Hensel K, Jedlovsky I, Lestinska L, et al. (2007) Emission spectroscopy of atmospheric pressure plasmas for bio-medical and environmental applications. *J Mol Spectrosc* 243: 194–201.
  28. Schulz-von der Gathen V, Schaper L, Knake N, Reuter S, Niemi K, et al. (2008) Spatially resolved diagnostics on a microscale atmospheric pressure plasma jet. *J Phys D-Appl Phys* 41: 6.
  29. Koban I, Matthes R, Hübner NO, Welk A, Meisel P, et al. (2010) Treatment of *Candida albicans* biofilms with low-temperature plasma induced by dielectric barrier discharge and atmospheric pressure plasma jet. *New J Phys* 12: 16.
  30. Rossi F, Kylian O, Hasiwa M (2006) Decontamination of surfaces by low pressure plasma discharges. *Plasma Process Polym* 3: 431–442.
  31. Pompl R, Jamitzky F, Shimizu T, Steffes B, Bunk W, et al. (2009) The effect of low-temperature plasma on bacteria as observed by repeated AFM imaging. *New J Phys* 11: 11.
  32. Joaquin JC, Kwan C, Abramzon N, Vandervoort K, Brelles-Marino G (2009) Is gas-discharge plasma a new solution to the old problem of biofilm inactivation? *Microbiology* 155: 724–732.
  33. von Keudell A, Awakowicz P, Benedikt J, Raballand V, Yanguas-Gil A, et al. (2010) Inactivation of Bacteria and Biomolecules by Low-Pressure Plasma Discharges. *Plasma Process Polym* 7: 327–352.
  34. Rupf S, Lehmann A, Hannig M, Schäfer B, Schubert A, et al. (2010) Killing of adherent oral microbes by a non-thermal atmospheric plasma jet. *J Med Microbiol* 59: 206–212.
  35. Schröder K, Meyer-Plath A, Keller D, Besch W, Babucke G, et al. (2001) Plasma-induced surface functionalization of polymeric biomaterials in ammonia plasma. *Contrib Plasma Phys* 41: 562–572.
  36. He M, Du MQ, Fan MW, Bian ZA (2007) In vitro activity of eugenol against *Candida albicans* biofilms. *Mycopathologia* 163: 137–143.
  37. Kudrle V, Vasina P, Talsky A, Mrázková M, Stec O, et al. (2010) Plasma diagnostics using electron paramagnetic resonance. *J Phys D-Appl Phys* 43: 13.
  38. Navrátil Z, Trunec D, Smid R, Lazar L (2006) A software for optical emission spectroscopy - problem formulation and application to plasma diagnostics. *Czech J Phys* 56: B944–B951.

### **5.3 “High Rate etching of Polymers by Means of an Atmospheric Pressure Plasma Jet”**

Katja Fricke, Hartmut Steffen, Thomas von Woedtke, Karsten Schröder, and Klaus-Dieter Weltmann

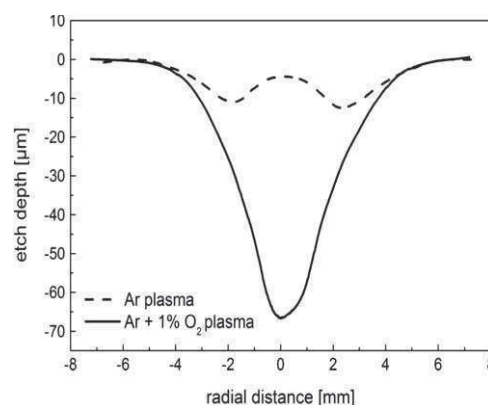
*Plasma Processes and Polymers*, vol. 8, no. 1, pp. 51-58, **2011**



# High Rate Etching of Polymers by Means of an Atmospheric Pressure Plasma Jet

Katja Fricke,\* Hartmut Steffen, Thomas von Woedtke, Karsten Schröder, Klaus-Dieter Weltmann

The impact of atmospheric pressure plasma on surfaces, in particular its potential application of modification and decontamination of different materials has been intensively investigated. In this study, the etching capability of an atmospheric pressure plasma jet is shown. A variety of polymers [e.g., polyethylene and poly (ether ether ketone)] was exposed to pure argon and argon/oxygen plasma. The influence of the oxygen admixture (up to 1%) and of the jet-nozzle to substrate distance on the etch rate of chemically different polymers was explored. Particular attention was applied on the feasible use of atmospheric pressure plasma on biofilm removal. For that reason a theory was postulated with each polymer representing a model compound of bacterial cells. The etch rates were obtained by determination of the mass loss and etch profiles after plasma exposure. The experiments showed that reactive oxygen species play an important role in the polymer removal which results in etch rates of 50 up to  $300 \text{ nm} \cdot \text{s}^{-1}$  depending on the polymeric material. These high etch rates imply that non-thermal atmospheric plasma jets could be used for removal of organic material including micro-organisms from surfaces.



## Introduction

Most polymer surfaces, especially hydrocarbon surfaces, are chemically inert, have low surface energies, and low adhesion properties which is disadvantageous for many practical applications. The use of non-thermal plasma treatment of polymers leads to changes of the chemical and physical surface characteristics without affecting the bulk properties. Additionally, considering that polymeric materials are very heat sensitive, non-thermal plasma is also a gentle method to alter the surface properties without destructive effects due to its low gas temperatures between 300 and 400 K.<sup>[1]</sup> The main processes observed in plasma

treatment of polymeric surfaces are modification, cross-linking and etching. The incorporation of atoms (e.g., O and N) into the surface during plasma exposure leads to the formation of polar groups such like hydroxyl-, carbonyl- and aldehyde groups. These functional groups influence the surface energy in such a way, that a better bonding capacity to other materials or bacteria cells can be achieved.<sup>[2–4]</sup> Furthermore, non-thermal plasma is also an environmentally friendly method to remove organic contaminants or to pattern surfaces.<sup>[5]</sup> Both applications are based on etching processes caused by ion bombardment and/or chemically reactive species. Etching of photoresist by an oxygen (O<sub>2</sub>) plasma with an etch rate of  $2 \text{ nm} \cdot \text{s}^{-1}$  was one of the first industrial applications of plasma etching in microelectronics.<sup>[6]</sup> Nowadays, plasma etching is one of the key processes used in microelectronic fabrication where CF<sub>4</sub> and CF<sub>4</sub>–O<sub>2</sub> are the widely applied gases in low-pressure plasmas. But apart from surface functionalization and

K. Fricke, H. Steffen, Th. von Woedtke, K. Schröder, K.-D. Weltmann  
Leibniz Institute for Plasma Science and Technology, Felix-  
Hausdorff-Str. 2, D-17489 Greifswald, Germany  
Fax: +49 3834 554301; E-mail: k.fricke@inp-greifswald.de



etching also cross-linking takes place during the plasma treatment. Surface cross-linking is based on the recombination of radicals generated by breaking the C–H bonds. Linkages results in a stabilization of the surface which makes for instance a further etching of the material more difficult.

But plasma sources are not only applied in the industry. Plasma medicine is a very promising field, too. Particularly, the plasma sterilization of polymeric materials is in the focus of attention.<sup>[7,8]</sup> It can be achieved with plasma that combines both, the inactivation or killing of bacteria – by producing charged particles, UV/VUV radiation, and reactive neutral species (excited atoms and molecules, radicals) – and the removal of dead cells or cell residues by plasma etching.<sup>[9,10]</sup> The atmospheric pressure plasma jet described in this paper has the capability to decontaminate polymer surfaces.<sup>[11–13]</sup> Hence, the work presented here is focused on the second requirement of plasma sterilization: the etching process at atmospheric pressure.

The surface chemical composition of bacteria cells deduced from XPS data reveals that micro-organisms mainly consist of carbohydrates, polypeptide, teichoic acids and lipids composed of C, H, O and N.<sup>[14,15]</sup> Whereby carbon is the most abundant element. For different bacteria strains the ratio of oxygen to carbon varies between 0.21 and 0.53 whereas the N/C ratio is between 0.04 and 0.082.<sup>[16]</sup> According to polymeric materials a similar elemental composition can be observed. Pelletier already pointed out, that the chemical structure of polymers is comparable to that of micro-organisms.<sup>[17]</sup> For that reason, we started this study with polymers of different chemical composition as model substances for cell components of micro-organisms. To etch organic films at atmospheric pressure, a gas mixture of argon and oxygen is often applied.<sup>[18]</sup> The main effect of the argon plasma is sputtering by ion bombardment, while oxygen admixtures produce chemically active species oxidizing organic compounds with the release of CO<sub>2</sub> and H<sub>2</sub>O. These two types of erosion may have a synergetic effect which leads to an increase of the etching capability.<sup>[19]</sup> In the uppermost polymer layers also UV/VUV photo degradation processes generated by the plasma jet operated with argon are important. This radiation leads not only to main chain scission and cross-linking of surface radicals but also the formation of low molecular weight species.

Previous investigations of plasma initiated polymer removal obtained at atmospheric pressure showed etch rates of 0.5–83 nm · s<sup>−1</sup>. For instance, Jung and Choi reported etch rates of 2 nm · s<sup>−1</sup> in Ar/O<sub>2</sub> plasma and 0.5 nm · s<sup>−1</sup> in pure Ar plasma.<sup>[20]</sup> But also other reactive gases can be used to etch materials. For instance, etching of Kapton results in an etch rate of 42–83 nm · s<sup>−1</sup> at atmospheric pressure with an helium/oxygen (He/O<sub>2</sub>)—plasma.<sup>[21]</sup> Compared to etch rates achieved at atmospheric

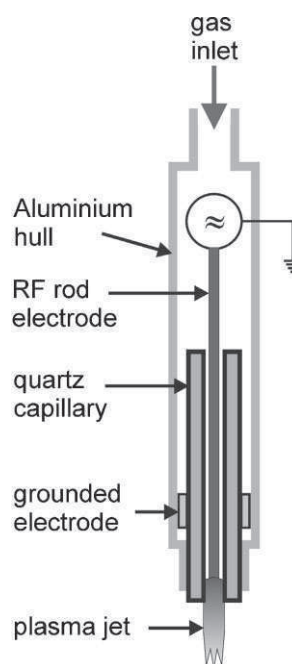
pressure, the rates reported at low-pressure plasma are much smaller. Benedikt et al. investigated the etching of hydrocarbon films exposed to mixtures of argon and oxygen and received a maximum etch rate of 0.8 nm · s<sup>−1</sup>.<sup>[19]</sup> Terlingen et al. obtained an etch rate of 0.01 nm · s<sup>−1</sup> for polyethylene with Ar plasma, Taylor and Wolf 0.5 nm · s<sup>−1</sup> for polystyrene in an O<sub>2</sub> plasma, and Pederson reported an etch rate of more than 12 nm · s<sup>−1</sup> for cellulose exposed to CF<sub>4</sub>/O<sub>2</sub> plasma.<sup>[22–24]</sup> The study described in this paper is focused on the estimation of etch rates caused by an atmospheric pressure Ar plasma and Ar/O<sub>2</sub> plasma. Results of dry etching of different polymeric materials are presented, focussing on the influence of oxygen admixture and of the jet-nozzle to substrate distance on the etch rate. Particular attention is paid on the application of the plasma jet to remove organic materials from surfaces.

## Experimental Part

### Miniaturized Atmospheric Pressure Plasma Jet

In Figure 1 the principle of the radio frequency (RF) driven (1 MHz) miniaturized atmospheric pressure plasma jet is schematically shown.

The jet is characterized by a grounded ring electrode and a centre rod electrode inside a quartz capillary (with an inner diameter of 1.6 mm and an outer diameter of 4 mm). The rod electrode is connected to the power source via a matching network. The RF power consumed by the discharge has not been measured directly; the overall electric power of 65 W applied was held constant

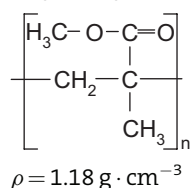


■ Figure 1. Schematic view of the plasma jet.

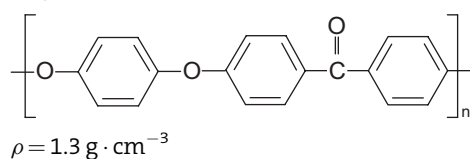


**Table 1.** Polymers used in etching experiments.

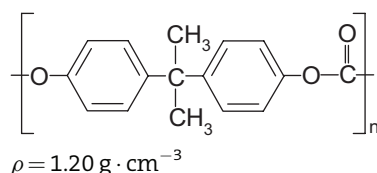
Polymethyl methacrylate (PMMA)



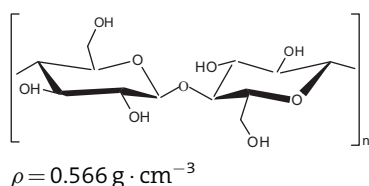
Poly(ether ether ketone) (PEEK)



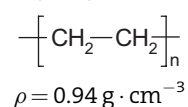
Polycarbonate (PC)



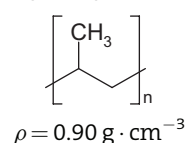
Filter paper (FP)



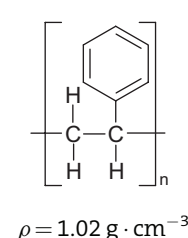
Polyethylene (PE)



Polypropylene (PP)



Polystyrene (PS)



throughout the experiments. Depending on the operating gas the length of the plasma jet varied between 12 mm (only Ar plasma) and 6 mm (Ar + 1% O<sub>2</sub> plasma). Further details of this jet are described elsewhere.<sup>[25,26]</sup> The polymers were treated localized with the plasma jet operating with argon at a flow rate of 5 slm and small admixtures of O<sub>2</sub> (0...1% in the gas flow).

## Materials

The different polymers and filter paper used during the experiments are listed in Table 1. The polymers were delivered by Goodfellow (Germany), and the filter paper (blue Ribbon filter paper 589/3) by Schleicher & Schuell Filters (Germany). From the large number of polymers special attention is paid to polyethylene, poly(ether ether ketone) and filter paper. The polymeric material was chosen according to the aspect of the removal of microorganisms by the used plasma jet. Each substrate describes a model constituent of microbial cells. For instance, PE represents long-chain hydrocarbon compounds like side chains of amino acid or lipids, proteins and sugar moieties. PEEK is an analogue to lipopolysaccharides, filter paper which consists of cellulosic fibres represents polysaccharides whereas PMMA and PC are model

compounds for amino acids. At the end of this contribution, a table of etch rates for all investigated polymers listed in Table 1 is presented.

## Determination of Etch Rates

The mass loss of the samples (size:  $1.3 \times 1.3 \text{ cm}^2$ ) was determined by weighing on an analytical ultra-microbalance (Sartorius SE 2, Göttingen, Germany). Before estimating the mass, every sample was treated with a high-performance ionizing air gun (Top Gun, SIMCO Industrial Static Control, USA). This ionizing air gun eliminates static charges which are responsible for the attraction of contaminants to the polymer surface. Furthermore, static charges hinder the mass measurements with the high sensitive microbalance.

Etch rates presented in this paper are calculated by two different methods. One way is to calculate the mass difference of the substrate after plasma etching (mass loss). This mass etch rate  $R_m$  is given by:

$$R_m = \frac{\Delta m}{t} \quad \text{with} \quad (1)$$

$\Delta m$  is the mass loss and  $t$  is the plasma treatment time. The linear etch rate which is commonly used to describe the etching of a material is given by:

$$R = \frac{R_m}{\pi r^2 \rho} \quad \text{with} \quad (2)$$

$r$  is the radius of the hole, etched during plasma exposure and  $\rho$  is the density of the etched material (see Table 1).

The radius  $r$  was estimated by measuring the radius of the hole created by the etch process. In case of Equation (2) a cylindrical shape of the etched hole is assumed, although this is definitely not the exact case in our experiments (see Figure 4). For that reason, Equation (2) gives only a rough estimation of the etch rate.

Another and more reliable possibility to determine etch rates is the measurement of surface profiles after plasma exposure. The depth profiles were recorded crossing the centre of the plasma treated polymer with a surface profiler (Dektak 3ST, Veeco, USA) with a scan speed of  $40 \mu\text{m} \cdot \text{s}^{-1}$  and a force of the stylus tip on the surface of 30 mg. These investigations were focused on PEEK, because of its very smooth and inflexible surface, being highly suitable for these investigations. But a similar etch profile was observed for all polymers.

## Results and Discussion

The effect of Ar/O<sub>2</sub> plasma on polyethylene is depicted in Figure 2. The etch rate was obtained by measuring the mass loss as a function of time. The jet-nozzle to substrate distance was chosen according to the length of the plasma jet so that the polymer surface was in close contact to the effluent and in downstream position. The data in Figure 2A suggest linear loss behaviour with increasing treatment time at different jet-nozzle to substrate distances. Because of the linearity of the results we can assume a constant mass etch rate. The surface attack by the etchant depends on the distance which might be attributed to the short

lifetimes of the reactive species and their reaction with ambient air or recombination processes during the longer pathway which results in a reduced number of etchants reaching the polymer surface. For this reason the highest weight loss is achieved at lower distance (5 mm) whereas mass differences and mass etch rates at 7 and 12 mm jet-substrate distance are almost equal.

Besides the jet-nozzle to substrate distance, also the admixture of oxygen was varied from 0 to 1%. The results are shown in Figure 2B. The etch rates increase when the gas mixture is enriched with oxygen probably to an increase of reactive oxygen species. Compared to Ar/O<sub>2</sub> plasma, the etch rate of pure Ar plasma (0% oxygen admixture) is five times smaller, attributed to the physical sputtering of Ar ions and the UV/VUV radiation which is significantly emitted in the Ar plasma.<sup>[27]</sup> Certainly, oxygen from ambient air which is admixed in the radial flowing afterglow outside the Ar effluent is involved in the etching process. The etch profiles confirm this assumption showing a remarkably different profile caused by Ar plasma compared to Ar/O<sub>2</sub> plasma (see Figure 4 and discussion there). Consequently, physical sputtering and etching by UV/VUV radiation play obviously a minor role in polymer degradation. An explanation might be the creation of unsaturated bonds on the substrate surface by the Ar plasma that do not undergo oxidizing processes because of the absence of chemically active species in the Ar plasma. Thus, unsaturated carbon-carbon bonds react with other carbons leading to cross-linking, that retards the etching process or reacts with the ambient air after plasma exposure, respectively.<sup>[28]</sup>

The mechanisms of polymer etching and modification were studied by a number of scientists.<sup>[18,29–31]</sup> For this reason only a short summary of the fundamental and important reactions is given here. As mentioned previously, depending on the gas mixture, the polymer removal is characterized by physical sputtering and chemical reac-

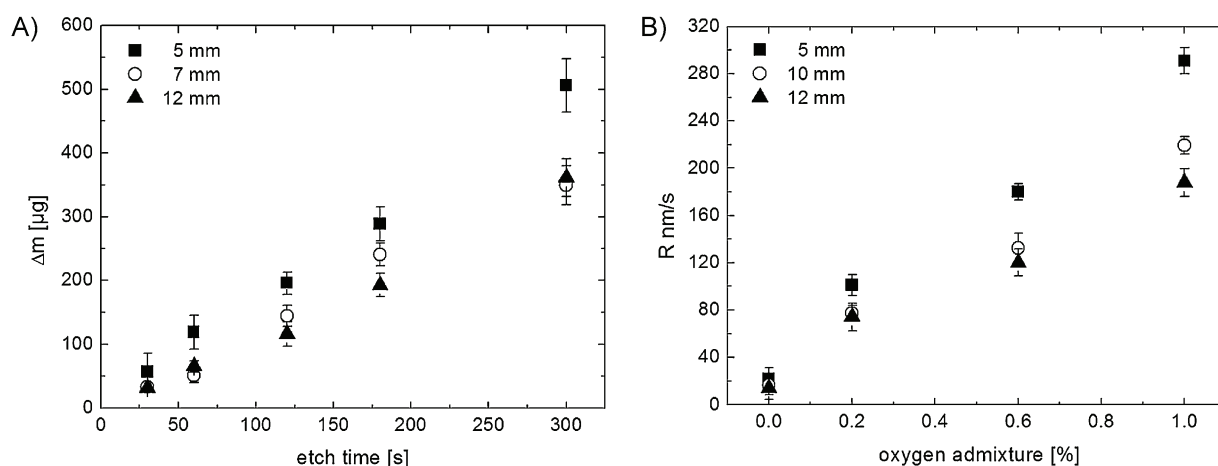
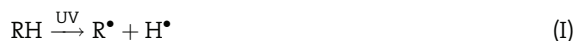


Figure 2. (A) Time dependent mass loss of polyethylene after plasma exposure with 5 slm Ar and 1% O<sub>2</sub> admixture. (B) Influence of oxygen admixture on the etch rate for 5 slm Ar at different jet-nozzle to substrate distances (mean  $\pm$  SD,  $n \geq 10$ ).

tions on the substrate surface as well as photolysis by UV radiation. The degradation, initiated by electron impact, reactive species and photons, leads to a dissociation of the polymer molecules (RH) and the formation of radicals according to:



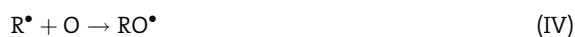
Due to the high reactivity of atomic oxygen further reaction occurs



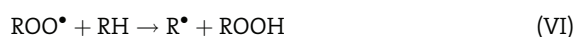
followed by



Reactive species and UV radiation produced in the plasma attacks selected carbon sites and causes an abstraction of hydrogen. The thereby formed alkyl radicals are characterized by short lifetimes and undergo various chemical reactions. In the presence of oxygen the oxidation of the surface is initiated leading to the formation of alkoxy radicals and peroxy radicals:

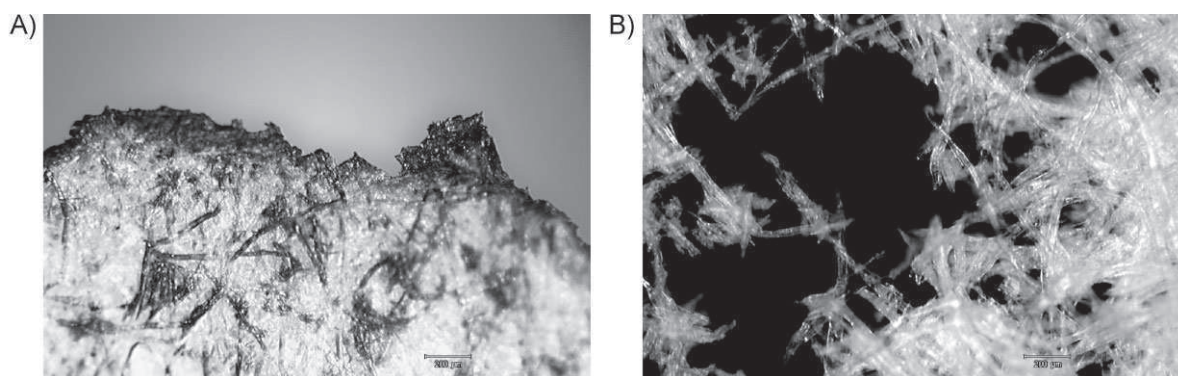


These radicals are starting points of the modification of the polymer surface, of chain scissions, and of the etching of the polymer:



End products of polymer etch reactions are CO, CO<sub>2</sub>, O<sub>2</sub>, OH and H<sub>2</sub>O. The etching and modification processes compete with the cross-linking of the substrate surface, initiated for example by peroxy radicals which results in a deactivation that can dramatically decrease the etch rates.<sup>[31]</sup> However, not only radiation and reactive species are emitted by the gas discharge, plasma treatment is also associated with the release of heat. It is known that high temperatures accelerate the etch rate, but polymers are very heat sensitive and heat damage must be prevented.<sup>[32]</sup> The difference between hot and cold burning is shown in Figure 3. The picture at Figure 3A taken after hot burning of filter paper is characterized by a melted edge, whereas the picture in Figure 3B, taken after etching with Ar/O<sub>2</sub> plasma, shows the etch hole and the residue of cellulose fibres indicating that the filter paper is etched fibre by fibre.

In order to clarify the influence of surface heating on the etch processes, additional experiments were carried out where the plasma on and plasma off times were varied (e.g., 20 s plasma on and 20 s plasma off). The size of the plasma etched hole as well as the weight loss after plasma treatment with or without plasma off times was nearly the same. This demonstrates that the temperature increase during the etch process might be negligible and that little temperature changes on the polymer surface do not significantly influence the etch rate. It should be mentioned that the oxygen admixture and the distance between substrate and jet-nozzle is crucial for the surface heating. With high oxygen admixtures (>2% O<sub>2</sub>) and at small jet-nozzle to substrate distances (<5 mm), the temperature increase becomes significant and a considerable damage of the polymer has to be expected. Surely, the extent of etching can be highly variable depending on the nature of the substrate. Taylor and Wolf figured out that strong bonds in the backbone or between backbone and side chains as in aromatic and polar functional groups make an etching more difficult.<sup>[24]</sup> Etch rates of different polymers treated with Ar/O<sub>2</sub> plasma are presented in Table 2. The etch rates are calculated by means of Equation (1) and (2).



■ Figure 3. Microscopically images of filter paper after (A) hot burning and (B) cold burning obtained by a Zeiss Axiovert 200M microscope.

**Table 2.** Etch rates of different polymers treated with 5 slm Ar and 1% O<sub>2</sub> admixture at a jet-nozzle to substrate distance of 5 mm. The radius  $r$  was estimated to about 2 mm and the etch rates were calculated according to Equation (2).

Rates	Substrates						
	FP	PP	PE	PMMA	PC	PS	PEEK
Etch rate $R$ (nm · s <sup>-1</sup> )	1 060	300	260	180	150	130	50
Mass etch rate $R_m$ (μg · s <sup>-1</sup> )	5.7	3.4	2.7	2.4	2.3	1.4	0.8

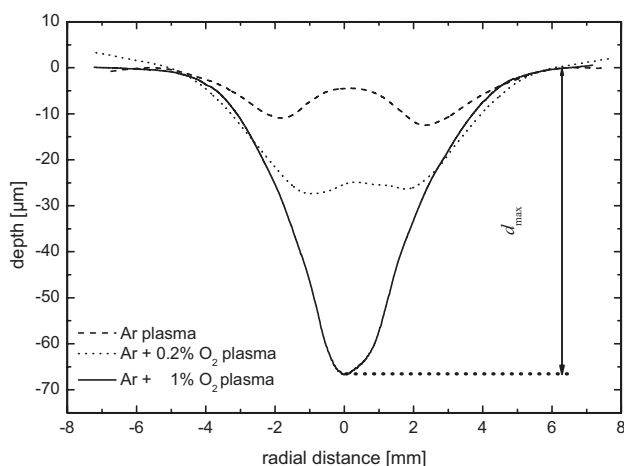


**Figure 4.** Depth profiles in PEEK after 20 min etching with 5 slm Ar, 0.2% O<sub>2</sub> and 1% O<sub>2</sub> admixture at 5 mm jet-nozzle to substrate distance. The maximum depth is 67 μm.

The etch rates of different polymers vary between 50 and 300 nm · s<sup>-1</sup>. The aromatic polymers PS and PEEK exhibit the lowest etch rates, because of the stabilization by aromatic functional groups like phenolic compounds which are more resistant against etching.

From measured depth profiles recorded with a surface profiler, etch rates can be calculated more accurately and the etch mechanism can be explored. Figure 4 gives an example of a depth profile of plasma treated PEEK. The measured depth depends strongly on the distance from the jet axis. The curve is almost symmetric. The observed irregularities (e.g., the shoulder on the right part) are assumed to be due to small asymmetries of the plasma jet and its orientation to the sample surface which is not exactly perpendicular to the surface. Figure 4 shows clearly the influence of the oxygen admixture on the etch rate profile. In case of a pure Ar plasma, the etching takes place mainly off the jet axis. The etched area shows the shape of a ring while at the jet axis almost no etching occurs. This etch ring is produced by eddies of the surrounding air and the Ar plasma which is assumed to lead to the formation of reactive oxygen species capable of etching. The etched profile can be described by two Gauss functions with their maxima at ±2 mm. The special shape of this profile shows the main influence of chemical etching by oxygen contain-

ing species clearly. Therefore, it can be assumed that ion sputtering delivers nearly no contribution to the erosion process. At low O<sub>2</sub> admixtures (Figure 4, dotted line) the etch depth increases but the entrainment of the ambient air is still remarkable. In case of Ar plasma admixed with 1% O<sub>2</sub> the etch rate has its maximum at the jet axis. The profile is almost symmetric and can be described by a single Gauss function.

Normalized depth profiles for several etch times are nearly congruent. Thus, any depth profile can be described by the product formula:

$$d(x, t) = f_n(x) d_{\max}(t) \quad \text{with} \quad (3)$$

$f_n(x)$  is the normalized depth profile with  $d_{\max} = 1$  which depends only on the distance to the jet axis ( $x$ ),  $d_{\max}(t)$  is the maximum depth which depends only on the etch time  $t$ .

The maximum etch depth depends linearly on the etch time (Figure 5). The slope of the linear fit function gives the maximum etch rate  $R_{\max} = 40.5 \text{ nm} \cdot \text{s}^{-1}$  in the centre of the hole which is in good agreement with the calculated etch rate above (Table 2) approving the measurements of the plasma generated hole.

Therefore, Equation (3) can be written as:

$$d(x, t) [\text{nm}] = f_n(x) 40.5 t [\text{s}] \quad (4)$$

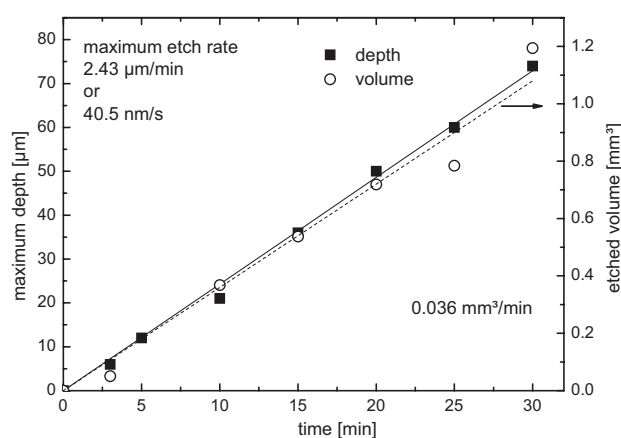


**Figure 5.** Maximum depth (filled squares) and etched volume (open circles) versus etch time for PEEK (5 slm Ar/O<sub>2</sub> (1% O<sub>2</sub>), 5 mm jet-nozzle to substrate distance).

From Equation (4) we can conclude that the etch rate is constant in time and depends only on the distance to the jet axis:

$$R(x) = f_n(x) 40.5 \frac{nm}{s} \quad (5)$$

Taking into account that the etched hole is axially symmetric, the etched volume can be calculated from the measured profile. A depth profile was fitted with Gauss functions and the volume was calculated according to:

$$V(t) = \pi \int_0^{\infty} x^2(d(t)) dx \quad (6)$$

Like the maximum depth, the etched volume depends linearly on the etch time. The slope of the linear fit function gives a volume etch rate of  $R_V = 0.6 \mu\text{m}^3 \cdot \text{s}^{-1}$ . Taking into account the density of PEEK  $\rho = 1.3 \text{ g} \cdot \text{cm}^{-3}$ , the mass etch rate can be calculated to  $R_m = 0.8 \mu\text{g} \cdot \text{s}^{-1}$  which correspond with the mass etch rate determined by weighing (see Table 2).

## Conclusion

The effect of etching with a miniaturized atmospheric pressure plasma jet on polymeric surfaces was investigated. The highest etch rates were obtained with Ar/O<sub>2</sub> plasma (up to 1% O<sub>2</sub> in the gas flow). The etch rate decreased with increasing jet-nozzle to substrate distance and increased with increasing oxygen admixture. The results show clearly that mainly chemical etching due to the reactive oxygen species is responsible for the polymer removal. Dependent on the different structures of the polymers, mass etch rates between  $3.4$  and  $0.8 \mu\text{g} \cdot \text{s}^{-1}$  and etch rates of  $50$ – $300 \text{ nm} \cdot \text{s}^{-1}$  are obtained. These values are very high compared to previous reported etch rates at atmospheric pressure. Considering that the surface of bacteria cells consists of proteins, polysaccharides and hydrocarbon like compounds, the results showed that cell components can be etched. Furthermore, taking into account that bacteria cells have a size of  $0.2$ – $4 \mu\text{m}$ , these high etch rates reveal a promising application not only for sterilizing polymeric medical devices, but also for removing organic contaminants such as micro-organisms from the polymer surface within a few seconds. First experiments concerning biofilm removal confirm this assumption, but are still under investigation. Etch profiles generated by the plasma jet were measured with a surface profiler. This method allows a better description than weighing and is thus more suitable for the investigation of etching behaviour of plasma jets. The etch profile can be calculated

by the product of a normalized profile function and the maximum depth. The normalized function depends on the jet-nozzle to substrate distance and the gas mixture. It is independent of etch time. The maximum depth depends linearly on the etch time. Assuming cylindrical symmetry, etched volume and mass etch rates can be calculated. In a further study, the chemical processes leading to polymer etching will be investigated in more detail by surface analyses with highly resolved XPS.

Received: July 12, 2010; Revised: September 27, 2010; Accepted: September 29, 2010; DOI: 10.1002/ppap.201000093

Keywords: atmospheric pressure; plasma etching; plasma jet; polymers; removal of micro-organisms

- [1] K. H. Becker, U. Kogelschatz, K. H. Schoenbach, R. J. Barker, "Non-equilibrium Air Plasmas at Atmospheric Pressure", IOP Publishing, London 2005.
- [2] U. Lommatzsch, D. Pasedag, A. Baalman, G. Ellinghorst, H. E. Wagner, *Plasma Process. Polym.* **2007**, *4*, 1041.
- [3] A. B. Gil'man, *High Energy Chem.* **2003**, *37*, 17.
- [4] B. Finke, F. Luethen, K. Schroeder, P. D. Mueller, C. Bergenian, M. Frant, A. Ohl, B. J. Nebe, *Biomaterials* **2007**, *28*, 4521.
- [5] R. Murillo, F. Poncin-Epaillard, Y. Segui, *Eur. Phys. J. Appl. Phys.* **2007**, *37*, 299.
- [6] S. J. Pearton, D. P. Norton, *Plasma Process. Polym.* **2005**, *2*, 16.
- [7] S. Lerouge, M. Tabrizian, M. R. Wertheimer, R. Marchand, L. Yahia, *Bio-Med. Mater. Eng.* **2002**, *12*, 3.
- [8] M. Moisan, J. Barbeau, M. C. Crevier, J. Pelletier, N. Philip, B. Saoudi, *Pure Appl. Chem.* **2002**, *74*, 349.
- [9] M. Laroussi, *IEEE Trans. Plasma Sci.* **2002**, *30*, 1409.
- [10] K. Stapelmann, O. Kylian, B. Denis, F. Rossi, *J. Phys. D-Appl. Phys.* **2008**, *41*, 6.
- [11] R. Brandenburg, J. Ehlbeck, M. Stieber, T. von Woedtke, J. Zeymer, O. Schluter, K. D. Weltmann, *Contrib. Plasma Phys.* **2007**, *47*, 72.
- [12] I. Koban, R. Matthes, N. O. Hubner, A. Welk, P. Meisel, B. Holtfrete, R. Sietmann, E. Kindel, K.-D. Weltmann, A. Kramer, T. Kocher, *New J. Phys.* **2010**, *12*, 16.
- [13] K. D. Weltmann, R. Brandenburg, T. von Woedtke, J. Ehlbeck, R. Foest, M. Stieber, E. Kindel, *J. Phys. D: Appl. Phys.* **2008**, *41*, 6.
- [14] Y. F. Dufrene, A. VanderWal, W. Norde, P. G. Rouxhet, *J. Bacteriol.* **1997**, *179*, 1023.
- [15] F. Ahimou, C. J. P. Boonaert, Y. Adriaensen, P. Jacques, P. Thonart, M. Paquot, P. G. Rouxhet, *J. Colloid Interface Sci.* **2007**, *309*, 49.
- [16] N. Mozes, A. J. Leonard, P. G. Rouxhet, *Biochim. Biophys. Acta* **1988**, *945*, 324.
- [17] S. Lerouge, M. R. Wertheimer, R. Marchand, M. Tabrizian, L. Yahia, *J. Biomed. Mater. Res.* **2000**, *51*, 128.
- [18] F. D. Egitto, *Pure Appl. Chem.* **1990**, *62*, 1699.
- [19] J. Benedikt, C. Floetgen, G. Kussel, V. Raballand, A. von Keudell, *J. Phys.: Conf. Ser.* **2008**, *133*.
- [20] M. H. Jung, H. S. Choi, *Thin Solid Films* **2006**, *515*, 2295.
- [21] J. Y. Jeong, S. E. Babayan, V. J. Tu, J. Park, I. Henins, R. F. Hicks, G. S. Selwyn, *Plasma Sources Sci. Technol.* **1998**, *7*, 282.
- [22] J. G. A. Terlingen, A. S. Hoffman, J. Feijen, *J. Appl. Polym. Sci.* **1993**, *50*, 1529.



- [23] L. A. Pederson, *J. Electrochem. Soc.* **1982**, *129*, 205.
- [24] G. N. Taylor, T. M. Wolf, *Polym. Eng. Sci.* **1980**, *20*, 1087.
- [25] K. D. Weltmann, E. Kindel, R. Brandenburg, C. Meyer, R. Bussiahn, C. Wilke, T. von Woedtke, *Contrib. Plasma Phys.* **2009**, *49*, 631.
- [26] A. Vogelsang, A. Ohl, H. Steffen, R. Foest, K. Schröder, K. D. Weltmann, *Plasma Process. Polym.* **2010**, *7*, 16.
- [27] R. Foest, E. Kindel, H. Lange, A. Ohl, M. Stieber, K. D. Weltmann, *Contrib. Plasma Phys.* **2007**, *47*, 119.
- [28] V. Stelmashuk, H. Biederman, D. Slavinska, M. Trchova, P. Hlidek, *Vacuum* **2004**, *75*, 207.
- [29] J. Friedrich, G. Kühn, J. Gähde, *Acta Polym.* **1979**, *30*, 470.
- [30] S. J. Moss, A. M. Jolly, B. J. Tighe, *Plasma Chem. Plasma Process.* **1986**, *6*, 401.
- [31] F. Clouet, K. Shi, *J. Appl. Polym. Sci.* **1992**, *46*, 1955.
- [32] A. M. Wrobel, B. Lamontagne, M. R. Wertheimer, *Plasma Chem. Plasma Process.* **1988**, *8*, 315.

#### **5.4 “Investigation of Surface Etching of Poly(ether ether ketone) by Atmospheric Pressure Plasmas”**

Katja Fricke, Stephan Reuter, Helena Tresp, Daniel Schröder, Volker Schulz-von der Gathen, Klaus-Dieter Weltmann, and Thomas von Woedtke

*IEEE Transactions on Plasma Science*, **2012**, DOI: 10.1109/TPS.2012.2212463





# Investigation of Surface Etching of Poly(ether ether ketone) by Atmospheric Pressure Plasmas

Katja Fricke, Stephan Reuter, Daniel Schröder, Volker Schulz-von der Gathen,  
Klaus-Dieter Weltmann, and Thomas von Woedtke

**Abstract**— An atmospheric pressure argon plasma jet with varying admixtures of molecular oxygen was used to study the etching mechanism of poly(ether ether ketone) (PEEK). Furthermore, a correlation between plasma-based etching processes on PEEK with the generation of chemically reactive plasma species is proposed. The surface analysis was performed by X-ray photoelectron spectroscopy (XPS), atomic force microscopy (AFM), and surface profilometry which showed a dramatic increase in the content of oxygen functionalities and surface roughness after long-time Ar/O<sub>2</sub> plasma treatment. For the plasma diagnostics two-photon absorption laser-induced fluorescence (TALIF) spectroscopy was applied. The obtained etching mass as well as the surface roughness for different molecular oxygen admixtures revealed strong dependence on the atomic oxygen density. Furthermore, the radial surface profile, affected by plasma etching, might be attributed to the distribution of plasma-generated oxygen species in the plasma jet effluent.

**Index Terms**—Atmospheric pressure plasma jet, surface topology, modification, plasma etching.

## I. INTRODUCTION

**P**OLY(ETHER ETHER KETONE) is a high performance semi-crystalline thermoplastic polymer which is characterized by good mechanical properties, high thermal (glass transition temperature  $T_g = 143^\circ\text{C}$  and melting temperature  $T_m = 343^\circ\text{C}$ ) as well as chemical stability, and resistance to radiation damage [1]. Consequently, PEEK has been widely used for many applications such as in aerospace, automotive, and medical industries. Especially, its prospective application as

substitute for titanium and its alloys for medical implants is of ongoing interests [2], [3]. The chemical structure of PEEK comprises an aromatic backbone molecular chain, interconnected by ketone and ether functional groups composed of the following repeating unit:

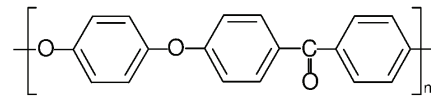


Fig. 1. Chemical structure of repeating units of poly(ether ether ketone).

Since most of the engineering thermoplastics exhibit low surface energies and poor adhesion and hence, do not possess the necessary surface characteristics for particular applications [4], [5], different processes are applied to activate the surface [6]. Among the different modification methods non-thermal plasmas have been widely used to alter the surface properties of various polymers which in turn resulted in improving the wettability and adhesion properties without affecting the bulk properties [7], [8]. According to the processing conditions (plasma gas, process parameter, and type of polymer) the plasma-exposed substrate surface is subjected to ion, radical and electron bombardment as well as ultraviolet radiation which influence the surface properties in various ways. Different surface modifications can be (i) surface functionalization resulting in chain scission and formation of chemical functionalities (ii) cross-linking on the surface and (iii) surface ablation (etching) [9]. During plasma exposure the processes i-iii are difficult to separate, because the predominance of the respective processes may vary according to the processing conditions.

This paper promotes the understanding of the mechanism at the interface between plasma and materials and extends our previous published work where the etching rates of chemically different polymers exposed to atmospheric pressure plasma were intensively studied [10]. In this work the impact of non-thermal atmospheric pressure plasma on PEEK concerning surface etching was studied in detail. Moreover, a correlation between surface effects and generated plasma species was investigated, linking elemental surface composition, surface roughness, as well as surface topology with the presence of plasma species in the altered surface properties of PEEK. For the investigations, the plasma jet was operated with noble gas (argon) with different admixtures of molecular oxygen in the order of 1 vol% O<sub>2</sub>.

Manuscript received April 14, 2012.

This work was supported by the Federal Ministry of Education and Research of Germany (BMBF, Grant No. 03Z2DN12 and No. 13N11188).

Corresponding author: K. Fricke (phone: +49 3834 554 3841; fax: +49 3834 554 301; k.fricke@inp-greifswald.de).

K. Fricke, K.-D. Weltmann, and Th. von Woedtke are with the Leibniz Institute for Plasma Science and Technology (INP Greifswald e.V.), Greifswald, Germany (e-mail: k.fricke@inp-greifswald.de, weltmann@inp-greifswald.de, woedtke@inp-greifswald.de).

S. Reuter is with the Centre for Innovation Competence plasmatic at the Leibniz Institute for Plasma Science and Technology (INP Greifswald e.V.), Greifswald, Germany (e-mail: stephan.reuter@inp-greifswald.de).

D. Schröder and V. Schulz-von der Gathen are with the Institute for Experimental Physcs II, Ruhr-Universität Bochum, Bochum, Germany (e-mail: svdvg@ep2.rub.de, daniel.schroeder@rub.de)

## II. MATERIALS AND METHODS

### A. Materials

Poly(ether ether ketone) (PEEK) were purchased from Goodfellow GmbH (Germany) in the form of 0.1 mm thin PEEK films and 1 mm thick PEEK plates.

### B. Atmospheric Pressure Argon Plasma Jet and Plasma Treatment Conditions

Fig. 2 shows a schematic setup of the atmospheric pressure argon plasma jet (kINPen, developed at the INP Greifswald, Germany) used in this study. The plasma device consists of a quartz capillary (inner radius of 0.8 mm) with a pin-type HF electrode (1.7 MHz) inside. The plasma is generated from the top of the centered electrode and expands to the surrounding air outside the nozzle. Further details of this type of jet, version kINPen09, are described elsewhere [11]. The plasma jet was operated with 5 standard liters per minute (slm) pure argon or with different admixtures of molecular oxygen.

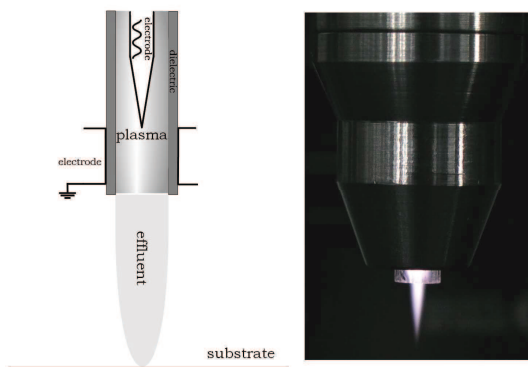


Fig. 2. (Left) Schematic setup of the plasma jet and (right) photograph of Ar/1%O<sub>2</sub> plasma jet.

PEEK samples were positioned perpendicular to the plasma jet and were treated locally at jet-nozzle-to-substrate distances of 5 mm and 7 mm for different treatment time.

### C. Physico-chemical Surface Analysis

The elemental surface composition and chemical binding properties were analyzed by X-ray photoelectron spectroscopy (XPS) using an AXIS Ultra DLD electron spectrometer (Kratos Analytical, Manchester, UK). The spectra were recorded by means of monochromated Al K $\alpha$  excitation (1486.6 eV) with a medium magnification (field of view 2) lens mode and by selecting the slot mode, providing an analysis area of approximately 250  $\mu$ m in diameter. A pass energy of 80 eV was used for estimating the chemical elemental composition and 10 eV for the high energy resolution of the C 1s peaks to investigate chemical functionalities. Charge neutralization was implemented by low energy electrons injected into the magnetic field of the lens from a filament located directly atop the sample. Valence band spectra were obtained using hybrid electrostatic system, to create an analyzed area of 300  $\mu$ m x 700  $\mu$ m, and a pass energy of 20 eV. Spectra were calibrated with reference to the

C 1s peak at 284.7 eV associated with aromatic C-C bonds of PEEK. Data acquisition and processing were carried out using CasaXPS software, version 2.14dev29 (Casa Software Ltd., UK). For the XPS analysis 0.1 mm thin PEEK films (1 cm x 1 cm) were used to reduce degassing in the XPS chamber to a minimum. The samples were analyzed by performing a line scan with an increment of 2 mm.

Changes in the surface roughness and topology were determined by an atomic force microscope (AFM) scanning probe microscope diCP2 (Veeco, Santa Barbara, CA, USA) in the non contact (tapping) mode. An area of 10  $\mu$ m x 10  $\mu$ m was scanned using a pyramidal silicon tip (Veeco, RTESPA-CP) doped with n-type phosphorus with a resonance frequency of 273-389 kHz and a force constant of 20 – 80 N/m. Five areas were measured for each sample and analyzed by means of the instrument software SPMLab Ver. 6.0.2 (Veeco).

The etched depth profiles were recorded crossing the centre of the plasma treated polymer with a stylus surface profiling system (Dektak 3ST, Veeco, USA) with a scan speed of 40  $\mu$ m/s and a force of the stylus tip on the surface of 10 mg.

The determination of the surface roughness and the radial analysis of the etching depth profile were performed on 1 mm thick PEEK plates.

### D. Optical Plasma Diagnostics

#### Two-photon Absorption Laser-induced Fluorescence (TALIF)

The measurement of absolute ground state atomic oxygen densities in the free effluent of the plasma jet by two-photon absorption laser-induced fluorescence is based on the simultaneous absorption of two UV-photons ( $\lambda = 225$  nm) exciting oxygen atoms from the ground state  $2p^4\ ^3P_1$  into the  $3p^1\ ^3P_2$  state. The deexcitation into the  $3s^1\ ^3S_0$  state results in the detected fluorescence at  $\lambda = 844$  nm which is proportional to the oxygen ground state density [12]. The necessary laser radiation is produced by a commercial laser system consisting of a Nd:YAG pumped tunable dye laser (Continuum Powerlite 800, Continuum ND6000) and a following frequency-doubling (KDP crystal) and -mixing (BBO crystal) unit generating laser pulses with a frequency of 10 Hz. The fluorescence light in the infrared is detected by an air-cooled photomultiplier (BURLE C31034A) synchronized to the laser system. As the plasma produces radiation of 842.42 nm by excited argon species, which is spectrally very close to the detected TALIF-Signal, the use of a interference filter (FWHM = 1 nm, T = 50%,  $\lambda_0 = 844.5$  nm) in front of the photomultiplier is mandatory to gain an acceptable signal to noise ratio [13]. By mounting the plasma discharge on a three-axis manipulator and keeping the optical setup fixed in space, space-resolved oxygen distributions can be recorded with a resolution of about 200  $\mu$ m. Detailed information about the experimental setup can be found in former own publications [13]. The absolute calibration of this diagnostics is performed by a comparing measurement in a xenon atmosphere at a defined pressure, described in detail in [14].

### III. RESULTS AND DISCUSSION

#### 1) Surface Chemical Analysis

For the determination of elemental surface composition and thus, to analyze the changes in surface chemistry, XPS was applied. The quantified surface composition reflects the effect of the plasma-initiated surface functionalization. Fig. 3 shows selected survey spectra of non-treated PEEK and PEEK treated for 300 s by Ar and Ar/1%O<sub>2</sub> plasma, respectively.

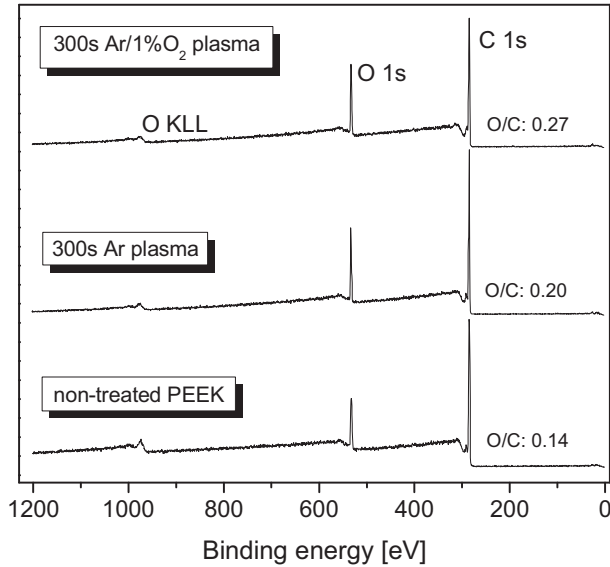


Fig. 3. XPS survey spectra of non-treated PEEK and PEEK exposed to Ar and Ar/1%O<sub>2</sub> plasma for 300 s, respectively, show the different amount of oxygen (O 1s) and carbon (C 1s).

Non-treated PEEK is composed of oxygen (O) and carbon (C) with an O/C ratio of 0.14 which is similar to the stoichiometric value of the PEEK repeat unit (see Fig. 1),  $O/C = 3/19 = 0.16$ . The O/C value of non-treated PEEK, obtained by XPS, is lower due to the contact of the sample with ambient air, which results in a contamination of C on the surface. However, after plasma treatment on all plasma-exposed polymers a decreased C content and an increased O content were measured. Hence, the degree of functionalization of the PEEK surface, expressed as O/C ratio, was increased after plasma exposure. Furthermore, the O/C value of PEEK after 300 s Ar/1%O<sub>2</sub> plasma was considerably higher compared to the O/C value of Ar plasma treated PEEK. The corresponding highly resolved measured C 1s core-level spectra of non-treated and plasma-treated PEEK as well as the identification of functional groups, based on binding energies of the peaks, are depicted in Fig. 4 for plasma exposure times of 30 s and 300 s.

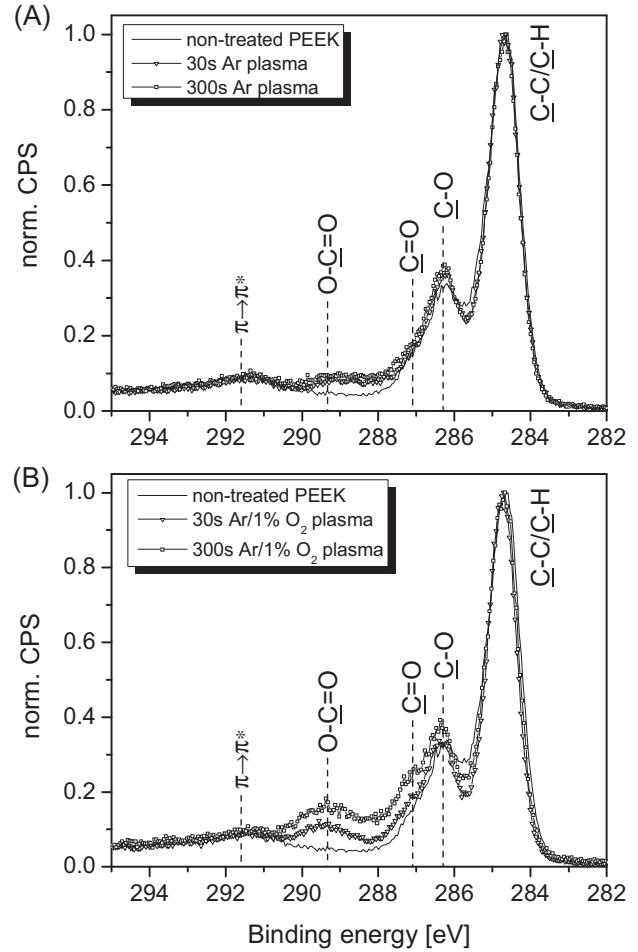


Fig. 4. Highly resolved measured C 1s spectra of non-treated PEEK and PEEK exposed to (A) Ar plasma and (B) to Ar/1%O<sub>2</sub> plasma for different exposure times.

The C 1s spectrum of non-treated PEEK was fitted using three components assigned to  $\underline{C}-C/\underline{C}-H$  (carbon atoms in the phenyl ring) at a binding energy (BE) of 284.7 eV,  $\underline{C}-O$  (ether group) at BE: 286.4 eV, and  $\underline{C}=O$  (ketone group) at BE: 287.2 eV [15]. The peak at BE: 291.7 eV is a shake-up satellite due to  $\pi \rightarrow \pi^*$  transition arising from electrons in the aromatic ring which is commonly present in aromatic structures. Hence, the  $\pi \rightarrow \pi^*$  shake-up satellite is associated with  $sp^2$  hybridized orbitals associated with benzenoid ring systems and carbon-carbon double bonds, which provides information on the degree of unsaturation of the surface [16]. From visual examination of the shape of the highly resolved C 1s spectra it is evident that the content of oxygen-functionalities was increased after plasma exposure. Five distinct peaks were fitted in the C 1s spectra of plasma-treated PEEK. Additionally to the above mentioned peaks of non-treated PEEK, a peak at higher binding energies (shift of 4.6 eV) which represents carboxyl groups,  $O-\underline{C}=O$ , in acid or ester bindings, was observed for all samples.

In Table I the relative percentages of the functional groups of PEEK in terms of gas mixture and plasma treatment time is listed.

TABLE I

RELATIVE PERCENTAGES (%) OF BONDING COMPONENTS IN DECONVOLUTED HIGH RESOLUTION C 1S SPECTRA (MEAN  $\pm$  SD, N = 5).

	$\underline{\text{C}}\text{-C}/\underline{\text{C}}\text{-H}^1$	$\underline{\text{C}}\text{-O}$	$\underline{\text{C}}=\text{O}$	$\text{O}-\underline{\text{C}}=\text{O}$
non-treated PEEK	75.4	19.7	4.9	
30 s Ar plasma	66.9 $\pm$ 0.2	22.0 $\pm$ 1.1	6.5 $\pm$ 1.3	4.6 $\pm$ 1.1
300 s Ar plasma	63.6 $\pm$ 0.1	24.7 $\pm$ 1.0	6.9 $\pm$ 0.3	4.7 $\pm$ 1.2
30 s Ar/1%O <sub>2</sub> plasma	62.9 $\pm$ 0.9	22.8 $\pm$ 0.8	5.6 $\pm$ 1.4	7.7 $\pm$ 0.7
300 s Ar/1%O <sub>2</sub> plasma	58.5 $\pm$ 0.7	23.3 $\pm$ 0.2	8.4 $\pm$ 0.2	9.8 $\pm$ 0.5

<sup>1</sup>including  $\pi \rightarrow \pi^*$  shake-up peak

The relative amount of functional features of non-treated PEEK was consistent with the theoretical values expected from its chemical structure [15].

Along with the increased O/C ratio demonstrated in Fig. 3, the highest relative percentages of functional groups were found to be after long-time Ar/1%O<sub>2</sub> plasma exposure. In comparison to Ar plasma-treated substrates, higher levels of oxygen-containing groups were achieved after Ar/1%O<sub>2</sub> plasma exposure. A considerable increase in  $\underline{\text{C}}=\text{O}$  and  $\text{O}-\underline{\text{C}}=\text{O}$  groups was observed, whereas slight changes occurred in the content of  $\underline{\text{C}}\text{-O}$  groups. Due to the increase of functional features, a relative reduction of  $\underline{\text{C}}\text{-C}/\underline{\text{C}}\text{-H}$  bonds can be seen. Nevertheless, the shake-up peak is still present in the C 1s core-level spectra of plasma-treated substrates suggesting that the aromaticity of PEEK is not destroyed. Furthermore, the full width at half maximum (FWHM) of the  $\underline{\text{C}}\text{-C}/\underline{\text{C}}\text{-H}$  peak at the binding energy of 284.7 eV showed no significant changes in terms of applied process gas and treatment time. In detail, the FWHM of the  $\underline{\text{C}}\text{-C}/\underline{\text{C}}\text{-H}$  peak of non-treated PEEK was 1.0 eV whereas the FWHM after 300 s Ar plasma and Ar/1%O<sub>2</sub> plasma was found to be 0.9 eV which made it difficult to fit the spectra using a component at 285.0 eV, assigned to aliphatic C-C/C-H bonds, which would indicate ring-opening after plasma treatment. Therefore, valence band (VB) spectra of these PEEK samples were acquired to reveal the information to what extent plasma-initiated ring-opening occurs since the chemical structure of the polymer backbone produces characteristics features, which represent the “fingerprint” of the particular polymer. These spectra are analyzed to obtain information on the chemical environment of the elements and hence, the molecular structure of the polymer surface [17]. The VB spectrum is characterized by electrons of low binding energy emitted from delocalized or bonding orbitals of the polymer [18]. Furthermore, the energy distribution of electrons involved in bonding between atoms of molecules is shown. Thus, it reveals information on features characterized by bonding, anti-bonding, and non-bonding state. Fig. 5 represent the VB spectra of non-treated PEEK (Fig. 5 A) and PEEK exposed to Ar (Fig. 5 B,C) and Ar/1%O<sub>2</sub> (Fig. 5 D, E) plasma after 30 s and 300 s, respectively.

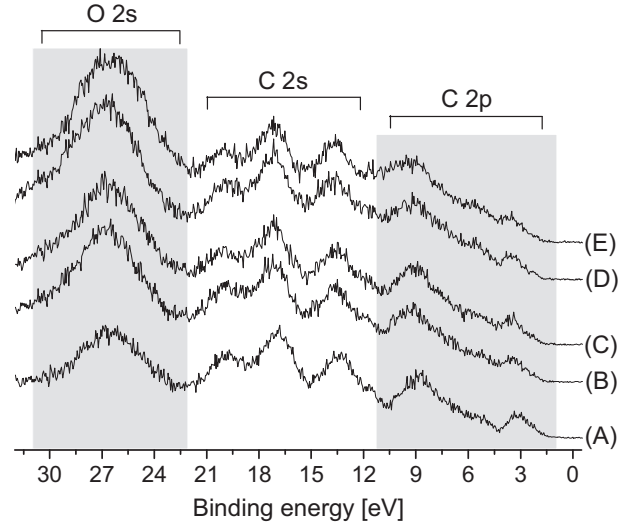


Fig. 5. Valence band spectra of (A) non-treated PEEK and PEEK exposed to (B) 30 s Ar, (C) 300 s Ar, (D) 30 s Ar/1%O<sub>2</sub>, and (E) 300 s Ar/1%O<sub>2</sub> plasma.

The VB spectrum of non-treated PEEK is dominated by a triplet pattern between 10.0 and 22.0 eV corresponding to molecular orbital with 2s character associated with C-C bonds localized on the phenyl ring [19]. In detail, the peak at 20.0 eV results from  $\sigma(\text{C}2\text{s}-\text{C}2\text{s})$ ;  $\text{C}2\text{s}-\text{O}2\text{s}$  bonding orbitals due to  $-\text{C}=\text{C}-$  of the phenyl ring,  $\text{C}=\text{O}$ , and  $\text{C}-\text{O}-$  bonds. The spectral features in the range of 17.0-12.0 eV are owing to  $\sigma(\text{C}2\text{s}-\text{C}2\text{s})$ ,  $\text{p}\sigma(\text{C}2\text{s}-\text{C}2\text{p})$  and  $\text{p}\sigma(\text{C}2\text{s}-\text{C}2\text{p})$ ,  $\text{p}\sigma(\text{C}2\text{s}-\text{O}2\text{p})$  bonding orbitals, respectively, assigned to  $-\text{C}=\text{C}-$  of the phenyl ring,  $\text{C}=\text{O}$ , and  $\text{C}-\text{O}-$  bonds [20], [21]. The distinct peak at a binding energy of 27.0 eV is related to molecular electronic levels where O 2s atomic orbital contributions are dominant from  $\sigma(\text{O}2\text{s}-\text{C}2\text{s})$  and  $\text{p}\sigma(\text{C}2\text{s}-\text{O}2\text{p})$  orbitals due to  $\text{C}-\text{O}/\text{C}=\text{O}$  functionalities. The O 2s band consist of two peaks where the higher binding energy peak arising from the ether ( $\text{C}-\text{O}$ ) and the lower binding energy peak being derived from the carbonyl groups ( $\text{C}=\text{O}$ ) [22]. The small features in the region below 11.0 eV are attributed to C 2p and O 2p states formed by extended  $\pi$  states. In particular, the region between 11.0-8.0 eV are determined by  $\text{p}\pi(\text{C}2\text{p}-\text{C}2\text{p})$  bonding of the phenyl ring ( $-\text{C}=\text{C}-$ ) and  $\text{p}\pi(\text{C}2\text{p}-\text{O}2\text{p})$  bonding orbitals of  $\text{C}=\text{O}$  whereas the peak located at around 3.0 eV is attributed to  $\text{p}\pi$  orbitals associated with the oxygen lone pair nonbonding orbitals in  $-\text{O}-$ ,  $=\text{O}$  functional groups [23]. The C 2p  $\pi$  orbitals produce the shake up satellite in C 1s core-level spectra [19], [24]. Bands in this region are derived from  $\pi$ -type bonding and nonbonding orbitals on the phenyl ring or carbonyl [25]. Since the atomic photo-ionization cross section of 2p-electron contributions is smaller compared to C 2s cross section, the intensity of features is less intense than those located at higher binding energy.

As can be seen in Fig. 5 the major effect in VB spectra after plasma treatment (Fig. 5 B-E) was a substantially increase in the intensity of the peak assigned to O 2s (BE: 27 eV), especially after 300 s Ar/1%O<sub>2</sub> plasma treatment (Fig. 5 E), concomitant with the increased O/C ratio and the enhanced



content of oxygen-containing functionalities after plasma treatment. To emphasize changes in VB spectra after plasma treatment and to simplify the comparison to the VB of non-treated PEEK, the background of the VB spectra was subtracted and digital signal processing (by using a FFT filter) was applied which is depicted in Fig. 6 for non-treated PEEK (lower curve) and PEEK exposed to Ar/1%O<sub>2</sub> plasma for 300 s, respectively. According to the prior discussion of the spectral feature at 27 eV, the VB spectra are only shown in the range of 22.0-0.0 eV.

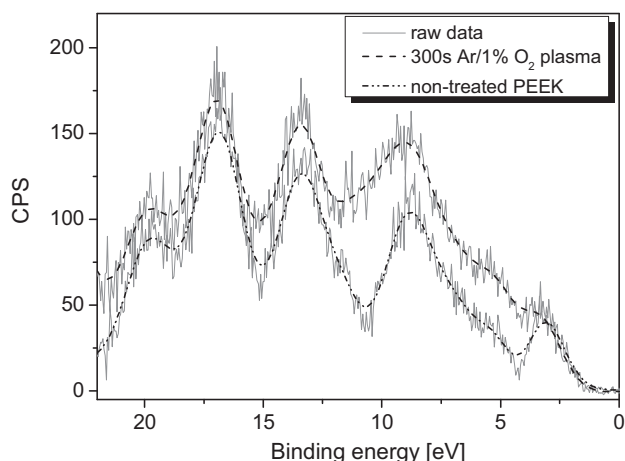
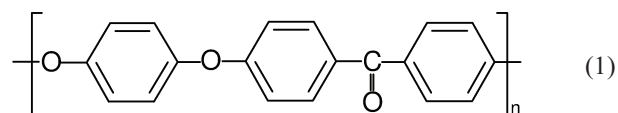


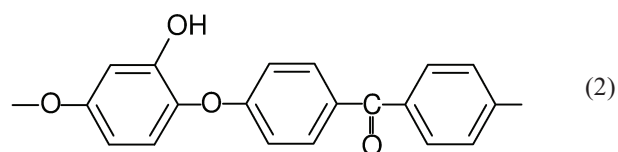
Fig. 6. Background subtraction of the valence spectrum of non-treated PEEK and Ar/1%O<sub>2</sub> plasma treated PEEK (300 s exposure time).

Additionally to the mentioned increase in the O 2s peak after plasma treatment, changes in the region between 2.0 and 11.0 eV were observed characterized by a broadening of the spectral features. This broadening is probably attributed to the presence of many electronic states where mainly O 2p and C 2p atomic orbitals participate [26]. Furthermore, the VB spectrum of Ar/1%O<sub>2</sub> plasma-treated PEEK shows that the original C 2s spectral features (20.0-10.0 eV) of non-treated PEEK were maintained after plasma treatment even after substantial incorporation of oxygen into the surface of the polymer. This suggests that the basic structure of PEEK is still intact. Furthermore, these observations show that the VB spectra sustain the conclusions from the peak fit of the core-level C 1s spectra. Consequently, it might be assumed that there is no indication of ring-opening by cleavage of the aromatic structure after plasma treatment. Therefore, due to the stability of ether-like bonds, which is attributed to the high radiation resistance of the ether linkage stabilized by the two contiguous benzene rings [27], it is most likely that the oxygen incorporation occurs into the benzene rings [28]. According to these results the changes in the chemical structure of PEEK are discussed hereinafter. Furthermore, proposed chemical structures, resulting from plasma treatment, are presented.

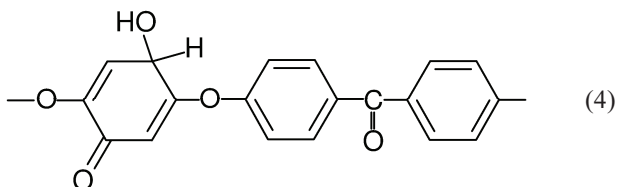
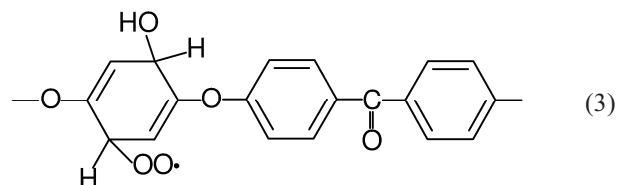
It is well known that oxygen atoms can react with aromatic rings to form phenols [29]. Consequently, starting from the PEEK structure (1)



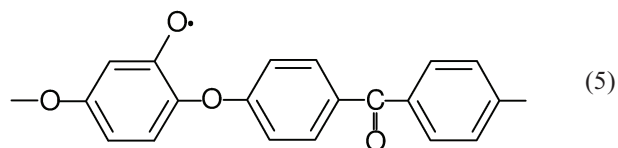
the initial step of oxidation is the attack of reactive species on the phenyl ring. In this way generated radicals at the phenyl ring of the polymer undergo further oxidation processes (e.g. through atomic oxygen, OH radical, or ozone) which results in the formation of a phenolic structure (2) [30]. This reaction leads to loss of plasma-generated oxygen species without forming free radicals or products involved in cleavage of the polymer backbone.



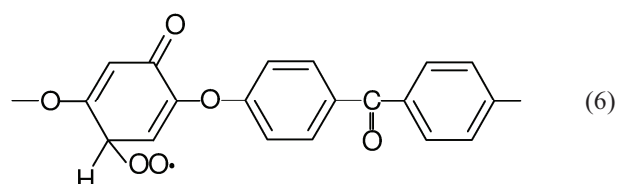
Subsequent reactions on the phenol result in further radical formation [31] where in the presence of oxygen species peroxy radical (3) is formed, a radical intermediate, which is converted for instance into a carbonyl group (4).



Furthermore, the attack of the phenol by radicals can also lead to the formation of phenoxyl radical for instance via hydrogen abstraction (5) [32].

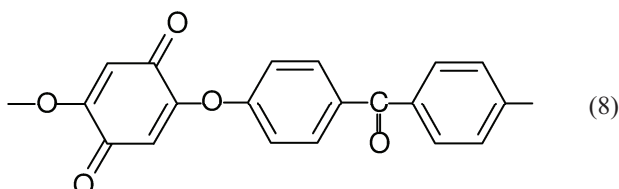
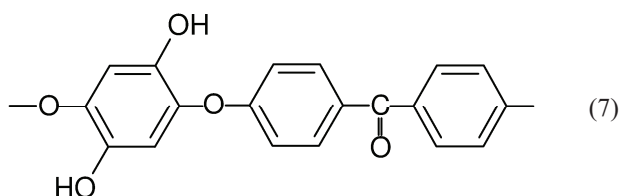


By the reaction of the phenoxyl radical peroxy radicals (6) can be formed.



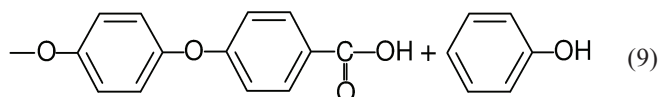
The peroxy radical can decompose to a hydroxyl group (7) or to a carbonyl group (8) [33].





Summarizing, structure (7) and (8), namely hydroquinone and quinone, are believed to be the mainly produced polymer structures after plasma treatment which was also postulated by Seidel *et al.* [28].

Since XPS data revealed a significant introduction of O=C-O functional groups onto the plasma-treated surface and, as already mentioned, ring-opening can not be derived from the results, a possible explanation might be the creation of O=C-O bonds caused by oxidation of the ketone group after chain scission according to (9) [28].



Furthermore, the content of O=C-O bonds was highest after Ar/1%O<sub>2</sub> plasma treatment which indicates that the capability of Ar/O<sub>2</sub> plasma in chain scission reactions is enhanced. This is not surprising because prior investigations on the etching efficiency of Ar and Ar/O<sub>2</sub> plasma showed significant etching behavior of the plasma jet when oxygen was added to the argon gas discharge [10]. Hence, extensive chain scission will result in polymer ablation influencing the surface morphology and topology of the plasma-treated PEEK surface.

## 2) Surface Morphology and Topology

In order to evaluate the impact of plasma-induced etching processes on PEEK atomic force microscopy (AFM) was applied. Representative 2-D images of non-treated PEEK and PEEK exposed to Ar and Ar/1%O<sub>2</sub> plasma for 30, 60, 120, and 300 s, respectively, are shown in Fig. 7.

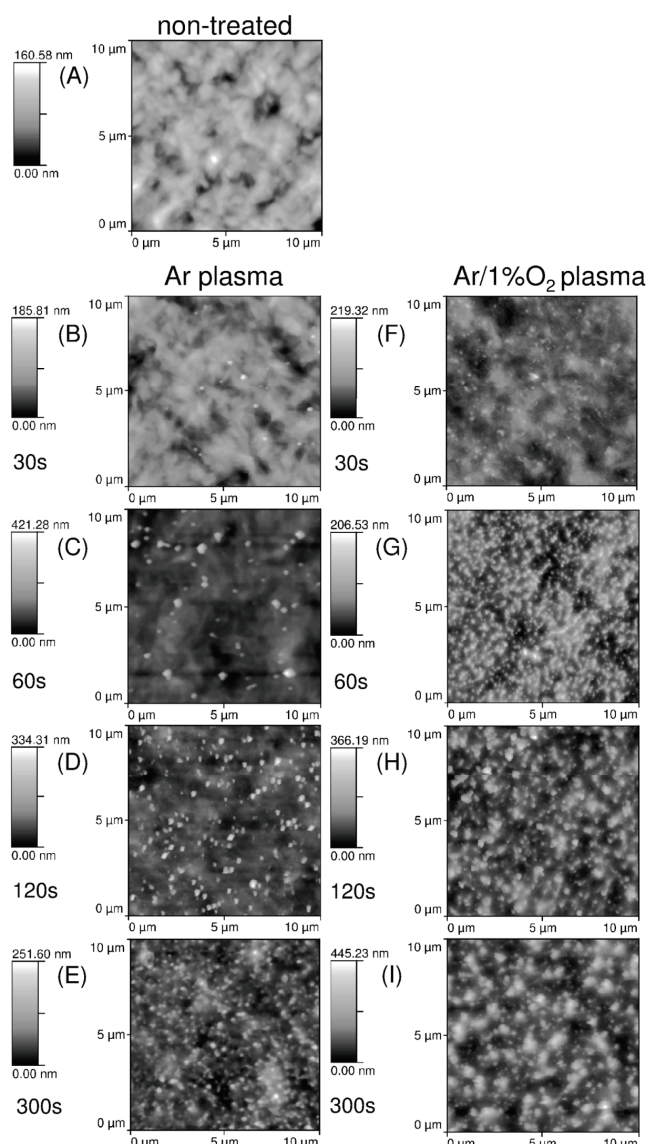


Fig. 7. 10  $\mu\text{m}$  x 10  $\mu\text{m}$  2-D AFM images of: (A) non-treated PEEK, PEEK exposed to (B) 30 s Ar plasma, (C) 60 s Ar plasma, (D) 120 s Ar Plasma, (E) 300 s Ar plasma, (F) 30 s Ar/O<sub>2</sub> plasma, (G) 60 s Ar/O<sub>2</sub> plasma, (H) 120 s Ar/O<sub>2</sub> plasma, and (I) 300 s Ar/O<sub>2</sub> plasma. The height information is represented according to a color code included on the right of each image.

Fig. 7 A displays the surface topography of non-treated PEEK, which is characterized by a rough-grained structure. After 30 s exposure to Ar (Fig. 7 B) and Ar/1%O<sub>2</sub> (Fig. 7 F) plasma, a few surface grains appeared on the surface but no significant changes compared to Fig. 7 A were observed. Whereas PEEK samples exposed to Ar and Ar/O<sub>2</sub> plasma for 60 s (Fig. 7 C and 7 G) exhibited initial changes in the surface topography characterized by the appearance of several small nanostructures on their surfaces especially after Ar/1%O<sub>2</sub> plasma. Long-time plasma treatment with exposure times of 120 s (Fig. 7 D and 7 H) led to an increase of the number of grains and the formation of spikes of considerable height. The difference between the surfaces treated with Ar and Ar/1%O<sub>2</sub> plasma is noticeable: after Ar/1%O<sub>2</sub> plasma treatment the surface was characterized by a multitude of spikes and grains.

Furthermore, the spikes on Ar plasma treated PEEK surface were not as dense packed as on PEEK after 120 s Ar/%O<sub>2</sub> plasma exposure. These dramatic changes in the surface topography can be attributed to the admixture of molecular oxygen leading to the generation of chemically reactive species etching the polymer surface. Only at treatment time of 300 s a nano-texturing of the surface was observed by using Ar plasma (Fig. 7 E). Furthermore, after 300 s Ar/1%O<sub>2</sub> plasma exposure (Fig. 7 I) it seems that the nanostructures are combined to broadened surface grains (nano-columns). Consequently, the 2-D images indicate an increase of the surface grain height with treatment time. A detailed look on the height profiles deduced from the recorded AFM images confirms this assumption. Fig. 8 shows the height profile of non-treated PEEK compared to those of PEEK exposed to Ar/1%O<sub>2</sub> plasma for 60 s and 300 s, respectively.

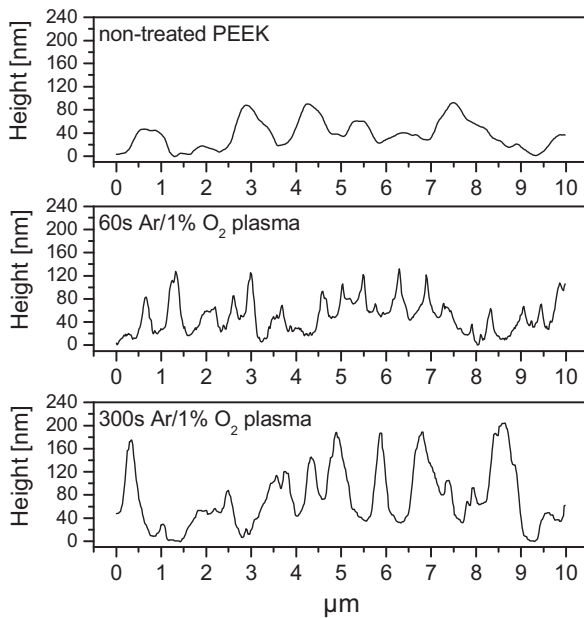


Fig. 8. Height profiles of non-treated PEEK and of PEEK exposed to Ar/1%O<sub>2</sub> plasma for 60 s and 300 s, respectively. The height profiles were obtained from the analysis of the AFM images.

The structure of non-treated PEEK revealed a grain-like structure of a maximum height of approximately 80 nm and a width of up to 1 μm. After 60 s plasma-exposure the grain height was increased to 120 nm whereas the width of these structures was reduced to 0.5 μm. A further increase of the grain height was observed after long-time plasma treatment (300 s), heights of approximately 200 nm were estimated and additionally, a broadening of these nano-structures was observed characterized by widths above 1 μm. According to these height profiles a dependence of the averaged surface roughness  $R_a$  on the treatment time and, of course, on the process gas was determined (see Fig. 9).

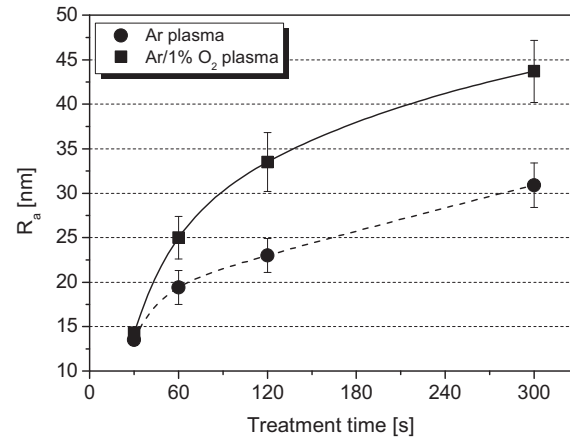


Fig. 9. Evolution of the averaged roughness ( $R_a$ ) versus the treatment time for Ar plasma (---●---) and Ar/1%O<sub>2</sub> plasma (—■—), respectively. The  $R_a$  value of non-treated PEEK was 13.5 nm ± 1.8 nm. (mean ± SD, n = 5)

An increase in the surface roughness with increasing treatment time was observed. Furthermore, the admixture of molecular oxygen to the argon gas discharge resulted in higher surface roughness due to the greater etching capability of Ar/O<sub>2</sub> plasma compared to Ar plasma [10].

Despite the localized plasma treatment a considerable larger area of the polymer is considered to be influenced by the gas discharge. In order to estimate the extent of plasma-affected changes in surface roughness a radial line scan across the plasma-treated PEEK surface was measured. The radial evolution of  $R_a$  examined after 180 s Ar/1%O<sub>2</sub> plasma treatment is depicted in Fig. 10.

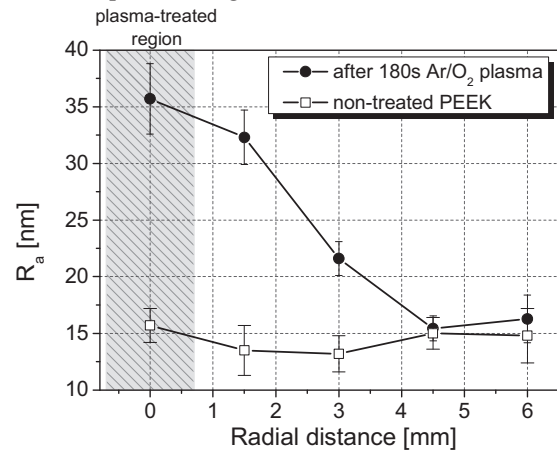


Fig. 10. Radial dependence of the averaged roughness ( $R_a$ ) after 180 s Ar/1% O<sub>2</sub> plasma treatment. (mean ± SD, n = 5).

It can be seen that with increasing radial distance to position '0', where the localized plasma treatment was performed, the  $R_a$  values declined. After a radial distance of 4.5 mm the  $R_a$  value is similar to the  $R_a$  value of non-treated PEEK. Hence, the plasma-based etching process is restricted to an area of less than 6-7 mm in diameter. Detailed information on the radial depth profile across the entire PEEK surface was received by means of a stylus surface profiler as function of the etching process. The surface profilometry is a simple method to study the influence of different operating parameter, such like

operating gas, treatment time, and operating distance, on the etching process (e.g. etching rate) [10]. Obtained from recorded depth profiles, etched mass can be calculated precisely and the etching mechanism can be explored. Fig. 11 gives an example of depth profiles of plasma treated PEEK exposed to Ar/1%O<sub>2</sub> plasma for 15 min obtained at jet-nozzle-to-substrate distances of 5 and 7 mm, respectively.

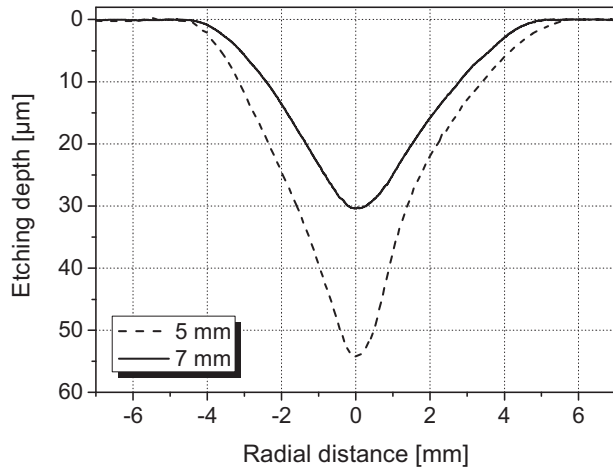


Fig. 11. Dependence of the etching depth on the axial distance. The PEEK substrates were exposed to Ar/1%O<sub>2</sub> plasma for 15 min at jet-nozzle-to-substrate distances of 5 and 7 mm.

Plasma-induced etching processes yield Gaussian shaped depth profiles. The measured etching depth depends strongly on the operating distance. Hence, the etching depth was reduced by a factor of approximately 1.8 at a jet-nozzle-to-substrate distance of 7 mm. Furthermore, in agreement with the radial measured surface roughness  $R_a$ , the changes in the surface profiles extend over an area of around 7 mm in diameter. However, a detailed investigation of these depth profiles relating to the results of the applied plasma diagnostics is presented in the following section.

### 3) Plasma Diagnostics

Key reactive species within the plasma jet effluent is expected to be atomic oxygen, a highly oxidizing species. To get information on the dependence of the atomic oxygen density within the plasma jet effluent TALIF-spectroscopy was applied, which directly yields spatially resolved absolute values for the concentration of oxygen atoms within the plasma jet effluent [37], [38].

Fig. 12 depicts the atomic oxygen densities (A), measured by TALIF spectroscopy, and the etching depth (B), determined by surface profilometry, as a function of the molecular oxygen admixture for different axial distances (5 and 7 mm). The etching depths were estimated on-axis at a radial distance of '0'.

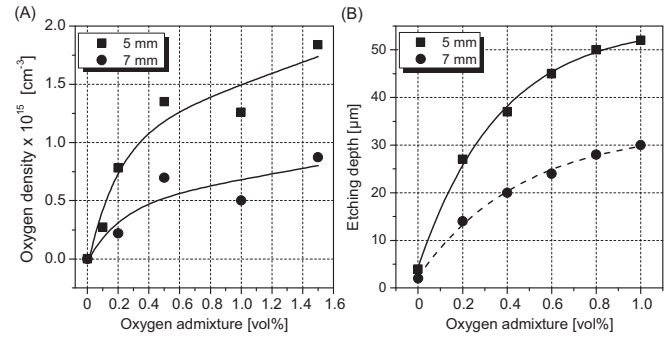


Fig. 12. A: Dependence of the oxygen density on the axial distance and the oxygen admixture. B: Etching depth vs. oxygen admixture obtained at different axial distances. The PEEK substrates were plasma-treated for 15 min.

At first, the two graphs in Fig. 12 A show similar behavior consisting of a steep increase for small admixtures up to 0.4 vol% oxygen, followed by a flattening for medium admixtures. This trend finally results in atomic oxygen densities of about  $1.75 \times 10^{15} \text{ cm}^{-3}$  at 5 mm distance and about  $0.8 \times 10^{15} \text{ cm}^{-3}$  at 7 mm for oxygen admixtures of 1.5 vol%. This flattening of the ascent is usually explained by the declining of the mean electron temperature, because of the increase of molecular oxygen in the discharge which is a sink for high energetic electrons. The model by Park predicts that at the used oxygen admixtures the electron temperature stays constant, but since oxygen is an electronegative gas, attachment processes become a loss channel for electrons [39]. The general behavior of the atomic oxygen density in Fig. 12 A does not change with increasing distance from the nozzle, but the atomic oxygen concentrations decrease about 50%. The dominating process for this lateral drop in the atomic oxygen density, is the formation of ozone [40]. In relation to the determined evolution of oxygen densities a similar tendency was observed for the dependence of the etching depth on the oxygen admixture (Fig. 12 B). The two graphs in Fig 12 B are characterized by a steep slope for oxygen admixtures up to 0.4 vol% whereas, between 0.4 and 1.0 vol% oxygen admixture, a shallower slope can be seen. Regarding the influence of the axial distance on the etching process, the etching depth was decreased about 43% at an axial distance of 7 mm which is in good agreement with the measured atomic oxygen density, too. Consequently the evolution of the oxygen density and the etching depth showed similarities that indicate that the etching process is mainly governed by oxygen species. For the elucidation of the assumed correlation between oxygen density and etching process the etched mass was calculated from the recorded depth profiles by the following considerations:

Taking into account that the etched profile is axially symmetric and that the depth profile is considered to have a Gaussian bell-like shape, the etched volume and hence, the etched mass, can be calculated from the radial measured profile. The volume was calculated according to

$$V_{etch} = \pi \int_a^b (f(x))^2 dx \quad (I)$$

The etched mass was calculated by

$$m_{etch} = V_{etch} \cdot \rho \quad (II)$$

with a density of  $\rho = 1.3 \text{ g/cm}^3$  for PEEK.

The calculated etched mass (obtained from axial distances of 5 and 7 mm with oxygen admixtures from 0 – 1 vol%, see Fig. 12) are displayed in Fig. 13.

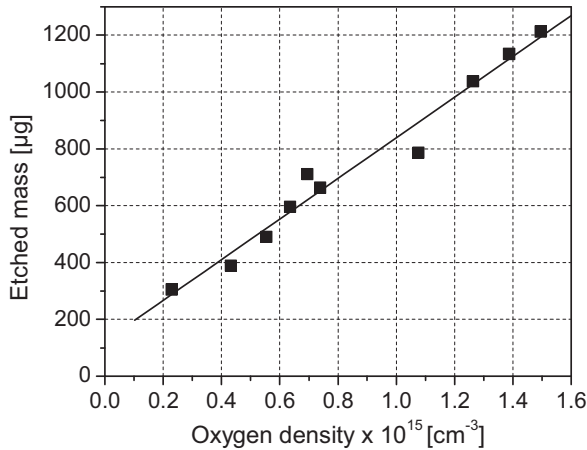


Fig. 13. Dependence of the etched mass on the oxygen density. The etched mass was calculated from the radial depth profiles of PEEK substrates exposed to Ar plasma with different oxygen admixtures (0-1 vol%  $\text{O}_2$ ) located at axial distances of 5 and 7 mm.

This graph shows a linear etching behavior which shows that the etching process is proportional to plasma-generated oxygen species. Regarding the reactive species, additional to atomic oxygen, high concentrations of ozone, of the order of  $10^{14} \text{ cm}^{-3}$ , is emitted by the plasma effluent [41]. In principal, the ozone concentration is proportional to the atomic oxygen concentration following an exponential law with increasing oxygen admixture and reaching a saturation towards higher oxygen admixtures [41]. Hence, it can be assumed, that both, atomic oxygen and ozone might be contributing equally to polymer etching.

As shown in Fig. 11 the etching process occurs not only on the jet axis, but also adjacent to the impinging plasma effluent. Therefore, the radial distribution of the oxygen density was investigated. Fig. 14 shows the correlation of measured radial atomic oxygen density profiles to the corresponding depth profiles at different axial distances.

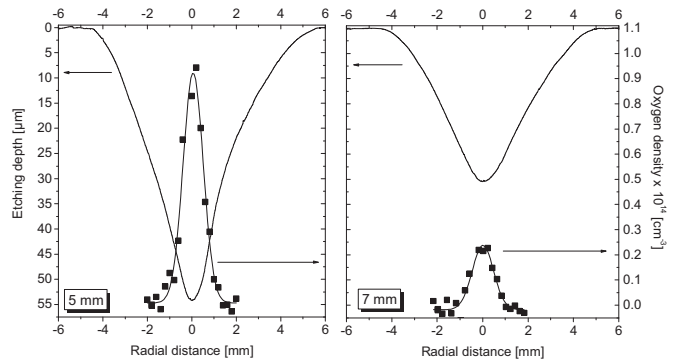


Fig. 14. Correlation of the etching profile and the radial distribution of the atomic oxygen density obtained at a jet-nozzle-to-substrate distance of 5 and 7 mm applying Ar/1% $\text{O}_2$  plasma. Both profiles of the oxygen density were fitted with a Gaussian function.

Analogous to Fig. 13, it can be seen that the etching depth of the surface was increased with the absolute atomic oxygen peak density, thus both depend on the distance between target and jet-nozzle. The oxygen distributions as well as the depth profiles are symmetrical to the jet axis and their full widths at half maximum do not change with increasing axial distance from 5 to 7 mm. But the radial profile of the oxygen density and the radial depth profile differ in width from each other. Thus, derived from the presented data, a FWHM of 3.4 mm for the depth profile and a FWHM of 1.2 mm for the oxygen profile was determined. Since the jet effluent has a conical shape, the FWHM of the oxygen profile is slightly smaller than the inner diameter of the quartz capillary. However, from the constant width of the oxygen profile it can be concluded that diffusion of atomic oxygen perpendicular to the gas beam, thus resulting in a broadening of the distribution, is negligible. The question that arises is why the oxygen and depth profile differs in width, although Fig. 13 and 14 suggest that the etched mass, and because of the constant radial distribution, the maximal etching depth are directly depending on the atomic oxygen density. One would expect a width of the area affected by etching according to the width of the atomic oxygen distribution, if atomic oxygen is the only candidate for etching and other reactive species or radiation, having a maybe wider radial distribution, are neglected. A possible explanation might be the influence of produced ozone. Previously studies analyzed the spatial distribution of ozone depending on the axial distance [41]. The results showed an ozone diffusion of several millimeters in radial direction forming a funnel-shaped profile with increasing axial distance. Therefore, the broadening of the depth profiles may result from the contribution of plasma generated ozone. Furthermore, it has to be noted that the conditions under which the two diagnostics (TALIF and surface profilometry) have been executed were different. The etching measurements were performed on a target surface, but the TALIF - measurements have not been carried out in front of a surface, thus the interaction of the target and the oxygen gas beam resulting in a possible broadening of the oxygen distribution was not investigated. Thus measurements in direct vicinity to the surface are



essential. Comparable measurements of the atomic oxygen density in front of a target surface, in the effluent of the helium-driven  $\mu$ -APPJ, offer a clue to this problem [42]. Here, dependent on the target material, a broadening of the radial oxygen distribution close to the surface was measured. For instance the oxygen signal was estimated to be up to five times wider directly on the metallic surface (gold) than in the free undisturbed effluent. But in contrast, using a polymeric target (PET) in front of the effluent did not result in a significant influence in the oxygen signal. Therefore, a broadening of the oxygen profile on the PEEK surface might be neglected but will be investigated in further studies.

#### IV. SUMMARY AND CONCLUSION

The etching mechanism of an argon atmospheric pressure plasma jet, impinging a PEEK surface, was investigated. The impact of admixtures of molecular oxygen on the surface properties was studied in detail. Physico-chemical surface analysis revealed that a number of new carbon-oxygen functionalities have been introduced into the polymeric surface. Especially after Ar/1%O<sub>2</sub> plasma a significant increase in the O/C ratio and in the content of oxygen-containing functionalities was measured. Furthermore, the fitted C 1s core-level spectra contained an additional peak which was assigned to carboxyl groups. From the FWHM of the aromatic C-C bonds, employed in the peak fit, and the still present shake-up peak plasma-induced ring-opening is unlikely. Also the analysis of the valence band spectra showed no indication for ring-opening after plasma treatment. Since the C 1s spectra exhibited no decrease in the carbonyl and ether bonds an oxidation on the benzene ring is considered which results in the formation of structures like phenol, hydroquinone, and quinone. The presence of carboxyl groups on the surface, which were observed especially after Ar/1%O<sub>2</sub> plasma treatment, indicates chain scission on the ketone group. The increased chain scission by using Ar/O<sub>2</sub> plasma is based on the enhanced etching capability of this plasma compared to pure argon plasma. This was also confirmed by atomic force microscopy. The surface roughness of PEEK was enhanced after Ar and Ar/1% O<sub>2</sub> plasma but the surface roughness was remarkably higher after Ar/1% O<sub>2</sub> plasma. From an initial relative smooth PEEK surface, grains of several hundred nanometers in height were measured after Ar/1%O<sub>2</sub> plasma treatment. However, radial measured depth profiles exhibited a symmetric-shaped etch crater which can be described by a Gaussian function. Furthermore, with increasing axial distance the etching depth, derived from the depth profiles, declined. In order to obtain more information on the etching process surface analysis was accomplished by two-photon absorption laser-induced fluorescence spectroscopy. Since the etching efficiency is increased when molecular oxygen is added, it can be assumed that plasma-generated oxygen species are mainly contributed in this plasma process. The absolute atomic oxygen density was determined by TALIF spectroscopy. The dependence of the atomic oxygen density on different gas

mixtures and axial distances was examined. It was found that the density increase became more pronounced with oxygen admixture. Moreover, the evolution of the oxygen density was characterized by a steep increase for small admixtures followed by shallow increase at higher oxygen admixtures reaching a saturation-like state. Regarding the determined etching depth a very similar tendency were observed. Deduced from these results it can be concluded that the etching process is proportional to the processes involved in the generation of reactive oxygen species. Additionally, the radial depth profiles nearly followed the radial evolution of the oxygen density. Certainly, the full widths at half maximum of the depth profiles were larger compared to those of the radial oxygen profiles. This observation implies that also other reactive species, that have a wider radial distribution, are involved in etching processes. A candidate for this assumption is ozone. Previously published data, performed with this jet, showed exactly the same exponential evolution of the ozone concentration with molecular oxygen admixture. Furthermore, the radial and axial ozone profile exhibited a funnel-shaped evolution based on the radial ozone diffusion of several millimeters. Hence, it can be assumed that the radial depth profile is also influenced by ozone.

#### REFERENCES

- [1] S. M. Kurtz, and J. N. Devine, "PEEK biomaterials in trauma, orthopedic, and spinal implants," *Biomaterials*, vol. 28, no. 32, pp. 4845-4869, Nov, 2007.
- [2] S. W. Ha, R. Hauert, K. H. Ernst *et al.*, "Surface analysis of chemically-etched and plasma-treated polyetheretherketone (PEEK) for biomedical applications," *Surf. Coat. Technol.*, vol. 96, no. 2-3, pp. 293-299, Nov, 1997.
- [3] F. Awaja, S. N. Zhang, N. James *et al.*, "Plasma Activation and Self Bonding of PEEK for the Use in the Encapsulation of Medical Implants," *Plasma Process. Polym.*, vol. 7, no. 9-10, pp. 866-875, Oct, 2010.
- [4] N. Inagaki, S. Tasaka, T. Horiuchi *et al.*, "Surface modification of poly(aryl ether ether ketone) film by remote oxygen plasma," *J. Appl. Polym. Sci.*, vol. 68, no. 2, pp. 271-279, Apr, 1998.
- [5] E. Gonzalez, M. D. Barankin, P. C. Guschl *et al.*, "Ring Opening of Aromatic Polymers by Remote Atmospheric-Pressure Plasma," *IEEE Trans. Plasma Sci.*, vol. 37, no. 6, pp. 823-831, Jun, 2009.
- [6] C. Oehr, "Plasma surface modification of polymers for biomedical use," *Nucl. Instrum. Methods Phys. Res. Sect. B-Beam Interact. Mater. Atoms*, vol. 208, pp. 40-47, Aug, 2003.
- [7] N. Gomathi, A. Sureshkumar, and S. Neogi, "RF plasma-treated polymers for biomedical applications," *Current Science*, vol. 94, no. 11, pp. 1478-1486, Jun, 2008.
- [8] A. Hollander, R. Wilken, and J. Behnisch, "Subsurface chemistry in the plasma treatment of polymers," *Surf. Coat. Technol.*, pp. 788-791, 1999.
- [9] M. R. Wertheimer, A. C. Fozza, and A. Hollander, "Industrial processing of polymers by low-pressure plasmas: the role of VUV radiation," *Nuclear Instruments & Methods in Physics Research Section B-Beam Interactions with Materials and Atoms*, vol. 151, no. 1-4, pp. 65-75, May, 1999.
- [10] K. Fricke, H. Steffen, T. von Woedtke *et al.*, "High Rate Etching of Polymers by Means of an Atmospheric Pressure Plasma Jet," *Plasma Process. Polym.*, vol. 8, no. 1, pp. 51-58, Jan, 2011.
- [11] K. D. Weltmann, E. Kindel, R. Brandenburg *et al.*, "Atmospheric Pressure Plasma Jet for Medical Therapy: Plasma Parameters and Risk Estimation," *Contrib. Plasma Phys.*, vol. 49, no. 9, pp. 631-640, Oct, 2009.
- [12] H. F. Doebele, T. Mosbach, K. Niemi *et al.*, "Laser-induced fluorescence measurements of absolute atomic densities: concepts and

- limitations," *Plasma Sources Sci. Technol.*, vol. 14, no. 2, pp. S31-S41, May, 2005.
- [13] S. Reuter, J. Winter, A. Schmidt-Bleker *et al.*, "Atomix oxygen in a cold argon plasma jet: TALIF spectroscopy in ambient air with modelling and measurements of ambient species diffusion," *Plasma Sources Sci. Technol.*, vol. 21, no. 024005, 2012.
  - [14] K. Niemi, V. Schulz-von der Gathen, and H. F. Dobebe, "Absolute calibration of atomic density measurements by laser-induced fluorescence spectroscopy with two-photon excitation," *J. Phys. D-Appl. Phys.*, vol. 34, no. 15, pp. 2330-2335, Aug, 2001.
  - [15] G. Beamson, and D. Briggs, *High resolution XPS of organic polymers. The Scienta ESCA 300 data base*, Chichester: John Wiley & Sons, 1992.
  - [16] D. T. Clark, and A. Dilks, "ESCA applied to polymers 23. RF glow-discharge modification of polymers in pure oxygen and helium-oxygen mixtures," *J. Polym. Sci. Pol. Chem.*, vol. 17, no. 4, pp. 957-976, 1979.
  - [17] D. Briggs, "Applications of XPS in Polymer Technology," *Practical Surface Analysis - Auger and X-ray Photoelectron Spectroscopy*, D. Briggs and M. P. Seah, eds., pp. 437-483: John Wiley & Sons Ltd., 1996.
  - [18] R. Foerch, G. Beamson, and D. Briggs, "XPS valence band analysis of plasma-treated polymers," *Surf. Interface Anal.*, vol. 17, no. 12, pp. 842-846, Nov, 1991.
  - [19] R. M. France, and R. D. Short, "Plasma treatment of polymers: The effects of energy transfer from an argon plasma on the surface chemistry of polystyrene, and polypropylene. A high-energy resolution X-ray photoelectron spectroscopy study," *Langmuir*, vol. 14, no. 17, pp. 4827-4835, Aug, 1998.
  - [20] S. Koizumi, A. Nakao, K. Endo *et al.*, "Analysis of valence XPS of hydrocarbon polymers modified by He-ion bombardment," *Polym. J.*, vol. 33, no. 8, pp. 621-628, 2001.
  - [21] K. Endo, C. Inoue, Y. Kaneda *et al.*, "Simulation of the Valence X-ray Photoelectron Spectra of 16 Polymers by the Semiempirical HAM/3 MO Method Using the Model Molecules," *Bull. Chem. Soc. Jpn.*, vol. 68, no. 2, pp. 528-538, Feb, 1995.
  - [22] D. Briggs, and G. Beamson, "XPS studies of the oxygen 1s and oxygen 2s levels in a wide-range of functional polymers," *Anal. Chem.*, vol. 65, no. 11, pp. 1517-1523, Jun, 1993.
  - [23] T. Otsuka, K. Endo, M. Suhara *et al.*, "Theoretical X-ray photoelectron spectra of polymers by deMon DFT calculations using the model dimers," *J. Mol. Struct.*, vol. 522, pp. 47-60, Apr, 2000.
  - [24] J. Riga, J. J. Pireaux, J. P. Boutique *et al.*, "X-ray photoelectron spectroscopic study of  $\pi$  electron delocalization in polyphenyls - a comparison with acenes and polystyrene," *Synth. Met.*, vol. 4, no. 2, pp. 99-112, 1981.
  - [25] S. R. Cain, and L. J. Matienzo, "Valence band x-ray photoelectron spectroscopy of poly(ether ketone) and poly(ether-ether ketone)," *J. Polym. Sci. Pt. B-Polym. Phys.*, vol. 30, no. 3, pp. 275-279, Mar, 1992.
  - [26] P. Boulanger, C. Magermans, J. J. Verbist *et al.*, "X-ray photoelectron-spectroscopy and x-ray emission spectroscopy of poly(ethylene oxide) and poly(vinyl alcohol): experiment and theory," *Macromolecules*, vol. 24, no. 10, pp. 2757-2765, May, 1991.
  - [27] G. Marletta, F. Iacona, and A. Toth, "Particle beam-induced reactions versus thermal degradation in PMDA-ODA polyimide," *Macromolecules*, vol. 25, no. 12, pp. 3190-3198, Jun, 1992.
  - [28] C. Seidel, C. Damm, and H. Muenstedt, "Surface modification of films of various high temperature resistant thermoplastics," *J. Adhes. Sci. Technol.*, vol. 21, no. 5-6, pp. 423-439, Apr, 2007.
  - [29] F. D. Egitto, V. Vukanovic, and G. N. Taylor, "Plasma etching of organic polymers " *Plasma deposition, treatment, and etching of polymers*, R. d'Agostino, ed., New York: Academic Press Inc., 1990.
  - [30] J. A. Macko, and H. Ishida, "Behavior of a bisphenol-A-based polybenzoxazine exposed to ultraviolet radiation," *J. Polym. Sci. Pt. B-Polym. Phys.*, vol. 38, no. 20, pp. 2687-2701, Oct, 2000.
  - [31] R. Volkamer, B. Klotz, I. Barnes *et al.*, "OH-initiated oxidation of benzene - Part I. Phenol formation under atmospheric conditions," *Phys. Chem. Chem. Phys.*, vol. 4, no. 9, pp. 1598-1610, 2002.
  - [32] C. Busset, P. Mazellier, M. Sarakha *et al.*, "Photochemical generation of carbonate radicals and their reactivity with phenol," *J. Photochem. Photobiol. A-Chem.*, vol. 185, no. 2-3, pp. 127-132, Jan, 2007.
  - [33] E. Gonzalez, M. D. Barankin, P. C. Guschl *et al.*, "Remote Atmospheric-Pressure Plasma Activation of the Surfaces of Polyethylene Terephthalate and Polyethylene Naphthalate," *Langmuir*, vol. 24, no. 21, pp. 12636-12643, Nov, 2008.
  - [34] J. W. Coburn, and M. Chen, "Optical emission spectroscopy of reactive plasmas: A method for correlating emission intensities to reactive particle density," *J. Appl. Phys.*, vol. 51, no. 6, pp. 3134-3136, 1980.
  - [35] K. Niemi, S. Reuter, L. M. Graham *et al.*, "Diagnostic based modeling for determining absolute atomic oxygen densities in atmospheric pressure helium-oxygen plasmas," *Appl. Phys. Lett.*, vol. 95, no. 15, pp. 3, Oct, 2009.
  - [36] H. M. Katsch, A. Tewes, E. Quandt *et al.*, "Detection of atomic oxygen: Improvement of actinometry and comparison with laser spectroscopy," *J. Appl. Phys.*, vol. 88, no. 11, pp. 6232-6238, Dec, 2000.
  - [37] N. Knake, S. Reuter, K. Niemi *et al.*, "Absolute atomic oxygen density distributions in the effluent of a microscale atmospheric pressure plasma jet," *J. Phys. D-Appl. Phys.*, vol. 41, no. 19, pp. 6, Oct, 2008.
  - [38] S. Reuter, K. Niemi, V. Schulz-von der Gathen *et al.*, "Generation of atomic oxygen in the effluent of an atmospheric pressure plasma jet," *Plasma Sources Sci. Technol.*, vol. 18, no. 1, pp. 9, Feb, 2009.
  - [39] G. Park, H. Lee, G. Kim *et al.*, "Global model of He/O-2 and Ar/O-2 atmospheric pressure glow discharges," *Plasma Process. Polym.*, vol. 5, no. 6, pp. 569-576, Aug, 2008.
  - [40] S. Reuter, *Formation Mechanisms of Atomic Oxygen in an Atmospheric Pressure Plasma Jet Characterised by Spectroscopic Methods*, Göttingen: Cuvillier Verlag, 2008.
  - [41] S. Reuter, J. Winter, S. Iseni *et al.*, "Detection of Ozone in a MHz Argon Plasma Bullet Jet," *Plasma Sources Sci. Technol.*, vol. 21, no. 3, pp.10, May, 2012
  - [42] D. Schröder, H. Bahre, N. Knake *et al.*, "Influence of target surfaces on the atomic oxygen distribution in the effluent of a micro-scaled atmospheric pressure plasma jet," *Plasma Sources Sci. Technol.*, vol. 21, no. 2, pp.7, Apr, 2012
- Katja Fricke** received the Diploma degree in environmental science at the Ernst Moritz Arndt University of Greifswald, Greifswald, Germany, in 2007. During her diploma thesis, she investigated the immobilization of biocatalysts for microbial bioelectrochemical systems and studied the anodic bioelectrocatalytic electron transfer in microbial fuel cells. Since 2008 she has been a researcher with the Leibniz Institute for Plasma Science and Technology (INP Greifswald e.V.), Greifswald. In her PhD thesis she elucidates the impact of non-thermal plasma on bio-relevant materials, particularly the influence of plasma on the physico-chemical and morphological surface properties. Her other research interests include plasma-based processes for biological decontamination and sterilization.
- Stephan Reuter** became an IEEE member in 2012. He received his Master of Engineering (Dipl. Phys.-Ing.) and his Master of Science (Dipl. Phys.) in plasma physics at the University of Duisburg-Essen. He was awarded his PhD (Dr. rer. nat.) in 2007 for the investigation of oxygen formation mechanisms in atmospheric pressure plasma jets. In 2008 he became a research fellow at the Centre for Plasma Physics at Queen's University Belfast, NI (UK). Currently he is head of the junior research group "Extracellular Effects" in the BMBF funded centre for innovation competence *plasmatis* at the Leibniz Institute for Plasma Science and Technology (INP Greifswald e.V.), Germany. Here he performs research on controlling the interaction of atmospheric pressure plasmas with biological liquids in the field of plasma medicine. The focus of his research group lies on optical diagnostics and modeling of atmospheric pressure plasma jets interacting with liquids. Stephan Reuter is an IEEE member, a member of the German Physical Society (DPG), the International Society for Plasma Medicine (ISPM), and the International Society for Plasma Chemistry (ISPC).
- Daniel Schröder** received his Master of Science (Dipl. Phys.) in plasma physics at the Ruhr-Universität Bochum in 2010 for his work on the interaction of reactive oxygen species, produced by an atmospheric pressure jet discharge, with surfaces of different materials. Since 2011 he is a PhD-Student at the Ruhr-Universität Bochum in the Department of Application oriented Plasma Physics and Member of the Research Unit FOR1123 'Physics of Microplasmas'. Daniel Schröder is a member of the German Physical Society (DPG).



**Volker Schulz-von der Gathen** received his doctorate degree (Dr. rer. nat.) at the University of Duisburg-Essen in 1990 for the investigation of an arc discharge by use of advanced optical diagnostics. He worked as senior scientist at the Institute of Laser- and Plasma Physics in Essen until he moved to the Institute for Application-oriented Plasma Physics at the Ruhr-University Bochum in 2005. His main research interest is the investigation of low-temperature non-equilibrium plasmas by optical methods as phase resolved optical emission spectroscopy or two-photon absorption laser-induced fluorescence spectroscopy. As a principal investigator in the Research Department Plasma he is now project leader in the Research Unit FOR1123 „Physics of Microplasmas“ concentrating on the diagnostics of micro discharges close to atmospheric pressure. In particular his group is investigating an at rf-frequency excited atmospheric pressure micro jet and micro plasma arrays operated at kHz frequencies. He is a member of the German Physical Society (DPG).

**Klaus-Dieter Weltmann:** This author became a Member of IEEE in 1995. Klaus-Dieter Weltmann received the diploma degree in electronics and the doctorate degree (Dr. rer. nat) in applied physics from the University of Greifswald, Germany, in 1989 and 1993, respectively. He worked on nonlinear dynamics in low temperature plasmas and plasma diagnostics. In 1994, he was Visiting Scientist at the Plasma Physics Laboratory, West Virginia University (USA). In 1995, he joined ABB Corporate Research Ltd., Baden-Dättwil, Switzerland, working in the research and development of HV and MV switchgear. In 1998, he became the head of High Voltage Systems Group, ABB Corporate Research Ltd. In 2000, he was appointed to lead R&D of Gas Insulated Switchgear (GIS, PASS) at ABB High Voltage Technologies Ltd., Zurich, Switzerland, 2002 he became Business Unit R&D Manager GIS. Since 2003, he is director and chairman of the board of the Leibniz Institute for Plasma Science and Technology e.V. (INP Greifswald) and Professor for Experimental Physics at the University of Greifswald. His present research interests include switchgears, arc physics, atmospheric plasmas, modeling and simulation, Plasma Medicine and plasma decontamination. Prof. Weltmann is member of IEEE, president of the International Society for Plasma Medicine (ISPM), member of the German Physical Society and member of several consulting committees in industry and research. He is initiator of three spin-off companies.

**Thomas von Woedtke** received the doctoral degree (Dr. rer. nat.) and the Habilitation degree (Dr. rer. nat. habil.) in Pharmaceutical Technology from the University of Greifswald, Greifswald, Germany, in 1996 and 2005, respectively. From 1987 to 2005, he worked on the application of biosensors in medicine and life science research as well as on alternative sterilization techniques for sensitive goods. Since 2005, he has been with the Leibniz Institute of Plasma Science and Technology e.V. (INP Greifswald), Greifswald, Germany. His research interests are in the field of plasma-based processes for biological decontamination and sterilization as well as in basic research problems of plasma-cell and plasma-tissue interactions. Dr. von Woedtke is Programme Manager Plasma Medicine/Decontamination at the INP Greifswald, Greifswald, Germany, and since 2011 Professor for Plasma Medicine at the University of Greifswald.

## **5.5 “Comparison of non-thermal Plasma Processes on the Surface Properties of Polystyrene and their Impact on Cell Growth”**

Katja Fricke, Kathrin Duske, Antje Quade, Barbara Nebe, Karsten Schröder, Klaus-Dieter Weltmann, Thomas von Woedtke

*IEEE Transactions on Plasma Science*, **2012**, DOI: 10.1109/TPS.2012.2204904



# Comparison of Nonthermal Plasma Processes on the Surface Properties of Polystyrene and Their Impact on Cell Growth

Katja Fricke, Kathrin Duske, Antje Quade, Barbara Nebe, Karsten Schröder, Klaus-Dieter Weltmann, *Member, IEEE*, and Thomas von Woedtke

**Abstract**—The initial adhesion and spreading of cells are crucial factors for the successful performance of a synthetic biomaterial used for cell culture disposables or human medical devices (e.g., implants). Surface properties which allow the control of the attachment of cells are decisive for the acceptance of the provided material. Hence, different surface preparation techniques are used to equip surfaces with functional groups to improve initial surface interactions. In this paper, polystyrene (PS) surfaces were modified by using different nonthermal plasma processes. In particular, low-pressure plasma and atmospheric-pressure plasma were applied to modify surfaces or to deposit thin films on surfaces. Furthermore, the behaviors of human osteoblastic cells with respect to cell viability and cell growth on differently plasma treated PS surfaces are investigated. A comparison is made between plasma-grafted PS and commercially available PS—such as tissue-culture PS and Primaria. The cell studies were accompanied by surface analysis comprising atomic force microscopy, determination of surface energies, and X-ray photoelectron spectroscopy measurements. This work demonstrates that the functionalization of PS substrates by applying low-pressure and atmospheric-pressure plasma processes are equally effective in the improvement of cell attachment and proliferation. Furthermore, it is shown that the enhanced metabolic activity and spreading behavior of osteoblastic cells correlate well with an increase in surface wettability and the introduction of polar oxygen- and/or nitrogen-containing functional groups after plasma treatment.

**Index Terms**—Atmospheric-pressure plasma, low-pressure plasma, osteoblastic cells, surface modification.

## I. INTRODUCTION

**P**OLYMERS exhibit advantageous properties, such as processability, recyclability, mechanical properties, and low cost; thus, they are well suited for different application; par-

ticularly, a wide variety of polymers is applied as artificial biomaterials [1]. However, because these materials are usually characterized by low surface energies and poor chemical reactivity, they do not possess the necessary surface characteristics for proper function [2]. Therefore, functionalization or coating processes are required to create chemical functionalities [3]. For this purpose, advanced nonthermal plasma processes exhibit an enormous technological potential for surface and material processing. Hence, two types of gas discharges are applied in nonthermal plasma technology [4]: 1) the use of low-pressure devices which ensure a uniform and well-defined surface modification, are stable, and can be easily controlled and 2) the use of atmospheric-pressure-plasma devices that do not require expensive vacuum equipment, can be easily implemented in continuous in-line processes, and, due to their scalability, offer the possibility to treat large products, even with a complex 3-D geometry. The application of gas-discharge plasmas can lead to surface activation and functionalization. Most of all, for biomedical applications, the functionalization is of particular importance, since functional groups control the conformation of biomolecules during adhesion and proliferation [3]. Hence, cell adhesion plays an important role in cellular physiological functions and in the integration of implantable biomedical devices to cells. The adhesion and proliferation of cells are strongly influenced by the presence of functional groups, surface energy, and roughness of the biomaterial [5]. Consequently, a good understanding of the relationships between the behavior of cells and the physicochemical properties of the substrates is of importance for the optimization of cell cultures. Current research is focused on the improvement of the biocompatibility (defined as the ability of a material to perform with an appropriate host response in a specific situation [6]) of biomaterials by using plasma-assisted surface modification and/or thin-film deposition [7], [8]. For this purpose, many studies have been reported using various plasma-based approaches and process gases [2]. Moreover, low-pressure plasma processes have gained considerable attention to improve the biocompatibility of different materials, usually using plasma-assisted coating methods [9]. As evidenced in previous work, those plasma processing procedures can be used to induce, for instance, nitrogen-containing groups (e.g., amino groups) on surfaces which are further capable of initiating cell adhesion and cell proliferation [10]–[12]. Hence, plasma processes for the surface grafting of biomaterials are traditionally performed

Manuscript received February 14, 2012; revised May 8, 2012; accepted June 7, 2012. This work was supported by the Federal Ministry of Education and Research of Germany within the joint research project “Campus Plasma-Med” under Grant 13N9779 and Grant 13N11188.

K. Fricke, A. Quade, K. Schröder, K.-D. Weltmann, and T. von Woedtke are with the Leibniz Institute for Plasma Science and Technology (INP Greifswald e.V.), 17489 Greifswald, Germany (e-mail: k.fricke@inp-greifswald.de; quade@inp-greifswald.de; weltmann@inp-greifswald.de; woedtke@inp-greifswald.de).

K. Duske and B. Nebe are with the Biomedical Research Center, Department of Cell Biology, University of Rostock, 18057 Rostock, Germany (e-mail: kathrin.duske@med.uni-rostock.de; barbara.nebe@med.uni-rostock.de).

Color versions of one or more of the figures in this paper are available online at <http://ieeexplore.ieee.org>.

Digital Object Identifier 10.1109/TPS.2012.2204904

at low pressure. However, due to the geometrical confinements of low-pressure plasmas and their need of vacuum systems, the interest toward the application of atmospheric-pressure plasmas in material processing is emerging worldwide [13].

In this paper, we analyze the effect of human osteoblastic cell spreading on polystyrene (PS) substrates of different surface properties, and a comparison is made between different plasma-treated PS surfaces. For instance, low-pressure nitrogen-containing plasma was applied either to functionalize the surface or to deposit a nanometer-thick aminofunctional thin film on the surface. Additionally, atmospheric-pressure plasma was applied with different operating gases (inert and reactive gases) to modify PS. Furthermore, conventional commercially available PS substrates, namely, tissue-culture PS (TCPS) and Primaria, were used as reference material. PS covered with a fluorine-containing thin film served as negative control. We investigated the effect of the different modification methods on cell-surface interactions in respect to the surface properties which were characterized by applying atomic force microscopy (AFM), X-ray photoelectron spectroscopy (XPS), water contact angle, and surface energy measurements, respectively. Here, we demonstrate that a similar improvement in cell spreading, compared to low-pressure plasma, was achieved using atmospheric-pressure plasma.

## II. MATERIALS AND METHODS

### A. Materials

PS cell culture dishes were obtained from the following commercial sources: Sterile Falcon non-tissue-culture-treated PS [PS (BD)] and Primaria were purchased from Becton Dickinson Bioscience (Heidelberg, Germany). Primaria features nitrogen-containing tissue-culture surfaces that support cell growth [14]. TCPS, whose surface was modified by using oxygen corona discharge, was purchased from Corning (Amsterdam, The Netherlands). Wafers with diameters of 15 mm were punched out of the bottom of the cell culture dishes. Only the PS (BD) wafers were used for plasma treatments. Primaria and TCPS served as reference material.

PS is an aromatic hydrocarbon polymer with a simple chemical structure containing no chemical functional groups which facilitates clear information on the impact of plasma on the chemical surface composition. Furthermore, PS was selected because of its particular relevance in biomedical applications.

### B. Plasma Sources and Plasma Treatments

For the comparative investigations, different plasma treatments were applied. The chosen process parameters are based on empirical data assessed by prior investigations [15]–[18]. Furthermore, considering the heat-sensitive property of PS, the applied plasma processes ensure a gentle surface treatment excluding material destruction.

1) *Low-Pressure Plasma*: For the plasma-assisted modification and thin-film deposition at low pressure, a microwave (MW)-excited (2.45 GHz) gas-discharge plasma (V55G,

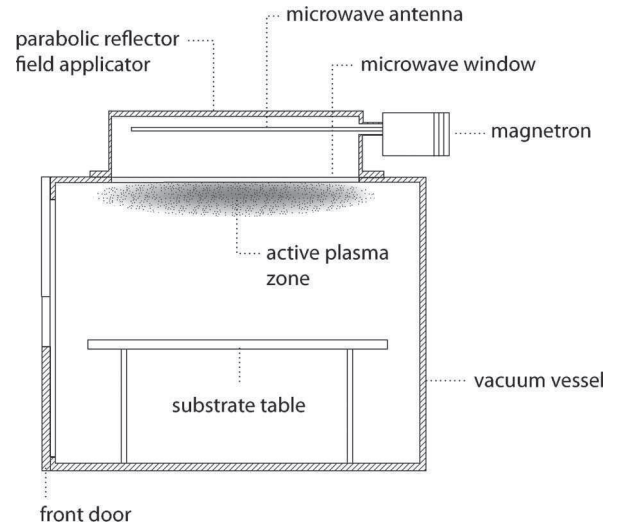


Fig. 1. Schematic drawing of the low-pressure-plasma processor with the MW source (according to [18]).

Plasma Finish, Germany) was applied (see Fig. 1), as described in [15]. The following plasma processes were used.

- 1)  $\text{NH}_3$ : Substrates were exposed to continuous wave (cw) ammonia plasma (40 sccm  $\text{NH}_3$ , 500 W, 50 Pa) in a downstream position of 5 cm from the MW coupling window for a duration of 30 s.
- 2)  $\text{O}_2$ : Functionalization of the substrates by using pulsed oxygen plasma (1200 W, 100 Pa, 60 sccm  $\text{O}_2$ /40 sccm Ar) for a time of 100 s at a downstream position of 11 cm from the MW coupling window. Note that the abbreviation “ $\text{O}_2$  MW” is used for this plasma process in this contribution.
- 3) Plasma polymerization of allylamine (PPAAm): Substrates were treated in a downstream position, 9 cm from the MW coupling window. The procedure is divided into two steps: 1) activation of the substrate by a cw oxygen plasma (500 W, 50 Pa, 100-sccm  $\text{O}_2$ /25 sccm Ar) and 2) PPAAm by an MW-excited pulsed gas-discharge plasma for 960 s (500 W, 50 Pa, 50 sccm Ar) [16].
- 4)  $\text{PPC}_6\text{F}_6$ : The deposition was carried out in a downstream position, 9 cm from the MW coupling window. The procedure is divided into two steps: 1) activation of the substrate by a pulsed argon plasma (800 W, 50 Pa, 50-sccm Ar) for a time of 330 s and 2) the plasma polymerization of hexafluorobenzene ( $\text{PPC}_6\text{F}_6$ ) by an MW-excited pulsed gas-discharge plasma for 1320 s (800 W, 50 Pa, 50 sccm Ar).

2) *Atmospheric-Pressure-Plasma Jet*: Fig. 2 shows a schematic setup of the atmospheric-pressure-plasma jet (kINPen, developed at the Leibniz Institute for Plasma Science and Technology) used in this study. The plasma device consists of a quartz capillary (inner diameter of 1.6 mm; outer diameter of 4 mm) with a pin-type HF electrode (1.7 MHz) inside. Further details of this type of jet, version kINPen09, are described elsewhere [19]. Feed gases 5 slm argon (labeled as “Ar jet”) or a mixture of 5 slm argon and 0.05 slm oxygen (1% oxygen admixture; labeled as “Ar/ $\text{O}_2$  jet”) were applied.



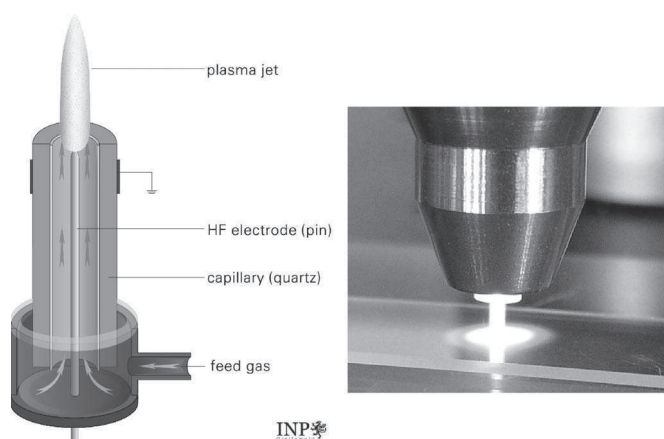


Fig. 2. (Left) Schematic setup of the plasma jet, according to [14], and (right) plasma treatment of a PS substrate.

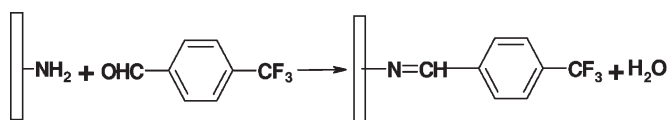


Fig. 3. Chemical derivatization for the determination of primary amino group density.

The PS samples were treated locally at a distance of 5 mm to the nozzle outlet (see Fig. 2, right) for 60 s.

### C. Physicochemical Surface Analysis

The elemental surface composition and chemical binding properties were analyzed by XPS using an AXIS Ultra DLD electron spectrometer (Kratos Analytical, Manchester, U.K.). The spectra were recorded by means of monochromated Al K $\alpha$  excitation (1486.6 eV) with a medium magnification (field of view 2) lens mode and by selecting the slot mode, providing an analysis area of approximately 250  $\mu\text{m}$  in diameter. A pass energy of 80 eV was used for estimating the chemical elemental composition, and a pass energy of 10 eV was used for the high-energy resolution of the C 1s peaks to investigate chemical functional groups. Charge neutralization was implemented by low-energy electrons injected into the magnetic field of the lens from a filament located directly atop the sample. Data acquisition and processing were carried out using CasaXPS software, version 2.14dev29 (Casa Software Ltd., U.K.).

Primary amino group density  $[-\text{NH}_2]$  cannot be measured with XPS directly. Therefore, a chemical derivatization with 4-trifluoromethylbenzaldehyde (TFBA) in a saturated gas phase (37  $^\circ\text{C}$  for 2 h) was used. According to Fig. 3,  $[-\text{NH}_2]$  values can be deduced from the measured fluorine concentration; more precisely, three fluorine atoms label one primary amino group.

For the determination of the wettability, water contact angle measurements on the surfaces were performed under ambient air at room temperature by the sessile drop method using a Digidrop contact angle analyzer (GBX Instrumentation Scientifique, France) and a drop of distilled water with a defined

volume (0.5  $\mu\text{L}$ ). The contact angle of the resting drop was determined, utilizing the software Windrop. Furthermore, the polar and dispersive components of surface energy were calculated from measurements of contact angles with different liquids. In particular, water, ethylene glycol, and ethylene iodine contact angles were determined using the OCA 30 contact angle measuring system (Data Physics Instruments GmbH, Filderstadt, Germany) with the sessile drop method. The surface energy was calculated according to the methods of Owens, Wendt, Rabel, and Kaelble [20].

Changes in the surface roughness were determined by a scanning probe microscope diCP2 (Veeco, Santa Barbara, CA, USA) in the noncontact mode, particularly tapping mode. An area of 10  $\mu\text{m} \times 10 \mu\text{m}$  was scanned using a pyramidal silicon tip doped with n-type phosphorus with a resonance frequency of 273–389 kHz and a force constant of 20–80 N/m (Veeco, RTESPA-CP). Five areas were recorded for each sample and analyzed by means of the software SPMLab Ver. 6.0.2 (Veeco).

### D. Cell Culture and Preparation of Human Osteoblastic Cells

For *in vitro* investigations, human osteoblastic cells (MG-63, ATCC, CRL-1427, Promochem, Wesel, Germany) were used. Probes were placed into 12-well chambers (Greiner Bio One, Frickenhausen, Germany), and cells were cultured with a density of  $4 \times 10^4$  cells/probe in Dulbecco's modified Eagle medium (Invitrogen GmbH, Darmstadt, Germany) with 10% fetal calf serum (PAA Laboratories, Pasching, Austria) and 1% gentamicin (Ratiopharm GmbH, Ulm, Germany) at 37  $^\circ\text{C}$  and in a 5%  $\text{CO}_2$  atmosphere.

Metabolic activity was analyzed after 24 h of cultivation, and the Cell-Titer-96 Aqueous One Solution Cell Proliferation Assay (Promega, Madison, USA) was used. With an Elisa Reader (Anthos Reader 2010, Anthos Mikrosysteme GmbH, Krefeld, Germany) at a wavelength of 492 nm, colorimetric measurements were performed.

For measurements of cell area, cells were trypsinated and washed with phosphate buffer saline. Before cells were seeded onto the probes, the cell membrane was stained with the red fluorescent linker PKH26 (PKH26 General Cell Linker Kit, Sigma-Aldrich Chemie GmbH, München, Germany). After cultivation of 1 and 24 h, cell fixation was performed using 4% paraformaldehyde, and the probes were fixed on a slide using double-face glue strip, and finally, cells were embedded with a cover slip. Cell areas of 40 cells per specimen were analyzed using the function "area measurement" of the confocal laser scanning microscope LSM 410 (Carl Zeiss, Jena, Germany).

### E. Statistical Analysis

The results are presented as *mean*  $\pm$  *standard deviation* (*SD*). Statistical analysis was performed on the data from the biological experiments at the significance level of less than 0.05 ( $p < 0.05$ ). The data from each surface were compared to those of the control PS (BD).



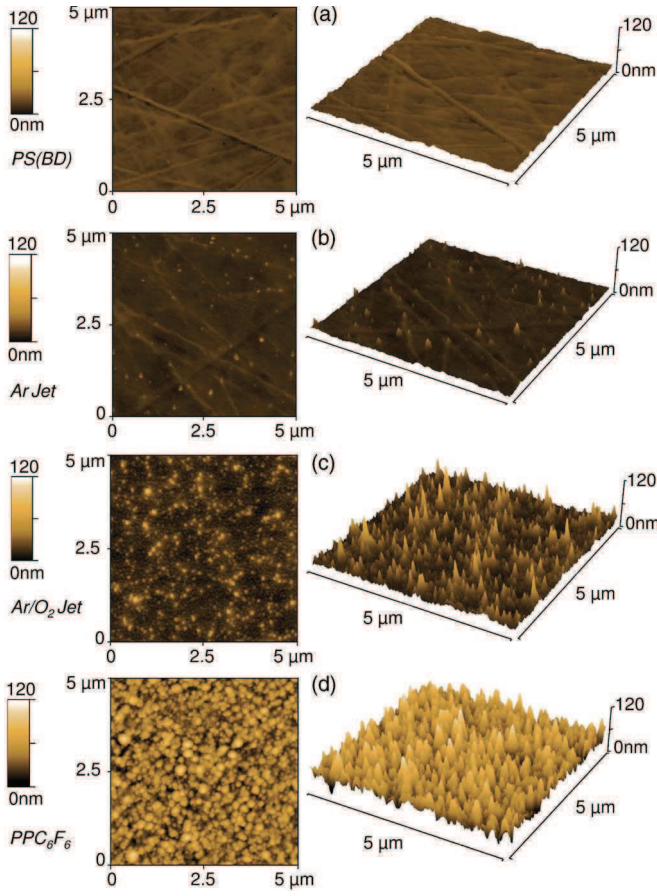


Fig. 4.  $5\ \mu\text{m} \times 5\ \mu\text{m}$  2-D and 3-D AFM images of (a) PS (BD), (b) Ar-jet-plasma-treated PS, (c) Ar/O<sub>2</sub>-jet-plasma-treated PS, and (d) PPC<sub>6</sub>F<sub>6</sub>-coated PS.

### III. RESULTS AND DISCUSSION

The first cell-surface interaction is based on physicochemical reactions such as ionic forces and van der Waals forces [21]. Subsequently, the cell attachment occurs via biomolecules, most commonly through integrins that are mobile nanometer-scaled (8–12 nm) transmembrane molecules [22]. Since the mechanism of cell response to the surface is based on proteins adsorbed on the surface, cell membrane receptors, and cytoskeleton molecules which are all in the nanometer scale, nanoscale topography might influence surface-specific biological responses such as cell activities [23], [24]. Plasma-based methods can initiate structural topographies on surfaces either by coating processes or by etching processes. In order to investigate the generation of nanotopographies on the studied polymeric surfaces, AFM measurements of plasma-treated PS were performed. Fig. 4 shows 2-D and 3-D images of PS (BD) [Fig. 4(a)], PS exposed to Ar [Fig. 4(b)] and Ar/O<sub>2</sub> jet plasma [Fig. 4(c)], and PPC<sub>6</sub>F<sub>6</sub>-coated PS [Fig. 4(d)], respectively. AFM images of the other PS substrates are not shown because no remarkable changes in the surface topography were observed.

The surface topography of PS (BD) exhibited an irregular structure composed of grooves and walls due to manufacturing processes. After Ar-plasma-jet exposure [Fig. 4(b)], the structure of the pristine PS was still retained, but a few surface

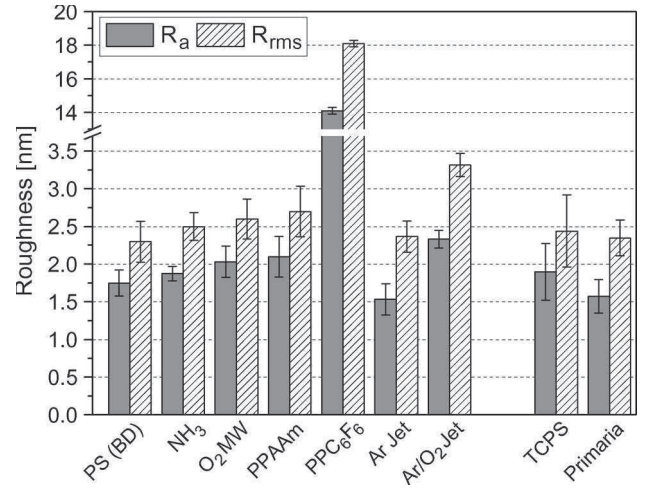


Fig. 5. Arithmetic roughness ( $R_a$ ) and root-mean-square ( $R_{rms}$ ) roughness ( $\text{mean} \pm \text{SD}$ ,  $n = 5$ ) obtained from an area of  $10\ \mu\text{m} \times 10\ \mu\text{m}$ .

grains with a dimension of several nanometers were distributed over the entire surface. Ar/O<sub>2</sub>-jet-plasma treatment [Fig. 4(c)] resulted in a spikelike structure displaying surface grains of 7–10 nm in diameter and an averaged height of 22 nm. The appearance of these grains can be explained by considering that Ar/O<sub>2</sub> plasmas have a strong etching capability due to the generation of reactive oxygen species owing to the dissociation of oxygen molecules in the gas discharge [25]. Fig. 4(d) shows the surface texture of PS after PPC<sub>6</sub>F<sub>6</sub> thin-film deposition. The surface appeared highly grainy with typical grain sizes of 30–100 nm in height and diameters of a few hundreds of nanometers. However, in Fig. 5, the surface roughness parameters, arithmetic roughness ( $R_a$ ), and root-mean-square roughness ( $R_{rms}$ ) of the different PS substrates are depicted.  $R_a$  is the arithmetic average of the height of peaks and depth of valleys from the center plane, whereas  $R_{rms}$  is defined as the SD of the height values relative to the mean line [26].

Although the surface topography of PS, treated by low-pressure plasma, exhibited the same surface texture compared to PS (BD), slight changes in the surface roughness were observed. In particular, Fig. 5 shows increased  $R_a$  and  $R_{rms}$  values for the mentioned PS substrates, particularly on the PPAAm-coated surface. The PS surfaces exposed to atmospheric-pressure plasma showed different results. Whereas the roughness of the Ar-jet-plasma-treated PS is reduced, the  $R_a$  and  $R_{rms}$  values of PS exposed to Ar/O<sub>2</sub> jet plasma were increased, which is based on the formation of the grainlike structure. The surface roughness of the reference TCPS was similar to PS (BD), and those of Primaria were similar to the Ar-jet-plasma-treated PS. The highest surface roughness was determined for the negative control (PPC<sub>6</sub>F<sub>6</sub>-coated PS) with roughness values of  $R_a = 14.1\ \text{nm} \pm 0.2\ \text{nm}$  and  $R_{rms} = 18.1\ \text{nm} \pm 0.2\ \text{nm}$ , respectively. Briefly, the roughness of the PS substrates varied between 1.6 and 2.4 nm for  $R_a$  and 2.25 and 3.3 nm for  $R_{rms}$ , respectively (excluding PPC<sub>6</sub>F<sub>6</sub>-coated PS). Furthermore, since the surface features created on Ar/O<sub>2</sub>-jet-plasma-treated PS are in the range of 7–10 nm in diameter and 22 nm in height, it is most unlikely that these structures diminish cell attachment [22].

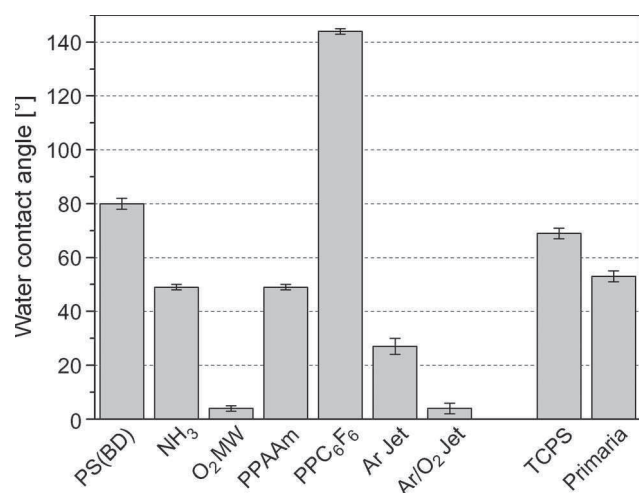


Fig. 6. Water contact angle ( $mean \pm SD$ ,  $n = 10$ ). Comparison of differently treated PS wafers.

Moreover, the influence of the chemistry of the substrate is certainly of high importance for cell adhesion and proliferation. For instance, many scientists pointed out that, *in vitro*, the adhesion of cells was favored on moderate to highly hydrophilic substrates [16], [21]. However, changes in the surface chemistry can be easily detected by contact angle measurements and by the determination of the surface energy. In Fig. 6, the wettability of the studied polymeric substrates is displayed.

It can be observed that PS (BD) is a poor wettable, i.e., slightly hydrophobic, surface, whereas plasma-treated surfaces as well as the reference surfaces exhibited hydrophilic properties. Additionally, the negative control (PPC<sub>6</sub>F<sub>6</sub>-coated PS) showed an increased water contact angle since fluorocarbons are considered as being one of the most hydrophobic molecules. A strongly hydrophilic character was determined for PS exposed to O<sub>2</sub> MW plasma as well as for PS treated by Ar/O<sub>2</sub> jet plasma.

Changes in the wettability are commonly related to changes in the surface energy. Complementary to the water contact angles, surface free energy on the references as well as on plasma-treated PS samples was examined. Fig. 7 shows the change of the total surface energy and of its polar and dispersive components.

The hydrocarbon chain in the PS backbone results in a high portion of dispersive component because dipole moments are absent in alkyl chains. Hence, PS (BD) showed a high amount of the dispersive component, whereas the polar component was lower. A strong increase in the surface energy was evident after plasma treatment in comparison to PS (BD). Only the negative control showed a significant decrease of the surface energy according to the hydrophobic surface. For PS (BD), a surface energy of 35 mN/m was estimated with only 6 mN/m polar components and a dispersive content of 29 mN/m. The results showed that the increase in surface energy was primarily due to the polar component increase on plasma-treated substrates. The dispersive component was found to decrease after plasma treatment or remained unchanged for PPAAm-coated PS and for the reference TCPS. According to the high wettability of O<sub>2</sub> MW-plasma- and Ar/O<sub>2</sub>-jet-plasma-treated PS, the polar com-

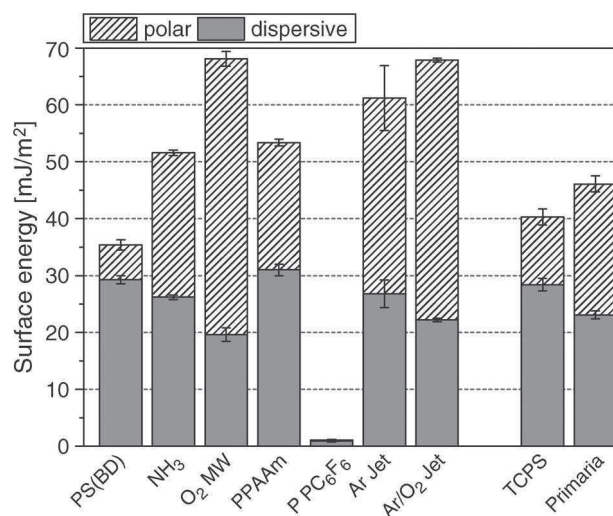


Fig. 7. Surface energy and its components of the modified PS surfaces ( $mean \pm SD$ ,  $n = 3$ ).

TABLE I  
ELEMENTAL SURFACE COMPOSITION (IN ATOMIC PERCENT) OF THE PS SURFACES DETERMINED BY XPS ( $Mean \pm SD$ ,  $n = 3$ )

	C	O	N	F	O/C	N/C	F/C
PS (BD)	98.4 ± 0.3	1.6 ± 0.3			1.6 ± 0.3		
PPAAm	73.7 ± 0.4	2.7 ± 0.3	23.6 ± 0.3		3.8 ± 0.4	32.0 ± 0.5	
NH <sub>3</sub>	91.9 ± 0.2	4 ± 0.3	4.1 ± 0.2		4.4 ± 0.3	4.4 ± 0.2	
O <sub>2</sub> MW	78.5 ± 0.2	20.5 ± 0.2	1 ± 0.1		26.1 ± 0.3	1.3 ± 0.2	
Ar Jet	88.1 ± 0.9	11.5 ± 0.7	0.4 ± 0.4		13.2 ± 0.9		
Ar/O <sub>2</sub> Jet	85.8 ± 1.6	14.2 ± 1.5			16.7 ± 1.5		
PPC <sub>6</sub> F <sub>6</sub>	53.9 ± 0.6	1.5 ± 0.2		44.6 ± 0.7	2.8 ± 0.3		82.8 ± 2.1
TCPS	90.4 ± 0.5	9.6 ± 0.5			10.7 ± 0.7		
Primaria	83.9 ± 0.5	11.6 ± 0.2	4.5 ± 0.3		13.8 ± 0.3	5.4 ± 0.4	

ponent was highest on these surfaces. The very hydrophobic PPC<sub>6</sub>F<sub>6</sub>-coated surface exhibited a surface energy of 1.1 mN/m including a dispersive content of 0.2 mN/m. The introduction of functional groups resulted in the formation of dipoles at the surface which, in turn, increased the polar component and, hence, the surface energy.

Consequently, it is well known that, along with changes in the wettability and the surface energy, the elemental surface composition is altered, too, which is indicated by the increase of the polar moieties. Hence, XPS has been employed to characterize the elemental surface composition of the PS substrates. In Table I, the relative amount of each element detected at the surfaces, namely, carbon (C), nitrogen (N), oxygen (O), and fluorine (F), as well as the element ratios are listed. The results revealed that the surfaces undergo substantial changes by plasma treatment.

Since atomic oxygen produced by the gas discharges is extremely reactive to hydrocarbons, Table I shows that higher surface atomic oxygen contents are generally observed after plasma treatment, whereas PS (BD) contained only traces of oxygen. Furthermore, on substrates exposed to nitrogen-containing plasmas, an increase in the N/C ratio was detected, due to the incorporation of nitrogen, with the highest N/C ratio of 32% for PPAAm-coated PS. TCPS showed an O/C ratio of 10.7%; Primaria showed an O/C ratio of 13.8% and, further, an N/C ratio of 5.4%, respectively. The highest O/C ratio was detected for O<sub>2</sub> MW (26.1%) and for Ar/O<sub>2</sub>-jet-plasma (16.7%)-treated PS, which corresponds to the determined

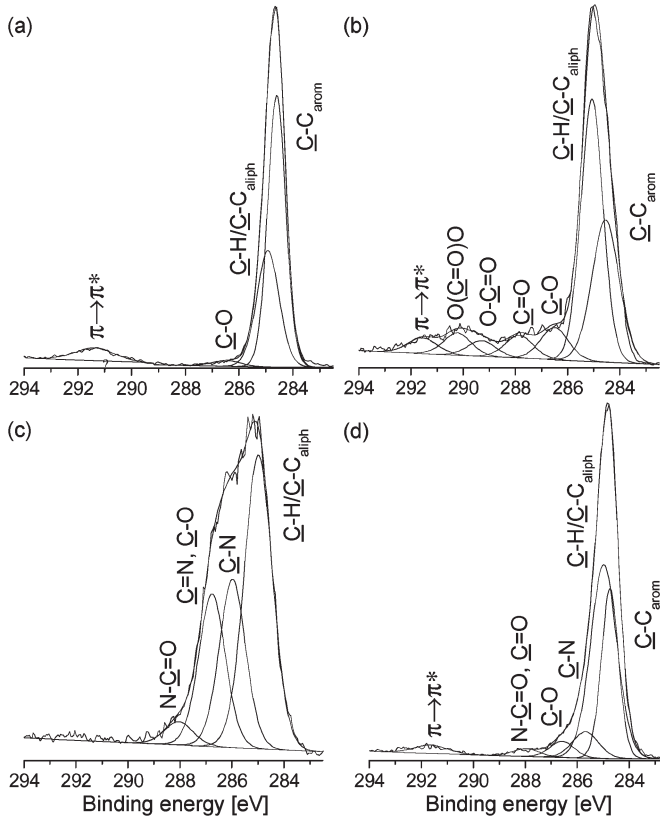


Fig. 8. High-resolution C 1s spectra. (a) PS (BD), (b) O<sub>2</sub> MW-plasma-treated PS, (c) PPAAm-coated PS, and (d) NH<sub>3</sub>-plasma-treated PS.

highly increased surface energy. Additionally to oxygen, small amounts of nitrogen (< 1%) were detected on O<sub>2</sub> MW- and Ar-jet-plasma-treated PS surfaces, which is probably based on postplasma reactions of low-pressure-plasma-treated substrates during air contact after plasma processing and admixing of ambient air during exposure to atmospheric-pressure plasma, respectively [20]. For ammonia-plasma-treated PS, the O/C and N/C ratios were almost equal. However, a part of the detected nitrogen belongs to amino groups which can be estimated by using TFBA. The results obtained by this derivatization technique indicated a primary amino group density,  $-\text{NH}_2/\text{C}$ , of  $3.28 \pm 0.08\%$  for PPAAm-coated PS,  $1.33 \pm 0.06\%$  for NH<sub>3</sub>-plasma-treated PS, and  $0.21 \pm 0.02\%$  for Primaria, respectively. As previously reported, these positively charged amino groups could play an important role to accelerate the initial adhesion of osteoblastic cells [11].

Fig. 8 shows the high-resolution XPS C 1s spectra of selected PS substrates [PS (BD) (a), O<sub>2</sub> MW-plasma-treated PS (b), PPAAm-coated PS (c), and NH<sub>3</sub>-plasma-treated PS (d)] which verify the existence of different oxygen-containing and nitrogen-containing bonds. The highly resolved measured C 1s spectrum of PS (BD) was deconvoluted into four components which were assigned to C-C<sub>arom</sub> (BE: 284.6 eV), C-C<sub>aliph</sub>/C-H (BE: 285.0 eV), C-O (BE: 286.5 eV), and the shake-up  $\pi \rightarrow \pi^*$  (BE: 291.7 eV). Depending on the applied plasma process, further components appeared, attributed to C-N (BE: 285.7 eV), C=O (BE: 288.0 eV), O-C=O (BE: 289.4 eV), and OC(=O)O (BE: 290.3 eV). On the PPAAm-coated PS, the components of pristine PS (BD) vanished,

TABLE II  
PERCENTAGES (IN PERCENT) OF BONDING COMPONENTS IN DECONVOLUTED HIGH-RESOLUTION C 1s SPECTRA

	C-C <sub>arom</sub> 284.6 eV	C-C <sub>aliph</sub> 285.0 eV	C-N 286.0 eV	C-O 286.5 eV	C=O 287.8 eV	O-C=O 289.3 eV	OC(=O)O 290.3 eV	$\pi\text{-}\pi^*$ 291.7 eV
PS (BD)	57.7	34.6		1.8				5.9
NH <sub>3</sub>	30.4	53.3	7.2	4.1	2.1			2.9
O <sub>2</sub> MW	22.0	46.8		8.8	10.0	6.3	3.4	2.7
Ar Jet	35.5	47.9		5.3	3.1	1.9	2.8	3.6
Ar/O <sub>2</sub> Jet	33.5	45.8		5.7	4.2	2.5	4.8	3.5
TCPS	38.8	48.5		4.7	1.6	2.3		4.1
Primaria	31.1	46.1	4.8	7.2	4.7	2.9		3.2
	C-C <sub>aliph</sub> 285.0 eV	C-N 286.0 eV	C-O, C=N 286.8 eV	N-C=O 288.1 eV				
PPAAm	47.5	25.4	23.3	3.8				
	C-C <sub>aliph</sub> 285.0 eV	C-CF 286.4 eV	CF 288.5 eV	CF <sub>2</sub> 290.8 eV	CF <sub>3</sub> 293.2 eV	OCF <sub>3</sub> 294.5 eV		
PPC <sub>6</sub> F <sub>6</sub>	3.1	29.7	40.3	19.3	5.5	2.1		

and the following components were determined: C-N (BE: 286.0 eV), C=N, C-O (BE: 286.8 eV), and N-C=O (BE: 288.0 eV).

Consequently, the highly resolved C 1s peaks showed drastic changes of the bond relations at the surfaces after plasma exposure. Furthermore, due to plasma processes, the number of oxygen-containing and nitrogen-containing functional groups on the surfaces was increased. The relative abundance of these components, obtained from curve fitting, of all samples is summarized in Table II.

Table II exhibits that the plasma processes resulted in the opening of the benzene ring and hydrogen abstraction accompanied with the formation of oxygen and/or nitrogen bonds. Therefore, percentage decrease in aromatic C-C bonds and  $\pi \rightarrow \pi^*$  shake-up components were determined, whereas a percentage increase of the aliphatic C-C bonds and of polar groups was observed. According to the elemental compositions, high percentages of different oxygen-containing functional groups were found for O<sub>2</sub> MW-plasma-treated and Ar/O<sub>2</sub>-jet-plasma-treated PS. In particular, the formation of hydroxyls (C-OH), ketones/aldehydes (C=O), carboxylic groups (O-C=O), and carbonates (OC(=O)O) was observed. Carboxylic groups have a strong nucleophilic character which, in turn, results in a high chemical reactivity. Moreover, the creation of oxygen-containing functionalities may implicate a negatively charged surface [28]. The deconvolution of the highly resolved C 1s spectra for NH<sub>3</sub>-plasma-treated PS yielded nitrogen(C-N)- and oxygen (C-O and C=O)-related functionalization. The C 1s peak of PPAAm-coated PS was dominated by aliphatic C-C bonds and nitrogen-containing groups assigned to amines (C-N), imines (C=N), and amides (N-C=O). It is most likely that the presence of nitrogen-containing groups, particularly amino groups, results in a positively charged surface [12], [28]. In terms of the enhanced surface energy of the plasma-modified surfaces, it is evident that the increase in the polar component is based on the formation of oxygen- and nitrogen-containing functional groups. Furthermore, it may be assumed that the polar component of oxygen-containing surfaces (O<sub>2</sub> MW and Ar/O<sub>2</sub>-jet-plasma-treated PS) is higher compared to nitrogen-containing surfaces (PPAAm-coated PS and



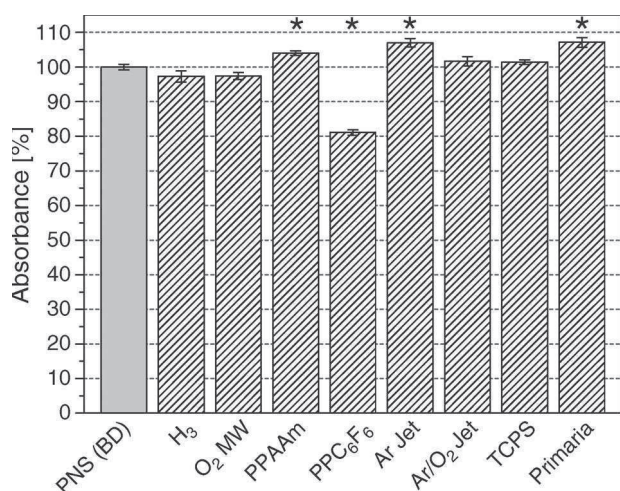


Fig. 9. Metabolic activity of MG-63 after 24 h of cultivation on PS, which was treated with different plasma sources. The absorbance of the control [PS (BD)] was set to 100%. Results are expressed as *means*  $\pm$  *SD* ( $n = 3$ ). *t*-test: \* $p < 0.05$  versus PS (BD). Note that a reduction of approximately 20% was obtained on PPC<sub>6</sub>F<sub>6</sub>-coated PS, compared to cells grown on PS (BD).

NH<sub>3</sub>-plasma-treated PS) since oxygen functionalities are highly polar. Owing to the reduced presence of polar functionalities on the fluorinated PS surface (PPC<sub>6</sub>F<sub>6</sub>-coated PS), the amount of the polar component in the surface energy was minute.

Deduced from the analysis of the physicochemical properties of the studied PS substrates, it can be assumed that the creation of different functional groups influences cell attachment and cell proliferation in many ways. Therefore, MG-63 osteoblastic cells were used to investigate this assumption in detail and to figure out which surface features are more important for cell growth.

The biocompatibility of the PS samples was evaluated by using MTT (3-(4,5-Dimethylthiazol-2-yl)-2,5-diphenyltetrazolium bromide) assay and cell spreading studies. The cell viability for each of the materials by performing an MTT assay 24 h after the cells were seeded on the differently treated samples is shown in Fig. 9. The MTT assay is a widely used procedure to measure metabolically cells to validate the biofunctionality of materials [29]. The yellow tetrazole (MTT) is metabolized (reduced) to purple formazan salt by mitochondrial enzymes in living cells. The assay detects only living cells, and the absorbance is proportional to the number of viable cells. The MTT assay was evaluated as percent absorbance compared to PS (BD) ( $p < 0.05$ ).

As can be seen in Fig. 9, almost all substrates showed no cytotoxic effects with the exception of PPC<sub>6</sub>F<sub>6</sub>-coated PS where the cell viability was significantly lower compared to PS (BD). Hence, considering the determined surface characteristics, the observed MTT assay data for PPC<sub>6</sub>F<sub>6</sub>-coated PS indicated a correlation between the physicochemical surface properties and the metabolic activity. More precisely, the non-polar character of this hydrophobic surface as well as the absence of polar oxygen- or nitrogen-containing functionalities resulted in a decrease in cell viability. Hence, the PPC<sub>6</sub>F<sub>6</sub> coating exhibited detrimental effects on the metabolic activity of osteoblastic cells. However, a slightly but still significantly enhanced metabolic activity was observed for PPAAm-coated

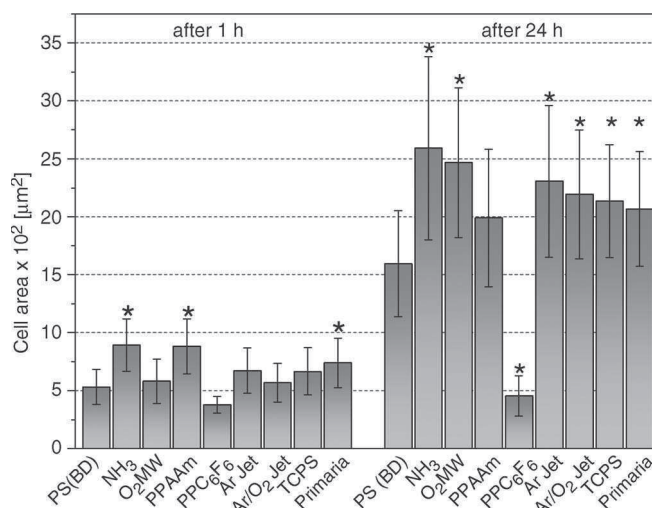


Fig. 10. Spreading of MG-63 osteoblasts after 1 and 24 h of cultivation on PS. Results are expressed as *means*  $\pm$  *SD* ( $n = 40$ ). One-way ANOVA post hoc Bonferroni: \* $p < 0.05$  versus PS (BD). Note that a coating with PPC<sub>6</sub>F<sub>6</sub> caused an approximately one-third smaller cell area after 24 h, compared to cells grown on PS (BD).

PS, Ar-jet-plasma-treated PS, and Primaria in comparison to PS (BD). The cell viability of ammonia-plasma-treated and of O<sub>2</sub> MW-plasma-treated PS was reduced, but the differences were not statistically significant. Deduced from the results, it can be concluded that the plasma-modified PS substrates were able to promote the early proliferation of MG-63 cells except for the negative control (PPC<sub>6</sub>F<sub>6</sub>-coated PS).

The cell spreading behavior of the osteoblastic cells on the differently plasma treated PS substrates was microscopically examined after 1 and 24 h of cultivation. The estimated cell area for each surface is shown in Fig. 10. Analysis of variance (ANOVA) was applied to evaluate differences in cell area related to PS (BD) ( $p < 0.05$ ).

After 1 h of cultivation, a significantly higher cell area was detected for ammonia-plasma-treated (893  $\mu\text{m}^2$ ) PS, PPAAm-coated (882  $\mu\text{m}^2$ ) PS, and Primaria (740  $\mu\text{m}^2$ ) relative to PS (BD) (533  $\mu\text{m}^2$ ). Concerning the examined physicochemical properties, it can be assumed that a quite hydrophilic surface is not decisive for cell spreading since the contact angles of these surfaces were found to be around 50°, whereas the most wettable surfaces having contact angles below 5° (O<sub>2</sub>-MW-plasma-treated and Ar/O<sub>2</sub>-plasma-treated PS) exhibited no significant increase in cell area after 1 h. Furthermore, the order of magnitude of the polar component was similar for ammonia-plasma-treated PS, PPAAm-coated PS, and Primaria, respectively. Deduced from these results and considering the elemental composition of these surfaces, it can be concluded that nitrogen-containing functional groups and, thus, a probably positively charged surface resulted in an improved initial spreading of MG-63 cells within 1 h. However, compared to the area of cells grown on PS (BD) (534  $\mu\text{m}^2$ ), Ar (672  $\mu\text{m}^2$ )-as well as Ar/O<sub>2</sub> (568  $\mu\text{m}^2$ )-jet-plasma-treated surfaces and TCPS (667  $\mu\text{m}^2$ ) exhibited a marginally increased cell area. A slight decrease in cell area was observed on PPC<sub>6</sub>F<sub>6</sub>-coated PS (378  $\mu\text{m}^2$ ) after 1 h in relation to PS (BD). After 24 h of cultivation, different results were obtained. Ammonia-plasma-treated

PS still showed the highest cell area ( $2593 \mu\text{m}^2$ ) relative to PS (BD) ( $1549 \mu\text{m}^2$ ), but also, for samples exposed to  $\text{O}_2$  MW plasma ( $2468 \mu\text{m}^2$ ) and Ar jet plasma ( $2307 \mu\text{m}^2$ ), a remarkable and significant increase in cell area was obtained. Furthermore, the cell areas were significantly increased for Ar/ $\text{O}_2$ -plasma-treated PS ( $2194 \mu\text{m}^2$ ), TCPS ( $2135 \mu\text{m}^2$ ), and Primaria ( $2067 \mu\text{m}^2$ ), too, but not as distinct as compared to those mentioned earlier. Interestingly, the PPAAm-coated surface exhibited no significantly increased cell area after 24 h compared to PS (BD). Since, on the PPAAm-coated surface, the O/C ratio was lower compared to the ones of the other plasma-treated surfaces, it can be assumed that, for the initial growth of osteoblastic cells, nitrogen-containing functionalities probably support cell spreading, whereas afterward, oxygen-containing functionalities lead to an additional enhancement in cell spreading. Apparently, the surfaces with increased O/C ratio and a certain level of oxygen functionalities supported cell growth. Therefore, the ammonia-plasma-treated PS surface exhibited enhanced cell spreading due to the presence of oxygen- and nitrogen-containing functional groups. Which one of the surface functional groups is the most effective in influencing cell-surface interaction is difficult to assess as the chemistry on the surface is very complex, and furthermore, cell response strongly depends on the type of cells, too [9], [30]. Until now, no specific mechanism of cell attachment can be attributed to only one functional group although, in the literature, a different dependence of cell proliferation on functional groups was proposed [9]. For instance, different scientists have reported enhanced cell performance with the formation of carboxyl functional groups on surfaces [30], [31]. It is also reported that an optimum cell growth of osteoblasts was obtained with a concentration of carboxylic groups ( $\text{O}=\text{C}-\text{O}$ ) less than 5% and, further, that the effect of alcohol/ether functionalities ( $\text{C}-\text{O}$ ) is little [30], [32]. However, this is not in accordance to the results presented in this contribution; e.g., on  $\text{O}_2$  MW-plasma-treated PS, the concentration of  $\text{O}=\text{C}-\text{O}$  groups was about 6% which resulted in enhanced cell spreading compared to Ar/ $\text{O}_2$ -jet-plasma-treated PS with an  $\text{O}=\text{C}-\text{O}$  concentration of about 2.5%. Furthermore, Daw *et al.* postulated that, in the absence of carboxylic groups, carbonyl groups ( $\text{C}=\text{O}$ ) do not promote the proliferation of osteoblastic cells [30]. This is a contradiction to the data obtained for ammonia-plasma-treated PS which exhibited the best cell proliferation results among the studied material. First, no  $\text{O}=\text{C}-\text{O}$  groups were found on this surface, and second, according to the assumption of Daw *et al.* that C-O groups play a minor role in the cell growth of osteoblastic cells, the obtained results would imply that nitrogen-containing groups are the important functional groups for cell proliferation. However, this was not confirmed by the results received for the PPAAm-coated PS surface. Hence, considering only surfaces grafted with oxygen-containing functional groups, cell proliferation almost correlated with increased O/C ratio and a high level of surface oxygen functionalities. Hence, it can be stated that the multifunctionality of the surface chemical composition promotes cell proliferation. However, substantially different data were obtained for  $\text{PPC}_6\text{F}_6$ -coated PS. The cell area was significantly lower in relation to PS (BD) and, moreover, remained within the range of cell area estimated after 1 h

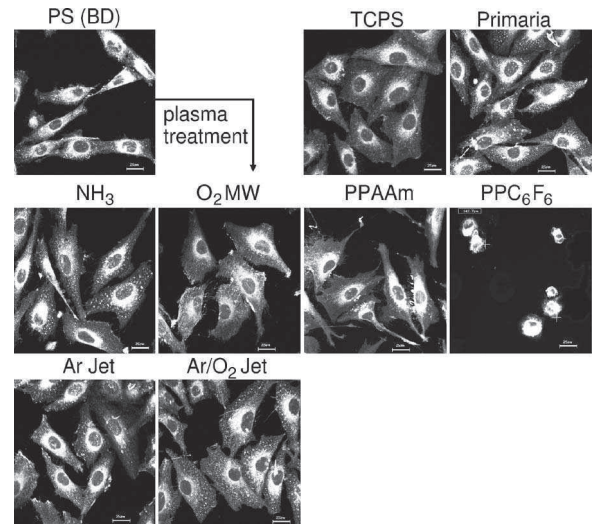


Fig. 11. Microscopic images of MG-63 cells grown for 24 h on PS. In comparison to cells on nontreated PS (BD), cells on  $\text{NH}_3$ -,  $\text{O}_2$  MW-, Ar-jet-plasma-, and Ar/ $\text{O}_2$ -jet-plasma-treated PS surfaces showed enhanced cell areas. In compliance with the results of cell area measurements, cells on  $\text{PPC}_6\text{F}_6$ -coated PS are not well spread after 24 h (bar =  $25 \mu\text{m}$ ; confocal microscopy LSM 410).

of cultivation. In agreement to the decreased metabolic activity of the osteoblastic cells, this result confirms the assumption that the lack of polar functionalities led to an impairment of cell growth and proliferation.

The different cell spreading behaviors of MG-63 cells on the studied surfaces after 24 h of cultivation are shown in Fig. 11. Furthermore, differences in cell morphology could be observed, too.

MG-63 cells on plasma-treated substrates were well attached and spread (excluding  $\text{PPC}_6\text{F}_6$ -coated PS). Moreover, a flat configuration showing a spherical body with cellular extensions in all directions on the samples was observed. In comparison to PS (BD), the extent of cell spreading was quite increased on plasma-modified surfaces. In contrast, cell spreading was inhibited on  $\text{PPC}_6\text{F}_6$ -coated PS in 24 h. According to the estimated cell area on this surface, it can be clearly noticed that the surface properties of  $\text{PPC}_6\text{F}_6$ -coated PS affect the interaction between cells and surface in an unfavorable way. The cells showed a clumplike rounded morphology due to very poor adherence. These results indicate that the  $\text{PPC}_6\text{F}_6$  coating prevents the osteoblastic MG-63 cells from proper cell function.

#### IV. CONCLUSION

Biocompatibility is of great importance for the design and application of polymeric biomaterials. Hence, efforts have been made for controlling the surface properties to improve cell adhesion since cells can sense the physical properties and chemical composition of surfaces and regulate their behavior. The results in this study strongly suggest that the applied plasma processes improved cell-surface interaction and, further, that low-pressure plasma and atmospheric-pressure plasma are equally effective in the improvement of cell attachment and proliferation. The effect of different physicochemical surface



properties, including wettability, surface energy, and chemical functionalities, on osteoblastic cell (MG-63) behavior has been examined, focusing on metabolic activity and cell spreading. No relation has been found between surface roughness and cell proliferation due to the relatively small increase in  $R_a$  and  $R_{rms}$  of all surfaces. Hence, differences in cellular response appeared to be due to surface properties. When observing contact angle and surface energy data in conjunction with XPS results, it can be concluded that the reduction in the contact angle and the increase in surface energy after plasma treatment (besides PPC<sub>6</sub>F<sub>6</sub>-coated PS) were attributed to the incorporation of oxygen and/or nitrogen into the surface. The analysis of the surface energy has shown that there were little changes in the dispersive component. In contrast, the polar component has changed in all modification techniques and shown the highest value on O<sub>2</sub> MW- and Ar/O<sub>2</sub>-jet-plasma-treated PS according to their highest O/C ratio. The major reason for the increase in the polar component is the enhanced total oxygen and/or nitrogen content of the surface through introducing new functional groups, namely, C–O, C=O, O=C–O, C–N, and C=N, which are highly polar. The results of the MTT assay have demonstrated that cells on surfaces equipped with oxygen and/or nitrogen functionalities showed a partly higher metabolic activity compared to PS (BD). In contrast, the marginal cell adhesion on PPC<sub>6</sub>F<sub>6</sub>-coated PS (negative control) has resulted in a slight impairment in metabolic activity. The analysis of cell spreading has exhibited that osteoblastic cells were able to adhere easily and spread out faster on the plasma-modified surfaces immediately after seeding (except for PPC<sub>6</sub>F<sub>6</sub>-coated PS). Proliferation results have suggested that cells proliferated with a significantly higher rate on surfaces with nitrogen-containing functionalities after 1 h of cultivation compared to the ones equipped with oxygen functional groups only, whereas after 24 h of cultivation, cells on nitrogen-containing and on oxygen-containing surfaces proliferated more readily on the plasma-modified surfaces than on PS (BD). Since cells seeded on PPAAm-coated PS have shown no significant increase in cell area after 24 h of cultivation, it can be concluded that both oxygen- and nitrogen-containing groups are important for cell spreading. In contrast, MG-63 cells on the PPC<sub>6</sub>F<sub>6</sub>-coated surface have revealed the inability of this hydrophobic surface to support the growth in cell area. Consequently, surfaces characterized by low wettability and surface energy as well as the absence of polar functionalities have shown less favorable adhesion conditions. Summarizing, a controlled modification of the interface chemistry from insufficient biomolecule attachment toward biocompatibility by different functionalities is beneficial for the proper function of biorelevant surfaces. In terms of the capability of nonthermal plasmas, atmospheric-pressure plasma offers a prospective application in the improvement of cell attachment and proliferation. Furthermore, plasma jets are able to penetrate into small structures, such like cavities, gaps, crevices, and tubes. Thus, even extremely small sized and complex miniaturized structures as well as the interior surfaces of small trenches can be treated by this plasma device. That might be a specific advantage of plasma jets over, e.g., low-pressure plasmas. However, further studies are needed to compare their potential to currently used plasma approaches.

## ACKNOWLEDGMENT

The authors would like to thank U. Kellner and R. Ihrke (Leibniz Institute for Plasma Science and Technology) for the excellent technical support.

## REFERENCES

- [1] N. Gomathi, A. Sureshkumar, and S. Neogi, "RF plasma-treated polymers for biomedical applications," *Current Sci.*, vol. 94, no. 11, pp. 1478–1486, Jun. 2008.
- [2] T. Desmet, R. Morent, N. De Geyter, C. Leys, E. Schacht, and P. Dubruel, "Nonthermal plasma technology as a versatile strategy for polymeric biomaterials surface modification: A review," *Biomacromolecules*, vol. 10, no. 9, pp. 2351–2378, Sep. 2009.
- [3] F. Hempel, H. Steffen, H. Busse, B. Finke, J. B. Nebe, A. Quade, H. Rebl, C. Bergemann, K.-D. Weltmann, and K. Schröder, "On the application of gas discharge plasmas for the immobilization of bioactive molecules for biomedical and bioengineering applications," *Biomedical Engineering-Frontiers and Challenges*, pp. 297–318, 2011.
- [4] J. Ehlbeck, R. Brandenburg, R. Foest, E. Kindel, U. Krohmann, K. Rackow, M. Stieber, K.-D. Weltmann, and T. Von Woedtke, "Decontamination of heat-sensitive polymer surfaces using low temperature plasma technology," in *Polymer Surface Modification: Relevance to Adhesion*, K. L. Mittal, Ed. Koninklijke Brill NV, 2010, pp. 381–394.
- [5] S. P. Massia, "Cell-extracellular matrix interactions relevant to vascular tissue engineering," in *Tissue Engineering of Vascular Prosthetic Grafts*, P. Zilla and H. P. Greisler, Eds. Austin, TX: Landes Bioscience, 1999.
- [6] D. F. Williams, "On the mechanisms of biocompatibility," *Biomaterials*, vol. 29, no. 20, pp. 2941–2953, Jul. 2008.
- [7] P. Kingshott, G. Andersson, S. L. McArthur, and H. J. Griesser, "Surface modification and chemical surface analysis of biomaterials," *Current Opinion Chem. Biol.*, vol. 15, no. 5, pp. 667–676, Oct. 2011.
- [8] R. Morent, N. De Geyter, T. Desmet, P. Dubruel, and C. Leys, "Plasma surface modification of biodegradable polymers: A review," *Plasma Process. Polym.*, vol. 8, no. 3, pp. 171–190, Mar. 2011.
- [9] K. S. Siow, L. Britcher, S. Kumar, and H. J. Griesser, "Plasma methods for the generation of chemically reactive surfaces for biomolecule immobilization and cell colonization—A review," *Plasma Process. Polym.*, vol. 3, no. 6/7, pp. 392–418, Aug. 2006.
- [10] K. Schröder, B. Finke, H. Jesswein, F. Lüthen, A. Diener, R. Ihrke, A. Ohl, K.-D. Weltmann, J. Rychly, and J. B. Nebe, "Similarities between plasma amino functionalized PEEK and titanium surfaces concerning enhancement of osteoblast cell adhesion," *J. Adhesion Sci. Technol.*, vol. 24, no. 5, pp. 905–923, 2010.
- [11] B. Finke, F. Hempel, H. Testrich, A. Artemenko, H. Rebl, O. Kylián, J. Meichsner, H. Biederman, B. Nebe, K.-D. Weltmann, and K. Schröder, "Plasma processes for cell-adhesive titanium surfaces based on nitrogen-containing coatings," *Surf. Coat. Technol.*, vol. 205, no. Supplement 2, pp. S520–S524, Jul. 25, 2011.
- [12] B. Nebe, B. Finke, F. Lüthen, C. Bergemann, K. Schröder, J. Rychly, K. Liefeth, and A. Ohl, "Improved initial osteoblast functions on amino-functionalized titanium surfaces," *Biomol. Eng.*, vol. 24, no. 5, pp. 447–454, Nov. 2007.
- [13] G. Da Ponte, E. Sardella, F. Fanelli, R. d'Agostino, and P. Favia, "Trends in surface engineering of biomaterials: Atmospheric pressure plasma deposition of coatings for biomedical applications," *Eur. Phys. J.-Appl. Phys.*, vol. 56, no. 2, pp. 1–4, Nov. 2011.
- [14] S. L. Barker and P. J. LaRocca, "Method of production and control of a commercial tissue culture surface," *J. Tissue Cult. Meth.*, vol. 16, no. 3/4, pp. 151–153, Sep. 1994.
- [15] A. Quade, K. Schröder, A. Ohl, and K. D. Weltmann, "Plasma deposition of nanoscale difluoromethylene dominated surfaces," *Plasma Process. Polym.*, vol. 8, no. 12, pp. 1165–1173, Dec. 2011.
- [16] B. Finke, F. Luethen, K. Schroeder, P. D. Mueller, C. Bergemann, M. Frant, A. Ohl, and B. J. Nebe, "The effect of positively charged plasma polymerization on initial osteoblastic focal adhesion on titanium surfaces," *Biomaterials*, vol. 28, no. 30, pp. 4521–4534, Oct. 2007.
- [17] K. Fricke, H. Tresp, R. Bussiahn, K. Schröder, T. Woedtke, and K. D. Weltmann, "On the use of atmospheric pressure plasma for the biodecontamination of polymers and its impact on their chemical and morphological surface properties," *Plasma Chem. Plasma Process.*, vol. 32, no. 4, pp. 801–816, May 2012.
- [18] C. Bergemann, A. Quade, F. Kunz, S. Ofe, E.-D. Klinkenberg, M. Laue, K. Schröder, V. Weissmann, H. Hansmann, K.-D. Weltmann, and B. Nebe, "Ammonia plasma functionalized polycarbonate surfaces improve cell migration inside an artificial 3D cell culture module," *Plasma Process. Polym.*, vol. 9, no. 3, pp. 261–272, Mar. 2012.



- [19] K. D. Weltmann, E. Kindel, R. Brandenburg, C. Meyer, R. Bussiahn, C. Wilke, and T. von Woedtke, "Atmospheric pressure plasma jet for medical therapy: Plasma parameters and risk estimation," *Contrib. Plasma Phys.*, vol. 49, no. 9, pp. 631–640, Nov. 2009.
- [20] N. De Geyter, R. Morent, and C. Leys, "Surface characterization of plasma-modified polyethylene by contact angle experiments and ATR-FTIR spectroscopy," *Surf. Interface Anal.*, vol. 40, no. 3/4, pp. 608–611, Mar./Apr. 2008.
- [21] K. Anselme, A. Ponche, and M. Bigerelle, "Relative influence of surface topography and surface chemistry on cell response to bone implant materials. Part 2: Biological aspects," *Proc. Inst. Mech. Eng. Part H, J. Eng. Med.*, vol. 224, no. H12, pp. 1487–1507, Dec. 2010.
- [22] K. Anselme, P. Davidson, A. M. Popa, M. Giazson, M. Liley, and L. Ploux, "The interaction of cells and bacteria with surfaces structured at the nanometre scale," *Acta Biomater.*, vol. 6, no. 10, pp. 3824–3846, Oct. 2010.
- [23] J. Takebe, S. Ito, S. Miura, K. Miyata, and K. Ishibashi, "Physicochemical state of the nanotopographic surface of commercially pure titanium following anodization–hydrothermal treatment reveals significantly improved hydrophilicity and surface energy profiles," *Mater. Sci. Eng. C, Mater. Biol. Appl.*, vol. 32, no. 1, pp. 55–60, Jan. 2012.
- [24] G. Legeay, A. Coudreuse, F. Poncin-Epaillard, J. M. Herry, and M. N. Bellon-Fontaine, "Surface engineering and cell adhesion," *J. Adhesion Sci. Technol.*, vol. 24, no. 13/14, pp. 2301–2322, 2010.
- [25] K. Fricke, H. Steffen, T. von Woedtke, K. Schröder, and K.-D. Weltmann, "High rate etching of polymers by means of an atmospheric pressure plasma jet," *Plasma Process. Polym.*, vol. 8, no. 1, pp. 51–58, Jan. 2011.
- [26] E. S. Gadelmawla, M. M. Koura, T. M. A. Maksoud, I. M. Elewa, and H. H. Soliman, "Roughness parameters," *J. Mater. Process. Technol.*, vol. 123, no. 1, pp. 133–145, Apr. 2002.
- [27] S. Bornholdt, M. Wolter, and H. Kersten, "Characterization of an atmospheric pressure plasma jet for surface modification and thin film deposition," *Eur. Phys. J. D*, vol. 60, no. 3, pp. 653–660, Dec. 2010.
- [28] K. Schröder, B. Finke, A. Ohl, F. Lüthen, C. Bergemann, B. Nebe, J. Rychly, U. Walschus, M. Schlosser, K. Liefeth, H.-G. Neumann, and K.-D. Weltmann, "Capability of differently charged plasma polymer coatings for control of tissue interactions with titanium surfaces," *J. Adhes. Sci. Technol.*, vol. 24, no. 7, pp. 1191–1205, Apr. 2010.
- [29] G. Ciapetti, E. Cenni, L. Pratelli, and A. Pizzoferrato, "In vitro evaluation of cell biomaterial interaction by MTT assay," *Biomaterials*, vol. 14, no. 5, pp. 359–364, Apr. 1993.
- [30] R. Daw, T. O'Leary, J. Kelly, R. D. Short, M. Cambray-Deakin, A. J. Devlin, I. M. Brook, A. Scutt, and S. Kothari, "Molecular engineering of surfaces by plasma copolymerization and enhanced cell attachment and spreading," *Plasma Polym.*, vol. 4, no. 2/3, pp. 113–132, 1999.
- [31] C. A. Scotchford, E. Cooper, G. J. Leggett, and S. Downes, "Growth of human osteoblast-like cells on alkanethiol on gold self-assembled monolayers: The effect of surface chemistry," *J. Biomed. Mater. Res.*, vol. 41, no. 3, pp. 431–442, Sep. 1998.
- [32] R. Daw, S. Candan, A. J. Beck, A. J. Devlin, I. M. Brook, and S. MacNeil, "Plasma copolymer surfaces of acrylic acid 1,7 octadiene: Surface characterisation and the attachment of ROS 17/2.8 osteoblast-like cells," *Biomaterials*, vol. 19, no. 19, pp. 1717–1725, Oct. 1998.

**Katja Fricke** received the Diploma degree in environmental science at the Ernst Moritz Arndt University of Greifswald, Greifswald, Germany, in 2007. During her thesis, she investigated the immobilization of biocatalysts for microbial bioelectrochemical systems and studied the anodic bioelectrocatalytic electron transfer in microbial fuel cells.

Since 2008, she has been a Researcher with the Leibniz Institute for Plasma Science and Technology (INP Greifswald e.V.), Greifswald. In her Ph.D. thesis, she elucidates the impact of nonthermal plasma on biorelevant materials, particularly the influence of plasma on the physicochemical and morphological surface properties. Her other research interests include plasma-based processes for biological decontamination and sterilization.

**Kathrin Duske** was born in Bergen auf Rügen, Germany, on May 29, 1978. She is currently working toward the Ph.D. degree in animal nutrition in the Leibniz Institute for Farm Animal Biology, Dummerstorf, Germany and is employed with the Biomedical Research Center, Department of Cell Biology, University of Rostock, Rostock, Germany.

She is also with the Unit of Periodontology, Department of Restorative Dentistry, Ernst Moritz Arndt University of Greifswald, Greifswald, Germany. Furthermore, her research interests include cellular behavior on surfaces treated with plasma.

**Antje Quade** received the Dr. rer. nat. degree in chemistry from the Ernst Moritz Arndt University of Greifswald, Greifswald, Germany, in 2001. During the Ph.D. thesis, she worked in the field of surface and interface analysis of thin films using X-ray diffractometry and reflectivity.

Since 2005, she has been a Researcher with the Leibniz Institute for Plasma Science and Technology (INP Greifswald e.V.), Greifswald. Her interests include the field of plasma surface modification for biomedical applications, hydrophobization of surfaces, and surface analysis techniques, e.g., X-ray photoelectron spectroscopy.

**Barbara Nebe** received the Ph.D. degree from the University of Rostock, Rostock, Germany, in 1995, on the field "integrin-mediated interactions with extracellular matrix molecules," and the Dr. agr. habil. degree from the University of Rostock and the *venia legendi* in 2005.

She is the Vice Chair of the Medical Faculty, Biomedical Research Center, Department of Cell Biology, University of Rostock, where she has been a Professor for cell biology (Assistant Professor) since 2011. Her research interests are in the field of cell biological investigations to understand the topographical and chemical influences of biomaterial surfaces on cell adhesion structures, cell signaling, cell growth, intracellular apoptotic cascades, adhesion receptor expression, cell function (transcription and translation level of proteins), and cell differentiation. The present focus of her research is on plasmachemical surface modifications and their impact on cell physiology. She is experienced in cross-disciplinary research on the research field of biosystem–material interaction.

Prof. Nebe has been a Member of the Executive Committee of the German Society of Biomaterials since 2008.

**Karsten Schröder** received the Dr. rer. nat. degree in chemistry from the Ernst Moritz Arndt University of Greifswald, Greifswald, Germany in 1992. During his Ph.D. thesis he worked in the field of Ziegler-Natta catalysts used in the synthesis of polymers.

Since 1996, he was a Researcher with the Leibniz Institute of Plasma Science and Technology e.V. (INP Greifswald), Greifswald, Germany. From 2006 to 2011, he was the head of the department plasma surface technology at the INP Greifswald. His research interests were in the field of plasma-based surface modification of materials for biomedical application, surface analysis techniques, and plasma chemistry. He passed away in August 2011.

**Klaus-Dieter Weltmann** (M'95) received the Diploma degree in electronics and the Dr. rer. nat. degree in applied physics from the Ernst Moritz Arndt University of Greifswald, Greifswald, Germany, in 1989 and 1993, respectively.

He worked on nonlinear dynamics in low-temperature plasmas and plasma diagnostics. In 1994, he was a Visiting Scientist with the Plasma Physics Laboratory, West Virginia University, Morgantown. In 1995, he joined ABB Corporate Research Ltd., Baden-Dättwil, Switzerland, working in the research and development (R&D) of HV and MV switchgear, where he became the Head of the High Voltage Systems Group in 1998. In 2000, he was appointed to lead the R&D of gas-insulated switchgear (GIS, PASS) with ABB High Voltage Technologies Ltd., Zurich, Switzerland, where he became the Business Unit R&D Manager of GIS in 2002. Since 2003, he has been the Director and Chairman of the Board of the Leibniz Institute for Plasma Science and Technology (INP Greifswald e.V.), Greifswald, and Professor for experimental physics with the Ernst Moritz Arndt University of Greifswald. He is the initiator of three spin-off companies. His present research interests include switchgears, arc physics, atmospheric plasmas, modeling and simulation, plasma medicine, and plasma decontamination.

Prof. Weltmann is the President of the International Society for Plasma Medicine, a member of the German Physical Society, and a member of several consulting committees in industry and research.

**Thomas von Woedtke** received the Dr. rer. nat. degree and the Dr. rer. nat. habil. degree in pharmaceutical technology from the Ernst Moritz Arndt University of Greifswald, Greifswald, Germany, in 1996 and 2005, respectively.

From 1987 to 2005, he worked on the application of biosensors in medicine and life science research as well as on alternative sterilization techniques for sensitive goods. Since 2005, he has been with the Leibniz Institute for Plasma Science and Technology (INP Greifswald e.V.), Greifswald, where he is the Program Manager for Plasma Medicine/Decontamination. Since 2011, he has been a Professor for plasma medicine with the Ernst Moritz Arndt University of Greifswald. His research interests are in the field of plasma-based processes for biological decontamination and sterilization as well as in basic research problems of plasma–cell and plasma–tissue interactions.

## **5.6 “New non-thermal atmospheric pressure plasma sources for decontamination of human extremities”**

Klaus-Dieter Weltmann, Katja Fricke, Manfred Stieber, Ronny Brandenburg, Thomas von Woedtke, and Uta Schnabel

*IEEE Transactions on Plasma Science*, **2012**, DOI: 10.1109/TPS.2012.2204279



# New Nonthermal Atmospheric-Pressure Plasma Sources for Decontamination of Human Extremities

Klaus-Dieter Weltmann, *Member, IEEE*, Katja Fricke, Manfred Stieber, Ronny Brandenburg, Thomas von Woedtke, and Uta Schnabel

**Abstract**—The research and development of plasma sources, which can be used for therapeutic applications in the new and emerging field of plasma medicine, has gained more and more interest during recent years. These applications require cold non-thermal plasmas operating at atmospheric pressure. Due to the fact that, in general, plasma on or in the human body is a challenge both for medicine and plasma physics, basic research combining experimental physical and biological investigation and modeling is necessary to provide the required knowledge for therapeutic applications. It turned out that each application needs a special tailor-made plasma source, passing a minimum set of physical and biological tests before it can be considered for medical use. In addition to atmospheric-pressure plasma jets, dielectric barrier discharges offer great potential for a variety of medical indications. A new 2-D and even 3-D acting plasma source is introduced, exemplified for a possible decontamination of human extremities or similar tasks. In contradiction to most of today's existing plasma sources with fixed electrodes and nozzles, the prototype uses flexible electrodes to automatically adapt the plasma under equal and stable conditions to nearly all surface structures. First, physical and biological investigations demonstrate the general potential for therapeutic applications on preferably intact skin surfaces.

**Index Terms**—Atmospheric-pressure plasmas, plasma applications, plasma medicine, sterilization.

## I. INTRODUCTION

NEW possibilities for plasma applications in medicine have opened up during recent years. Today, the number and type of clinical placements that might be feasible in future are significantly increasing, comparable to the launch of laser technology into medicine years ago. The development of cold plasma sources working at atmospheric pressure was the basis for a new independent medical field, i.e., plasma medicine, that is emerging worldwide. Its main focus, in addition to the treatment of implants and the decontamination of heat-sensitive medical devices, is the direct application of physical plasmas on

or in the human or animal body. Regarding their potential for biomedical applications, various plasma sources have been investigated such as the plasma needle [1], atmospheric-pressure plasma plume [2], floating-electrode dielectric barrier discharge (DBD) [3], microhollow cathode discharge air plasma jet [4], several different plasma jets [5]–[8], and DBD [9]. The most promising field in terms of scientific and economic impact seems to be the plasma treatment of chronic wounds [10], [11]. The reason for this is the successful combination of a selective antimicrobial (antiseptic) effect, which does not damage the surrounding tissue, with a well-controlled stimulation of tissue regeneration. In addition, dental applications such as the removal of biofilms, tissue engineering, tumor treatment based on specific apoptotic processes, or the treatment of skin diseases are promising fields. The plasma sources developed and investigated here focus on infectious skin diseases.

## II. MATERIALS AND METHODS

### A. Plasma Sources

Most of the currently available plasma sources are intended to be used for local treatment of small areas. Important plasma parameters such as temperature, concentration of reactive species, charged particles, and intensity of radiation change with distance to the place the discharge is ignited, usually the electrodes. Investigations in [12] have shown that the results of the intended treatment depend very sensitively on the combination of these parameters, and thus on the distance to the treated object. Today, stable conditions are controlled by fixed-distance holders [5], [13], which work accurately enough as long as the surface is only slightly curved. To guarantee well-defined treatment conditions for complex structured surfaces, other practicable solutions are needed. Therefore, several plasma sources have been developed by the Leibniz Institute for Plasma Science and Technology (INP Greifswald) that allow the treatment of various curved surfaces such as infectious skin diseases at tissue tolerable temperature. All these plasma sources are based on the principle of surface DBD [14]–[16]. Figs. 1 and 2 display the electrode arrangement of the two plasma sources used for the present investigations.

**Plasma Array:** Fig. 1 shows the array of single electrodes, which are movable and independent from each other. This guarantees stable and safe treatment parameters even on complex 3-D geometries. In this case, the glass-covered pin electrodes are connected with the high-voltage (HV) plug of the power supply, whereas the surface to be treated serves as a grounded electrode.

Manuscript received February 14, 2012; revised April 26, 2012; accepted June 4, 2012. Part of this work was realized within the joint research project "Campus PlasmaMed" supported by the German Federal Ministry of Education and Research (BMBF) under Grant 13N11188 and the project "ConPlas" supported by the Ministry of Education, Research and Culture of the State of Mecklenburg-Vorpommern under Grant AU 07139. This work was also supported in part by the German Federal Ministry of Food, Agriculture and Consumer Protection (BMELV) through research project "FriPlas" under Grant 2816300707.

The authors are with the Leibniz Institute for Plasma Science and Technology Greifswald e.V. (INP Greifswald), 17489 Greifswald, Germany (e-mail: uta.schnabel@inp-greifswald.de).

Color versions of one or more of the figures in this paper are available online at <http://ieeexplore.ieee.org>.

Digital Object Identifier 10.1109/TPS.2012.2204279

### Plasma array

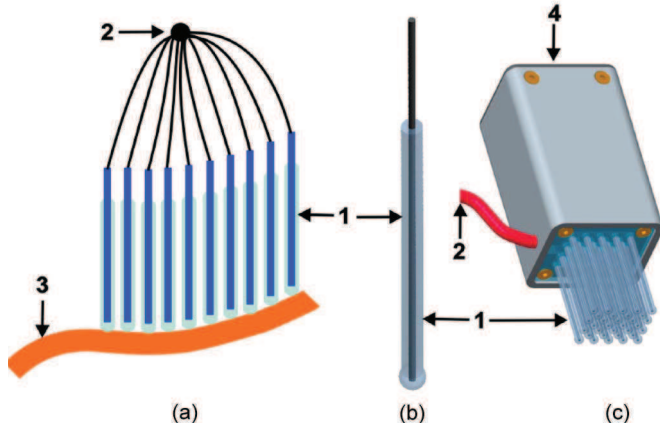


Fig. 1. Flexible electrode array arrangement (hereafter called the plasma array): (a) schematic view of independent electrodes, (b) single electrode, and (c) laboratory prototype with  $6 \times 6$  electrodes (area of  $9 \text{ cm}^2$ ); (1) glass-covered HV pin electrode, (2) electrical connection cable to the power supply, (3) surface to be treated (grounded electrode), and (4) housing of the array arrangement.

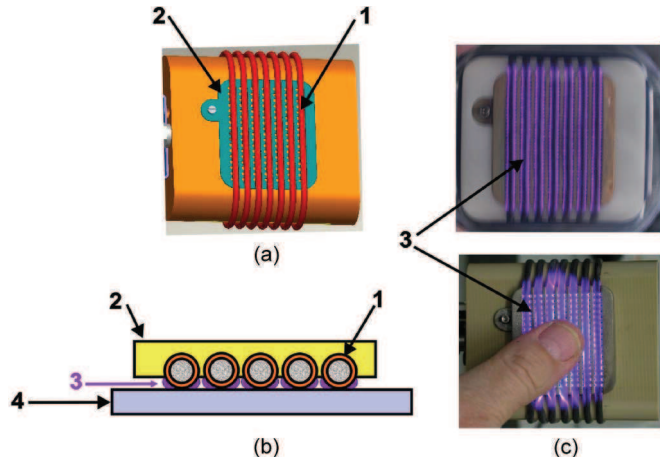


Fig. 2. Functional principle of the plasma source ConPlas: (a) 3D-CAD model, (b) schematic side view of the plasma handheld unit, and (c) plasma unit of a laboratory prototype in operation; (1) isolated wires as HV electrodes, (2) grounded electrode, (3) plasma, and (4) object to be treated.

**Plasma Source ConPlas:** The second plasma source used for the investigations, as shown in Fig. 2, is labeled as the registered brand name “Contacted Plasma” (ConPlas). This type of plasma source combines the advantages of surface DBD and plasma jet and is highly versatile concerning its application for plasma surface treatment under atmospheric conditions [17]. As shown in the schematic view in Fig. 2(b), both types of electrodes (i.e., HV and grounded electrodes) are component parts of the plasma source itself. Hence, in contrast to the electrode array arrangement in Fig. 1, the treated object is not integrated in the electrode arrangement, and thus, it is not influencing the discharge by its stray capacitance values. In the present case, a handheld type of the ConPlas device with a changeable treatment unit is applied.

If the treated surface completely consists of flexible materials [14], this plasma source is suitable for the treatment of various curved shapes similar as the array arrangement in Fig. 1.

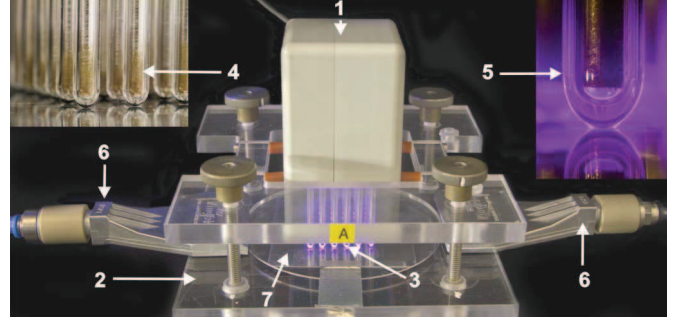


Fig. 3. Experimental setup with plasma array: (1) laboratory prototype of plasma array with  $6 \times 6$  electrodes, (2) adjustable adapter between plasma array and sample holder, (3) plasma, (4) and (5) magnified views of the glass-covered HV pin electrodes, (6) gas nozzles for additional mixing of argon (Ar), and (7) plastic sheet placed on the grounded electrode.

### B. Experimental Arrangement

**Treatment With Plasma Array:** Fig. 3 shows the experimental setup for inactivation of bacteria and yeast by treatment of microbially contaminated plastic sheets (PET: polyethylene terephthalate) by using the plasma array.

For plasma operation, an HV pulse generator RUP3-7bip (GBS Elektronik GmbH, Germany) is used. The fast HV MOSFET switching module “HTS 161-06-GSM” (Behlke Power Electronics GmbH) is incorporated in that device in order to generate square-wave pulses in the range up to 15-kV peak-to-peak voltage  $U_{pp}$ . This HV pulse generator operates with a broad range of load capacitance (50 pF–1 nF). Rise and decay times are on the order of 100–200 ns, dependent on voltage and load capacitance. The pulse parameters (i.e., frequency, pulsewidth, and amplitude) are freely adjustable in a wide range. In this case, the process conditions of the plasma treatment are characterized, on the one hand, by electrical power  $P$ , pulse parameter frequency  $f$ , and peak-to-peak voltage  $U_{pp}$ , and on the other hand, by the process gas and the treatment time.

**Treatment With ConPlas:** Fig. 4 exhibits the experimental setup for the plasma treatment of bacteria-inoculated agar plates with a handheld type of a ConPlas device with an interchangeable treatment unit.

The HV power supply of the handheld ConPlas device is placed in the handheld part (see 1 in Fig. 4). The HV is generated by a line transformer from the amplified sine-wave signal of a signal generator. The process conditions of the plasma treatment are characterized by the electrical parameters such as peak-to-peak value voltage  $U_{pp}$ , frequency  $f$  of the applied sinusoidal HV, and electrical power  $P$ . The electrical power was determined by the method of the voltage–charge Lissajous figure, as described in [12].

### C. Temperature Measurements

Temperature is one of the most critical parameters regarding medical applications. To avoid thermal influences on the skin surface, a maximum temperature of  $40^\circ\text{C}$  should not be exceeded. The surface temperature of the sample material, close to the plasma source during the plasma treatment, has been



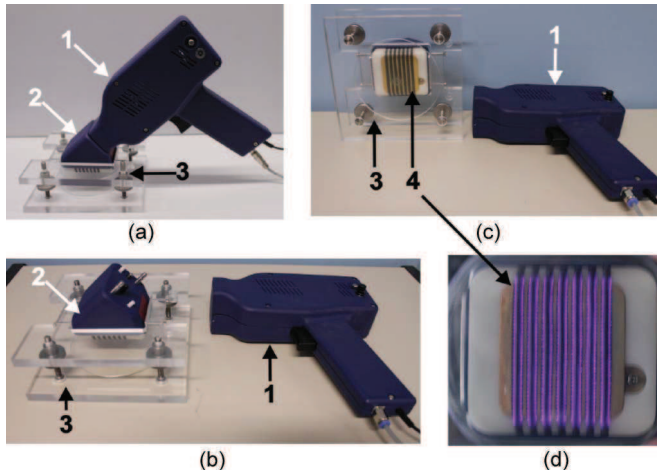


Fig. 4. Experimental setup with ConPlas handheld laboratory prototype: (a) complete treatment unit, (b) and (c) parts of the handheld laboratory prototype separated from one another in different views, and (d) plasma unit in operation; (1) handheld part with incorporated HV power supply, (2) interchangeable plasma unit, (3) adjustable adapter between plasma unit and sample holder, and (4) plasma unit in operation.

measured by the fiber-optic temperature sensor “FOTEMP” (Optocon AG). The FOTEMP instrument enables failure-free measurements of temperatures in the range of 0 °C to 300 °C under the influence of electromagnetic fields caused by plasma sources.

#### D. Microbiological Tests

For microbiological experiments, *Escherichia coli* (*E. coli*) K-12 (NCTC 10538), *Staphylococcus aureus* (*S. aureus*; ATCC 6538), and *Candida albicans* (*C. albicans*; ATCC 10231) were used. Bacteria and yeast were obtained from the Leibniz Institute DSMZ - German Collection of Microorganisms and Cell Culture. For the investigations, two different specimens were used. Plastic sheets (25 cm<sup>2</sup>) were treated with the plasma array and petri dishes (diameter of 90 mm) with the ConPlas source. The sheets were inoculated, centered on an area of 2 cm<sup>2</sup> by pipetting, and dried under aseptic conditions. The recovery of microorganisms on the sheets was realized by using the surface-spread-plate count method with tryptic soy agar plates. The sheets were shaken in tryptic soy broth for 15 min before. The detection limit of this procedure was 100 colony-forming units per milliliter (cfu · mL<sup>-1</sup>). In case the number of microorganisms fell below the detection limit, i.e., no viable microorganisms have been found, these values are set at 1.5 in the graphs. The petri dishes were filled with 20-mL CASO agar (Merck, Darmstadt, Germany), resulting in a constant agar surface area of 63.6 cm<sup>2</sup>. Overnight cultures of *S. aureus* were diluted using a physiological saline solution (0.85% NaCl) to obtain concentrations of 10<sup>7</sup>–10<sup>8</sup> cfu · mL<sup>-1</sup>. The agar plates were inoculated with the bacteria suspension under aseptic conditions using dilutions ranging from 1 : 1 to 1 : 1 000 000. In addition, 100 µL of bacteria suspension of the respective solution have been plated on each agar plate.

The number of viable *S. aureus* on the agar surface (in cfu · cm<sup>-2</sup>) was estimated by manually counting the grown colonies on each agar plate after overnight incubation at 35 °C–37 °C.

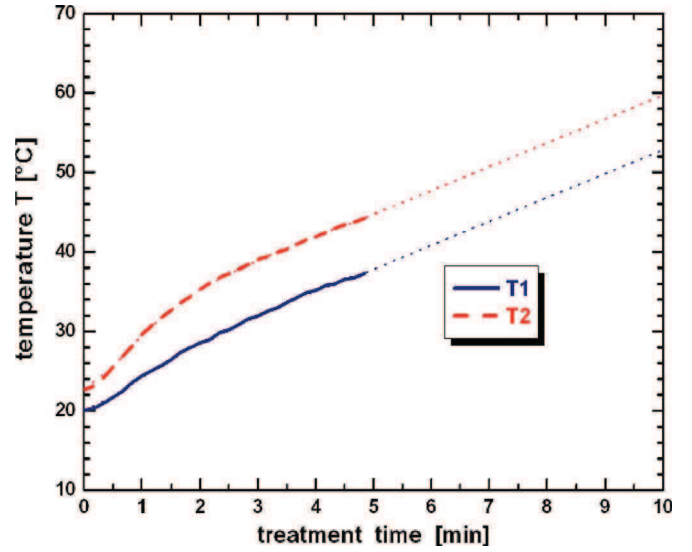


Fig. 5. Temperature–time curves for the plasma source ConPlas: Treatment time is 5 min in pulse operation (on time is 1 s; off time is 2 s);  $U_{pp} = 10$  kV;  $f = 11$  kHz, and  $P = 4$  and 5 W. For longer treatment times, the curves were extrapolated. (T1) Surface temperature of the treated object at a distance of 3 mm from the plasma source. (T2) Surface temperature of the HV electrodes.

Colony counting was performed on a defined circular area of 22.57 cm<sup>2</sup> in the center of the agar plate, only, to exclude nontreated colonies. According to manual counting, a maximum number of 350 colonies were countable on the counted area of 22.57 cm<sup>2</sup>. Consequently, the upper detection limit was at 15 cfu · cm<sup>-2</sup>. Because the minimum number of countable colonies on the counted area of 22.57 cm<sup>2</sup> was 1, the lower detection limit was 0.04 cfu · cm<sup>-2</sup>.

Logarithmic reduction factors ( $\lg R$ ) were calculated as the differences of number of viable microorganisms on nontreated references ( $N_0$ ; cfu · cm<sup>-2</sup>) and countable plasma-treated samples ( $N_a$ ; cfu · cm<sup>-2</sup>)

$$\lg R = \lg N_0 - \lg N_a. \quad (1)$$

Inactivation kinetics of microorganisms were depicted in semilogarithmic plots. In case the number of cfu fell below the detection limit, i.e., no colonies have been found, these values are set at  $-1.35$  for clearness sake.

### III. EXPERIMENTAL RESULTS AND DISCUSSION

#### A. Results of Temperature Measurements

In the case of the plasma source array, the maximum value of the temperature close to the electrodes was approximately 28 °C, measured after 10 min. The electrodes were in direct contact to the treated plastic sheets.

For the tests with the plasma source ConPlas, temperature–time curves were measured. Fig. 5 exhibits the surface temperature curves of the ConPlas source depending on the treatment time, which were measured directly on the electrodes and the treated object (agar plates), respectively. As shown, with longer treatment times, the linear temperature increase continued. Therefore, an adaptation in pulse operation (e.g., by increasing the off time) is necessary to reduce the temperature on the



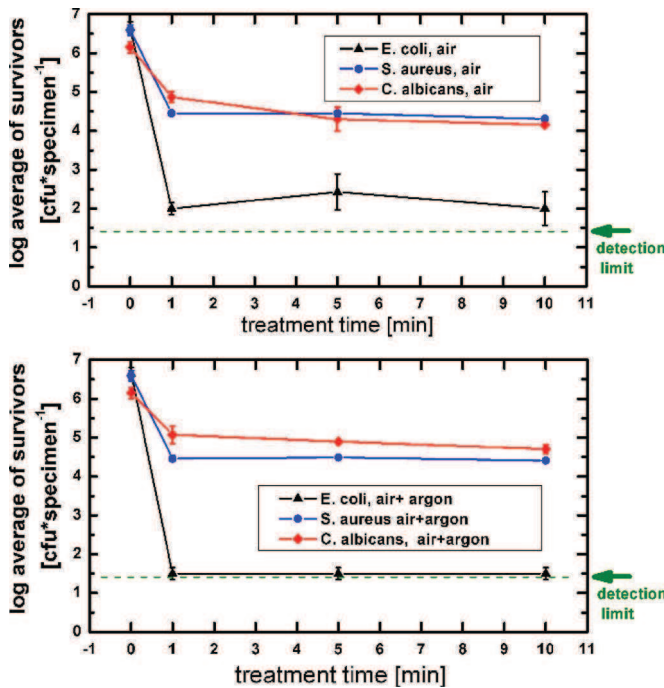


Fig. 6. Inactivation of *E. coli*, *S. aureus*, and *C. albicans* on plastic sheets as a result of treatment by the plasma array;  $U_{pp} = 10$  kV, and  $f = 4$  kHz. (mean  $\pm$  SD,  $n = 3$ , each) The upper graphics show the inactivation curves of air treatment, and the lower graphics show those of air and argon treatment.

substrate surface. However, critical temperatures that might initiate thermal damage were not reached within treatment times.

Deduced from the temperature measurements, it was demonstrated that the applied plasma devices operate in a moderate temperature range without exceeding critical temperatures that might initiate thermal damage. Consequently, the plasma sources can be used for the treatment of human skin.

### B. Inactivation of Bacteria and Yeast by the Plasma Array

To investigate the antimicrobial efficacy of the plasma array, *E. coli*, *S. aureus*, and *C. albicans* were chosen as possible colonizers of skin and wounds. In Fig. 6, the survival curves for all studied microorganisms depended on plasma treatment times, and different gas compositions (air and air + argon) are shown. It can be observed that the inactivation of *E. coli* bacteria rapidly decreased for each gas composition. After 1-min treatment time, a reduction of  $\geq 4.5 \log_{10}$  was reached. Unlike *E. coli*, the inactivation of *S. aureus*, obtained at the same operating conditions, exhibited lower inactivation rates. The exposure of this bacterium to the plasma up to 10 min led to a maximum inactivation of  $2.2 \log_{10}$ . Furthermore, a lower lethal effect was also observed for the inactivation curves of *C. albicans* compared with those of *E. coli* and *S. aureus*. A maximum reduction of  $2 \log_{10}$  by air plasma and of  $1.4 \log_{10}$  by air with argon plasma treatment was detected. The admixture of argon did not strengthen the bactericidal effect, and furthermore, only minor differences in terms of gas composition were observed. The immediate lethal effect of plasma might be due to the point that most reactive species are generated in the first seconds of plasma ignition and can react with species

of surrounding air. Furthermore, because of the high initial concentrations of bacteria and fungi, the shielding effects of stacked microorganisms cannot be excluded.

Generally, plasma generates numerous active components that are considered to be responsible for the inactivation of microorganisms. Plasma components with antimicrobial effects are heat, VUV/UV radiation, radicals (reactive oxygen and reactive nitrogen species), and ions [18]–[21]. In the present investigations, heat as an antimicrobial component can be excluded, which was confirmed by temperature measurements. Hence, radicals such as oxygen ( $O_2^-$ ,  $O^\cdot$ ), hydroxyl ( $OH^\cdot$ ), nitrogen monoxide ( $NO^\cdot$ ), nitrogen dioxide ( $NO_2^\cdot$ ), and ozone ( $O_3$ ) play a major role for the inactivation of microorganisms.

Three different mechanisms may lead to microbial inactivation: 1) deterioration of the cell membranes' integrity by oxidation of unsaturated fatty acids of the membrane lipids; 2) oxidation of integrated membrane proteins of the double lipid layer; and 3) oxidation of deoxyribonucleic acid molecules [22]. Therefore, concerning plasma treatments, the main targets of microorganisms are the membrane lipids, which, in turn, probably explain the higher bactericidal effects of plasma on Gram negative bacteria. Due to their cell membrane structure, Gram negative bacteria are more susceptible to plasma than Gram positive bacteria, fungi, and spores. Damages of the outer membrane and, thus, cell lysis rapidly occurred for the Gram negative bacterium *E. coli*. [22], [23]. Gram positive bacteria such as *S. aureus* and *Bacillus subtilis* showed no detectable morphological changes in the same treatment time. Longer treatment times were necessary to observe changes in cell membranes and cell breakage [22], [24].

Similar observations were done in our experiments. *E. coli* showed much higher inactivation than *S. aureus* and *C. albicans* did. By analogical conclusion, the aforementioned inactivation mechanisms may be the reason for observed effects, taking the inactivation kinetics into account. However, further investigations of plasma and microorganisms are necessary to get deeper insights into inactivation mechanisms.

### C. ConPlas Treatment of *Staphylococcus Aureus*

The electrode arrangement of the used ConPlas setup has an area of  $4 \times 5 \text{ cm}^2$ . Consequently, a simultaneous effective plasma treatment of an area of about  $20 \text{ cm}^2$  can be realized where the treatment time can be continuously varied. The treatment of bacteria-inoculated agar plates resulted in time-dependent inactivation, which can be observed in Figs. 7 and 8. As shown in Fig. 7, more than  $4 \log_{10}$  reduction of *S. aureus* was estimated after 60-s plasma treatment. Furthermore, an enhanced decline of the number of viable microorganisms within 120-s plasma exposure can be observed. After 540-s plasma treatment, only few viable microorganisms were detectable. The intensity of the reduction is dependent on the initial concentration and treatment time, which is depicted in Fig. 7 too. The observed dilution dependence of the inactivation may be a dosage effect due to the same concentration of radicals, but fewer counts of bacteria and fungi. However, a commonly accepted unit for a plasma dosage does not exist. The different

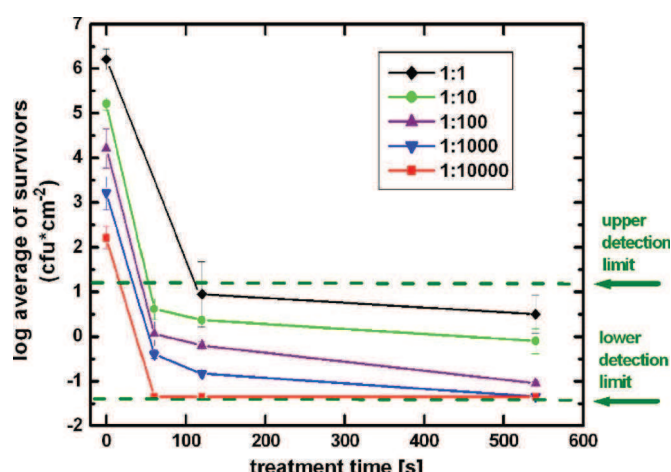


Fig. 7. Inactivation kinetics of *S. aureus* on agar plates as a result of ConPlas treatment (in air);  $U_{pp} = 10$  kV,  $f = 11$  kHz, and  $P = 4$  and  $5$  W. (mean  $\pm$  SD,  $n = 3$ , each) Detection limits are set at the level of count limits, as described above. The upper detection limit is at the logarithm of  $15 \text{ cfu} \cdot \text{cm}^{-2}$ , and the lower one is at the logarithm of  $0.04 \text{ cfu} \cdot \text{cm}^{-2}$ .

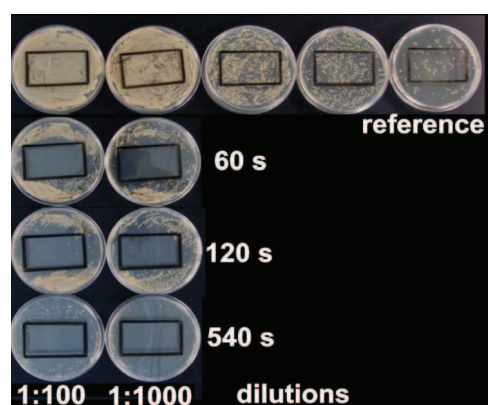


Fig. 8. Exemplary pictures of *S. aureus*-inoculated and ConPlas-treated agar plates. For nontreated agar plates (reference), dilutions from 1:100 to 1:1 000 000 are shown, and for treated agar plates, dilutions 1:100 and 1:1000 are shown. Black-surrounded area was counted only ( $22.57 \text{ cm}^2$ ).

kinds of plasma (e.g., thermal, nonthermal, atmospheric, and low pressure), plasma setups, and therefore, the produced cocktails of reactive species, radiation, ions, and molecules make it difficult to define a common unit [25]. The order of magnitude of microbial inactivation is comparable but depends on the investigated microorganism and environment (e.g., substrate and humidity). For special applications, a plasma dosage may be defined, as it was done for corona discharge treatments of synthetic materials in industrial applications [26]. It might be also possible that higher microbial concentrations implicate physical shielding by stacked microorganisms resulting in the formation of multiple layers, which hinder complete penetration of radicals [25].

However, Fig. 8 illustrates an exemplary sequence of *S. aureus* on agar plates after 60-, 120-, and 540-s plasma treatments for dilutions of 1:100 and 1:1000, respectively. For comparison, nontreated agar plates (labeled as reference) are depicted also. The black-rimmed areas show the results of impinging plasma species leading to a remarkable decrease



Fig. 9. Demonstration test: Plasma treatment of human extremity model with plasma source array; (1) glass-covered HV pin electrodes and (2) plasma.

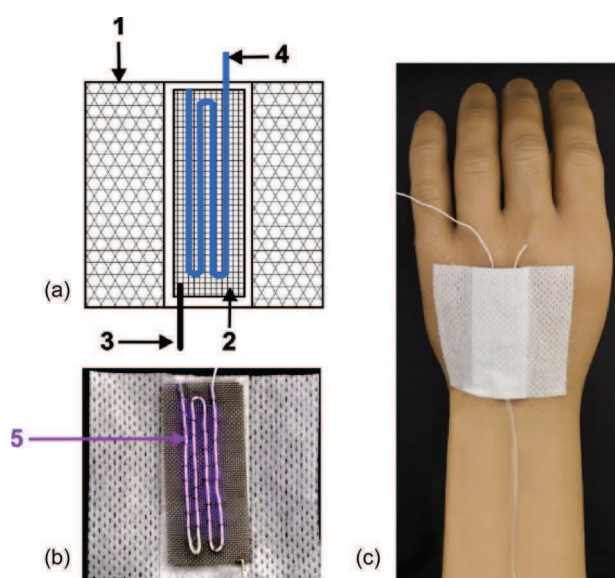


Fig. 10. Demonstration test: plasma treatment of human extremities with a small-sized plasma source ConPlas, integrated in a sticking plaster. (a) Schematic view: (1) sticking plaster, (2) gaze made from an electrically conductive material as the grounded electrode, (3) electrical connection cable to the ground, and (4) isolated wire as an HV electrode. (b) Test arrangement. (c) Demonstration of an application example: plasma treatment of a human hand model.

in cfu even after 60-s plasma exposure. Furthermore, the agar plates, plasma-treated for 60 and 120 s, exhibited nontreated regions according to the geometrical confinements of the used plasma device. In contrast, agar plates exposed to plasma for 540 s showed a homogenous inactivation of *S. aureus* over the entire agar plates. Observed broadening of the plasma-affected area may result from the radial diffusion of plasma-generated reactive in or on the agar.

Owing to their low temperatures and their capability of inactivating microorganisms, the developed and investigated plasma devices can be applied for medical purposes. The images in Figs. 9 and 10 demonstrate the possibilities of these plasma sources for medical applications, particularly the plasma treatment of human extremities. However, these are still models, and they only provide possible applications. The studies to human skin have not been completed yet and are still under research.

## IV. CONCLUSION

The possible application of two novel nonthermal plasmas sources for the treatment of human extremities has been in focus. The approached plasma sources are well adaptable on complex structure objects and have shown an antimicrobial activity on various microorganisms. The *in vitro* testing of microorganisms alone showed promising results. Plasma parameters and composition and, thus, antimicrobial effects can be controlled by operation parameters and gas.

## ACKNOWLEDGMENT

The authors would like to thank S. Krafczyk, S. Horn, and K. Loyal for technical assistance.

## REFERENCES

- [1] E. Stoffels, A. J. Flikweert, W. W. Stoffels, and G. M. W. Kroesen, "Plasma needle: A non-destructive atmospheric plasma source for fine surface treatment of (bio)materials," *Plasma Sources Sci. Technol.*, vol. 11, no. 4, pp. 383–388, Nov. 2002.
- [2] M. Laroussi and X. Lu, "Room-temperature atmospheric pressure plasma plume for biomedical applications," *Appl. Phys. Lett.*, vol. 87, no. 11, pp. 113902-1–113902-3, Sep. 2005.
- [3] G. Fridman, M. Peddinghaus, H. Ayan, A. Fridman, M. Balasubramanian, A. Gutsol, A. Brooks, and G. Friedman, "Blood coagulation and living tissue sterilization by floating-electrode dielectric barrier discharge in air," *Plasma Chem. Plasma Process.*, vol. 26, no. 4, pp. 425–442, Aug. 2006.
- [4] J. F. Kolb, A. H. Mohamed, R. O. Price, R. J. Swanson, A. Bowman, R. L. Chiavarini, M. Stacey, and K. H. Schoenbach, "Cold atmospheric pressure air plasma jet for medical applications," *Appl. Phys. Lett.*, vol. 92, no. 24, p. 241 501, Jun. 2008.
- [5] T. Shimizu, B. Steffes, R. Pompl, F. Jamitzky, W. Bunk, K. Ramrath, M. Georgi, W. Stolz, H.-U. Schmidt, T. Urayama, S. Fujii, and G. E. Morfill, "Characterization of microwave plasma torch for decontamination," *Plasma Process. Polym.*, vol. 5, no. 6, pp. 577–582, Aug. 2008.
- [6] A. Shashurin, M. Keidar, S. Bronnikov, R. A. Jurjus, and M. A. Stepp, "Living tissue under treatment of cold plasma atmospheric jet," *Appl. Phys. Lett.*, vol. 93, no. 18, p. 181 501, Nov. 2008.
- [7] S. Rupf, A. Lehmann, M. Hannig, B. Schäfer, A. Schubert, U. Feldmann, and A. Schindler, "Killing of adherent oral microbes by a non-thermal atmospheric plasma jet," *J. Med. Microbiol.*, vol. 59, no. 2, pp. 206–212, Feb. 1, 2010.
- [8] H. J. Lee, C. H. Shon, Y. S. Kim, S. Kim, G. C. Kim, and M. G. Kong, "Degradation of adhesion molecules of G361 melanoma cells by a non-thermal atmospheric pressure microplasma," *New J. Phys.*, vol. 11, no. 11, p. 115 026, Nov. 2009.
- [9] M. Kuchenbecker, N. Bibinov, A. Kaemling, D. Wandke, P. Awakowicz, and W. Viöl, "Characterization of DBD plasma source for biomedical applications," *J. Phys. D, Appl. Phys.*, vol. 42, no. 4, p. 045 212, Feb. 2009.
- [10] G. Lloyd, G. Fridman, S. Jafri, G. Schultz, A. Fridman, and K. Harding, "Gas plasma: Medical uses and developments in wound care," *Plasma Process. Polym.*, vol. 7, no. 3/4, pp. 194–211, Mar. 2010.
- [11] G. Isbary, G. Morfill, H. U. Schmidt, M. Georgi, K. Ramrath, J. Heinlin, S. Karrer, M. Landthaler, T. Shimizu, B. Steffes, W. Bunk, R. Monetti, J. L. Zimmermann, R. Pompl, and W. Stolz, "A first prospective randomized controlled trial to decrease bacterial load using cold atmospheric argon plasma on chronic wounds in patients," *Brit. J. Dermatol.*, vol. 163, no. 1, pp. 78–82, Jul. 2010.
- [12] K. D. Weltmann, E. Kindel, T. von Woedtke, M. Hänel, M. Stieber, and R. Brandenburg, "Atmospheric-pressure plasma sources: Prospective tools for plasma medicine," *Pure Appl. Chem.*, vol. 82, no. 6, pp. 1223–1237, 2010.
- [13] N. Bibinov, P. Rajasekaran, P. Mertmann, D. Wandke, W. Viöl, and P. Awakowicz, "Basics and biomedical applications of dielectric barrier discharge (DBD)," in *Biomedical Engineering, Trends in Materials Science*, A. N. Laskovski, Ed. Rijeka, Croatia: InTech, 2011, pp. 123–150.
- [14] S. Horn, R. Brandenburg, K.-D. Weltmann, M. Stieber, and T. von Woedtke, "Device for the planar treatment of areas of human or animal skin or mucous membrane surfaces by means of a cold atmospheric pressure plasma," WO2011/023478 A1, Mar. 3, 2011.
- [15] J. Ehlbeck, R. Foest, E. Kindel, N. Lembke, M. Stieber, and K.-D. Weltmann, "Method and device for the plasma-aided treatment of surfaces," WO2009/019156 A2, Dec. 2, 2009.
- [16] K.-D. Weltmann, M. Stieber, S. Horn, R. Brandenburg, M. Hänel, Plasmaquellen-Array zur Behandlung von Freiformflächen, DE202010004332U1, Oct. 19, 2011.
- [17] R. Brandenburg, private communication, 2012.
- [18] R. Brandenburg, H. Lange, T. von Woedtke, M. Stieber, E. Kindel, J. Ehlbeck, and K.-D. Weltmann, "Antimicrobial effects of UV and VUV radiation of nonthermal plasma jets," *IEEE Trans. Plasma Sci.*, vol. 37, no. 6, pp. 877–883, Jun. 2009.
- [19] K. Oehmigen, M. Hänel, R. Brandenburg, C. Wilke, K.-D. Weltmann, and T. von Woedtke, "The role of acidification for antimicrobial activity of atmospheric pressure plasma in liquids," *Plasma Process. Polym.*, vol. 7, no. 3/4, pp. 250–257, Mar. 2010.
- [20] K. Oehmigen, J. Winter, M. Hänel, C. Wilke, R. Brandenburg, K.-D. Weltmann, and T. von Woedtke, "Estimation of possible mechanisms of *Escherichia coli* inactivation by plasma treated sodium chloride solution," *Plasma Process. Polym.*, vol. 8, no. 10, pp. 904–913, Oct. 2011.
- [21] J. Ehlbeck, U. Schnabel, M. Polak, J. Winter, T. von Woedtke, R. Brandenburg, T. von dem Hagen, and K.-D. Weltmann, "Low temperature atmospheric pressure plasma sources for microbial decontamination," *J. Phys. D, Appl. Phys.*, vol. 44, no. 1, p. 013 002, Jan. 2011.
- [22] T. C. Montie, K. Kelly-Wintenberg, and J. R. Roth, "An overview of research using the one atmosphere uniform glow discharge plasma (OAugDP) for sterilization of surfaces and materials," *IEEE Trans. Plasma Sci.*, vol. 28, no. 1, pp. 41–50, Feb. 2000.
- [23] M. Laroussi, G. S. Sayler, B. B. Glascock, B. McCurdy, M. E. Pearce, N. G. Bright, and C. M. Malott, "Images of biological samples undergoing sterilization by a glow discharge at atmospheric pressure," *IEEE Trans. Plasma Sci.*, vol. 27, no. 1, pp. 34–35, Feb. 1999.
- [24] M. Laroussi, J. Richardson, and F. Dobbs, "Biochemical and morphological effects of non-equilibrium atmospheric pressure plasmas on bacteria," in *Proc. 15th ISPC*, Orléans, France, 2001, pp. 729–734.
- [25] M. G. Kong, G. Kroesen, G. Morfill, T. Nosenko, T. Shimizu, J. van Dijk, and J. L. Zimmermann, "Plasma medicine: An introductory review," *New J. Phys.*, vol. 11, p. 115 012, Nov. 2009.
- [26] Ahlbrandt System GmbH, Apr. 18, 2012. [Online]. Available: <http://neu.ahlbrandt.de/index.php?page=corona-behandlung-2>

**Klaus-Dieter Weltmann** (M'95) received the Diploma degree in electronics and the Doctorate degree (Dr. rer. nat.) in applied physics from the University of Greifswald, Greifswald, Germany, in 1989 and 1993, respectively.

He worked on nonlinear dynamics in low-temperature plasmas and plasma diagnostics. In 1994, he was a Visiting Scientist at the Plasma Physics Laboratory, West Virginia University, Morgantown. In 1995, he joined ABB Corporate Research Ltd., Baden-Dättwil, Switzerland, working in the research and development (R&D) of HV and MV switchgear. In 1998, he became the Head of the High Voltage Systems Group, ABB Corporate Research Ltd. In 2000, he was appointed to lead the R&D of gas insulated switchgear (GIS, PASS) at ABB High Voltage Technologies Ltd., Zurich, Switzerland; in 2002, he became the Business Unit R&D Manager of GIS. Since 2003, he has been the Director and Chairman of the Board of the Leibniz Institute for Plasma Science and Technology e.V. (INP Greifswald), Greifswald, and a Professor of experimental physics at the University of Greifswald. His current research interests include switchgears, arc physics, atmospheric plasmas, modeling and simulation, plasma medicine, and plasma decontamination.

Prof. Weltmann is the President of the International Society for Plasma Medicine, a member of the German Physical Society, and a member of several consulting committees in industry and research. He is the initiator of three spin-off companies.

**Katja Fricke** received the Diploma in environmental science from the Ernst-Moritz-Arndt University of Greifswald, Greifswald, Germany, in 2007. During her thesis, she investigated the immobilization of biocatalysts for microbial bioelectrochemical systems and studied the anodic bioelectrocatalytic electron transfer in microbial fuel cells.

Since 2008, she has been a Researcher with the Leibniz Institute for Plasma Science and Technology (INP Greifswald), Greifswald. In her Ph.D. thesis, she elucidates the impact of nonthermal plasma on biorelevant materials, particularly the influence of plasma on the physicochemical and morphological surface properties. Her other research interests include plasma-based processes for biological decontamination and sterilization.



**Manfred Stieber** received the Diploma degree in physics (Dipl.-Phys.) and the Doctorate degree (Dr. rer. nat.) in experimental physics from the University of Greifswald, Greifswald, Germany, in 1969 and 1973, respectively.

From 1969 to 1991, he was a Scientist at the Central Institute of Electron Physics (ZIE) of the Academy of Sciences, Greifswald Division, where he worked on low-temperature plasmas and plasma diagnostics. Since 1992, he has been a Scientist at the Leibniz Institute for Plasma Science and Technology e.V. (INP Greifswald), Greifswald, in the field of plasma physics and plasma technology. His current scientific interests are focused on discharge physics and applications of atmospheric plasmas.

**Ronny Brandenburg** received the Diploma degree in physics (Dipl.-Phys.) and the Doctorate degree (Dr. rer. nat.) in experimental physics from the University of Greifswald, Greifswald, Germany, in 2000 and 2005, respectively.

From 2001 to 2005, he was with the Institute of Physics, University of Greifswald, where he worked on the diagnostics of nonthermal plasmas. In 2005, he was with Vanguard AG Berlin, where he investigated nonthermal plasma processes for reprocessing of medical devices. Since 2008, he has been with the Leibniz Institute for Plasma Science and Technology (INP Greifswald), Greifswald. Since 2009, he has been the Head of the Department of "Plasma Sources," INP Greifswald, and since 2010, he has been the Program Manager for the topic "exhaust treatment." His particular scientific interests are focused on discharge physics, plasma diagnostic, and plasma chemistry, as well as the use of plasmas for environmental issues and life-science applications.

**Thomas von Woedtke** received the Doctoral degree (Dr. rer. nat.) and the Habilitation degree (Dr. rer. nat. habil.) in pharmaceutical technology from the University of Greifswald, Greifswald, Germany, in 1996 and 2005, respectively.

From 1987 to 2005, he worked on the application of biosensors in medicine and life science research, as well as on alternative sterilization techniques for sensitive goods. Since 2005, he has been with the Leibniz Institute for Plasma Science and Technology e.V. (INP Greifswald), Greifswald. He is currently a Program Manager for plasma medicine/decontamination at INP Greifswald, and since 2011, he has been a Professor of plasma medicine at the University of Greifswald. His research interests are in the field of plasma-based processes for biological decontamination and sterilization, as well as in basic research problems of plasma-cell and plasma-tissue interactions.

**Uta Schnabel** received the Diploma degree in biology from the University of Rostock, Rostock, Germany, in 2005.

She worked on microbiology and plant genetics, particularly cytoplasmic male sterility at the PEF1 cytoplasm of *Helianthus spp.* From 2006 to 2008, she was a Scientist at Klinikum Großhadern Hospital, Munich, Germany, where she investigated the JNK/Jun (c-Jun N-terminal kinases/Jun) signal pathway signal pathway in human liver cells with molecular biology, proteomics, and *in vivo* (animal trials). Since 2009, she has been a Scientist at the Leibniz Institute for Plasma Science and Technology e.V. (INP Greifswald), Greifswald, Germany, in the field of plasma medicine and decontamination. Her recent research deals with decontamination of medical devices, food, and packaging.





## **IV Eidesstattliche Erklärung/Affirmation**

Hiermit erkläre ich, dass diese Arbeit bisher von mir weder an der Mathematisch-Naturwissenschaftlichen Fakultät der Ernst-Moritz-Arndt-Universität Greifswald noch einer anderen wissenschaftlichen Einrichtung zum Zwecke der Promotion eingereicht wurde.

Ferner erkläre ich, dass ich diese Arbeit selbständig verfasst und keine anderen als die darin angegebenen Hilfsmittel und Hilfen benutzt und keine Textabschnitte eines Dritten ohne Kennzeichnung übernommen habe.

Greifswald, den 20. September 2012



## V Curriculum Vitae

### Persönliche Daten

Name: Katja Fricke  
Geburtstag/-ort: 30.10.1982 in Rostock  
Nationalität: deutsch

### Schulbildung

1989 – 1993 Grundschule Reutershagen, Rostock  
1993 – 2002 Gymnasium am Goetheplatz, Rostock  
2002 Abitur

### Hochschulstudium

2002 – 2007 Diplom-Studium Umweltwissenschaften an der Ernst-Moritz-Arndt-Universität Greifswald  
Okt 2006 – Juni 2007 Diplomarbeit: „Grundsatzuntersuchungen zur Biokatalysator-Immobilisierung in mikrobiellen Brennstoffzellen“ im Arbeitskreis Analytische Chemie und Umweltchemie, Institut für Biochemie  
Juni 2007 Abschluss als Diplom-Umweltwissenschaftler an der Ernst-Moritz-Arndt-Universität Greifswald

### Beruflicher Werdegang

Aug 2007 - Sept 2007 wissenschaftliche Hilfskraft am Institut für Biochemie der Ernst-Moritz-Arndt-Universität Greifswald  
Okt 2007 – Aug 2008 wissenschaftliche Mitarbeiterin am Institut für Biochemie der Ernst-Moritz-Arndt-Universität Greifswald  
Seit Sept 2008 Wissenschaftliche Mitarbeiterin am Leibniz-Institut für Plasmaforschung und Technologie (INP Greifswald e.V.) in der Abteilung Plasmaoberflächentechnik

### Promotion

seit Sept 2008 Promotionsstudium im Bereich Pharmazeutische Technologie  
Sept 2010 Gewinner des „Best Student Award“ auf der 3<sup>rd</sup> International Conference on Plasma Medicine (ICPM-3)

Greifswald, den 20.09.2012



## VI List of all publications

### Peer-reviewed publications

#### **2008**

“On the Use of Cyclic Voltammetry for the Study of the Anodic Electron Transfer in Microbial Fuel Cells”

K. Fricke, F. Harnisch, U. Schröder, *Energy Environ. Sci.*, vol. 1, no. 1, pp. 144-147, 2008

“Improvement of the Anodic Bioelectrocatalytic Activity of Mixed Culture Biofilms by a Simple Consecutive Electrochemical Selection Procedure”

Y. Liu, F. Harnisch, K. Fricke, R. Sietmann, U. Schröder, *Biosensors & Bioelectronics*, vol. 24, no. 4, pp. 1006-1011, 2008

#### **2010**

“The study of electrochemically active microbial biofilms on different carbon-based anode materials in microbial fuel cells”

Y. Liu, F. Harnisch, K. Fricke, R. Sietmann, U. Schröder, *Biosensors & Bioelectronics*, vol. 25, no. 9, pp. 2167-2171, 2010

#### **2011**

“High Rate Etching of Polymers by Means of an Atmospheric Pressure Plasma Jet”

K. Fricke, H. Steffen, Th. von Woedtke, K. Schröder, K.-D. Weltmann, *Plasma Process. Polym.*, vol. 8, no. 1, pp. 51-58, 2011

#### **2012**

“On the Use of Atmospheric Pressure Plasma for the Bio-Decontamination of Polymers and Its Impact on Their Chemical and Morphological Surface Properties”

K. Fricke, H. Tresp, R. Bussiahn, K. Schröder, Th. von Woedtke, K.-D. Weltmann, *Plasma Chem. Plasma Process.*, vol. 32, pp. 801-816, 2012

“Grain boundary corrosion of the surface of annealed thin layers of gold by OH center dot radicals”

U. Hasse, K. Fricke, D. Dias, G. Sievers, H. Wulff, F. Scholz, *J. Solid State Electrochem.*, vol. 16, no. 7, pp. 2383-2389, 2012

“Atmospheric Pressure Plasma: A high-performance tool for the efficient removal of biofilms”

K. Fricke, I. Koban, H. Tresp, L. Jablonowski, K. Schröder, A. Kramer, K.-D. Weltmann, Th. von Woedtke, Th. Kocher, *PLOS ONE*, vol. 7, no. 8, pp. 1-8, 2012



“New non-thermal atmospheric pressure plasma sources for decontamination of human extremities”

K.-D. Weltmann, K. Fricke, M. Stieber, R. Brandenburg, Th. von Woedtke, U. Schnabel  
*IEEE Trans. Plasma Sci.*, 2012, DOI: 10.1109/tps.2012.2204279

“Comparison of non-thermal Plasma Processes on the Surface Properties of Polystyrene and their Impact on Cell Growth”

K. Fricke, K. Duske, A. Quade, B. Nebe, K. Schröder, K.-D. Weltmann, Th. von Woedtke  
*IEEE Trans. Plasma Sci.*, 2012. DOI: 10.1109/TPS.2012.2204904

“Investigation of Surface Etching of Poly(ether ether ketone) by an Atmospheric Pressure Plasma Jet”

K. Fricke, S. Reuter, D. Schröder, V. Schulz-von der Gathen, K.-D. Weltmann, Th. von Woedtke, *IEEE Trans. Plasma Sci.*, 2012, DOI:10.1109/TPS.2012.2212463

### Invited talk

*“Plasma: Technologie der Zukunft zur Dekontamination/Sterilisation und Erzeugung bioaktiver Implantatoberflächen”*

K. Fricke, K.-D. Weltmann, Th. von Woedtke, Otti-Fachforum für funktionale Implantatoberflächen – Biointegration vs. Biofilm, 17.09.-18.09.2012, Regensburg, Germany

### Talks

#### **2010**

*“Modification and Bio-Decontamination of Polymers utilizing Cold Atmospheric Plasma”*

K. Fricke, K. Schröder, Th. von Woedtke, K.-D. Weltmann

3<sup>rd</sup> International Conference on Plasma Medicine (ICPM-3), 19.09.-24.09.2010, Greifswald, Germany

*“Cold Atmospheric Pressure Plasma for the Modification and Etching of Biomedical relevant Surfaces”*

K. Fricke, K. Schröder, Th. von Woedtke, K.-D. Weltmann, Material Science and Engineering (MSE) - 2010, 24.08.-26.08.2010, Darmstadt, Germany

#### **2011**

*“Modification of the physicochemical surface properties of polymers during the plasma-based decontamination”*

K. Fricke, H. Tresp, R. Bussiahn, K. Schröder, K.-D. Weltmann, Th. von Woedtke

20<sup>th</sup> International Symposium on Plasma Chemistry (ISPC-20), 24.07.-29.07.2011, Philadelphia, USA

*“Comparison of low-temperature plasma processes on the surface properties of polystyrene and their impact on the growth of osteoblastic cells”*

K. Fricke, K. Duske, A. Quade, B. Nebe, K. Schröder, Th. v. Woedtke, Eighth International Symposium on Polymer Surface Modification: Relevance to Adhesion, 20.06.-22.06.2011, Danbury, USA

## Posters

### **2008**

*“The Anodic Electron Transfer in Microbial Fuel Cells: Comparative Studies of Shewanella putrefaciens and Geobacter sulfurreducens”*

K. Fricke, F. Harnisch, U. Schröder, 10. Frühjahrssymposium 2008, Jungchemikerforum, 27.03.-29.03.2008, Rostock, Germany

*“Electrochemical Characterization of the Anodic Electron Transfer of Shewanella putrefaciens and Geobacter sulfurreducens”*

K. Fricke, F. Harnisch, Th. R. Neu, U. Schröder, Balitc Conference on Electrochemistry, 30.04.-03.05.2008, Tartu, Estonia

*“Improvement of the Anodic Bioelectrocatalytic Activity of Mixed Culture Biofilms by a Simple Consecutive Electrochemical Selection Procedure”*

Y. Liu, F. Harnisch, K. Fricke, R. Sietmann, U. Schröder, Balitc Conference on Electrochemistry, 30.04.-03.05.2008, Tartu, Estonia

### **2009**

*“Comparison of surface functionalization of different polymers by means of an Atmospheric Pressure Plasma Jet”*

K. Fricke, A. Quade, A. Ohl, K. Schröder, Th. von Woedtke, K.-D. Weltmann  
DPG-Frühjahrstagung Plasmaphysik, 30.03.-02.04.2009, Greifswald, Germany

*“Comparison of chemical surface modification by an Atmospheric Pressure Plasma Jet on different polymers”*

K. Fricke, A. Quade, A. Ohl, K. Schröder, Th. von Woedtke, K.-D. Weltmann  
19<sup>th</sup> International Symposium on Plasma Chemistry (ISPC-19), 27.7-31.07.2009, Bochum, Germany

### **2010**

*“Impact of Atmospheric Pressure Plasma on Polymers: Modification vs. Etching”*

K. Fricke, H. Steffen, K. Schröder, Th. von Woedtke, K.-D. Weltmann  
12<sup>th</sup> International Conference on Plasma Surface Engineering (PSE), 13.09.-17.09.2010, Garmisch Partenkirchen, Germany

*“Removal of plaque from extracted teeth by atmospheric pressure plasma jets”*

Th. Kocher, I. Koban, L. Jablonowski, K. Schröder, K. Fricke, E. Kindel, K.-D. Weltmann,

A. Kramer, N.-O. Huebner, 3<sup>rd</sup> International Conference on Plasma Medicine (ICPM-3), 19.09.-24.09.2010, Greifswald, Germany

## **2012**

*“Plasma-generated species and its effect on surface chemistry and morphology of polymers exposed to atmospheric pressure plasma - a prospective application for biomedical purposes”*

K. Fricke, S. Reuter, H. Tresp, I. Koban, L. Jablonowski, D. Schröder, V. Schulz-von der Gathen, A. Kramer, T. Kocher, K.-D. Weltmann, T. von Woedtke, 4<sup>th</sup> International Conference on Plasma Medicine (ICPM-4), 17.06.-21.06.2012, Orléans, France

*“Biofilm removal from rough titanium surfaces using different methods and/or atmospheric pressure plasma”*

L. Jablonowski, K. Fricke, K. Duske, I. Koban, R. Schlüter, K.-D. Weltmann, T. von Woedtke, T. Kocher, 4<sup>th</sup> International Conference on Plasma Medicine (ICPM-4), 17.06.-21.06.2012, Orléans, France

*“Removal of dental plaque biofilm on titanium discs using different plasma devices and settings”*

I. Koban, K. Fricke, L. Jablonowski, R. Bussiahn, K.-D. Weltmann, T. von Woedtke, A. Kramer, T. Kocher, 4<sup>th</sup> International Conference on Plasma Medicine (ICPM-4), 17.06.-21.06.2012, Orléans, France

*“Atmospheric pressure plasma treatments inside meander-like cavities”*

A. Quade, K. Fricke, and K.-D. Weltmann, 13<sup>th</sup> PSE, 10.09.-14.09.2012, Garmisch Partenkirchen, Germany

## Conference proceedings

## **2009**

*“Comparison of chemical surface modification by use of an Atmospheric Pressure micro-Plasma Jet on different polymers”*

K. Fricke, A. Quade, A. Ohl, K. Schröder, Th. von Woedtke  
19<sup>th</sup> International Symposium on Plasma Chemistry (ISPC-19), 27.7-31.07.2009, Bochum, Germany, P1.8.29

## **2010**

*“Abtöten und Abtragen von dentalen Biofilmen von Titanimplantatoberflächen”*

I. Koban, L. Jablonowski, N.O. Hübner, P. Meisel, K. Schröder, K. Fricke, E. Kindel, K.-D. Weltmann, A. Kramer, T. Kocher, BMT 2010, 05.10-08.10.2010, Rostock-Warnemünde, Germany

*“Ätzen von Polymeren mit Jetplasmen bei Normaldruck“*

K. Fricke, H. Steffen, Th. von Woedtke, K. Schröder, K.-D. Weltmann, 18. NDVaK, 2010, Dresden, Germany

## **2011**

*“Modification of the physicochemical surface properties of polymers during the plasma-based decontamination”*

K. Fricke, H. Tresp, R. Bussiahn, K. Schröder, K.-D. Weltmann, Th. von Woedtke  
20<sup>th</sup> International Symposium on Plasma Chemistry (ISPC-20), 24.07.-29.07.2011, Philadelphia, USA, Nr. 184

## **2012**

*“Atmospheric pressure plasma treatment inside meander-like cavities”*

A. Quade, K. Fricke, K.-D. Weltmann 13<sup>th</sup> International Conference on Plasma Surface Engineering (PSE) 2012, 10.09.-14.09.2012, Garmisch Partenkirchen, Germany, PO2040

## Non peer-reviewed publications

*“Plasma aus dem Stift“*

A. Vogelsang, K. Fricke, M. Häckel, R. Lambrich, B. Russ  
*Kunststoffe*, vol. 6, pp. 34-36, 2010

*“Kalte Normaldruck-Jetplasmen zur lokalen Oberflächenbehandlung“*

R. Foest, K. Fricke, E. Kindel, H. Lange, J. Schäfer, M. Stieber, K.-D. Weltmann  
*Vakuum in Forschung und Praxis*, vol. 21, no. 6, pp. 17-21, 2009



## VII Acknowledgement

At this point I would like to thank everyone that has contributed to the success of this work.

First I would like to express my deepest gratitude to my supervisors Prof. Dr. Thomas von Woedtke and Dr. Karsten Schröder. Without their theoretical and practical knowledge, valuable guidance, support, and encouragement the results in this thesis could never have been developed. I am very thankful for giving me this interesting topic and further, that I had the chance to present this work at many international and national conferences. Thank you for introducing me into the world of plasma.

For the opportunity to work at the Leibniz Institute for Plasma Science and Technology (INP Greifswald e.V.), I would like to thank the director of this Institute, Prof. Dr. Klaus-Dieter Weltmann. I greatly appreciate the additional activities he gave me to improve my experiences in the field of plasma medicine.

In addition to the aforementioned people, there are several others I would like to acknowledge, especially my colleagues from the department "Plasma Surface Technology". In particular: Dr. Antje Quade, Urte Kellner, Dr. Martin Polak, Dagmar Jasinski, Sebastian Peters, Gerd Friedrichs, Uwe Lindemann, Roland Ihrke, Dr. Frank Hempel, Dr. Birgit Finke, Dr. Andreas Ohl, Dr. Jan Schäfer, and Dr. Rüdiger Foest. I am very grateful for the scientific discussions and for all you have done to support my research. It was a pleasure to work with you and to discuss ideas and to find solutions for problems that arose during this work. Further, I would like to express my sincere thanks to the following colleagues: Rüdiger Titze, Christiane Meyer, Dr. René Bussiahn, and Dr. Eckhard Kindel for the technical support and for the insights you gave me in the work principles of the plasma jet, Dr. Stephan Reuter, Helena Tresp, and Dr. Jörn Winter with whom I closely collaborated, and Liane Kantz for helping me to perform the microbial investigations and for her encouraging words.

Many thanks also to my colleagues in the PhD office which were responsible for the good working environment, day and night. I really enjoyed the time with you!!! Our funny conversations and the fruitful discussions are memorable for me. Thank you so much!!!

I also give my best thanks to the colleagues of the universities I worked with: Daniel Schröder and Dr. Volker Schulz-von der Gathen from the "Universität Bochum", Ina Koban from the Dental School, University of Greifswald, and Kathrin Duske from the Department of Cell Biology, University of Rostock.

Last but not least, I would like to extend my gratitude to my friends and family. Especially, I would like to thank Philipp Schnaase and Franklin Martinez. Thank you, for your straight talk and that you were always willing to listen to my worries as well as many thanks for carefully reading my publications. I deeply thank my family for their love and support during the completion of this work. Without you none of this has been possibly happened.